ice
Institution of Civil Engineers
publishing

Steel-Concrete Composite Bridges

Designing with Eurocodes

Second edition

David Collings
Independent consultant, Technical Director RB International

Published by ICE Publishing, One Great George Street, Westminster, London SW1P 3AA.

Full details of ICE Publishing sales representatives and distributors can be found at: www.icevirtuallibrary.com/info/printbooksales

First edition published 2005

Other titles by ICE Publishing

Prestressed Concrete Bridges, Second edition.
N. Hewson. ISBN 978-0-7277-4113-4
Designers' Guide to Eurocode 1: Actions on bridges.
J.-A. Calgaro, M. Tschumi and H. Gulvanessian. ISBN 978-0-7277-3158-6
Bridge Construction Equipment.
M. Rosignoli. ISBN 978-0-7277-5808-8

www.icevirtuallibrary.com

A catalogue record for this book is available from the British Library

ISBN 978-0-7277-5810-1

Commissioning Editor: Rachel Gerlis
Production Editor: Imran Mirza
Market Specialist: Catherine de Gatacre

Typeset by Academic + Technical, Bristol
Printed and bound in Great Britain by CPI Group (UK) Ltd, Croydon, CR0 4YY

Steel–concrete Composite Bridges
ISBN 978-0-7277-5810-1

http://dx.doi.org/10.1680/scb.58101.001

ice Institution of Civil Engineers publishing

Introduction

The Eurocodes with their ten volumes, some of these with 20 parts, each with their own national annex, some with 370 separate clauses or subclauses, amounting to some 5000 sheets of paper, can seem a daunting set of documents.

Bridges work today in much the same way as they always have, obeying the same basic laws of nature, although we now have more sophisticated ways to analyse them. Having a grasp of how the structure works, of how bridges stand, is more important than being able to quote clause by clause from codes. We should be aware that these codes have been a long time in gestation (Johnson, 2009) and, while they may appear to be more sophisticated than older codes, they may in fact already be outdated in some areas. But, we must have some knowledge of these documents; their drafters were, after all, trying to capture the best of our current state of knowledge. The Eurocodes, with their ten volumes, some of these with 20 parts, each with their own national annex, some with 370 separate clauses or subclauses, amounting to some 5000 sheets of paper, can seem a daunting set of documents. I am reminded of the words of Isambard Kingdom Brunel regarding rules for the design of bridges; he was concerned that to 'lay down rules to be hereafter observed [will] embarrass and shackle the progress of improvements of tomorrow by recording and registering as law the prejudices and errors of today' (Vaughn, 1991). To avoid a situation where the Eurocodes shackle the designer, the documents must be understood. This chapter reviews and looks at a number of the Eurocode volumes relevant to the design of bridges, and outlines which parts of the various volumes are relevant to the design of bridges, and steel–concrete composite bridges in particular.

Eurocodes 0 and 1

These first two Eurocodes outline the principles used and the basis of design, and give the definitions of basic loads and load factors.

Basis of design – Eurocode 0

Eurocode 0 (BSI, 2002a) is a relatively compact document of only one part. It outlines the basis of the Eurocodes, the fundamentals around which the others are based. Section 1 gives definitions of terms used in the code and the key symbols used. Similar symbols are used (with some simplification) in this book and are defined in the Notation section that precedes this Introduction. Section 2 defines a number of requirements, including the design life; for bridges this is notionally 100 years, which is significantly longer than the design life used in the same codes for building structures, which have a notional design life of 50 years. The UK National Annex (BSI, 2002b) for this section modifies this life to 120 years, a figure that has been used in the UK for a number of decades. However, material strengths, concrete covers, etc., used in the UK are very similar to those practices used elsewhere in Europe, and so may have had some political influence (Johnson, 2009). Section 3 of Eurocode 0 outlines the principles of limit state design, which should not be new to most designers. This section contains a useful hint: 'verification shall be carried out for all relevant design situations … verification of one of the two categories of limit states may be omitted provided that

sufficient information is available to prove that it is satisfied by the other'. There is no need to check, clause by clause, every situation for every aspect of every limit state; some thinking, some discretion is allowed. With experience, the designer will know which limit state and which load combination is more critical in various situations. Section 4 outlines the basic definitions of actions (which are based on time, that is, permanent (G), variable (Q) or accidental (A)), materials and geometric data. Section 5 describes structural analysis and design assisted by testing – this is an important concept. The theoretical models must be based on reality. I have seen some four-dimensional modelling that failed to converge on the answer given by simpler more empirical methods based on physical testing. Significant failures have occurred in the past where the current theory and reality diverge (Collings, 2005), and often such complex models must be calibrated by testing. Some of the examples of composite construction used in this book are based on physical tests, the earliest I have found being from 1908 (Burr, 1912).

Section 6 outlines the basic partial factor method for loads and actions, or effects (E) and resistance (R). Stated simply, the design resistance should be larger than the design effects:

$$E_{\mathrm{d}} \leq R_{\mathrm{d}} \tag{0.1}$$

The design effect is a load, or characteristic action, multiplied by various partial factors (usually to increase it for the design situation):

$$E_{\mathrm{d}} = \gamma f \psi F_{\mathrm{k}} \tag{0.2}$$

The design resistance is the characteristic strength of the materials being designed divided by a partial factor (usually to reduce it for the design situation):

$$R_{\mathrm{d}} = R_{\mathrm{k}}/\gamma m \tag{0.3}$$

Eurocode 0, like other Eurocodes, contains a number of annexes. These do not have the same status as the main body of the code, but contain relevant data that may be used. They are normally classed as informative (giving additional information) or normative (giving standard methods that could generally be used). Annex 2 is relevant to steel–concrete composite bridges, and gives values for load combinations of actions for various bridge types; some important serviceability criteria for railway bridges are also presented (see Chapter 4).

Actions on structures – Eurocode 1

Eurocode 1, 'Actions on structures', has ten parts outlining the various actions to be considered when designing a structure. Part 1-1, 'General actions – densities, self-weight and imposed loads for buildings' (BSI, 2002c), is useful. Section 5 of Part 1-1 outlines some requirements specifically for bridges, and Annex A outlines densities to be used in the calculation of the structure self-weight and non-structural permanent loads (see Chapter 2). Part 1-2, 'General actions – Actions on structures exposed to fire' (BSI, 2002d), is generally not applicable to bridges, although in some special circumstances may be useful. The consideration of fire on bridges (and other risks) is outlined in Chapter 12. Part 1-3, 'General actions – Snow loads' (BSI, 2003a), outlines snow loads on roofs. This document is not considered in this book, but where bridges are in mountainous areas or are shaped such that large drifts can occur, then some consideration may need to be given to this document.

Part 1-4, 'General actions – Wind actions' (BSI, 2005a), defines the primary lateral loads experienced by a structure; this is outlined in more detail in Chapter 10. For wind actions the UK National Annex (BSI, 2008a) is particularly important, as it contains the basic wind-speed map for the UK, and also

contains (some slightly confusing) amendments to the main part that significantly modify some aspects of the methodology for determining the wind force or pressures on a bridge. Annex E of Part 1-4 contains information on vortex shedding and aeroelastic instabilities that are particularly important for longer span bridges or lighter footbridges (see Chapter 10). Part 1-5, 'General actions – Thermal actions' (BSI, 2003b), outlines temperature actions to be considered, and Section 6 of this part is specific to bridges (see Chapter 3). Part 1-6, 'General actions – Actions during execution' (BSI, 2005b), considers the construction stage. For composite beams and slabs that have concrete elements this is relevant and may give a critical load case, unless props are used. Annex A2 gives supplementary rules for bridges. Part 1-7, 'General actions – Accidental actions' (BSI, 2006a), is also relevant to the robustness of the structure and the prevention of collapse of part or all of the structure, particularly for impact loads. Section 4 of this part considers impact from road vehicles, trains and ships. Annex B outlines information on risk assessments, which the designer should always carry out early in the design of a bridge (see Chapters 1 and 12). The UK National Annex to this part (BSI, 2008b) contains further data on clearances and impact forces on bridge supports.

Part 2 (BSI, 2003c) outlines traffic loads on bridges from roads and railways, and is a key document for the bridge designer. Section 4 outlines actions specifically for road bridges (see Chapter 2); section 5 outlines actions on footbridges, and section 6 looks at actions on railway bridges (see Chapter 4). The annexes to this part also contain useful data: Annex F outlines criteria where dynamic analysis is not required, and annex G gives the requirements with regard to track structure interaction, which is a key issue for most modern railway bridges. For most bridges, Part 3, 'Actions induced by cranes and machinery' (BSI, 2005c), will not be applicable, but for some movable bridges or long-span structures with their own maintenance gantries this part may be useful. Part 4 (BSI, 2005d) outlines actions on silos and tanks. This is generally not used for bridges, but may be useful in part for special bridges such as aqueducts.

Table 0.1 outlines the various parts to Eurocodes 0 and 1, and indicates the relevance of each part (high, medium, low) to steel–concrete bridges. Eurocode 1 and its various parts will generally give enough information for the designer to determine the value of E_d in Equations 0.1 and 0.2. The values of the resistance R_d in Equations 0.1 and 0.3 can be found in Eurocodes 2, 3 or 4.

Eurocodes 2, 3 and 4

These three Eurocodes are key documents and contain details on materials used in a bridge, and how to safely calculate strength and avoid collapse at the ultimate limit state; and to ensure the structure is usable and durable at the serviceability limit state.

Concrete structures – Eurocode 2

Eurocode 2, 'Design of concrete structures', has four parts. Part 1-1, 'General rules and rules for buildings' (BSI, 2004a), is useful for the bridge designer, as it contains a lot of the basic requirements. Section 6 of this part outlines the methods for determining R_d for the ultimate axial, shear and bending resistance in concrete elements. An understanding of this section is needed, as concrete behaviour has a significant influence in steel–concrete composite bridge design. Section 7 outlines serviceability issues for concrete, the control of cracking being particularly important.

Part 2, 'Concrete bridges – Design and detailing rules' (BSI, 2005e), is useful, but needs to be read in conjunction with Part 1-1 as it refers to that extensively. Section 3 outlines the properties of concrete to be used in design (see Chapter 2). Section 5 outlines structural analysis requirements for concrete structures. Part 2 also contains a series of annexes. Annex B outlines creep and shrinkage effects on

Table 0.1 Eurocodes 0 and 1, title, parts and relevance to steel–concrete composite bridges

BS EN No.	Eurocode	Volume title	Part No.	Part title	Relevance
1990	0	Basis of structural design	–	–	H
1991-1-1	1	Actions on structures	1-1	General actions. Densities, self weight, imposed loads for buildings	M
1991-1-2			1-2	General actions. Actions on structures exposed to fire	L
1991-1-3			1-3	General actions. Snow loads	L
1991-1-4			1-4	General actions. Wind actions	H
1991-1-5			1-5	General actions. Thermal actions	M
1991-1-6			1-6	General actions. Actions during execution	H
1991-1-7			1-7	General actions. Accidental actions	H
1991-2			2	Traffic loads on bridges	H
1991-3			3	Actions induced by cranes and machinery	L
1991-4			4	Silos and tanks	L

H, high; M, medium; L, low

concrete elements (see Chapter 1). Annex G looks at soil–structure interaction (see Chapter 3), which is relevant to steel and steel–concrete composite structures as well as concrete bridges. Part 3 (BSI, 2006b) gives specific rules for liquid-retaining structures, and is therefore not considered in this book.

Steel structures – Eurocode 3

Eurocode 3 has 20 parts, and getting to grips with these is something the composite-bridge engineer has to do. Part 1-1, 'General rules and rules for buildings' (BSI, 2005f), contains much of the basic design basis. Section 5.5 outlines the classifications of a steel element, a particularly important aspect of steel, as the rules are very different for relatively stocky and compact class 1 and 2 sections and the more slender class 3 and 4 sections where local buckling effects may influence behaviour. The rules in Part 1-1 are primarily for building structures, where class 1 and 2 sections are the norm. Section 6 of this part outlines the methods for determining R_d for the ultimate axial, shear and bending resistance in the steel element.

Part 1-2 (BSI, 2005g) outlines the general rules for fire resistance, and Part 1-3 (BSI, 2005h) gives rules for cold-formed thin gauge structures. Parts 1-2 and 1-3 are not normally used by the composite-bridge designer, although Part 1-3 may be needed where enclosure of the steelwork is being considered (see Chapter 8). Part 1-4, 'General rules – Supplementary rules for stainless steels' (BSI, 2006c), may be useful, as stainless steel is used where durability or aesthetics is a key issue (see Chapter 10). Part 1-5, 'Plated structural elements' (BSI, 2006d), gives rules for stiffened plate subject to in-plane forces. Part 1-5 is useful for the bridge designer, particularly in understanding plate buckling (see Chapter 10). Annex D of Part 1-5 gives rules for girders with corrugated webs (see Chapter 11). Parts 1-6 and 1-7 (BSI, 2007a,b) are for steel-shell structures or plates subject to out-of-plane forces; they are not so useful for most steel–concrete composite bridges, and are therefore not considered in this book.

Part 1.8, 'Design of joints' (BSI, 2005i), is a useful document, as there will be welded or bolted joints in all steel elements of a bridge (see Chapters 4 and 8), the methods for calculating joint stiffness are particularly useful in some buckling problems associated with through-girder or truss bridges. Part 1-9 (BSI, 2005j) considers fatigue, and it is useful to have a copy of table 8 of this part, which outlines visually various construction details and fatigue crack locations. Part 1-10, 'Material toughness and through-thickness assessment' (BSI, 2005k), is important for many bridges where steel thickness can be large (see Chapter 1). The UK National Annex to Part 1-10 (BSI, 2009) outlines particular requirements for UK practice. Part 1-11, 'Design of structures with tension components' (BSI, 2006e), outlines additional rules and requirements for bridge elements such as cable stays (see Chapter 10). Part 1-12 (BSI, 2007c) outlines additional rules for the use of higher strength steels (see Chapter 8).

Part 2 (BSI, 2006f) outlines rules for steel bridges; these rules tend to be supplementary to those found in Parts 1-1 to 1-12 of Eurocode 3. Annexes A and B of Part 2 deal with bearings and expansion joints – elements that the bridge engineer must get right, as most durability problems on bridges stem from these two elements.

Parts 3-1 and 3-2 (BSI, 2006g,h) deal with towers, masts and chimneys. For cable-stayed and suspension bridge structures some knowledge of these parts could be useful. Parts 4-1, 4-2 and 4-3 (BSI, 2007d,e,f) deal with silos, tanks and pipes, and are generally not used for bridge design. Part 5, 'Piling' (BSI, 2007g), may be useful, as many steel–concrete composite bridges use piled foundations (see Chapter 12). Part 6 (BSI, 2007h) on crane supporting structures is not generally used for bridges, but could be applicable for some special structures.

Composite steel and concrete structures – Eurocode 4

Eurocode 4, 'Design of composite steel and concrete structures', has three parts and is the main document for composite structures. Part 1-1, 'General rules and rules for buildings' (BSI, 2004b), contains the basic rules. Section 5.5 outlines modifications to the class of the steel element where it is composite (usually making it more compact and less susceptible to buckling). Again, as with both the steel and the concrete codes, section 6 outlines the methods for determining R_d for axial, shear and bending resistance of composite beams and columns at the ultimate limit state. Section 7 outlines serviceability issues, such as cracking deflection, vibration, etc. Section 8 outlines some additional requirements for joints in composite structures supplementary to those in Eurocode 3: Part 1-8 (BSI, 2005i). Section 9 outlines the behaviour of composite slabs. This part contains three annexes: annex A outlines modifications to joint stiffness for composite structures; annex B, on the testing of connectors and composite action, is useful; and annex C, on shrinkage, should be used with caution for composite bridges (see Chapter 2). Part 1-2 (BSI, 2005l) outlines fire design for composite structures (see Chapter 12).

Part 2, 'General rules and rules for bridges' (BSI, 2005m), gives modifications to Part 1-1 relevant to composite bridges, but many of the requirements of Part 1-1 remain valid. More details on the design of filler beams (a type of beam not common in buildings) is outlined throughout this part (see Chapter 12). Composite plates in bridge decks are also introduced in section 9 (see Chapter 7). There is no annex A or B (strangely); however, there is an annex C, which outlines where splitting forces from shear connectors can occur.

Table 0.2 outlines the various parts to Eurocodes 2, 3 and 4, and indicates the relevance of each part (high, medium, low) to steel–concrete bridges. Eurocode 4 and its various parts will generally give enough information for the designer to determine the value of the resistance R_d in Equations 0.1 and 0.3.

Table 0.2 Eurocodes 2, 3 and 4, title, parts and relevance to steel–concrete composite bridges

BS EN No.	Eurocode	Volume title	Part No.	Part title	Relevance
1992-1-1	2	Design of concrete structures	1-1	General rules and rules for buildings	M
1992-1-2			1-2	General rules. Structural fire design	L
1992-2			2	Concrete bridges. Design and detailing rules	H
1992-3			3	Liquid retaining and containment structures	L
1993-1-1	3	Design of steel structures	1-1	General rules and rules for buildings	M
1993-1-2			1-2	General rules. Structural fire design	L
1993-1-3			1-3	General rules. Supplementary rules for cold-formed members and sheeting	L
1993-1-4			1-4	General rules. Supplementary rules for stainless steels	M
1993-1-5			1-5	Plated structural elements	H
1993-1-6			1-6	Strength and stability of shell structures	L
1993-1-7			1-7	Plated structures subject to out of plane loading	L
1993-1-8			1-8	Design of joints	H
1993-1-9			1-9	Fatigue	M
1993-1-10			1-10	Material toughness and through-thickness properties	M
1993-1-11			1-11	Design of structures with tension components	M
1993-1-12			1-12	Additional rules for the extension of EN 1993 up to steel grades S700	H
1993-2			2	Steel bridges	H
1993-3-1			3-1	Towers, masts and chimneys. Towers and masts	M
1993-3-2			3-2	Towers, masts and chimneys. Chimneys	L
1993-4-1			4-1	Silos	L
1993-4-2			4-2	Tanks	L
1993-4-3			4-3	Pipelines	L
1993-5			5	Piling	M
1993-6			6	Crane supporting structures	L
1994-1-1	4	Design of composite steel and concrete structures	1-1	General rules and rules for buildings	H
1994-1-2			1-2	General rules. Structural fire design	L
1994-2			2	General rules and rules for bridges	H

H, high; M, medium; L, low

Eurocodes 5 to 9

These Eurocodes are not the primary documents for designing steel–concrete composite structures, but they contain useful items of information and, for completeness of this review of the Eurocodes, they are considered briefly here. Eurocode 5, 'Design of timber structures', is not considered in this book. However, with the growing interest in sustainable structures, a knowledge of Part 2 on timber bridges (BSI, 2005n) is useful. It is possible to use the composite action between steel and timber for laminated timber decks (Bahkt and Krisciunas, 1997), and the principles outlined in this book on composite action can be transferred to this related composite material. Eurocode 6, 'Design of masonry structures' (BSI, 2006i), is also not considered, but structures that rely on composite action between metal and masonry do exist, and may be encountered if an assessment of their strength is required.

Table 0.3 Eurocodes 5 to 9, title, parts and relevance to steel–concrete composite bridges

BS EN No.	Eurocode	Volume title	Part No.	Part title	Relevance
1995-1-1	5	Design of timber structures	1-1	General. Common rules and rules for buildings	L
1995-1-2			1-2	General. Structural fire design	L
1995-2			2	Bridges	L
1996-1-1	6	Design of masonry structures	1-1	General. Rules for reinforced and unreinforced masonry structures	L
1996-1-2			1-2	General rules. Structural fire design	L
1996-2			2	Design considerations, selection of materials and execution of masonry	L
1996-3			3	Simplified calculation methods for unreinforced masonry structures	L
1997-1	7	Geotechnical design	1	General rules	M
1997-2			2	Ground investigation and testing	L
1998-1	8	Design of structures for earthquake resistance	1	General rules, seismic actions and rules for buildings	L
1998-2			2	Bridges	M
1998-3			3	Assessment and retrofitting of buildings	L
1998-4			4	Silos, tanks and pipelines	L
1998-5			5	Foundations, retaining structures and geotechnical aspects	M
1998-6			6	Towers, masts and chimneys	L
1999-1-1	9	Design of aluminium structures	1-1	General rules. General rules and rules for buildings	L
1999-1-2			1-2	General rules. Structural fire design	L
1999-1-3			1-3	Structures susceptible to fatigue	L
1999-1-4			1-4	Cold-formed structural sheeting	L
1999-1-5			1-5	Shell structures	L

H, high; M, medium; L, low.

Eurocode 7, 'Geotechnical design', has two parts. Part 1, 'General rules' (BSI, 2004c), outlines the basis of geotechnical limit state design and the derivation of safe foundation structures. Section 9 deals with earth-retaining structures, and the methods in this section and annex C are applicable to integral steel–concrete composite bridges (see Chapter 3).

Eurocode 8: Part 1, 'Design of structures for earthquake resistance. General rules, seismic actions and rules for buildings' (BSI, 2004d), contains some useful information, particularly for those designing composite bridges outside the UK (where the consideration of seismic effects is not normally required). Section 2 outlines some fundamental requirements, including when seismic design is required. Section 7 outlines specific rules for composite steel–concrete buildings. Part 2, 'Bridges' (BSI, 2005o), gives more specific rules for bridges in earthquakes; however, like other additional parts applicable to bridges, it tends to be supplementary to the main rules outlined in the first part.

Eurocode 9 covers the design of aluminium structures. Aluminium is not commonly used for major structural elements in bridges, although it is often used on parapets. There are five parts to this Eurocode but they are not considered relevant to this book.

Table 0.3 outlines the various parts to Eurocodes 5 to 9, and indicates the relevance of each part (high, medium, low) to steel–concrete bridges.

REFERENCES

Bakht B and Krisciunas R (1997) Testing a prototype steel–wood composite bridge. *Structural Engineering International* **7(1)**: 35–41.

BSI (2002a) BS EN 1990:2002. Eurocode. Basis of structural design. BSI, London.

BSI (2002b) NA to BS EN 1990:2002 + A1:2005. UK National Annex to Eurocode. Basis of structural design. BSI, London.

BSI (2002c) BS EN 1991-1-1:2002. Eurocode 1. Actions on structures. General actions. Densities, self weight, imposed loads for buildings. BSI, London.

BSI (2002d) BS EN 1991-1-2:2002. Eurocode 1. Actions on structures. General actions. Actions on structures exposed to fire. BSI, London.

BSI (2003a) BS EN 1991-1-3:2005. Eurocode 1. Actions on structures. General actions. Snow loads. BSI, London.

BSI (2003b) BS EN 1991-1-5:2003. Eurocode 1. Actions on structures. General actions. Thermal actions. BSI, London.

BSI (2003c) BS EN 1991-2:2003. Eurocode 1. Actions on structures. Traffic loads on bridges. BSI, London.

BSI (2004a) BS EN 1992-1-1:2004. Eurocode 2. Design of concrete structures. General rules and rules for buildings. BSI, London.

BSI (2004b) BS EN 1994-1-1:2004. Eurocode 4. Design of composite steel and concrete structures. General rules and rules for buildings. BSI, London.

BSI (2004c) BS EN 1997-1:2004. Eurocode 7. Geotechnical design. General rules. BSI, London.

BSI (2004d) BS EN 1998-1:2004. Eurocode 8. Design of structures for earthquake resistance. General rules, seismic actions and rules for buildings. BSI, London.

BSI (2005a) BS EN 1991-1-4:2005. Eurocode 1. Actions on structures. General actions. Wind actions. BSI, London.

BSI (2005b) BS EN 1991-1-6:2005. Eurocode 1. Actions on structures. General actions. Actions during execution. BSI, London.

BSI (2005c) BS EN 1991-3:2005. Eurocode 1. Actions on structures. Actions induced by cranes and machinery. BSI, London.
BSI (2005d) BS EN 1991-4:2005. Eurocode 1. Actions on structures. Silos and tanks. BSI, London.
BSI (2005e) BS EN 1992-2:2005. Eurocode 2. Design of concrete structures. Concrete bridges. Design and detailing rules. BSI, London.
BSI (2005f) BS EN 1993-1-1:2005. Eurocode 3. Design of steel structures. General rules and rules for buildings. BSI, London.
BSI (2005g) BS EN 1993-1-2:2005. Eurocode 3. Design of steel structures. General rules. Structural fire design. BSI, London.
BSI (2005h) BS EN 1993-1-3:2005. Eurocode 3. Design of steel structures. General rules. Supplementary rules for cold-formed members and sheeting. BSI, London.
BSI (2005i) BS EN 1993-1-8:2005. Eurocode 3. Design of steel structures. Design of joints. BSI, London.
BSI (2005j) BS EN 1993-1-9:2005. Eurocode 3. Design of steel structures. Fatigue. BSI, London.
BSI (2005k) BS EN 1993-1-10:2005. Eurocode 3. Design of steel structures. Material toughness and through-thickness properties. BSI, London.
BSI (2005l) BS EN 1994-1-2:2005. Eurocode 4. Design of composite steel and concrete structures. General rules. Structural fire design. BSI, London.
BSI (2005m) BS EN 1994-2:2005. Eurocode 4. Design of composite steel and concrete structures. General rules and rules for bridges. BSI, London.
BSI (2005n) BS EN 1995-2:2005. Eurocode 5. Design of timber structures. Bridges. BSI, London.
BSI (2005o) BS EN 1998-2:2005. Eurocode 8. Design of structures for earthquake resistance. Bridges. BSI, London.
BSI (2006a) BS EN 1991-1-7:2006. Eurocode 1. Actions on structures. General actions. Accidental actions. BSI, London.
BSI (2006b) BS EN 1992-3:2006. Eurocode 2. Design of concrete structures. Liquid retaining and containment structures. BSI, London.
BSI (2006c) BS EN 1993-1-4:2006. Eurocode 3. Design of steel structures. General rules. Supplementary rules for stainless steels. BSI, London.
BSI (2006d) BS EN 1993-1-5:2006. Eurocode 3. Design of steel structures. Plated structural elements. BSI, London.
BSI (2006e) BS EN 1993-1-11:2006. Eurocode 3. Design of steel structures. Design of structures with tension components. BSI, London.
BSI (2006f) BS EN 1993-2:2006. Eurocode 3. Design of steel structures. Steel bridges. BSI, London.
BSI (2006g) BS EN 1993-3-1:2006. Eurocode 3. Design of steel structures. Towers, masts and chimneys. Towers and masts. BSI, London.
BSI (2006h) BS EN 1993-3-2:2006. Eurocode 3. Design of steel structures. Towers, masts and chimneys. Chimneys. BSI, London.
BSI (2006i) BS EN 1996-2:2006. Eurocode 6. Design of masonry structures. Design considerations, selection of materials and execution of masonry. BSI, London.
BSI (2007a) BS EN 1993-1-6:2007. Eurocode 3. Design of steel structures. Strength and stability of shell structures. BSI, London.
BSI (2007b) BS EN 1993-1-7:2007. Eurocode 3. Design of steel structures. Plated structures subject to out of plane loading. BSI, London.
BSI (2007c) BS EN 1993-1-12:2007. Eurocode 3. Design of steel structures. Additional rules for the extension of EN 1993 up to steel grades S700. BSI, London.
BSI (2007d) BS EN 1993-4-1:2007. Eurocode 3. Design of steel structures. Silos. BSI, London.
BSI (2007e) BS EN 1993-4-2:2007. Eurocode 3. Design of steel structures. Tanks. BSI, London.

BSI (2007f) BS EN 1993-4-3:2007. Eurocode 3. Design of steel structures. Pipelines. BSI, London.
BSI (2007g) BS EN 1993-5:2007. Eurocode 3. Design of steel structures. Piling. BSI, London.
BSI (2007h) BS EN 1993-6:2007. Eurocode 3. Design of steel structures. Crane supporting structures. BSI, London.
BSI (2008a) NA to BS EN 1991-1-4:2008. UK National Annex to Eurocode 1. Actions on structures. General actions. Wind actions. BSI, London.
BSI (2008b) NA to BS EN 1991-1-7:2008. National Annex to Eurocode 1. Actions on structures. General actions. Accidental Actions. BSI, London.
BSI (2009) NA to BS EN 1993-1-10:2009. National Annex (informative) to Eurocode 3. Design of steel structures. Material toughness and through-thickness properties. BSI, London.
Burr WH (1912) Composite columns of concrete and steel. *Minutes of the Proceedings of the ICE* **188**: 114–126.
Collings D (2005) Lessons from historical failures. *Proceedings of the ICE – Civil Engineeering* **161(6)**: 20–27.
Johnson RP (2009) Eurocodes 1970–2010: why 40 years? *Proceedings of the ICE – Structures and Buildings* **6(1)**: 371–379.
Vaughn A (1991) *Isambard Kingdom Brunel*, *Engineering Knight-Errant*. John Murray, London.

Preface to the second edition

> The bridge crossing it, with its numberless short spans and lack of bigness, beauty and romance he gazed upon in instant distain. It appeared to creep, cringing and apologetic, across the wide waters which felt the humiliation of its presence … Yet he received a shock of elation as the train had moved slowly along the bridge, carrying him with it, and he gazed downward upon flowing waters, again he marvelled at what men could do; at the power of men to build; to build a bridge so strong …
>
> (Sullivan, 1958)

I saw the first edition of this book (Collings, 2005) as a journey. A journey of experience from the first simple river crossing to the more complex suspended spans of today. A journey across the world from the bleak post-industrial landscapes that are still scattered across Britain, around the broad untamed rivers of Bengal, and into the racing development of South East Asia. But it was also a subjective journey, over and under the numberless spans of motorway bridges that are the 'bread and butter' of many bridge designers, through to the countless bridges today that perform their task with pride, and always marvelling at how we build so strong, always questioning. For me, the journey continues; this second edition was written while I was outside Europe in South East Asia, still learning, building, marvelling.

The first edition of this book had its origins in the composite bridge chapter of the *Manual of Bridge Engineering* (Ryall *et al*., 2000), for which I wrote the chapter on composite bridges, and which has also seen a second edition (Parke and Hewson, 2008). The first edition of this book expanded that chapter and provided details of more steel–concrete composite bridges. It was intended to show how composite bridges may be designed simply from basic concepts, without the need for clause-by-clause checking of codes and standards. I am glad it was successful. Since these books on bridges, I have also written one on composite steel–concrete buildings, using Eurocodes (Collings, 2010). This second edition of the bridges book draws on that knowledge, but keeps the format of the first book and adds detail of the relevant Eurocodes and uses them throughout the book. All chapters of this edition use examples of various bridges to illustrate design using the methods outlined in the Eurocodes. The construction methods used to build the bridges are outlined in a little more detail. I am glad my readers want to build and not just to design.

The book looks impartially at this important construction form and compares composite bridges with other types, particularly concrete structures, and often places limits on their use. I have added a short section on environmental issues (carbon dioxide, embodied energy, etc.) – research work (Collings, 2006) I carried out after the first edition shows that steel–concrete composite bridges can have a low carbon footprint if properly designed. This issue is touched upon in other parts of the book – I have a particular dislike for distorting structures for a perceived aesthetic benefit, and the increase in material quantities required seems wasteful, as well as usually making the structure more difficult to build.

The book is intended for a number of readers. First, those who use the *Manual of Bridge Engineering* and wish to find out more detail about steel–concrete composite bridges. Second, it is for those engaged in design who require a deeper understanding of the methods used, as well as how they are

verified against design codes. The book aims to show how to choose the bridge form, and how to design element sizes to enable drawings to be produced. The book covers a wide range of examples, all of which the author has had a personal involvement or interest in. In this second edition, I am also exploring the background to the rules in the Eurocode, giving test data where possible, or some derivation of the key formulae used. In some places, the Eurocode is also compared with other codes so that its results can be put into an international perspective.

REFERENCES

Collings D (2005) *Steel–Concrete Composite Bridges*. Thomas Telford, London.

Collings D (2006) An environmental comparison of bridge forms. *Proceedings of the ICE, Bridge Engineering* **159**: 163–168.

Collings D (2010) *Steel–Concrete Composite Buildings, Designing with Eurocodes*. Thomas Telford, London.

Parke GAR and Hewson N (eds) (2008) *ICE Manual of Bridge Engineering*, 2nd edn. Thomas Telford, London.

Ryall MJ, Parke GAR and Harding JE (eds) (2000) *Manual of Bridge Engineering*. Thomas Telford, London.

Sullivan LH (1958) *The Autobiography of an Idea*. Dover Publications, New York.

Contents

Steel–concrete Composite Bridges
ISBN 978-0-7277-5810-1

http://dx.doi.org/10.1680/scb.58101.011

ice
Institution of Civil Engineers
publishing

Chapter 1
General concepts

... the composite whole being substantially stronger and stiffer than the sum of the parts ...

1.1. Introduction

Composite bridges are structures that combine materials like steel, concrete, timber or masonry in any combination. In common usage today, composite construction is normally taken to mean steel and concrete construction. The term 'composite' is also used to describe modern materials such as glass or carbon-reinforced plastics, which are becoming more common but are beyond the scope of this book. Steel–concrete composite structures are a common and economical form of construction in Europe and the USA; such structures occur in a wide variety of structural types. This book looks first at the concepts of composite action, then reviews the forms of structure in which composite construction is used, and then the more common forms of composite construction are considered in more detail.

Compliance with codes and regulations is necessary in the design of a structure, but in itself it is not sufficient for the design of an efficient, elegant and economic structure. An understanding of the behaviour, what physically happens and how failure occurs is vital for any designer, as without this understanding the mathematical equations are a meaningless set of abstract concepts. It is also vital to understand how structures are constructed and the effect this can have on the stress distribution. One aim of this book is to give the reader this understanding of the behaviour of composite structures. Examples of designs of composite structures are used extensively throughout the book. Where possible, these examples are based on designs or checks carried out by the author.

1.2. Structural forms

Most commonly, steel–concrete composite structures take a simple beam and slab form. However, composite structures are very versatile and can be used for a considerable range of structures – from foundations, substructures (Kerensky and Dallard, 1968; Hill and Johnstone, 1993) and superstructures, through a range of forms (beams, columns, towers and arches) (Dajun, 2001; Chen and Wang, 2009), to a diverse range of bridge structures, including tunnels (Narayanan *et al.*, 1997), viaducts (Dickson, 1987; Mato, 2001), elegant footbridges, and major cable-stayed bridges (Withycome *et al.*, 2002) and integral bridges (Prichard, 1993; England and Tsang, 2001).

Steel–concrete composite bridges generally occupy the middle ground between concrete and steel structures. Economically they become competitive with concrete bridges from spans of about 20 m in basic beam and slab forms. For heavier loads, such as railways, deeper through girders or truss forms are more likely. From 50 m to 500 m steel–concrete composite arches and cable-stayed bridges are competitive. For the longer span bridges, lighter all-steel structures are usually preferred, although extensive use of concrete in back spans as a counterweight to the main span is common, giving a mixed structure rather than a composite structure. Figure 1.1 illustrates the typical span ranges for the more common composite bridge forms.

Figure 1.1 Span ranges for various bridge types

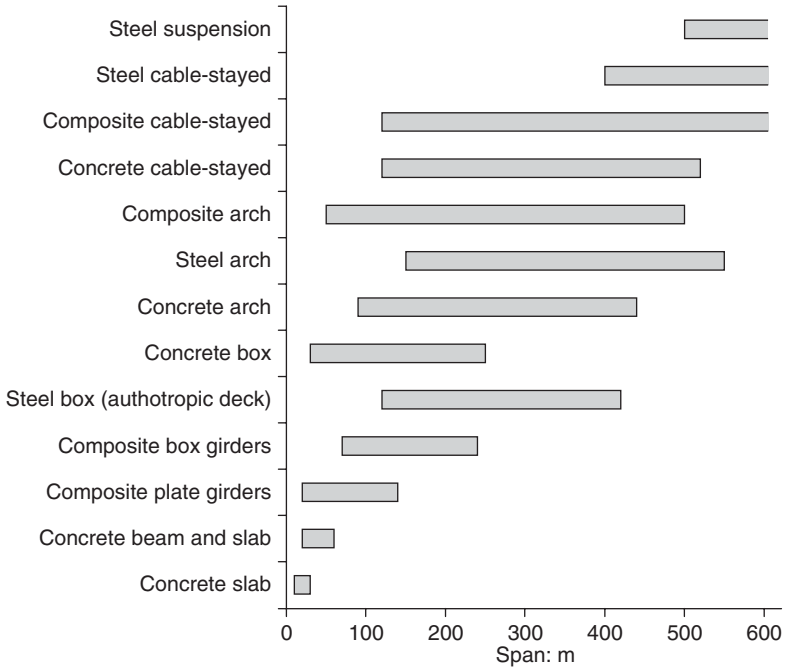

1.3. Materials

The behaviour of the composite structure is heavily influenced by the properties of its component materials. The reader wanting to understand composite bridges should first have a good understanding of the properties of and design methods for the individual materials. In particular, the reader should note the differences between materials, as it is the exploitation of these different properties that makes composite construction economic. Concrete has a density of approximately 25 kN/m^3, a compressive strength of 25–100 N/mm^2 and almost no tensile strength. Steel has a density of 77 kN/m^3, a tensile strength of 250–1880 N/mm^2 and is prone to buckling where thin sections are loaded in compression. The use of a concrete slab on a steel girder uses the strength of concrete in compression and the high tensile strength of steel to overall advantage in forming a composite structure.

1.3.1 Concrete

Concrete is a material formed of cement, aggregate and water. The proportions of the components are varied to get the required strength (generally, the more cement and less water added, the stronger the resulting concrete). Admixtures to improve workability, retard strength gain etc., may also be added. The primary property of concrete of interest to the engineer is its compressive strength. Traditionally, in the UK, codes of practice have required the use of concrete cubes to determine the ultimate compressive strength (f_{cu}). In the USA and Europe, cylinders have been used to determine strength (f_{ck}). Generally, cylinder strengths are 80–85% of cube strengths. Eurocodes use cylinder strength. In the examples given in this book, cylinder strengths are used.

The tensile strength of concrete is normally ignored for design; however, in some circumstances (i.e. when looking at the cracking of concrete) it may be useful to have an estimate of the tensile strength.

The tensile strength of concrete f_{ct} is about 10% of its compressive strength, with a minimum value of 2.9 N/mm^2, or

$$f_{ct} = 0.3(f_{ck})^{1/2} \tag{1.1}$$

However, given the variability of this parameter, a value of double this is used when considering tension stiffening of composite structures (see Chapter 4). The tensile strength should not be relied on in the strength calculations for major structural elements.

A stress–strain curve used for the design of concrete elements is shown in Figure 1.2a. The ultimate failure strain is typically 0.0035, with a limit of elasticity at a strain of 0.00175 for concrete strengths

Figure 1.2 (a) Concrete stress–strain curve. (b) Concrete shrinkage strain curve

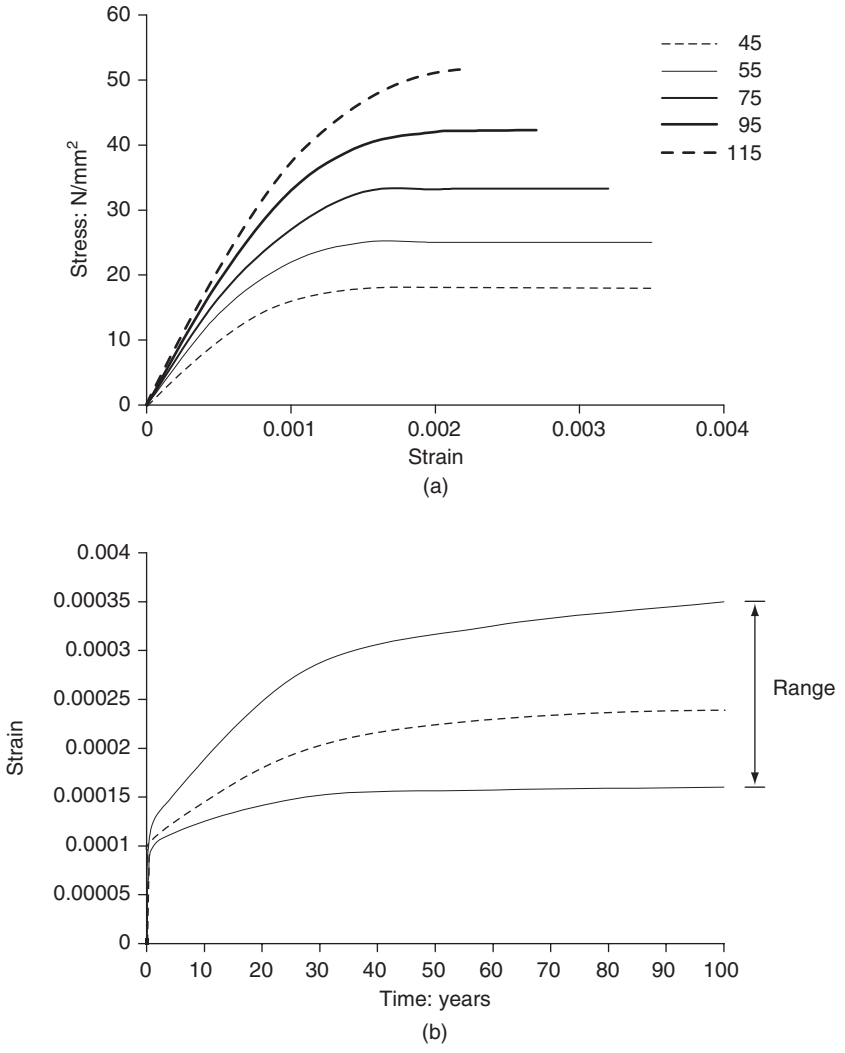

Table 1.1 Concrete modulus (E_c) for various concrete strengths

Strength, f_{ck}: N/mm^2	Short-term static modulus: kN/mm^2	Modulus range: kN/mm^2
30	33	23–40
40	35	25–42
50	37	26–44
70	41	33–49
90	44	35–52

below $f_{ck} = 50$ N/mm^2. For higher strengths the ultimate strain will be smaller. The concrete modulus is required in composite structures to determine the distribution of load between each material. The modulus for concrete (E_c) is summarised in Table 1.1 for various concrete strengths. There will be a variation in concrete modulus, and a range of values should be considered if this variation has a significant effect on the force distribution within the bridge.

When mixed and placed into the structure, the concrete is a fluid and will flow to take up the shape of the supporting formwork. As the concrete hydrates and hardens, the chemical reactions occurring give off a significant heat, which will cause expansion, and any restraint on this expansion (from the steel element) may cause cracking. Reinforcement is required to control this early-age cracking (Highways Agency, 1987; BSI, 2005a). For a typical 200–250 mm thick slab of a composite beam bridge, the minimum reinforcement required is approximately

$$A_s = 0.35(A_c/100) \tag{1.2a}$$

this reinforcement being placed approximately equally in the top and bottom faces. If the slab is constructed using an infill bay system (which is common for continuous structures, see Chapters 4 and 5) the infill bays will be restrained and require additional reinforcement:

$$A_s = 0.9(A_c/100) \tag{1.2b}$$

As the concrete hydrates further over a period of months or years it will shrink slightly. The amount of shrinkage will depend on the concrete thickness, mix parameters and environmental conditions (primarily humidity). Figure 1.2b shows a typical shrinkage strain over time for a 200–250 mm slab in the UK. Shrinkage can be important for some types of composite structure, as it can tend to create additional stress at the steel–concrete interface. Design procedures to allow for these stresses are given in the examples in subsequent chapters. It can be seen from Figure 1.2b that the shrinkage is of the order of 0.5 mm/m, which is slightly larger than the 0.32 mm/m outlined for building structures in Eurocode 4: Part 1.1, 'General rules and rules for buildings' (BSI, 2004). For buildings where the underside is often sealed by the use of steel sheeting and the upper surface with screeds and finishes, this may be appropriate, but for bridges a more realistic value should be considered if shrinkage has an effect on the composite structure (see Chapter 3).

The final property of concrete to be considered is creep. The amount of creep depends on the magnitude and duration of applied stresses, concrete mix parameters and environmental conditions.

The creep affects the concrete modulus; a creep-affected modulus can be calculated from the following equation:

$$E_c' = \frac{1}{1 + \psi\phi} \tag{1.3}$$

The changing of the modulus will influence the distribution of load between materials. Typical creep coefficients (ϕ) and creep multipliers are 1.0 for precast decks to 1.5 for in situ concrete. Generally, assuming $E_c = 0.4E_c$ to $0.5E_c$ will give a reasonable estimate for most circumstances.

For a concrete element, such as a deck slab acting as part of a composite structure, there are two key design criteria: axial compressive capacity and bending resistance. For a concrete element subject to a compressive load, the ultimate stress in the concrete is limited to 85% of the cylinder strength. The ultimate axial design compressive resistance (N_{cd}) of the concrete section is simply the ultimate stress multiplied by the area:

$$N_{cd} = 0.85 f_{ck} A_c / \gamma_{cm} \tag{1.4a}$$

$$N_{cd} = 0.57 f_{ck} bd \tag{1.4b}$$

For concrete elements subject to a bending compression moment (C), the ultimate moment of resistance (M_u) can be derived by assuming a concrete failure (M_{cd}) or a failure in tension (T) of the embedded reinforcing steel (M_{sd}) as illustrated Figure 1.3.

For the failure of the concrete

$$M_{cd} = N_c z$$

Assuming the limiting value of N_c occurs when $0.8x = d/2$ and, $z = 0.8d$

$$M_{uc} = 0.2 bd^2 f_{ck} \tag{1.5a}$$

Figure 1.3 Idealised bending stresses in a concrete element

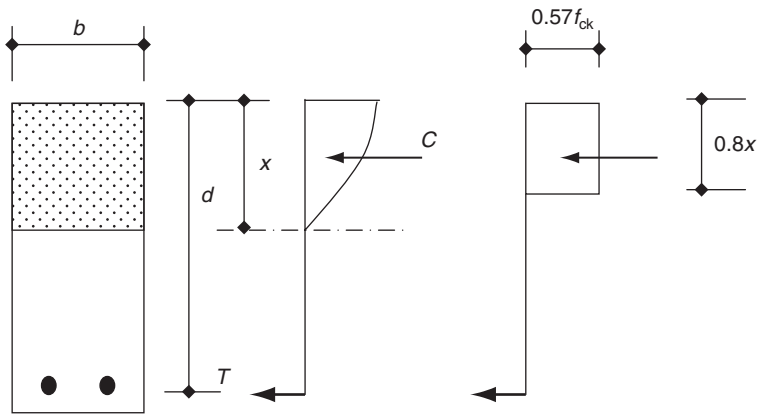

Table 1.2 Strengths for various steel components

Component	Yield stress: N/mm^2 (or ultimate tensile stress where noted*)
Universal beams, channels and angles. Grade S275	275
Universal beams, channels and angles. Grade S355	355
Plates and flats. Grade S355	Varies, see Figure 1.4
Mild steel reinforcing bar (plain)	250
High-yield reinforcing bar (ribbed)	460–500
Prestressing bars	880–1200*
HSFG bolts	880*
Prestressing strand	1770–1880*

For failure of the steel reinforcement

$$\mathrm{M_{sd}} = N_{\mathrm{T}} z,\ N_{\mathrm{T}} = A_{\mathrm{s}} f_{\mathrm{y}}/\gamma_{\mathrm{am}} \text{ and } z = 0.8d$$

$$M_{\mathrm{us}} = 0.7 d A_{\mathrm{s}} f_{\mathrm{y}} \tag{1.5b}$$

To achieve ductility it is normal to ensure that the steel fails before the concrete and that M_{cd} is greater than M_{sd}. Where an axial force occurs with the moment (as in an arching action, see Chapter 5) there will be an increase in the bending capacity. The concrete may also fail in shear, direct tension or by a combination of axial force and moment; these other, less common, design criteria are introduced in subsequent chapters if required by the example being considered.

1.3.2 Steel

The steel used in composite bridges tends to be of two primary forms: structural steel, in the form of rolled sections or fabricated plates; and bar reinforcement within the concrete element. Occasionally, prestressing steel in the form of high tensile strand or bars may be used. The key property for design is, again, the material strength; this is outlined in Table 1.2.

The limiting stress in tension or compression is similar for small or compact sections, but may be less for thicker fabricated sections (Figure 1.4a). A stress–strain curve used for the design of steel elements is shown in Figure 1.4b.

For composite structures, the steel elastic modulus is required to determine the distribution of load between each material. The modulus for steel (E_{a}) is generally constant for all steel grades, and can be taken as 210 kN/mm^2 for plates; however, there may be some slight variation with temperature. For bar reinforcement the modulus is slightly lower at 200 kN/mm^2.

Structural steel fabrications are prone to buckling. The buckling of steelwork elements when compressed may occur in a number of ways. Local buckling of the flange or stiffener outstand is suppressed by the use of outstand ratios. The value of the limiting flange outstand ratio or web depth will depend on the class of the structure. Eurocode 3: Part 1-1, 'General rules and rules for buildings' (BSI, 2005b), defines four classes. Class 1 and 2 are ductile and will achieve full plasticity. Class 3 will achieve yield but may not achieve full plasticity. A class 4 structure may buckle prior to achieving

Figure 1.4 (a) Yield strength for grade S355 steel plate of various thickness. (b) Steel stress–strain curve for various elements

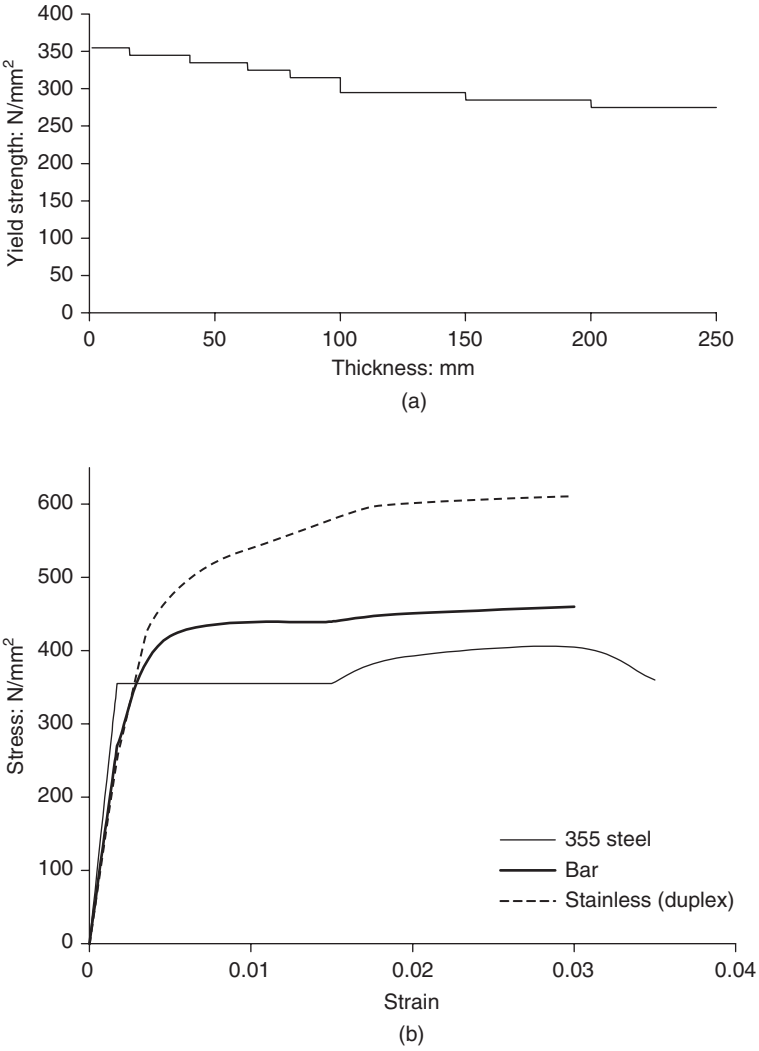

yielding. Table 1.3 summarises the key requirements for outstand ratios to prevent local buckling. Where flanges or webs are larger than these limits, stiffeners can be applied to suppress the buckling tendency. For composite flanges, connectors may suppress local buckling, provided minimum spacing requirements are met. Eurocode 4: Part 1-1 (BSI, 2004) outlines modifications to the basic ratios for steel structures when they are acting compositely (see Table 1.3).

The entire steel section may be prone to buckling under compressive loads, and is normally braced to limit this buckling tendency. For columns and members loaded primarily in compression, the classic Euler buckling is assumed and bracing is provided to limit the effective length of the member. For beams, the buckling may be a lateral–torsional form (Wang and Nethercot, 1989; Jeffers, 1990), where the instability of the compression flange leads to lateral movement of the whole section. The

Table 1.3 Geometric limits to prevent local buckling of steel plates (BSI, 2004, 2005b)

Element	Limit
Class 2 steel flange in compression	$8t_f$
Class 2 steel flange composite with concrete in compression	$18t_f$
Class 3 steel flange in compression	$11t_f$
Steel flange in tension	$16t_f$
Class 2 steel web in bending	$67t_w$
Class 3 steel web in bending	$100t_w$
Class 3 steel web in bending/tension	$220t_w$
Class 2 steel web in compression	$30t_w$
Class 3 steel web in compression	$34t_w$
Plate stiffener	$9t_s$
Class 2 steel circular section	$D_o = 46t_o$
Class 3 steel circular section	$D_o = 60t_o$
Class 2 connector spacing	$18t_f$ longitudinal, $7t_f$ edge distance
Class 3 connector spacing	Six times slab thickness or 600 mm
Composite circular section (without connectors)	$D_o = 73t_o$

tendency to buckle can be estimated from the slenderness parameter λ, which is a function of the ratio of the applied force (or moment) to the critical buckling force, this force being dependent on the effective length (L_{eff}) and section properties, primarily the radius of gyration (i):

$$\lambda = (N_E/N_{cr})^{1/2} \tag{1.6a}$$

$$\lambda = L_{eff}/ik_1 \tag{1.6b}$$

where N_E is the design load effect, N_{cr} is the critical buckling load and $k_1 = \pi(E/f_y)^{1/2}$. Figure 1.5 shows the typical reductions in stresses required to limit the tendency to buckle.

Typical effective lengths for elements of composite bridge design are outlined in Table 1.4; these are generally based on annex D of Eurocode 3: Part 2 (BSI, 2006a). The buckling of the steel section in many composite structures is most likely to occur during construction, when the concrete loads the steelwork but the concrete has not hardened and so provides no restraint.

For many steel–concrete composite structures the steel forms a major element of the structure, and the design issues most commonly encountered are bending, shear and axial loads. For a steel element subject to a tensile load, the maximum stress in the steel is limited to the yield strength. Where wires strands, bars or other elements that cannot carry compression are used, special rules are given in Eurocode 3: Part 1-11, 'Design of structures with tension components' (BSI, 2006b):

$$N_{TD} = f_y A_{ae}/\gamma_{am} \tag{1.7a}$$

$$N_{TD} = f_y A_{ae} \tag{1.7b}$$

where A_{ae} is the effective area of the steel allowing for any bolt holes.

Figure 1.5 Limiting compressive stress for buckling

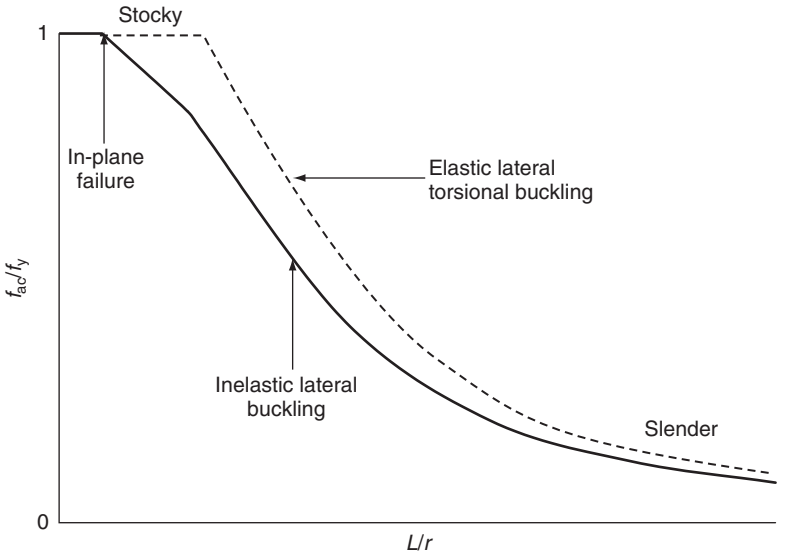

For a compressive load the maximum stress will also be limited to yield or a proportion of yield, where χ will be determined from the slenderness parameter and limiting compressive stress curves like those shown in Figure 1.5:

$$N_{CD} = \chi f_y A_{ae} / \gamma_{am} \tag{1.7c}$$

$$N_{CD} = 0.9 \chi f_y A_{ae} \tag{1.7d}$$

Table 1.4 Typical effective lengths for composite structures

Element	Effective length	
Steel girders, prior to casting slab	$1.0L_B$	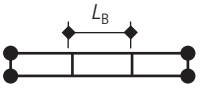
Compression chord of truss	$0.85L_c$	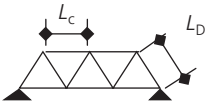
Truss diagonal	$0.7L_D$	
Column fixed to foundation but free at top	$2.0L_c$	
Column fixed to foundation but pinned at top	$1.5L_c$	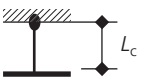
Column fixed to foundation and integral with deck	$1.0L_c$	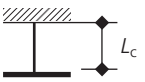

For a class 1 or 2 steel beam subject to bending, the moment of resistance (M_D) is given by

$$M_D = f_y W_p / \gamma_{am} \tag{1.8a}$$

$$M_D = f_y W_p \tag{1.8b}$$

where W_p is the section plastic modulus. For a class 3 steel beam subject to bending, the moment of resistance (M_D) is given by

$$M_D = f_y W_e / \gamma_{am} \tag{1.8c}$$

$$M_D = f_y W_e \tag{1.8d}$$

where W_e is the section elastic modulus. For a class 4 steel beam subject to bending, the moment of resistance (M_u) is given by

$$M_D = \chi f_y W_e / \gamma_{am} \tag{1.8e}$$

$$M_D = 0.9 \chi f_y W_e \tag{1.8f}$$

Section moduli for standard rolled sections are pre-calculated (SCI and BCSA, 2007), and for fabricated sections the properties will need to be calculated by the designer. Appendices B and D outline the calculation of elastic section properties.

For a steel beam the ultimate design shear resistance of the section is

$$V_D = V_{web} + V_{flange} \leq 1.2 f_y \, h_w t_w / \sqrt{3} \gamma_m \tag{1.9a}$$

$$V_{web} = \chi_w f_y h_w t_w / \sqrt{3} \gamma_m \tag{1.10}$$

$$V_{flange} = b_f t_f^2 f_y / c \gamma_m \tag{1.11}$$

where χ_w is a web buckling coefficient from Figure 1.6. This coefficient is dependent on the web slenderness parameter λ_w and the shear buckling coefficient k_v:

$$\lambda'_w = \frac{h}{31 t_w} \sqrt{k_v} \tag{1.12}$$

$$k_v = 5.34 + 4(h_w/a)^2 \tag{1.13}$$

$$c = a(0.25 + 1.6 b t_f^2 / t_w h_w^2) \tag{1.14}$$

where h is the web height and a is the distance between transverse stiffeners. Where the beam is shallow and has large flanges, it may be worth considering the flange contribution to shear; however, if the flanges are used for bending or are relatively small, it is common practice to neglect this part of the equation.

For unstiffened webs with a slenderness ratio (h_w/t) less than 70, or webs with transverse stiffeners at $10h_w$ or less with a slenderness less than 50, the full shear capacity can be assumed:

$$V_D = 0.58 f_y h_w t_w \tag{1.9b}$$

Figure 1.6 Web slenderness curve and typical limiting shear capacity curves for steel beams with panel geometry

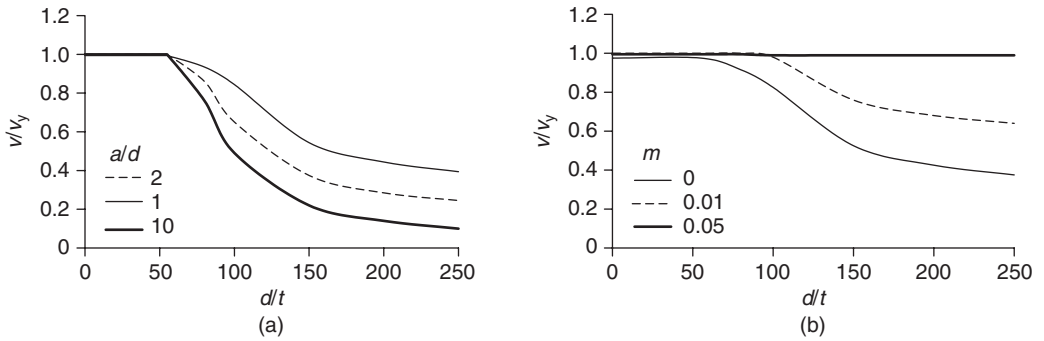

For higher web slenderness values there may be a reduction in capacity due to web buckling effects. Figure 1.6 shows a typical web shear capacity curve. The limiting values depend on the slenderness (h_w/t), the web panel ratio (a/h_w) and flange stiffness (m):

$$V_D = 0.58 f_y \chi_w h_w t_w \tag{1.9c}$$

Most steel sections used in composite bridge structures are fabricated sections. The fabrication of a girder or steelwork element involves the assembly of the pieces of steel that will form it in a factory or workshop. The process starts with taking the design and breaking it down into its component elements. For example, the simple girder shown in Figure 1.7 is made up of 12 elements; a top and bottom flange, a web, two end plates, four bearing stiffener plates, two intermediate stiffeners and the shear connectors. A drawing of each element will be produced to enable the cutting area of the fabrication shop to produce each part. In many factories the process has been automated and the dimensions of the part are transferred to a cutting machine without the need for a paper copy of the drawing.

Once cut, the plates are assembled. The main girder is likely to be put together in one of two ways – either by using a T&I machine, or by using the side-to-side method. The T&I machine takes a web and flange and welds them together to form an inverted T-section; this is turned, and the other flange added and welded. In the side-to-side method, all three elements are clamped together, with the girder on its side, and the welds on that side are laid; the beam is turned to the other side, and the welds there laid. In practice, the process is more complex, as plates come in 6–18 m lengths and so each flange or web will be formed from a number of plates. The structure is also likely to be larger than can be assembled in the factory or transported easily, and so it is broken down into a number of subparts. Figure 1.8 outlines the plates, diaphragms and stiffeners needed for a double composite box girder (see Chapters 6 and 7).

The total cost of the steelwork in a composite bridge will be influenced by fabrication costs. In Europe, fabrication costs will be relatively high (see Figure 1.7) and the design should aim to simplify stiffening details such that as much of the fabrication as possible can be carried out using automated processes. In Asia, where labour is relatively less costly, material costs will be more significant, and the designer should aim to reduce the amount of steel used (Figure 1.9).

Today, plates are joined primarily by welding. This involves the laying of molten metal along joints; when cooled this metal has fused with the plates on each side to form a joint. There are a number

Figure 1.7 Typical elements making up a simple steel girder; (pie chart) fabrication costs

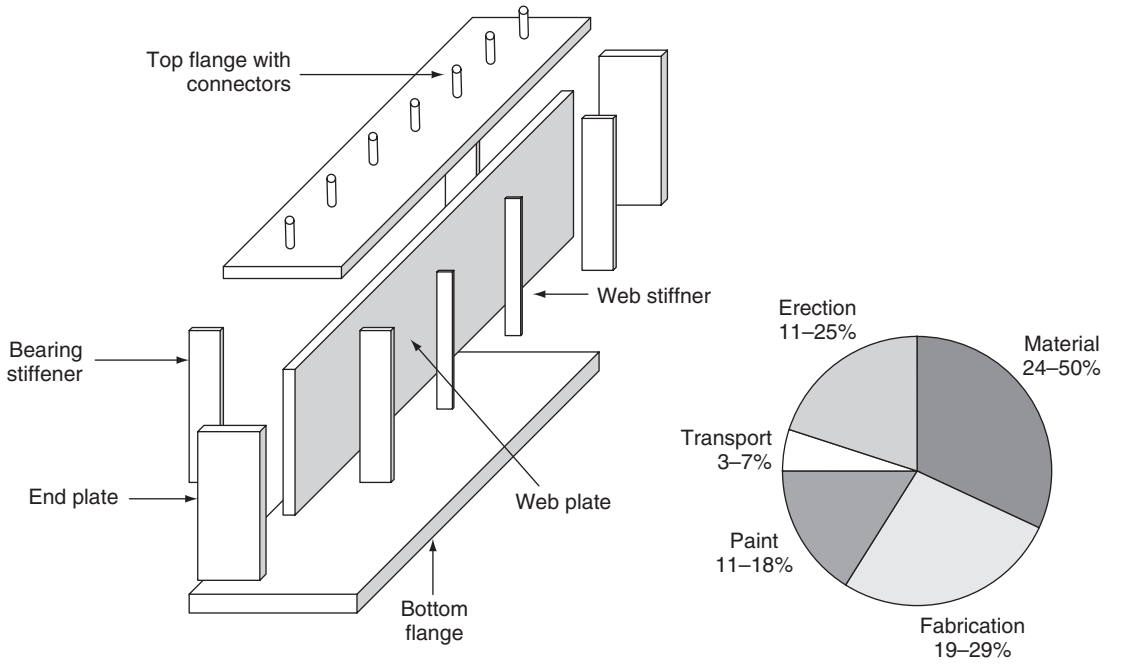

of processes in which the weld can be formed: submerged arc welding (SAW), metal active gas (MAG) and metal arc welding (MAW). The MAW and SAW processes are used for the more automated ways of welding, and MAG is the most widely used manual welding method. For the bridge designer, two weld types are usual – a butt weld and a fillet weld. The welds are formulated such that they have similar properties to the parent metal being joined, so that the limiting yield and shear stresses are unaffected. The welding and fabrication process is complex, and significant testing and quality control regimens should be in place (BSI, 1999). On drawings and sketches produced by the designer, welding is normally indicated using shorthand symbols.

Fatigue is a phenomenon primarily affecting the steel elements of a composite structure. Eurocode 3: Part 1-9, 'Bridges' (BSI, 2005c), deals with this issue in detail, and for composite structures the additional information on shear connectors in Eurocode 4: Part 2, 'General rules and rules for bridges' (BSI, 2005d), will also be useful. Fatigue is primarily influenced by the stress fluctuations in an element (the maximum range of stress, as opposed to the maximum stress), the structure geometry and the number of load cycles. The stress range prior to significant damage varies with the number of load cycles. At high stress ranges the number of cycles to damage is low; there is a stress range below which an indefinitely large number of cycles can be sustained. For design, it is critically important to obtain a detail with the maximum fatigue resistance, and this is achieved by avoiding sudden changes in stiffness or section thickness, partial penetration welds, intermittent welding or localised attachments. Composite highway structures, if properly detailed, are not particularly sensitive to fatigue problems. The design of shear connectors near midspan may be governed by fatigue where static strengths dictate only minimum requirements. Railway bridges, with their higher ratio of live to permanent loads, are more sensitive to fatigue.

Figure 1.8 Plates, diaphragms and stiffeners fabrication model for a double composite box; note that each part has a unique reference

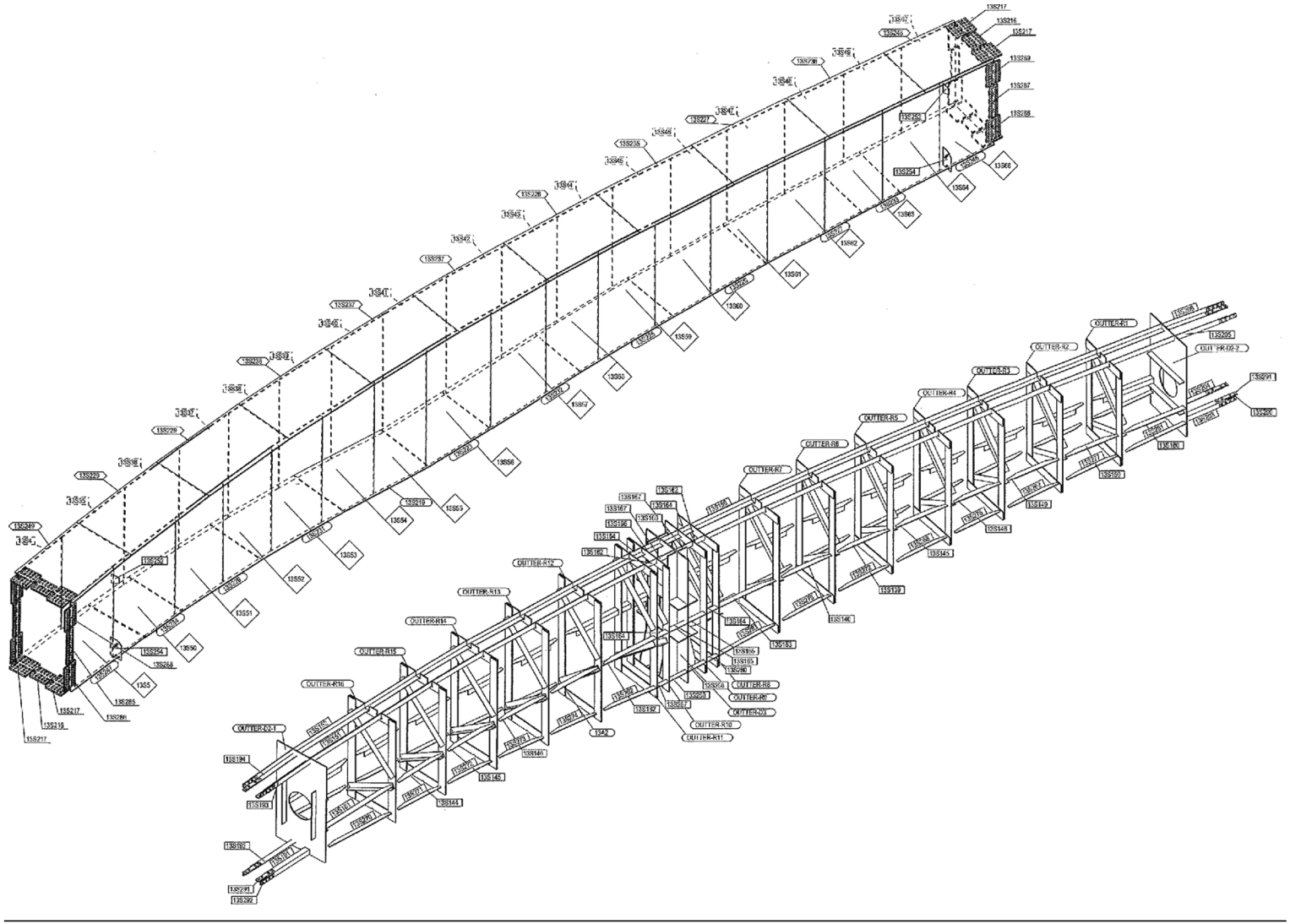

Figure 1.9 A fabrication factory in China working on a major truss structure (see Chapter 8)

At low temperatures steel can become brittle. Thicker sections containing more impurities or laminations are more likely to have significant residual stresses during fabrication, and are the most likely to be affected. Charpy impact testing values are used to measure this; for bridge works in the UK a minimum Charpy value of 27 J is required. Eurocode 3: Part 1.10, 'Material toughness and through-thickness properties' (BSI, 2005e), outlines the requirements in more detail. For temperatures below about -20°C or sections above 65 mm thickness subjected to a tensile stress a grade of steel with higher Charpy values may be required. Figure 1.4 gives the maximum stresses at the serviceability limit state for S355 steel based on Eurocode limits in the UK; the value is 65 mm if the stress is less than $0.75f_y$, 120 mm if the stress is half of yield, and 170 mm if the stresses are less than $0.25f_y$.

1.4. Composite action

There are two primary points to consider when looking at the basic behaviour of a composite structure.

- The differences between the materials.
- The connection of the two materials.

1.4.1 The modular ratio

Differences between the strength and stiffness of the materials acting compositely affect the distribution of load in the structure. Stronger, stiffer materials, such as steel, attract proportionally more load than does concrete. In order to take such differences into account, it is common practice to transform the properties of one material into those of another by the use of the modular ratio.

At working or serviceability loads the structure is likely to be within the elastic limit, and the modular ratio is the ratio of the elastic modulus of the materials. For a steel–concrete composite the modular ratio is

$$n = \frac{E_a}{E_c} \text{ or } \frac{E_a}{E'_c} \tag{1.15a}$$

The value of this ratio varies from 6 to 18 depending on whether the short-term or long-term creep-affected properties of concrete are used. Typical values of the concrete modulus are given in Table 1.1. It should also be noted that the quoted value for E_c is normally the instantaneous value at low strain, and lower values based on the secant modulus may be appropriate at higher strains. At ultimate loads the modular ratio is the ratio of material strengths, and this ratio is dependent on the grade of steel and concrete used. For design, the different material factors will need to be considered to ensure a safe structure. For a steel–concrete composite

$$n = \frac{R_{aD}}{R_{cD}} \tag{1.15b}$$

where R_{aD} and R_{cD} are the ultimate strengths of steel and concrete. These values will depend on the codes of practice being used and the value of the partial factors, but for Eurocodes n is approximately

$$n = 1.5\frac{f_y}{f_{ck}} \tag{1.15c}$$

1.4.2 Interface connection

The connection of the two parts of the composite structure is of vital importance. If there is no connection, the two parts will behave independently. If adequately connected, the two parts act as one whole structure, potentially greatly increasing the structure's efficiency.

Imagine a small bridge consisting of two timber planks placed one on the other, spanning a small stream. If the interface between the two planks is smooth and no connecting devices are provided, the planks will act independently; there will be significant movement at the interface, and each plank will, for all practical purposes, carry its own weight and half of the imposed loads. If the planks are subsequently nailed together such that there can be no movement at the interface between them, the two parts will be acting compositely; the structure will have an increased section for resisting the loads and could carry about twice the load of two non-composite planks. The deflections on the composite structure would also be smaller by a factor of approximately four, the composite whole being substantially stronger and stiffer than the sum of the parts. A large part of the criteria presented in the following chapters is aimed at ensuring that this connection between parts is adequate.

The force transfer at the interface for composite sections is related to the rate of change of force in the element above the connection. The longitudinal shear flow V_l is:

$$V_l = \frac{dy}{dx} N \, dx \tag{1.16a}$$

Considering a simple composite beam at the ultimate limit state, assuming it is carrying its maximum force, as Equation 1.4, the maximum change in force in the slab over a length from the support to midspan is

$$N = 0.57 f_{ck} bt \tag{1.4}$$

and the shear flow at this stage is

$$V_1 = N/0.5L \tag{1.17a}$$

which is often written as

$$V_1 = N/L_v \tag{1.17b}$$

where L_v is the shear length. If the section is capable of significant plastic deformation, the shear flow may be considered to be uniform. A consideration of Equation 1.16 will yield that, for a simple beam, the rate of change in the force in the slab is proportional to the rate of change in moment, or the shear force. For most sections the number of connectors should generally follow the shape of the shear diagram. Typically, codes allow a 10–20% variation from the elastic shear distribution:

$$V_1 = \frac{VA_c y}{I} \tag{1.16b}$$

1.5. Shear connectors

Shear connectors are devices for ensuring force transfer at the steel–concrete interface; they carry the shear and any coexistent tension between the materials. Without connectors slip would occur at low stresses. Connectors are of two basic forms: flexible or rigid. Flexible connectors, such as headed studs (Figure 1.10), behave in a ductile manner, allowing significant movement or slip at the ultimate limit state. These are the most common form of connectors for both buildings and bridges, and the rules of Eurocode 4: Part 1.1, 'General rules and rules for buildings' (BSI, 2005b), and Eurocode 4: Part 2, 'General rules and rules for bridges' (BSI, 2005d) are based on the assumption that headed stud connectors are used. Rigid connectors, such as fabricated steel blocks or bars, behave in a more brittle fashion; failure is either by fracture of the weld connecting the device to the beam, or

Figure 1.10 Typical shear connector types for steel–concrete composite construction: studs, bars with hoops and channels

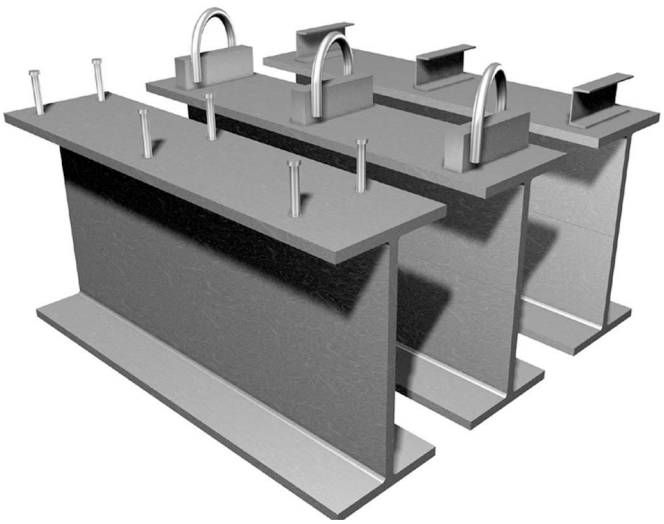

Table 1.5 Nominal static strengths of shear connectors

Type of connector	Connector material	Nominal static strength per connector for concrete grade 32
Headed studs, 100 mm or more in height, and diameter:	Steel $f_y = 385$ N/mm^2 and minimum elongation of 18%	
19 mm		109 kN
22 mm		139 kN
25 mm		168 kN
50 × 40 × 200 mm bar with hoops	Steel $f_y = 250$ N/mm^2	963 kN
Channels:	Steel $f_y = 250$ N/mm^2	
127 × 64 × 14.9 kg × 150 mm		419 kN
102 × 51 × 10.4 kg × 150 mm		364 kN

by local crushing of the concrete. Some types of connector, such as the combined block and bar types (see Figure 1.10), can resist direct tensile forces as well as shear. Channel connectors are an intermediate type, and may be found on older composite bridges. Typical nominal static strengths P_k for various connector types for grade 32 N/mm^2 concrete are given in Table 1.5. Other forms of shear connector are also available, such as perforated plates (Oguejiofor and Hosain, 1992), undulating plates or toothed plates (Schlaich *et al.*, 2001).

$$P_d = P_k/\gamma_m \tag{1.18a}$$

The type and number of connectors used should reflect the type of load. For normal, relatively uniform shear flows, stud connectors are economic; for heavier shear flows, bar or perforated plate connectors may be more applicable than larger studs at close centres. Where shear flows are more concentrated with sudden changes in magnitude, the larger rigid plate connectors are more appropriate. Care must be taken in mixing connector types. Where there is a likelihood of tensile loads occurring with the shear, then hoop connectors or long studs should be used, such that the tensile load can be resisted in the main body of the concrete, and suitable reinforcement should be detailed around the hoop or stud head. Where the shear connectors are used with coexisting tension (T), the shear capacity will be reduced:

$$V_{l\,max} = (V_l^2 + 0.33T^2)^{1/2} \tag{1.19}$$

Where the tension exceeds about 10% of the shear detailing of the tensile resistance, the load path should be considered, with the use of longer connectors or additional tensile link reinforcement in the concrete.

The number of connectors required (n) is determined by dividing the longitudinal shear force by the capacity of a connector, at the ultimate limit state:

$$n = V_l/P_d \tag{1.20}$$

The capacity of the connectors depends on a number of variables, including material strength, stiffness (of the connector, steel girder and concrete) and the width, spacing and height of the connector. For

headed stud connectors with diameter d, ultimate strength f_{vu} and a height of more than $4d$, the design strengths can be estimated from the following equation. For failure in the steel

$$P_d = 0.8 f_{vu}(\pi d^2/4)/\gamma_m \tag{1.21a}$$

and for failure in the concrete

$$P_d = 0.29\alpha d^2 (f_{vu} E_{cm})^{1/2}/\gamma_m \tag{1.21b}$$

which, for design, simplifies to the lesser of Equation 1.17c or 1.17d:

$$P_d = 0.55 f_{uv} d^2 \tag{1.21c}$$

$$P_d = 11 f_{ck} d^2 \tag{1.21d}$$

Similar equations are given below for other types of connector. For the relatively flexible channel connectors, where A_f is the projected area (Bh):

$$P_d = 0.7 A_f f_{ck} \tag{1.22}$$

For the stiffer bar connector:

$$P_d = 2.5 A_f f_{ck} \tag{1.23}$$

For hoop connectors:

$$P_d = 1.1 f_y d^2 \tag{1.24}$$

For the combination of hoop and bar connectors in Table 1.5, the capacity is that of the bar plus 70% of the hoop. The capacity of the bar or channel connector may also be governed by the size of the weld between the connector and girder:

$$P_d = (1.2D + 1.45B) f_y w \tag{1.25}$$

where B is the width and D the depth (along the girder) of the connector, w is the weld size and $f_y w$ is the yield strength of the weld (taken as the lower of the girder or connector strength). Bar connectors should not be used on their own as they have little resistance to uplift; the author has used them successfully on the inside of steel tubes (see Chapter 9), where the constrained nature of the concrete means that tensile separation cannot occur in the same way as in a simple beam. The author has also used channel connectors to carry more concentrated loads; groups of connectors would be the preference with Eurocode designs. A combination of hoop and bar connectors at ends of beams (with high shear, torsion and tensile loads) and stud connectors through the remainder of the span has also been used on many bridges.

1.5.1 Shear interface strength

At the ultimate limit state the failure of shear planes (Figure 1.11) other than at the interface (x–x) may need to be investigated. These shear planes will be around the connector (y–y) or through the slab (z–z).

Figure 1.11 Typical shear planes in a steel–concrete composite structure

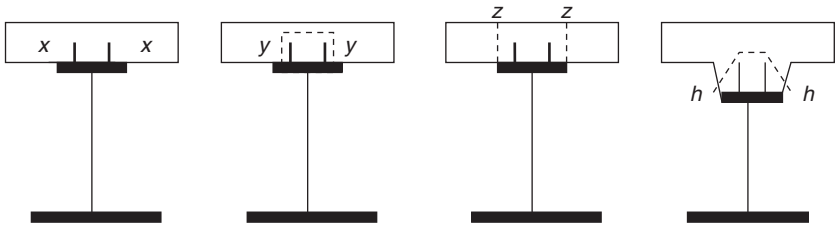

Where haunches are used, a check on shear planes (h–h) through the haunch may be required. Where permanent formwork is used, other planes may also occur.

The shear planes around the connectors rely on the shear strength of concrete v_d, the length of the shear plane L_d, and any reinforcement passing through the shear planes. The maximum force that can be carried by the shear plane is limited by the concrete strength.

$$V_l \leq 0.57 f_{ck} L_d k_v \sin \theta f \cos \theta f \tag{1.26a}$$

where k_v is a shear strength reduction factor, which varies with the concrete strength but which can be taken as 0.5 for most circumstances. θf is the angle of the notional compressive strut, and is usually assumed to be between 27° and 45°. It is noted that the assumptions regarding the steel, concrete and steel–concrete composite parts are not always compatible, the assumptions regarding shear flow being one such example. For concrete structures L_d is reduced, thus effectively increasing the shear flow for concrete parts. To avoid the need to recalculate, a simpler equation is used for design purposes:

$$V_l \leq 0.08 f_{ck} L_d \tag{1.26b}$$

Where this limit governs, a wider or taller connector layout is required to increase the shear plane within the concrete, or stronger concrete must be used. Typically, 0.17% A_c of reinforcement should be provided through the shear plane to ensure a robust structure with a ductile behaviour. The strength of the shear plane reinforcement may be taken as

$$V_l = 1.7 A_s f_y \tag{1.26c}$$

1.5.2 Testing of shear connectors

The strength of the standard connectors outlined in Table 1.5 and Equations 1.17 have been calibrated by tests. Newer forms of perforated plate connectors are also tested as part of the development process (Oguejiofor and Hosain, 1992). In the UK, much of the testing has used the standard small test (BSI, 1978), which comprises a push-out test on a pair of connectors (Figure 1.12a). At least three tests should be carried out and the lowest value used. The standard small test can underestimate connector strengths, particularly for connectors with limited resistance to separation. A modified and larger test is the standard test in Eurocode 4 (Figure 1.12b). The larger standard test will more accurately reflect the structure geometry and connector capacities.

In the standard test, the surface of the steel beam in contact with the concrete is normally greased to ensure that the bond between the steel and concrete does not influence the results. At least three tests

Figure 1.12 Test layout for connectors: (a) small test; (b) standard test

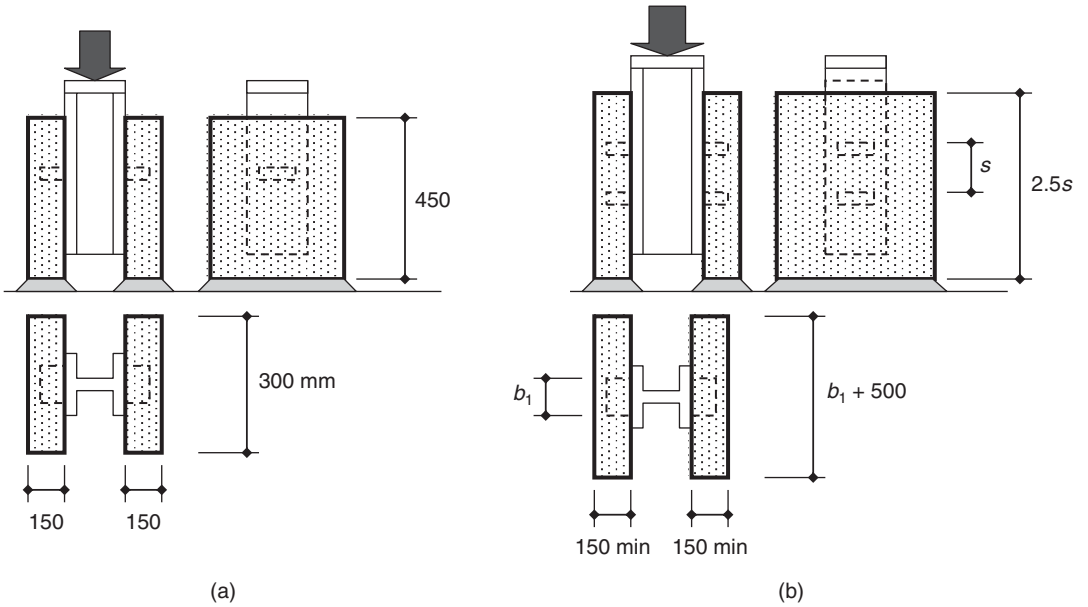

are required, and the test resistance P_T is taken as the mean of the test values. The characteristic strength P_k is taken as 90% of this value. Headed stud connectors are required to be ductile, and to achieve ductility these should have a slip capacity δk of at least 6 mm.

1.6. Example 1.1: Connector test

Push-out tests were carried out using a layout approximating the standard test. The slab was formed using a permanent formwork system, giving a non-continuous contact with the steel. The connectors were standard 19 mm diameter, headed studs in concrete, with a cylinder strength of 21 N mm^2. Using Equations 1.17, the characteristic strength of the connectors is estimated as

$$P_{ka} = 0.8 f_{vu}(\pi d^2/4) = 0.63 \times 500 \times 19^2 = 113{,}700 \text{ N, or } 114 \text{ kN}$$

$$P_{kc} = 0.29 \alpha d^2 (f_{vu} E_{cm})^{1/2} = 14 \times 21 \times 19^2 = 106{,}100 \text{ N, or } 106 \text{ kN}$$

The test results are outlined in Figure 1.13a with other test data for various types of slab and various concrete strengths. The failure loads from the tests are 50, 80, 85 and 120 kN, giving an average of 84 kN and a characteristic capacity of $0.9 \times 84 = 75$ kN, which is significantly lower than the calculated capacity. The load-slip data from the test is plotted in Figure 1.13b together with the idealised requirement (in thick line). Again it is clear that the test results depart from the ideal, and at 6 mm slip the loads have reduced on three of the four specimens.

These tests and others (Johnson and Yuan, 1998; Hicks, 2007) indicate that, where the slabs are not solid, the capacities of the connectors reduce, and Equation 1.14 becomes

$$P_d = k P_k / \gamma_m \tag{1.18b}$$

Figure 1.13 Test results: (a) characteristic capacity with concrete strength for various slab-test data; (b) load–slip plots for connectors

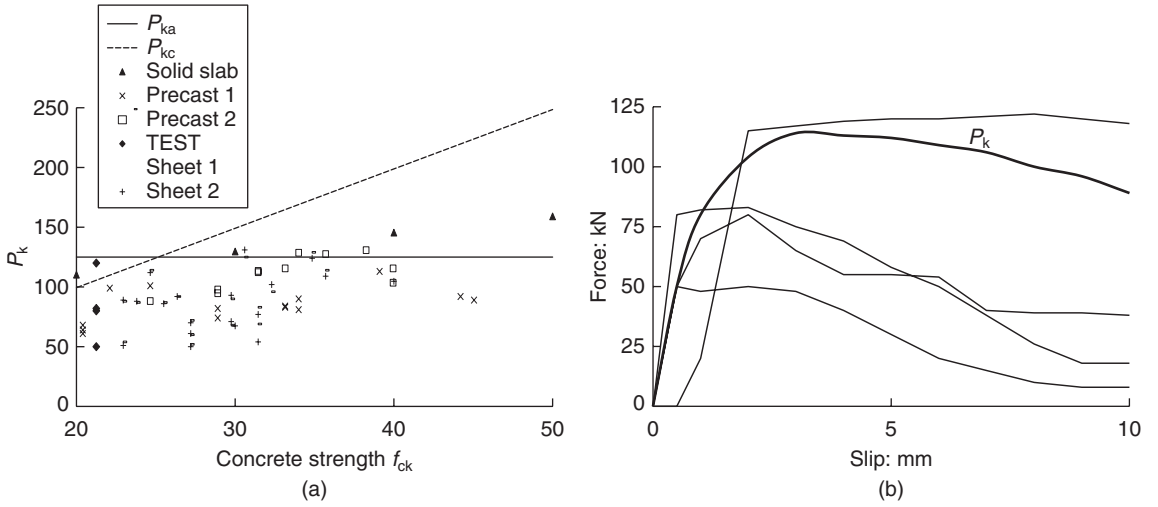

where k is a reduction coefficient for non-solid slabs, and varies from 0.5 when the indents are approximately 80 mm to 1.0 for solid slabs.

REFERENCES

BSI (1978) BS 5400-5:1978. Steel, concrete and composite bridges. Code of practice for design of composite bridges. BSI, London.

BSI (1999) BS 5400-6:1999. Steel, concrete and composite bridges. Specification for materials and workmanship, steel. BSI, London.

BSI (2004) BS EN 1994-1-1:2004. Eurocode 4. Design of composite steel and concrete structures. General rules and rules for buildings. BSI, London.

BSI (2005a) BS EN 1992-2:2005. Eurocode 2. Design of concrete structures. Concrete bridges. Design and detailing rules. BSI, London.

BSI (2005b) BS EN 1993-1-1:2005. Eurocode 3. Design of steel structures. General rules and rules for buildings. BSI, London.

BSI (2005c) BS EN 1993-1-9:2005. Eurocode 3. Design of steel structures. Fatigue. BSI, London.

BSI (2005d) BS EN 1994-2:2005. Eurocode 4. Design of composite steel and concrete structures. General rules and rules for bridges. BSI, London.

BSI (2005e) BS EN 1993-1-10:2005. Eurocode 3. Design of steel structures. Material toughness and through-thickness properties. BSI, London.

BSI (2006a) BS EN 1993-2:2006. Eurocode 3. Design of steel structures. Steel bridges. BSI, London.

BSI (2006b) BS EN 1993-1-11:2006. Eurocode 3. Design of steel structures. Design of structures with tension components. BSI, London.

Chen BC and Wang TL (2009) Overview of concrete filled steel tube arch bridges in China. *Practice Periodical on Structural Design and Construction* **14(2)**: 70–80.

Dajun D (2001) Development of concrete-filled tubular arch bridges, China. *Structural Engineering International* **11(4)**: 265–267.

Dickson DM (1987) M25 Orbital Road, Poyle to M4: alternative steel viaducts. *ICE Proceedings*, *Part 1* **82(2)**: 309–326.

England G and Tsang N (2001) Towards the design of soil loading for integral bridges. Concrete Bridge Development Group Technical Paper 2. Paper presented at the Annual Conference of the Concrete Bridge Development Group. Magdalene College, Cambridge.

Hicks SJ (2007) Strength and ductility of headed stud connectors welded in modern profiled steel sheeting. *The Structural Engineer* **85(10)**: 32–38.

Highways Agency (1987) BD 28, Early thermal cracking of concrete. In *Design Manual for Roads and Bridges*, Vol. 1. The Stationery Office, London.

Hill GJ and Johnstone SP (1993) Improvements of the M20 Maidstone bypass, junctions 5–8. *Proceedings of the ICE – Civil Engineering* **93**: 171–181.

Jeffers E (1990) U-frame restraint against instability of steel beams in bridges. *The Structural Engineer* **68(18)**.

Johnson RP and Yuan H (1998) Existing rules and new tests for stud shear connectors in troughs of profiled sheeting. *Proceedings of the ICE – Structures and Buildings* **126**: 244–251.

Kerensky OA and Dallard NJ (1968) The four level interchange at Almonsbury. *Proceedings of the ICE* **40**: 295–322.

Mato F (2001) Comparative analysis of double composite action launched solutions in high speed railway viaducts. *Composite Bridges – State of the Art in Technology and Analysis. Proceedings of the 3rd International Meeting*, Madrid.

Narayanan R, Bowerman HG, Naji FJ, Roberts TM and Helou AJ (1997) *Application Guidelines for Steel–Concrete Sandwich Construction: Immersed Tube Tunnels*. Technical Report 132. Steel Construction Institute, Ascot.

Oguejiofor EC and Hosain MU (1992) Behaviour of perfobond rib shear connectors in composite beams: full size tests. *Canadian Journal of Civil Engineering* **19**: 224–235.

Prichard B (ed.) (1993) Continuous and integral bridges. *Proceedings of the Henderson Colloquium*, Cambridge.

Schlaich J, Schlaich M and Schmid V (2001) Composite bridges: recent experience. The development of teeth connectors. *Composite Bridges. Proceedings of the 3rd International Meeting*, Madrid, pp. 760–790.

SCI and BCSA (Steel Construction Institute and British Constructional Steelwork Association) (2007) *Steelwork Design Guide to BS 5950*, *Vol. 1*, *Section Properties and Member Capacities*, 4th edn. Publication 202. Steel Construction Institute, Ascot.

Wang Y and Nethercot D (1989) Ultimate strength analysis of three dimensional braced I-beams. *ICE Proceedings*, *Part 2* **87(1)**: 87–112.

Withycome S, Firth I and Barker C (2002) The design of the Stonecutters Bridge, Hong Kong. *Current and Future Trends in Bridge Design*, *Construction and Maintenance. Proceedings of the International Conference*, Hong Kong. Thomas Telford, London.

Steel–concrete Composite Bridges
ISBN 978-0-7277-5810-1

http://dx.doi.org/10.1680/scb.58101.051

ice Institution of Civil Engineers
publishing

Chapter 3
Integral bridges

. . . integral bridges are used for all bridges up to 60 m long . . .

3.1. Introduction

Integral bridges are structures where joints are not required, as the substructure and superstructure are monolithic. Integral bridges have significant maintenance advantages over conventionally articulated bridges. Leaking joints are a major source of water ingress (Highways Agency, 1994), causing deterioration. In the UK, the Highways Agency (2003) recommends that integral bridges are used for all bridges up to 60 m long, unless there are good reasons not to. However, integral bridges can be used for longer lengths; in the USA, lengths of double this are common in some states.

Integral bridges come in two forms: semi-integral or fully integral. The semi-integral form has no joints, but has bearings to give some rotational flexibility to the end of the deck. The fully integral bridge has no joints or bearings. Ideally, the abutment is kept as shallow as possible by the use of a bank-seat-type structure (Figure 3.1a–c), thus limiting the amount of soil affected by the movement. When a bank seat is not viable, a full-height wall of concrete or steel sheet piles is required, forming a portal structure (Figure 3.1d,e).

Bridges move primarily due to thermal effects, although the concrete shrinkage and vehicle traction may also cause some movement. The bridge will undergo a series of cyclic movements as temperatures fluctuate between day and night and between summer and winter. The thermal mass of the structure has some influence in damping the fluctuations. In the UK, typical thermal strains are +0.0004 for concrete bridges and +0.0006 for steel bridges, with steel–concrete composite bridges being in between the two (Highways Agency, 2003). More detailed thermal strains can be estimated using the coefficient of thermal expansion and the likely extreme bridge temperatures outlined in Eurocode 1: Part 1-5, 'Actions on structures. General actions. Thermal actions' (BSI, 2003a). For structures located in the south of England or which use concrete with a lower coefficient of thermal expansion (limestone or lightweight aggregates for instance) some reduction in the thermal strains may be found.

3.2. Soil–structure interaction

If the likely thermal movement is in the range of 20 mm, an asphaltic plug (BSI, 2007) in the carriageway surfacing will be capable of accommodating any tendency to crack, and no expansion joint is required. With no expansion joint the bridge structure will be in contact with the soil backfill, and the bridge movement will induce pressures in the soil; these pressures will in turn need to be resisted by the structure. It is common to visualise the soil–structure interaction as a change in soil pressures between active (K_a) and passive (K_p), with the static pressure being near the at-rest (K_o) state. Eurocode 7: Part 1, 'Geotechnical design. General rules' (BSI, 2004) defines the resulting soil

Figure 3.1 Bank-seat abutment: (a) semi-integral; (b) integral; (c) piled integral. Portal structure: (d) on pad foundations; (e) on embedded piles

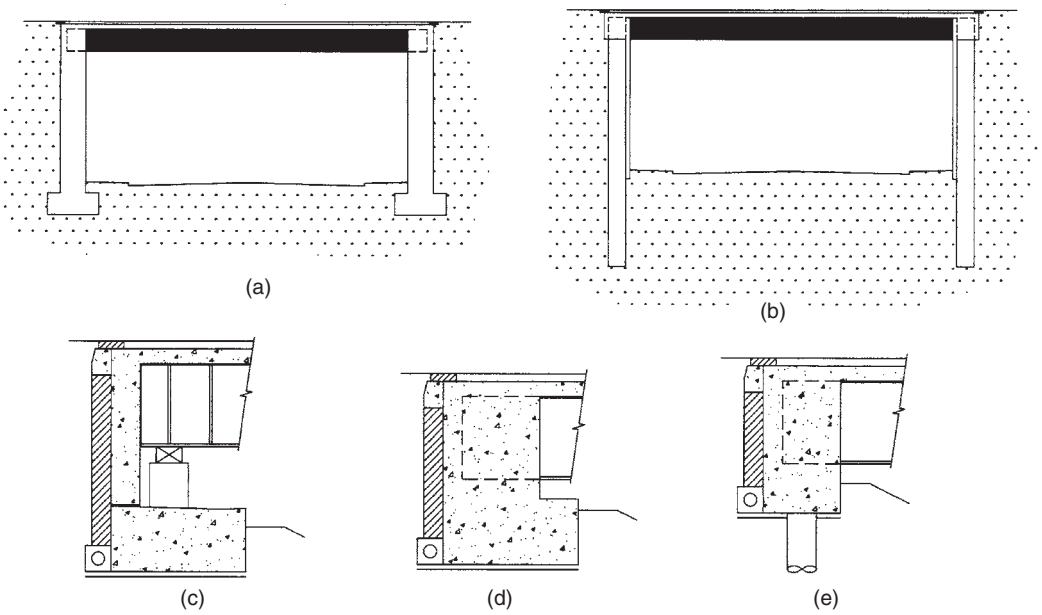

pressures (σ_a and σ_p) as

$$\sigma_a = K_a(\gamma z + q) - 2c\sqrt{k_a} \tag{3.1a}$$

$$\sigma_{pa} = K_p(\gamma z + q) + 2c\sqrt{k_a} \tag{3.1b}$$

where γ is the soil density, z is the distance down from the top of the wall or ground surface, q is any surcharge load on the ground and c is the ground cohesion. For most bridges that use a selected backfill, which is generally cohesionless, the second term in each of the above equations can be neglected, thus simplifying the calculation of soil pressure. For vertical walls with a drainage layer behind the wall, such that there is little friction between wall and soil, the soil pressure is assumed to act perpendicularly to the wall. The various soil pressure coefficients can be estimated using the following equations:

$$K_a = \frac{1 - \sin\phi}{1 + \sin\phi} \tag{3.2a}$$

$$K_o = 1 - \tan\phi \tag{3.2b}$$

$$K_p = \frac{1 + \sin\phi}{1 - \sin\phi} \tag{3.2c}$$

where ϕ is the soil angle of shear resistance. If there is some friction between wall and soil there will be some change in the soil pressure coefficients – slightly reducing the active, but significantly increasing

Figure 3.2 (a) Estimated values of passive soil coefficients obtained using Equation 3.1c (K_p) and with wall friction (K_{pf}). (b) Variation in soil pressure with movement for two wall heights

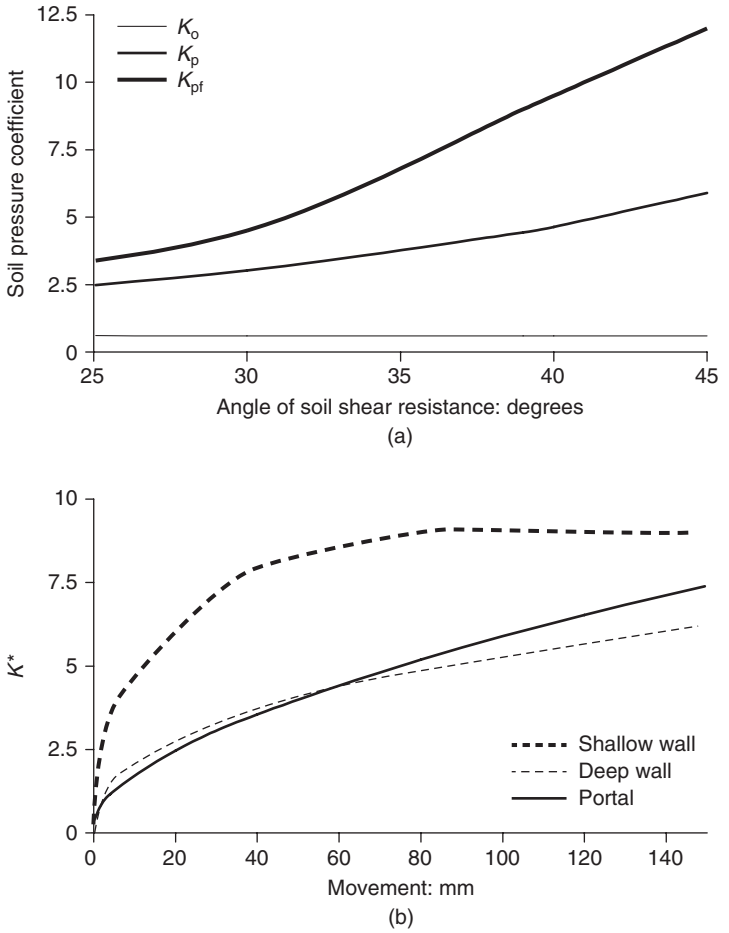

the passive. A friction angle of 50% of the soil shear strength is generally assumed; values of K_p taking wall friction into account are shown in Figure 3.2a.

The pressures induced by the thermal movements depend primarily on the level of movement of the bridge, the point about which movement occurs and the properties of the soil. Eurocode 7: Part 1 gives some indication of this; typically active pressures are generated at movements of 0.1–0.2% of the wall height, and passive pressures require movements of 3–10% of the wall height. Traditionally, backfill behind bridge abutments has been of a good quality, usually better than the adjacent embankments. Fill of good quality will, however, generate very high passive soil pressures, leading to larger forces on the structure. For integral bridges, it is normal to specify a maximum soil strength to avoid very high passive pressures. Care needs to be taken in the minimum soil strength, as the fill will need to resist the highway loads and too weak a fill will not give a good transition between the embankment and the structure.

The backfill behaves in a non-linear manner during loading, and on repeated loading it will tend to undergo some volume change and residual strains will occur, with the accumulation of strain occurring in a ratcheting effect (England and Tsang, 2000). The relationship between maximum soil pressure (K^*) and the wall movement is normally expressed as:

$$K^* = K_o + \text{function}\ (K_p, \Delta) \tag{3.2}$$

The function of K_p depends on the wall height and form. Figure 3.2b shows a typical variation in K^* for a wall with $K_p = 9$ and wall heights of 2.5 m and 7.5 m.

3.3. Example 3.1: A semi-integral bridge

The first example in this chapter is another simply supported river bridge, this time of a semi-integral form. The bridge was designed in the early 2000s as part of a new motorway around Birmingham. The bridge is shown in Figures 3.3 and 3.4; it is a multi-beam form of 37.5 m span that is formed from weathering steel girders. The bridge abutments are formed from reinforced earth walls, with a bank-seat supporting the bridge deck. The bridge is semi-integral rather than fully integral to limit

Figure 3.3 River Blythe Bridge: details

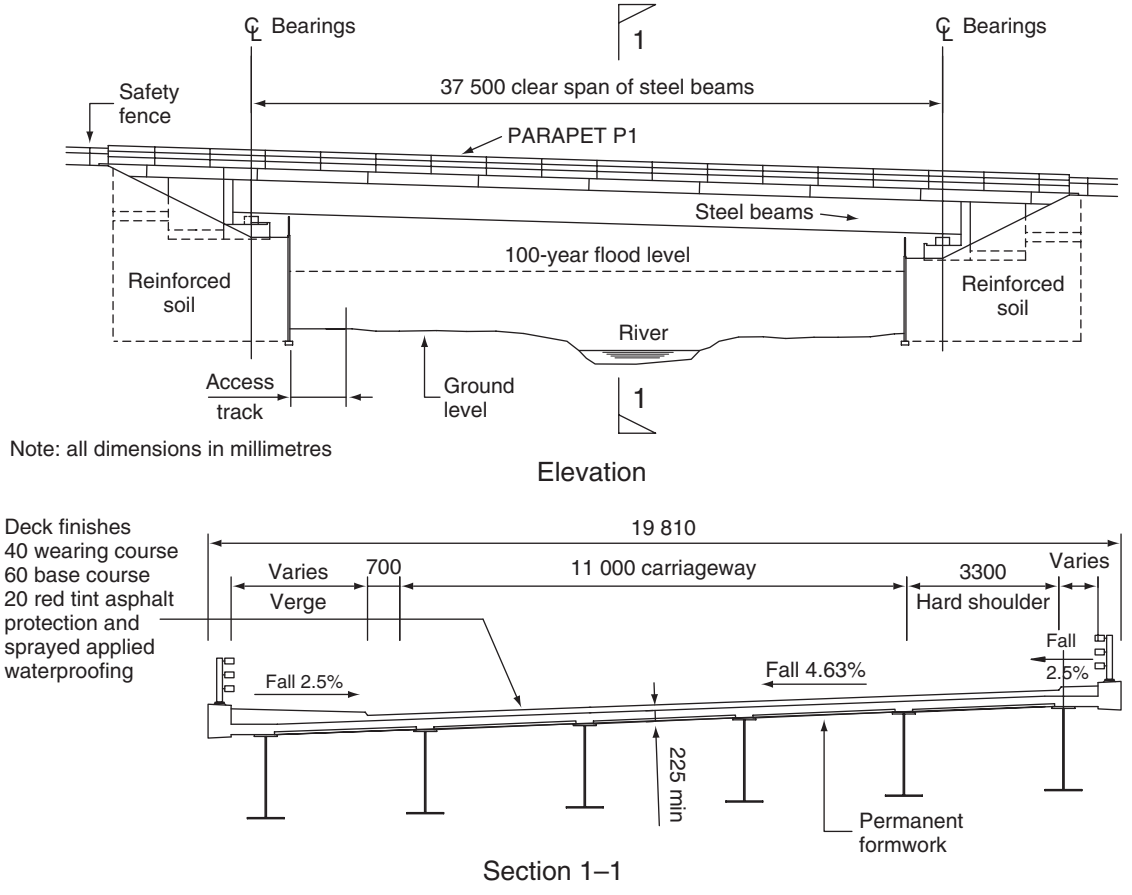

Figure 3.4 The River Blythe Bridge: view of semi-integral abutment and weathering steel girder

the additional strains on the reinforced earth substructure. The bridge has been sized (in a similar way to the example in Chapter 2) for load model 1 (LM1) loading.

3.3.1 Loads for Example 3.1

The dead loads of the steelwork, concrete and surfacing can be determined from the outline sizing and the layout drawing. Weights of parapets and parapet coping, together with additional surfacing at the footway will also be established for this detailed stage. Live loads for LM1, the uniformly distributed load (UDL), the tandem axle load (TA) and the footway load, are determined from the codes (BSI, 2003b). The soil loading can be established from Figure 3.2, from work by England and Tsang (2000) (Peel-Cross *et al*., 2001) or by using the equations in the codes (BSI, 2004). To estimate the soil loading the temperature movement and soil characteristics must be known. The bridge bank-seat is supported on a reinforced soil wall with a selected granular material. The soil fill behind the bank-seat is of a similar material with a density of 19 kN/m^3 and angle of shearing resistance of 42°, giving an estimated K_p of 5–9 (see Figure 3.2a). Assuming a thermal strain of 0.0005 for a steel–concrete composite structure, the movement for a 37.5 m long structure is 10 mm ($0.0005 \times 37.5/2$). A conservative estimate of the maximum soil pressure coefficient K^* is 4.5 (from Figure 3.2b). The peak soil pressure at the base of the abutment wall is

$$\sigma_q = K^* \gamma z \tag{3.3}$$

The wall height is 2.5 m, and so for this example

$$\sigma_q = K^* \gamma z = 4.5 \times 19 \times 2.5 = 214 \text{ kN/m}^2$$

The maximum soil force, assuming a triangular pressure distribution, is

$$F_s = 0.5\sigma_q z \tag{3.4}$$

which for this example gives a characteristic force of 267 kN/m due to soil loading. With a partial load factor of 1.5 and the spacing of beams at 3.46 m the ultimate force per beam is 1385 kN. This force is assumed to act parallel to the girders.

Another loading action to be considered in detailed design is concrete shrinkage and differential temperature. Both these loads stress the concrete slab in a different way to the underlying steel beam, causing a force at the steel–concrete interface. The loading is self-equilibrating and will not cause the structure to fail, and so can generally be ignored at the ultimate limit state if compact class 1 or 2 sections are used. However, for the more slender class 3 sections, it should at least be considered. Shrinkage and differential temperature will cause additional deflections, which again may need consideration. Shrinkage of the slab on a simply supported beam results in longitudinal shears of an opposite sign to the shears from loading on the span (see Figure 3.14 and accompanying text). For the differential temperature case where the slab is cooler than the beam, longitudinal shears are again of opposite sign to the general dead and live loads. Where the slab is hotter than the beam, positive shears can result; however, they are unlikely to be significantly larger than the permanent shrinkage shears, and so for simply supported structures both shrinkage and temperature effects can usually be safely ignored in the interface design.

3.3.2 Analysis for Example 3.1

The modelling of any bridge, even the simplest of single-span, beam and slab layout, involves some generalisation. Provided the limitations of the models are recognised, a series of simple models is usually preferable to a more complex model that tries to represent all aspects of the structure. For a beam and slab deck the most popular form of analysis is the grillage, which models the bridge deck in two-dimensions only, and represents only the shear, bending and torsional interactions in the structure. The limitations of this method are well known (Hambley, 1991), but in general it provides sufficient accuracy for design of the main girders for most bridges. The grillage method does not consider longitudinal load effects. For the soil loading a separate line model is used; this could be carried out by hand methods, but the use of a computer model with nodes at similar points to those in the grillage allows the superposition of results more easily. The grillage can also be used to determine slab moments and shears if the transverse members are proportioned to suit an effective strip method (Hillerborg, 1996). Some designers advocate the use of an influence surface (Pucher, 1964) in combination with the grillage to design the slab; this complicates analysis and leads to a very conservative design. If more detailed slab models are to be considered the methods should recognise the significant in-plane or arching effects (Peel-Cross *et al.*, 2001) that occur in these structures (see Chapter 5). If the slab span is less than 3.2 m, the simplified methods of taking arching into account (Highways Agency, 2002) may be appropriate.

The three-dimensional grillage model layout for this bridge is shown in Figure 3.5. In this case, three grillage models are used – a non-composite beam and zero slab stiffness, short-term concrete properties for the composite sections, and long-term composite properties – and soil loads on the composite section are also modelled. The temperature fluctuation causing the soil pressures is composed of annual and daily fluctuations. The model could have considered part of the load applied to a short-term composite section, but this additional complication is not worthwhile for such a small structure (it is more applicable to larger structures).

Figure 3.5 Models for an integral bridge deck slab

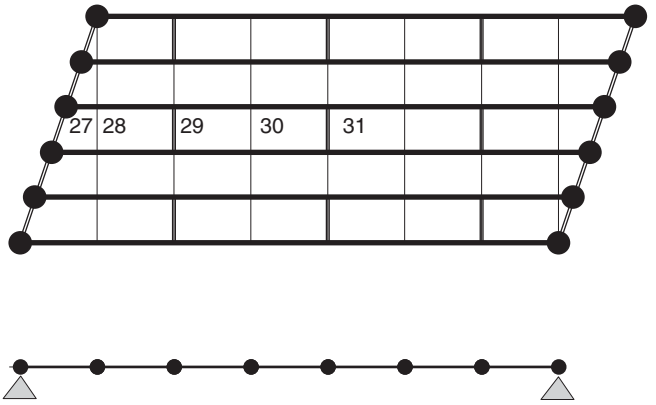

Table 3.1 shows the relevant section properties for the grillage (for calculation of section properties see Appendix B). It should be noted that the torsional properties of the beams are effectively those of the slab as the torsional stiffness of the girders are negligible. The torsional properties are halved to more accurately represent this form of structure (Hambley, 1991) (for a structure of this form setting the torsional stiffness to zero and only considering shear and bending effects would also lead to a safe solution). The end diaphragms and intermediate bracing have been included in the grillage, this generally gives a less conservative estimate of forces than an alternative method; which is to not model these restraints, and later design them to accommodate the displacements of the grillage. As weathering steel is used the section properties used are those where a 1 mm corrosion allowance has been made on all exposed surfaces (Highways Agency, 2001).

3.4. Weathering steel

Weathering steel has an enhanced resistance to corrosion compared to normal steel, as the initial rust layer forms a protective barrier that dramatically slows further corrosion (Dolling and Hudson, 2003). Typically, an allowance of 1 mm to each exposed face should be allowed as a loss of section for a typical British structure with a 120-year design life. For the interiors of box girders or other enclosed

Table 3.1 Blythe River Bridge section properties

Section	A: m^2	I: m^4	C_J: m^4	Z: m^3
Girder, non-composite	0.070	0.036	0	0.052
Girder, composite, $n = 12$	0.100	0.088	0.0005	0.67
Girder, composite, $n = 6$	0.200	0.106	0.001	0.07
Bracing	0.006	0.006	0	–
Bracing, $n = 12$	0.070	0.0115	0.0005	–
Bracing, $n = 6$	0.120	0.0115	0.001	–
End wall	0.100	0.050	0.0004	–
Slab, $n = 12$	0.064	0.0003	0.0005	–

Table 3.2 River Blythe Bridge analysis results

Node No.		Serviceability limit state			Ultimate limit state		
		M: MN m	*V*: MN	*N*: MN	*M*: MN m	*V*: MN	*N*: MN
Non-composite	27	0	0.55	0	0	0.60	0
	29	3.6	0.27	0	4.0	0.30	0
	31	5.2	0	0	5.7	0	0
Composite, $n = 12$	27	0	0.15	0.93	0	0.22	1.4
	29	1.1	0.07	0.93	1.6	0.10	1.4
	31	1.35	0	0.93	1.9	0	1.4
Composite, $n = 6$	27	0	1	0	0	1.3	0
	29	5.4	0.75	0	7.5	1	0
	31	7.5	0.35	0	10.5	0.45	0

sections not subject to damp conditions this allowance may be reduced. In some locations the allowance may need to be increased. If the steel parts are continually wetted, are in coastal regions, or in areas likely to be affected by de-icing salts the corrosion rates can be significant and weathering steels should not be used.

The cost of painting may be 11–18% of the steelwork cost (see Figure 1.7) and the primary advantage of using weathering steel is to eliminate this cost. Furthermore, the need for future repainting is removed and future maintenance costs are reduced.

3.4.1 Design for Example 3.1

For this example, three elements will be looked at in more detail: the girder bottom flange, the shear connectors and the deck slab at the interface with the girder. The moments, shears and axial loads from the analysis at the ultimate and serviceability limit state for a midspan section and a support section (nodes 31 and 27 in Figure 3.5) are given in Table 3.2. The steelwork layout is shown in Figure 3.6.

Assuming the section is to be checked as a non-compact class 3 section, the stress in the bottom flange at node 31 is

$$f_{ab} = \frac{N_1}{A_1} + \frac{M_1}{Zb_1} + \frac{N_2}{A_2} + \frac{M_2}{Zb_2} + \frac{N_3}{A_3} + \frac{M_3}{Zb_3} \tag{3.5}$$

$$f_{ab} = 0 + 129 + 0 + 32 + 8 + 165 = 334 \text{ N/mm}^2$$

For a steel of thickness 28 mm the yield stress f_y is 345 N/mm^2, and so the section is just satisfactory. Another way of expressing Equation 3.5 is

$$\frac{M}{M_D} + \frac{N}{N_D} < 1 \tag{3.6a}$$

Figure 3.6 Steelwork details for River Blythe Bridge

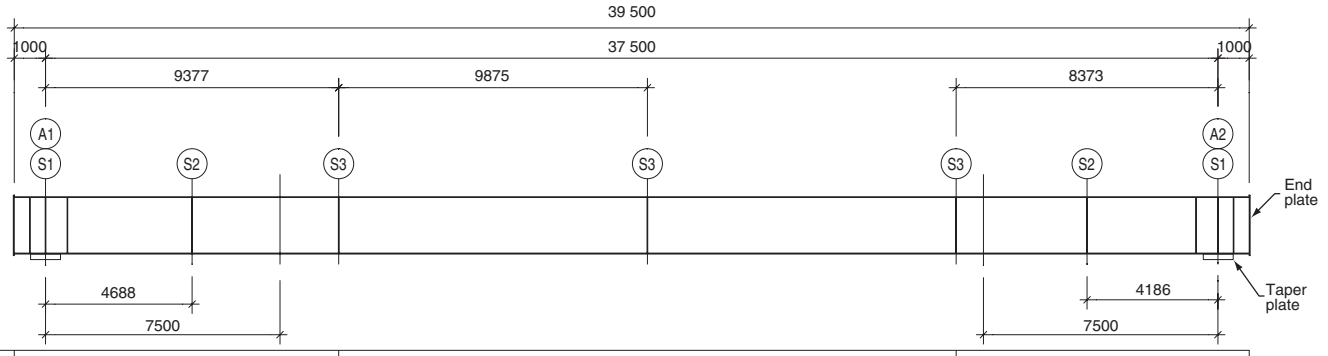

Shear connector	2 @ 150		2 @ 150		2 @ 150
Top flange	600 × 25				
Web plate	1780 × 20				
Bottom flange	800 × 30		950 × 30		800 x 30
Geometry					
Steel	0	12	20	12	0
Concrete	0	31	50	31	0
Precamber	0	92	155	92	0

Note: all dimensions in millimetres

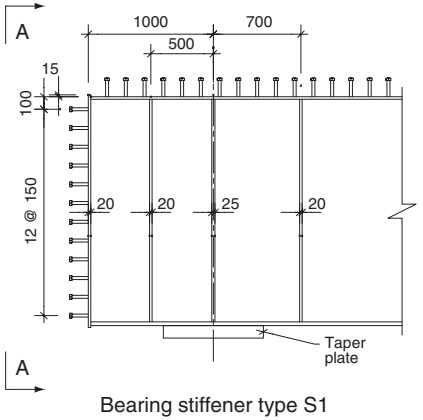

Bearing stiffener type S1
(1:50)

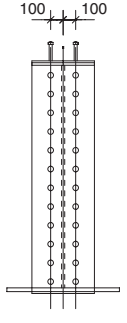

Section A–A
(1:50)

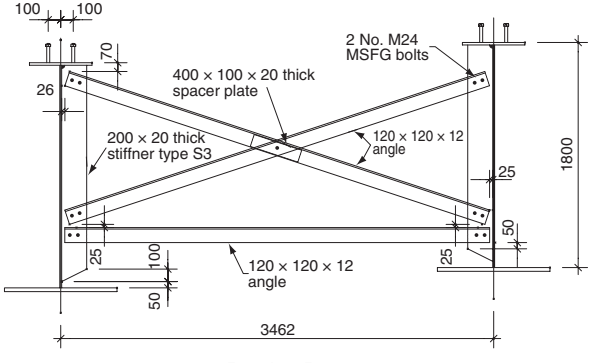

Bracing B1
(1:50)

where

$$M = M_1 \frac{Zb_3}{Zb_1} + M_2 \frac{Zb_3}{Zb_2} + M_3 \tag{3.6b}$$

$$N = N_1 \frac{A_3}{A_1} + N_2 \frac{A_3}{A_2} + N_3 \tag{3.6c}$$

These equation are preferred by the author, as rather than checking stresses at each node the moments and axial forces can be modified by an additional section factor during the analysis with the partial load factors; the moment diagrams can then be plotted directly and the M_D diagram superimposed. For the simply supported beam example, there is little difference in the number of calculations to be carried out; however, for a more complex structure the use of spreadsheets to calculate stresses can be virtually eliminated. The use of a graphic method of design also aids reviews and checking, which is more difficult with tabulated data on stresses. The form of Equation 3.6a is also used where axial loads are more predominant (see Chapters 8 to 11).

The longitudinal shear flow is calculated at the ultimate limit state from the vertical shear (see Equation 1.16). It is a maximum at the support (node 27) and again is summed at all stages:

$$V_l = V_{l1} + V_{l2} + V_{l3} \tag{3.7}$$

From the section properties the V_l/V ratio is known at each stage (see Appendix C).

$$V_l = 0 + 0.58 \times 0.22 + 0.53 \times 1.3 = 0.82 \text{ MN or } 820 \text{ kN}$$

Using 19 mm diameter studs with $P_u = 108$ kN (see Table 1.6) and Equation 1.17b,

$$n = \frac{V_l}{0.7P_u} = \frac{820}{75} = 11$$

The connectors required are calculated at the other nodes and plotted as shown in Figure 3.7 Two connectors at 150 mm centres give sufficient capacity at the support; the connectors could be curtailed

Figure 3.7 Longitudinal shear diagram, with connector requirements

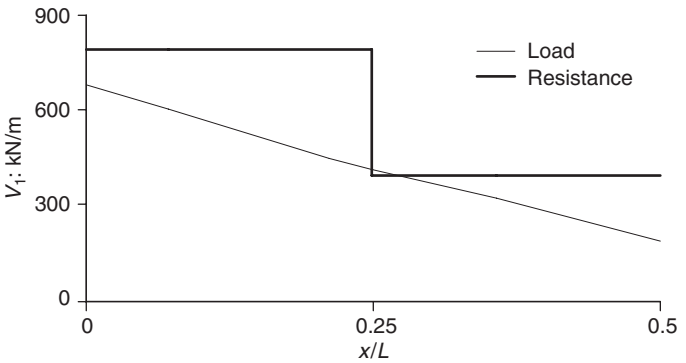

Figure 3.8 Detailing of reinforcement at precast permanent formwork

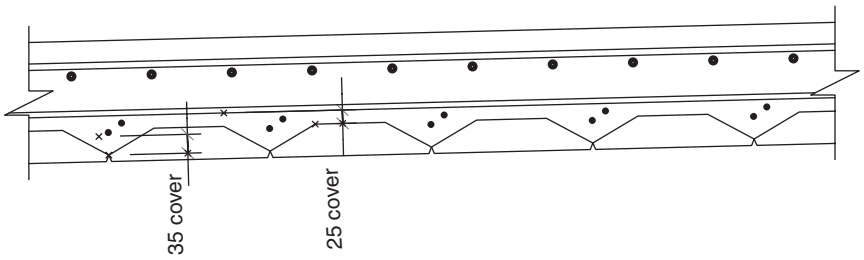

Note: all dimensions in millimetres

between nodes 28 and 29 to two at 300 mm centres. In general, connector spacing should be kept constant for at least 10% of the span. At the supports, the connection capacity should exceed the applied shear; at other locations the shear flow can locally exceed capacity by up to 10%.

Having confirmed that the shear plane is satisfactory through the connectors, the longitudinal shear capacity of the concrete slab should be checked using Equation 1.22. At node 27 (at the support) the shear flow at the ultimate limit state is 820 kN/m. For a pair of 150 mm high connectors placed 200 mm apart, the length of plane y–y is 520 mm (see Figure 1.11b), the length of plane z–z (see Figure 1.11c) is 330 mm (ignoring the lower 60 mm of the slab where the plane runs along the edge of the precast formwork), and

$$V_{1\,\max} = 0.14 L_{\mathrm{d}} f_{\mathrm{ck}} = 0.08 \times 330 \times 32 = 1478 \text{ kN/m}$$

for z–z the shortest plane. This is greater than the applied shear and satisfactory. Plane y–y has the least reinforcement with two T12 bars at 300 mm centres running between the permanent formwork, giving an area of reinforcement of 747 mm^2/m each time the reinforcement crosses the shear plane. Using Equations 1.22b and 1.22c:

$$V_1 = 1.7 \times 747 \times 460 \times 2 = 1168 \text{ kN/m}$$

This is again greater than the applied shear. Both shear planes are satisfactory.

The detailing rules for reinforcement through the shear plane require that 50% of the bars are below 50 mm of the connector top. To achieve this one of the two bars passing between the precast units should be fixed low, as shown in Figure 3.8, or taller connectors should be used.

3.5. Compact class 1 and 2 sections

So far we have considered class 3 beams using elastic analysis and elastic section properties. However, where sections meet the flange outstand and web slenderness limits and the connector spacing requirements for compact class 1 and 2 sections (see Table 1.3) the increased plastic section properties may be used (see Appendix D). For steel beams the plastic modulus is typically 10–20% higher than the elastic modulus. For steel–concrete composite sections with the concrete slab element in compression the plastic modulus is approximately 5–20% higher, but will be dependent on the modular ratio of the section. A primary advantage of using a compact or plastic section is that all loads may be assumed

Figure 3.9 Variation in steelwork tonnage with depth and class of section

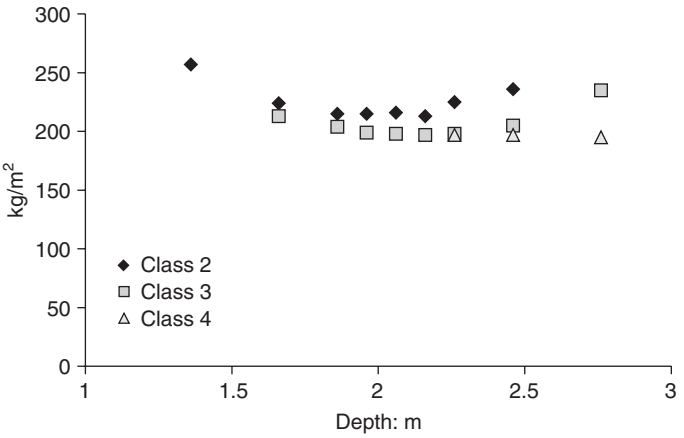

to act on the final section, such that Equation 3.6a may be used, with Equations 3.8a and 3.8b:

$$\frac{M}{M_D} + \frac{N}{N_D} < 1 \tag{3.6a}$$

where

$$M = M_1 + M_2 + M_3 \tag{3.8a}$$

$$N = N_1 + N_2 + N_3 \tag{3.8b}$$

However, to take advantage of this additional bending capacity the shear connection should be designed to carry the entire shear:

$$V_1 = (V_1 + V_2 + V_3)Ay/I \tag{3.9}$$

Compact section design therefore tends to allow smaller sections for bending but necessitates higher shear connector requirements. For larger bridges the web limitations for class 1 or 2 structures may be onerous and over-thick webs required, leading to additional steel.

An analysis of the bridge in Example 3.1 was undertaken for various depths of girder and various classes of section. The results are plotted in Figure 3.9. It can be seen that the curve is fairly flat and that girder depths between 1.6 and 1.9 m give a similar steelwork tonnage. For this span, the class 3 structures generally give lighter structures than the class 1 or class 2 sections.

3.6. Portal frame structures

Integral portal structures are formed from the composite deck structure being connected to the full-height abutment. The advantage of this form is that the moments are nearer those of a fixed-end beam rather than a simply supported one (Figure 3.10), and deflections are also significantly reduced. A disadvantage, structurally, is that a larger moment range has to be considered due to the variation in soil pressures, which range from low active to high almost passive.

Figure 3.10 Comparison of moments and deflections for fixed and simply supported structures

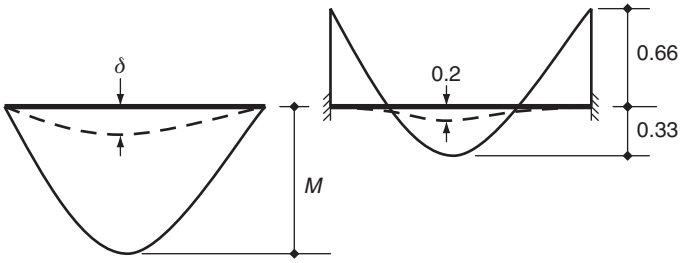

3.7. Example 3.2: Composite portal frame

The second example in this chapter is a fully integral portal structure, the bridge being an alternative design proposal for a new road in Staffordshire, UK. The structure is similar to the one shown in Figure 3.1e, and has a 22.5 m span, multiple rolled, universal beam bridge deck supported on high-modulus steel piles, the abutment being part of a longer retaining wall system.

3.7.1 Loads and analysis for Example 3.2

The soil loads on the wall will vary from low active pressures (K_a) to the larger integral pressures (K^*). The maximum and minimum soil pressures are shown in Figure 3.11a. For a wall of this form, the high integral pressures occur in the top half to two-thirds of the wall height. They may be assumed to be back to the at-rest condition (K_o) near the front ground line, this distribution being dependent on the relative stiffness of the wall and soil. The characteristic soil loads are approximately 4.5 MN maximum (K^*) and 0.7 MN minimum (K_a). It is common that for integral structures such as the one in this example the soil is modelled as elastic or semi-elastic spring. These models will allow a more accurate assessment of the typical soil pressures on the wall. However, they will not take the effects of soil ratcheting (England and Tsang, 2000) into account, and so care needs to be taken when using them. The model will give a good indication of where the soil is moving, and so allow a more accurate assessment of the K^* pressures.

Characteristic deck loadings of 0.5 MN, 0.225 MN and 1.3 MN for dead, surfacing and live loads are also assumed. Analysis of the structure is carried out as a portal frame strip; the results are summarised in Figure 3.11b. The maximum sagging moment at midspan is in combination with the minimum soil loads on the wall; the maximum hogging moment is in combination with the maximum soil loads. The moment at the portal knee is similar to the maximum midspan moment, but causes tensions in the concrete elements (see Chapter 4).

It is common for integral structures such as the one in this example that the soil is modelled as an elastic or semi-elastic spring. These models will allow a more accurate assessment of the typical pressures on the wall. They will generally not take into account the ratcheting effects of multiple movements, and so care needs to be taken when using them. The modelling will, however, give a good indication of where the soil is moving, and so allow a more accurate placing of the K^* pressures.

To reduce the effects of the range of maximum and minimum soil pressures the walls may be inclined. If the wall of the portal is leaning to an angle near the shear resistance of the soil, the range of pressures will be minimised, leading to an inclined portal or arch form as the best portal shape.

Figure 3.11 Example 3.2: (a) maximum and minimum soil pressures; (b) bending moments on the portal

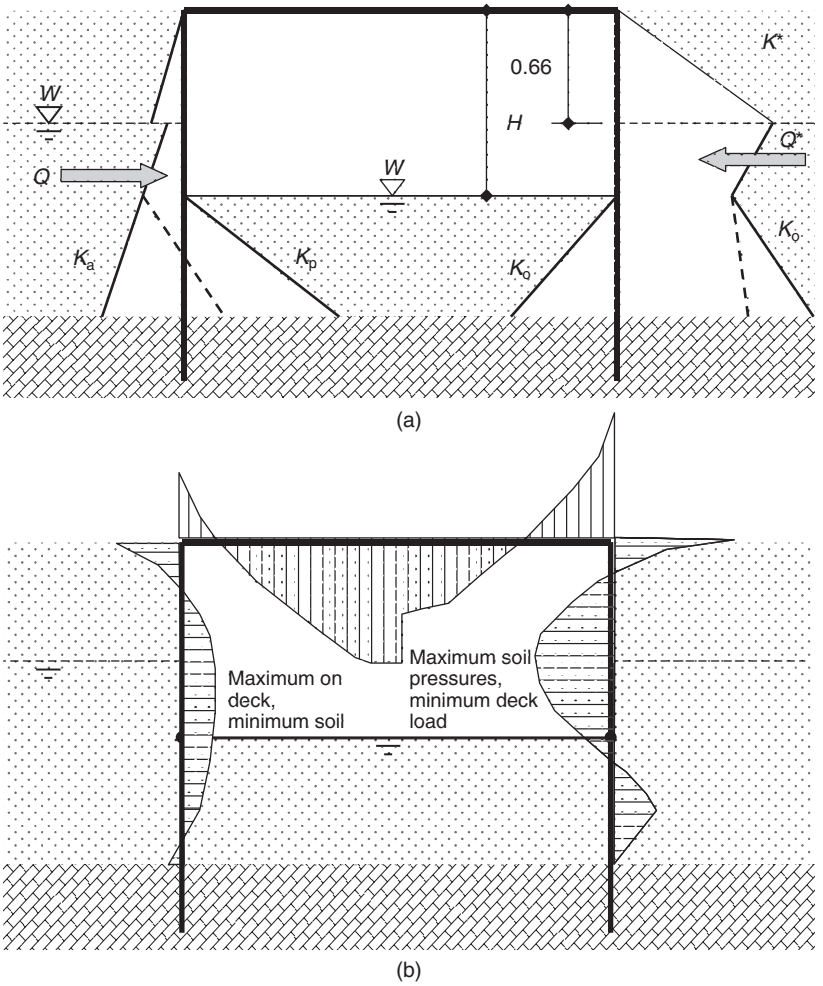

3.8. Effects of skew

The structures considered in Examples 3.1 and 3.2 have only a small skew. For bridges with a larger skew angle (θ) the soil forces (F_s) are offset (see Figure 3.11b). If the eccentricity (e) of the forces becomes too large, some rotational movement of the abutment may occur. For stability, a shear force will occur along the abutment:

$$V = F_s e/L \tag{3.10}$$

where e increases with the skew

$$e = L \tan\theta \tag{3.11}$$

The limiting value of V is estimated from the friction on the abutment, assuming a factor of safety from sliding of γ_{ms}:

$$V_{max} = \frac{F_s}{\gamma_{ms}} \tan 0.67\phi \tag{3.12}$$

where ϕ is the soil angle of shearing resistance; a value of 0.67 is used, as the failure surface is likely to be at the interface with the wall. With $\phi = 42^\circ$, $V = V_{max}$ at approximately 28°. Hence for skews above this value the behaviour of the structure should be considered carefully.

For a high skew, crossing the arrangement of the beams could be modified such that they form a square span with no eccentricity, this gives a larger deck area than the skewed bridge (Figure 3.12c). For bridges where the width is greater than the span and the girders are square with only skewed edge beams (Figure 3.12d), the maximum soil pressures are higher adjacent to the points a–b, c–d. The limiting skew angle increases as the width/span ratio (B/L) of the deck increases (Figure 3.12e).

Figure 3.12 Beam layouts for integral bridges: (a) square bridge with no load eccentricity; (b) narrow skew bridge with eccentricity of load; (c) over-wide bridge; (d) wide bridge with skew ends; (e) limiting skew angles for integral bridges with various width/span ratios (B/L)

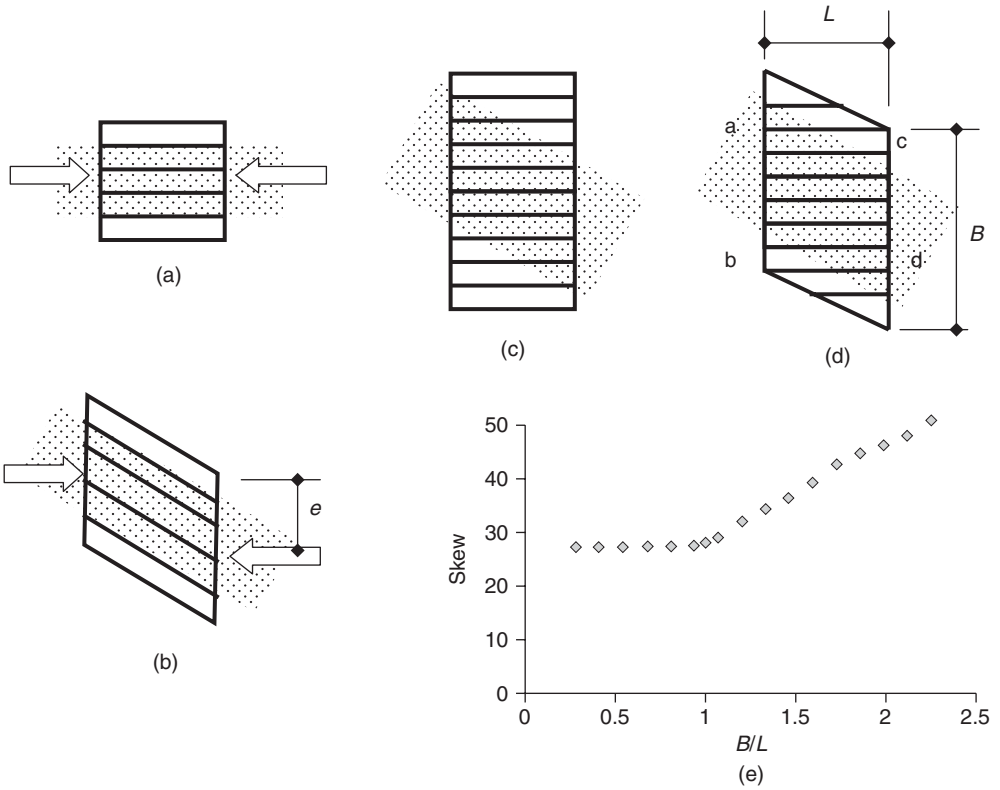

3.9. Example 3.3: Very high skew bridge

It is possible to design integral bridges outside the range outlined in Figure 3.12. The final example in this chapter is the Nanny Bridge (Bell, 2003), where a dual carriageway crosses a river at a skew of 48° (Figure 3.13). To overcome the issues of skew, this design is formed using a portal beam arrangement with reinforced earth walls. The portal is fully fixed at one end, with movement occurring at one end only; the top of the portal only is in contact with the soil, limiting the height in which the soil–structure interaction is accommodated. The fixing at one end does, however, limit the length of structure that can be used to about half that of a conventional integral structure (40 m rather than 80 m). The portal also allows the beam to be profiled, an aesthetic requirement stipulated for this structure.

At the portal end the tensile load is initially carried by the steel flange only. There is some strain incompatibility with the concrete, which has no load. Where a force is applied to one element only of a composite section the force cannot be transferred instantaneously, rather it must spread over a finite length (L_s). The length over which the applied force spreads is dependent on the stiffness of

Figure 3.13 The Nanny Bridge: details

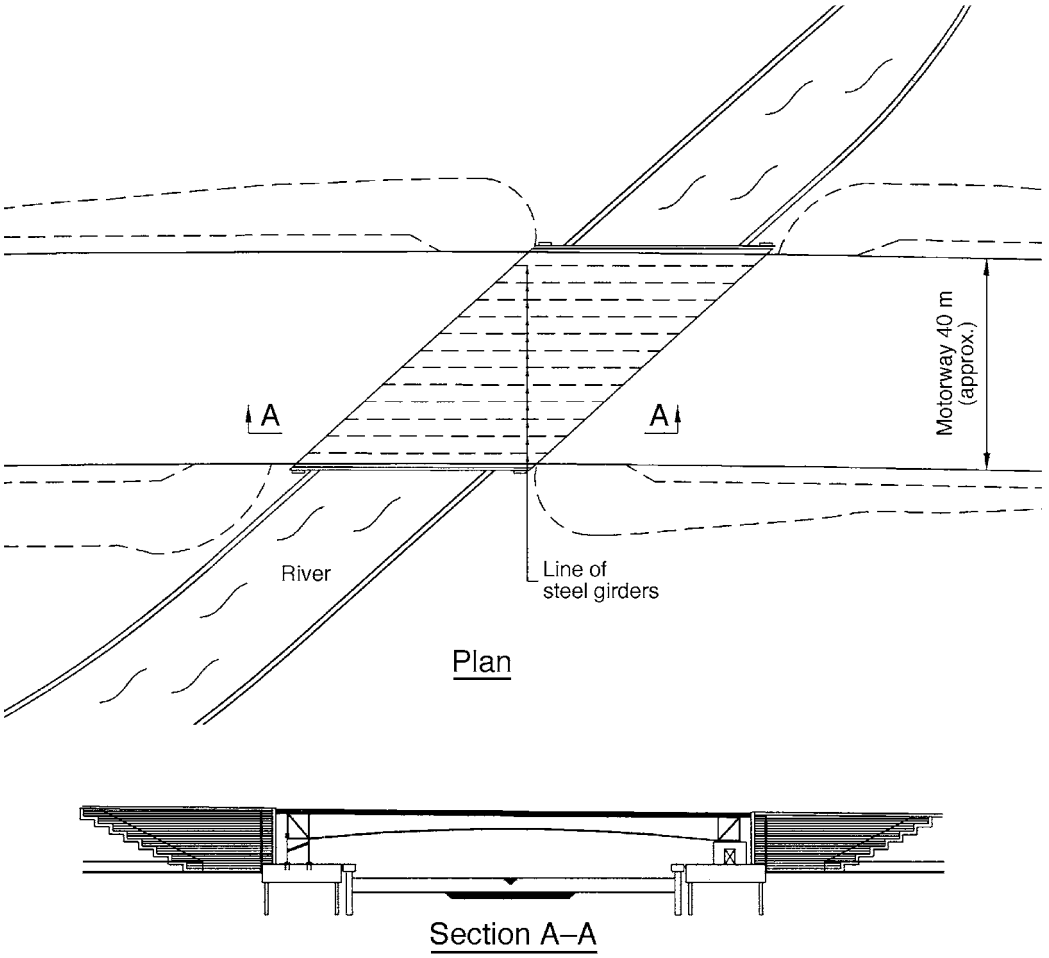

the connector between the two elements, and can be estimated from

$$L_s = 2(S_c\ \partial N/\partial\varepsilon)^{1/2} \tag{3.13}$$

where $S_c = 0.003\ \text{mm}^2/\text{N}$ for stud connectors or 0.0015 for other connectors (BSI, 1978), $\partial\varepsilon$ is the difference in free strain between steel and concrete. The stud connector flexibility given above is based on the initial stiffness of the connector with limited slip. At the ultimate limit state, if more slip is allowed then the length over which the force will spread will be increased. Alternatively, according to more simplified Eurocode methods, the length (L_s) can be approximated as the effective width of the beam.

At the end of the beam the connector requirement is calculated from the longitudinal shear and the additional that is required to transfer the loads from the steel to the concrete. The shear at the end of the beam for this example is 1.4 MN. V_l/V is 0.34 (see Appendix C):

$$V_l = 0.34 \times 1.4 = 0.48\ \text{MN/m}$$

The force in the tensile stiffener and flange at the joint with the all-steel portal is 4.4 MN. Only about 35% of this force will transfer into the slab:

$$\partial N = 4.4 \times 0.35 = 1.54\ \text{MN}$$

The flange has an area of $0.0225\ \text{m}^2$, and its stress is $4.4/0.0225 = 195\ \text{N/mm}^2$, so

$$\varepsilon_a = \frac{f}{E_a} = \frac{195}{210\,000} = 0.00093$$

$$\varepsilon_c = 0$$

$$\partial\varepsilon = 0.65\varepsilon_a - \varepsilon_c = 0.00061$$

Using Equation 3.13:

$$L_s = 2(S_c\ \partial N/\partial\varepsilon)^{1/2} = 2(0.003 \times 1.54/0.00061)^{1/2} = 5.50\ \text{m}$$

$$V_l' = \partial N/L_c = 1.54/5.5 = 0.28\ \text{MN/m}$$

The total longitudinal shear is $0.48 + 0.28 = 0.76$ MN/m, or 760 kN/m.

An alternative way of estimating L_s is to assume a 1 : 2 spread from the end of the beam to the midspan of the slab. The beam is non-composite at the start of spread and fully composite beyond L_s, with the force being transferred uniformly between this length. For the Nanny Bridge, using this method $L_s = 3.4$ m, which is smaller than the previous estimate.

Aesthetic requirements on this structure dictated that the steel would be painted and covered with an architectural feature, rather than using a weathering steel. For the Nanny Bridge, the steelwork for the girders was provided with a 450 μm minimum thickness glass flake epoxy in the fabrication shop, with a polyurethane finishing coat applied on site. For the portal legs, which could be submerged in flood conditions, an extra 1 mm of steel was allowed all around, together with an aluminium spray and a 350 μm multicoat paint system.

3.10. Painting

The corrosion of steel is an electrochemical process, where the steel in the presence of oxygen and water converts to a hydrated ferric oxide, or 'rust'. The rate of corrosion will be heavily influenced by the amount of time for which the steelwork is wet. If the bridge can be detailed such that the steel section is protected, the rate of corrosion will be reduced. Atmospheric pollutants such as sulphates and chlorides will also have an effect on the corrosion rate, and consequently industrial and coastal regions will have higher corrosion rates. The steel is normally painted to protect it from corrosion. The effectiveness of the paint system will depend on the surface condition of the steel, the paint or protective system used, the procedures used to apply the protective system, and the environment in which it is applied.

The performance of a protective system is highly influenced by its ability to adhere properly to the steel. Mill-scale, rust, oil, water or other surface contamination of the steel will need to be removed. Blast cleaning is usually used to clean the steel. The cleaning also creates a rough surface profile that helps the adhesion of the paint system. The process used to apply the paint and the environmental conditions when the paint is applied are also significant to the adherence of the paint. Most specifications for new bridges require the surface preparation to be done and the first coats of metal and paint to be applied at the place of fabrication, where the environmental conditions can be controlled and the paint applied by spraying. Site brush-applied paint systems are usually to be avoided except for the final finishing coat.

The protective system used will depend on the environment, access conditions and the intended life of the paint until first maintenance. Bridges in coastal regions or with difficult access will generally require a better (and usually more expensive) system than will inland structures with better access. Table 3.3 outlines some common systems for highway and railway structures. The systems use paint, or a metal coating system with paint. The metal coating is a thermal-sprayed aluminium coating.

Paint systems consist of three basic stages: a primer applied directly to the steel or to the sealed metal coating; the main intermediate stage, which may be one thick coating or several thinner layers; and,

Table 3.3 Protective systems for bridges

Environment/ access	Preparation	First coat	Second coat	Third coat	Fourth coat	Thickness: μm	Relative cost
Protected (interior of box)	Blast clean	Zinc epoxy primer	Micaceous iron oxide (MIO)			200	0.85
Inland with good access	Blast clean	Zinc epoxy primer	MIO	MIO	Polyure-thane finish	300	1
Inland with poor access	Blast clean	Epoxy primer	Glass flake epoxy	Polyure-thane finish		450	1.25
Marine or industrial	Blast clean, aluminium spray	Epoxy sealer	Zinc epoxy primer	MIO	Polyure-thane finish	400	1.6

finally, the finishing coat. The intermediate coating chosen will depend on the environment and, to some degree, the fabricator applying the system. Glass flake epoxy coating has the advantage of building up a thick layer in a single application, whereas micaceous iron oxide epoxy is applied in three or four layers. The outer layer of paint is the layer that provides the finish to the structure, particularly its final colour.

The final colour of the bridge significantly affects its character. Battleship grey has been a common colour, particularly for motorway bridges, meaning that they look very like concrete structures. The use of a dark grey or black paint can enhance the shadow effects and draw the eye to the thinner parapet coping (see Figure 4.1). Earthy green and brown colours are used particularly in rural areas; a deep blue can also blend in well. Brighter colours such as yellow or red can be used if the structure is spectacular. White or silver is popular, modern and fashionable; however, it can get dirty very quickly and require a good cleaning and maintenance regimen. The designer should take great care in the choice of colour; it is a major factor in the layman's view of the structure.

3.11. Shrinkage

In Example 3.1 it was noted that for a simply supported span the effects of concrete shrinkage can be ignored as the effects are of different signs. For a cantilever or the hogging area of a beam the effect of shrinkage is additional to the bending effects (Figure 3.14b).

For a deck slab, the shrinkage strain is estimated from Figure 1.3 and is typically 0.5 mm/m. If restrained, this shrinkage would induce a tensile force in the slab of

$$G_{cs} = \varepsilon_s E_c' A_c \tag{3.14}$$

In the actual structure, there will not be a rigid restraint and the force will be shared between the beam and slab. The proportion of the force carried by the beam or slab is dependent on its stiffness compared with that of the whole composite section:

$$G_a = G_{cs} \frac{A_a}{A_{ac}} \tag{3.15}$$

Figure 3.14 Relative free movement of slab: (a) simply supported with shrinkage and under loading; (b) cantilever with shrinkage and under loading

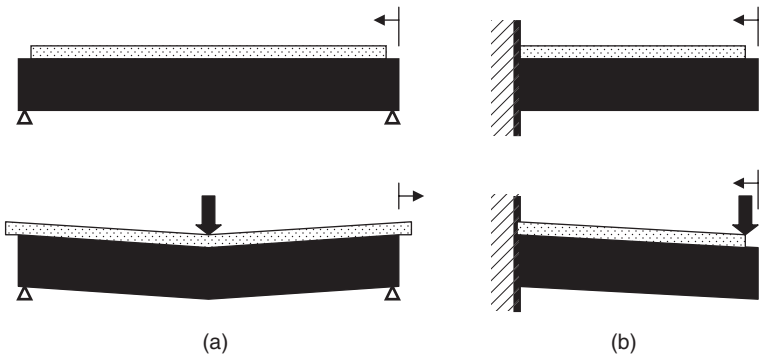

The force has to be transferred into the steel by shear connectors, and this will occur near the ends of the beam. The length over which the force is transferred will depend on the connector stiffness and can be estimated using Equation 3.13. The longitudinal shear flow (V_l) is assumed to vary from a maximum at the end of the girder to zero at a distance L_s from the end:

$$V_l = 2G_a/L_s \tag{3.16}$$

3.12. Differential temperature

Eurocode 1: Part 5, 'Actions on structures. General actions. Thermal actions' (BSI, 2003a), considers temperature effects. Generally, two types of temperature effects are considered: uniform temperature and temperature difference. The uniform temperature affects the overall movement of the bridge and may generate the K^* soil pressures considered previously in this chapter; it will also influence the design of bearings and expansion joints (see Chapter 5). The temperature difference may induce interface stresses in a composite structure, and may require consideration. Two temperature distributions across a girder are considered: a positive temperature difference with the slab hotter than the girder, and a reverse temperature difference. These temperature distributions induce forces in the slab and girder. The reverse temperature difference has an effect similar to that of shrinkage.

For Example 3.3, which is restrained rotationally at the ends producing a significant fixing moment (see Figure 3.8), the effects of shrinkage and differential shrinkage will be considered. The shrinkage strain for a slab in a damp environment is estimated as 0.035 mm/m. The concrete modulus from Equation 1.3 is

$$E'_c = 0.5E_c = 0.5 \times 34\,000 = 17\,000 \text{ MN/m}^2$$

giving a modular ratio n of 12.

The section properties are given in Appendices B and C. $A_a = 0.093 \text{ m}^2$, $A_c = 0.765 \text{ m}^2$ and $A_{ac} = 0.157 \text{ m}^2$. Using Equation 3.14, the restrained slab force is:

$$G_{cs} = \varepsilon_s E'_c A_c = 0.00035 \times 17\,000 \times 0.765 = 4.55 \text{ MN}$$

Using Equation 3.15, the force transferred to the steel girder is

$$G_a = G_{cs}\frac{A_a}{A_{ac}} = 4.55 \times 0.093/0.157 = 2.7 \text{ MN}$$

Similarly, for differential temperature the force to be transferred is 0.38 MN.

For this structure, the transfer length has already been calculated as $L_s = 5.5$ m. Using Equation 3.16, the maximum longitudinal shear is:

$$V_l = 2G_a/L_s = 2 \times (1.15 + 0.38)/4.46 = 0.67 \text{ MN/m}$$

This force is added to that previously calculated. Where critical, the effects of shrinkage and differential temperature will increase the connector requirement locally to the ends of the bridge.

REFERENCES

Bell B (2003) An integral composite bridge of high skew. *Proceedings of the ICE – Bridge Engineering* **156(4)**: 191–198.

BSI (1978) BS 5400-5:1978. Steel, concrete and composite bridges. Code of practice for design of composite bridges. BSI, London.

BSI (2003a) BS EN 1991-1-5:2003. Eurocode 1. Actions on structures. General actions. Thermal actions. BSI, London.

BSI (2003b) BS EN 1991-2:2003. Eurocode 1. Actions on structures. Traffic loads on bridges. BSI, London.

BSI (2004) BS EN 1997-1:2004. Eurocode 7. Geotechnical design. General rules. BSI, London.

BSI (2007) BS EN 1993-4-1:2007. Eurocode 3. Design of steel structures. Silos. BSI, London.

Dolling C and Hudson R (2003) Weathering steel bridges. *Proceedings of the ICE – Bridge Engineering* **156(1)**: 39–44.

England GL and Tsang CN (2000) *A Fundamental Approach to the Time–Temperature Loading Problem*. Thomas Telford, London.

Hambley E (1991) *Bridge Deck Behaviour*, 2nd edn. E&F Spon, London.

Highways Agency (1994) BD 33, Expansion joints for use in highway bridge decks. In *Design Manual for Roads and Bridges*, Vol. 2. The Stationery Office, London.

Highways Agency (2001) BD 7, Weathering steel for highway structures. In *Design Manual for Roads and Bridges*, Vol. 2. The Stationery Office, London.

Highways Agency (2002) BD 81, Use of compressive membrane action in bridge decks. In *Design Manual for Roads and Bridges*, Vol. 3. The Stationery Office, London.

Highways Agency (2003) BA 42, The design of integral bridges. In *Design Manual for Roads and Bridges*, Vol. 1. The Stationery Office, London.

Hillerborg A (1996) *Strip Method Design Handbook*. E&F Spon, London.

Peel-Cross J, Rankin G, Gilbert S and Long A (2001) Compressive membrane action in composite floor slabs in the Cardington LBTF. *Proceedings of the ICE – Structures and Buildings* **146(2)**: 217–226.

Pucher A (1964) *Influence Surfaces of Elastic Plates*. Springer-Verlag, Berlin.

Steel–concrete Composite Bridges
ISBN 978-0-7277-5810-1

http://dx.doi.org/10.1680/scb.58101.073

ice Institution of Civil Engineers publishing

Chapter 4
Continuous bridges

... the key benefit of continuity is a reduction in (or elimination of) bearings and joints ...

4.1. Introduction

The bridges considered so far have been single-span structures. For many bridges, two or more spans are required. If a bridge is required to span a 50 m wide motorway it is often more economic to use two 25 m spans rather than a single 50 m span. For most highway bridges of two or more spans it is now fairly standard to use a continuous bridge with full continuity over intermediate piers, unless there are significant settlement issues that require the flexibility given by a series of simply supported spans. Overall, a continuous structure tends to be more efficient structurally. The continuity over the intermediate piers produces a hogging moment, inducing a tension in the concrete slab and compression in the lower flange of the bridge, which reduces the efficiency of the composite structure. The concrete is poor in carrying tension and must have additional reinforcing steel added; the steel flange in compression is unrestrained by the concrete slab and more prone to buckling. There are also further complications in that high shears occur at the intermediate supports, together with large moments, which require a consideration of the shear–bending interaction.

Continuous bridges tend to be stiffer than simply supported bridges of the same span, and so the span/depth ratios can be increased (Table 4.1) compared to simply supported structures (see Table 2.1). Overall there is only a little difference in the cost of steelwork between a continuous structure and a series of simply supported spans, and the key benefit of continuity is a reduction in (or elimination of) bearings and joints.

Figure 4.1 shows a typical two span bridge over the M5 motorway to the west of Birmingham (Collings, 1994) with continuity across the spans. This motorway was widened, with the new bridges being primarily steel–concrete composite structures, which were relatively quick and simple to erect over the existing road, causing minimum disruption to traffic using the motorway.

4.2. Motorway widening

When constructing a new motorway it has been a common practice to provide structures that simply span the proposed highway. The significant growth in traffic on motorways in the UK since their construction has meant that many have required widening to increase capacity. Given the relatively short period since the original construction it has been argued that providing overlong structures to allow for future road widening would be beneficial. The benefit of this can be demonstrated by the use of a net present value calculation (Arya and Vassie, 2004), where the value of the future costs (C_f) are discounted at a chosen rate (i) over a number of years (N) to the net present value (C_{np}):

$$C_{np} = \frac{C_f}{(1+i)^N} \tag{4.1}$$

Table 4.1 Typical span/depth ratios for continuous bridges

Element	Span/depth ratio	Remarks
Constant-depth main steel girders (highway bridges)	20–25 16–20	Internal spans End spans
Haunched main girders (highway bridges)	20–30 12–20	Midspan At supports
Transverse beams for ladder-beam type (highway bridges)	10–22	
Constant-depth main steel girders (rail bridges)	10–20 8–18	Internal spans End spans
Haunched main girders (rail bridges)	15–20 9–15	Midspan At supports
Transverse beams for ladder-beam type (rail bridges)	5–20	

Consider, for example, a motorway bridge with an initial cost of £800 000 for the minimum span or £1 000 000 for an overwide layout. With a discount rate of 6% and a time to widening of 25 years the additional cost of building the minimum span and rebuilding at a future date is, using Equation 4.1,

$$C_{\mathrm{np}} = \frac{C_{\mathrm{f}}}{(1+i)^N} = \frac{1\,000\,000}{(1+0.06)^{25}} = £233\,000$$

So, the effective cost of the minimum span plus future rebuilding is £800 000 + £233 000 = £1 033 000, which is similar to the cost of building with provision for widening. This offers only a rough guide; the chosen discount rate and time to rebuilding will significantly affect costs. The issues of costs of delays

Figure 4.1 Continuous steel–concrete bridge spanning the M5 motorway (Collings, 1994)

are also ignored, although for major roads these additional costs can be significant and may be more than the rebuilding cost of the structure (Highways Agency, 1992) (see also Chapter 12). However, the over-wide bridge also has a larger carbon footprint and higher embedded energy, which should also be considered (see Chapter 2).

The discount interest rate will depend on the state of the country's economy, inflation rate, etc. The 6% used in the example was a common interest rate at the time of the first edition of this book; it still could be applied to some economies, but a lower rate should be used in Europe. If 3% is used, there is no advantage to over-widening. Such over-widening also could cause issues with regard to potential changed code requirements (see Chapter 12), further increasing costs.

Motorways may be widened in a number of ways: using symmetric or asymmetric widening, by parallel widening, or by the addition of feeder roads. In symmetric widening, the hard shoulders of the motorway are reconstructed to form a new lane, and additional shoulders are constructed. Asymmetric widening reconstructs the hard shoulder and extends the carriageways on one side only. Both these methods tend to cause significant disruption to the existing carriageways. The parallel widening technique involves the construction of a complete new carriageway adjacent to the existing one, and when this is complete modifications to the existing can be carried out. This method requires more land and is not suitable in urban locations, but causes less disruption to road users. The fourth method, constructing additional feeder roads adjacent to the existing road, causes the least disruption to traffic but can only be used if some segregation of traffic is accepted and additional land is available.

Minimising the disruption to traffic on the motorway is a key element of motorway widening, and the rebuilding of bridges requires methods that facilitate this (Iles, 1992). Steel–concrete composite bridges are one of the best ways of achieving this, as the steelwork can be prefabricated offsite and lifted in during night-time closures of the motorway. The layout of the reconstructed bridges will be different for each widening type, their character being affected by the form of widening required (Figure 4.2). For symmetric and asymmetric widening a single-span structure is favoured in order to minimise disruption during the construction of a pier. For widening to four or five lanes the spans become long and it may be more economic to provide a central pier and accept some small additional traffic disruption. For parallel widening, an asymmetric two-span layout is required to allow the new bridge to span the existing carriageways prior to its reconstruction or removal. The feeder road option gives a multi-span form.

4.3. Moment–shear interaction

The maximum design bending capacity (M_D) of a beam is derived from its section properties, including the web. In Examples 2.1 and 3.1, the web accounts for about 10–20% of the bending capacity (see also Appendix A). The maximum design shear capacity (V_d) of a beam is derived from the section, including the flanges. Equations 1.9 to 1.11 show that there is an increase in shear capacity for a beam with stiff flanges, particularly at small panel ratios. The moment–shear interaction occurs primarily at the onset of tension field action in the web (Rockey and Evans, 1981), where some local web buckling occurs and the shear is carried as a diagonal tie. If the flange is stiff, the width of the tension field is larger and the shear capacity is increased; the failure in shear involves a local bending failure in the flange.

If the beam bending capacity is derived only using the flanges such that the web is ignored (M_{flange}) there will be no interaction and the full shear capacity of the web can be utilised. If the shear capacity is derived from the web (V_{web}) assuming no flange interaction (with $V_{flange} = 0$ in Equation 1.9a) the

Figure 4.2 Bridge spans for motorway widening. (a) Single span; (b) two span – both for use with symmetric or asymmetric widening; (c) two asymmetric spans for parallel widening; (d) multi-span for feeder roads

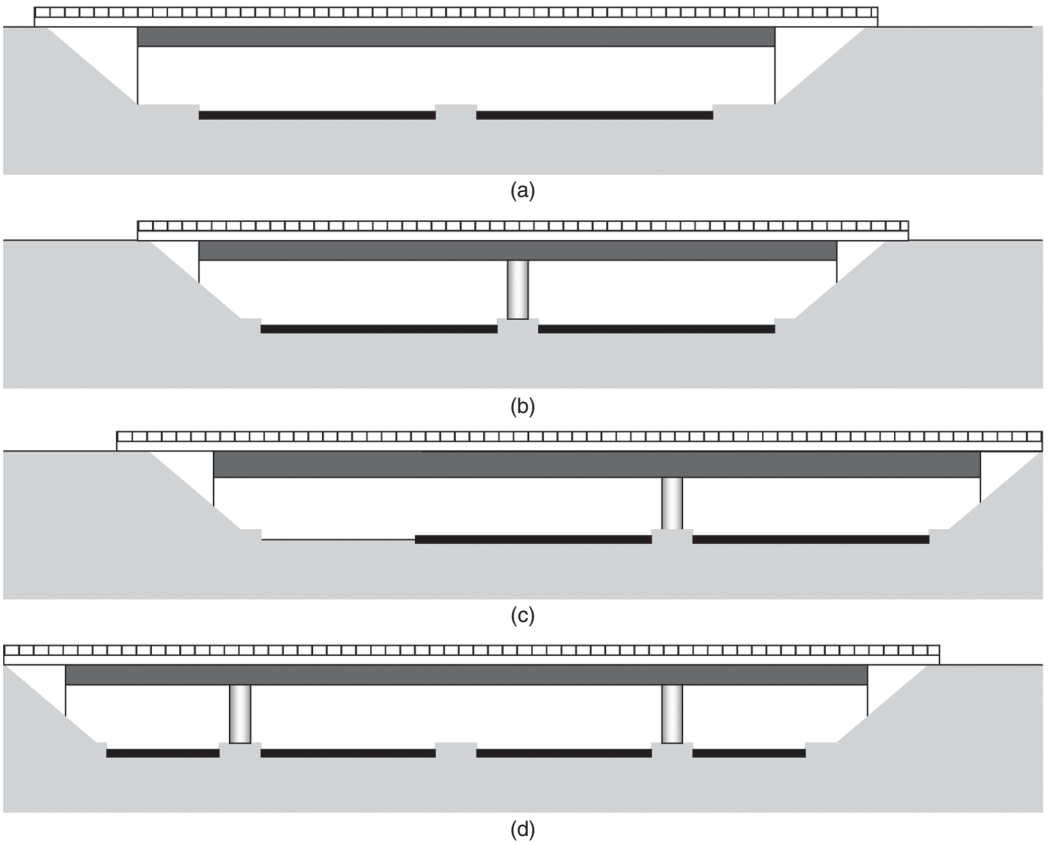

full moment capacity of the section can be carried. These simple interactions are shown in Figure 4.3a. For multi-beam bridges of 20–40 m span the difference between M_{flange} and M_{D} or V_{web} and V_{d} is small, and the simple interaction will not lead to significant conservatism. Where the girder webs and flanges are more substantial the simple interaction may lead to conservatism, and a less conservative interaction curve (see Figure 4.3b) may need to be considered (Rockey and Evans, 1981; BSI, 2000). For the interaction it is assumed that full bending can be carried at half V_{web} and that full shear can be carried at half M_{flange}. For moments greater than M_{flange} when $V_{\text{web}} = V_{\text{d}}$,

$$\frac{M}{M_{\text{D}}} + \left(1 - \frac{M_{\text{f}}}{M_{\text{D}}}\right)\left(\frac{2V}{V_{\text{d}}} - 1\right) = 1 \tag{4.2a}$$

The Eurocode method (BSI, 2005c) used a reduced bending method. For shears up to $0.5V_{\text{d}}$ the full bending capacity (M_{D}) can be used; beyond this limit a reduced moment (M_{VD}) is used:

$$M_{\text{VD}} = M_{\text{D}}(1 - \rho_{\text{v}}) \tag{4.2b}$$

where $\rho_{\text{v}} = [(2V_{\text{E}}/V_{\text{d}}) - 1]^2$. Again the resulting interaction curve is drawn in Figure 4.3b.

Figure 4.3 Shear–bending interaction: (a) simple criteria; (b) simple interaction and Eurocode interaction curve (based on example 4.1)

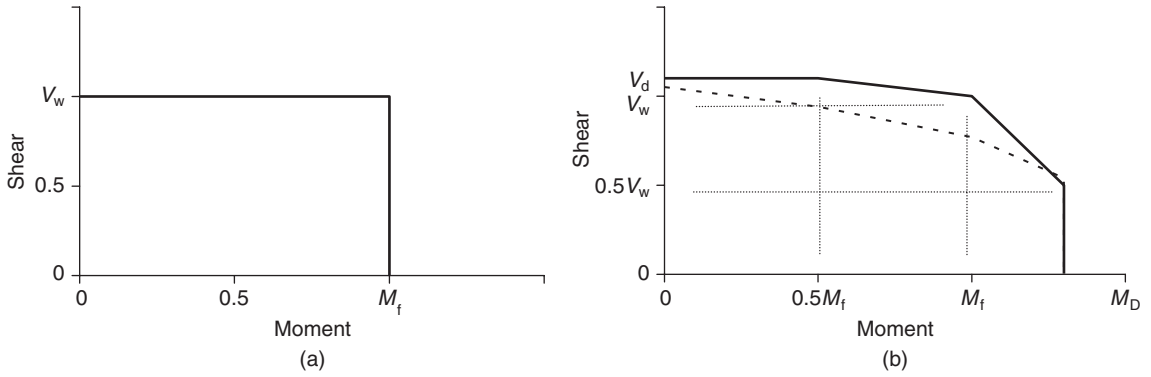

4.3.1 Tension stiffening

In a composite girder, at hogging regions near supports the top slab will be subject to a tensile force. The behaviour of the beams slab under predominantly tensile effects can be complex and involves the estimation of first cracking and tension stiffening as outlined in the stress–strain diagram shown in Figure 4.4.

Initially the concrete will be uncracked, and then at a load approaching N_{ct} the concrete will start to crack (line O–A in Figure 4.4). At loads beyond N_{ct} to approximately $1.3N_{ct}$ further cracking occurs and force is transferred to the reinforcement (line A–B).

$$N_{ct} = A_c f_{ct} \tag{4.3}$$

Figure 4.4 Stress–strain diagram outlining cracking and tension stiffening of a slab under tensile loads

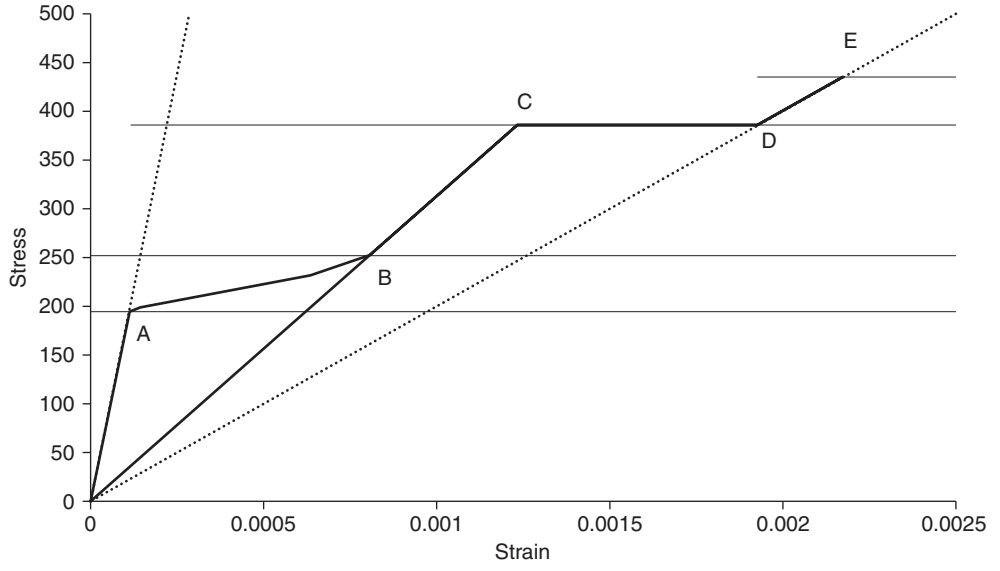

where f_{ct} is the tensile strength of concrete (see Chapter 1). Between $1.3N_{ct}$ and $2.0N_{ct}$ the load will be carried by the tension stiffened section (line B–C), which will have an effective stiffness less than the concrete section but larger than the reinforcement only (by a factor of k):

$$(EA)_{eff} = kE_sA_s \tag{4.4}$$

$$k = \frac{n\rho + (1 - \rho)}{n\rho + 0.6(1 - \rho)} \tag{4.5}$$

where n is the modular ratio and ρ is the reinforcement ratio ($\rho = A_s/A_c$).

Beyond $2N_{ct}$ tension the load is assumed to be carried by the steel only until its maximum load N_s (line C–D–E):

$$N_s = 0.87A_sf_{ys} \tag{4.6}$$

For subsequent load cycles the concrete will be cracked and the stiffness is given by Equation 4.5 for all loads (line O–B–C). This model requires sufficient reinforcement to be provided in the slab to prevent yielding of the reinforcement when the concrete cracks, or

$$A_{s2} = 1.0A_c/100 \tag{4.7}$$

This is more than the normal minimum requirements outlined in Chapter 1 (Equation 1.7a).

4.4. Example 4.1: A continuous bridge

The first example in this chapter is another bridge on a motorway around Birmingham, UK, located near the bridge in Example 3.1. The new motorway was constructed to relieve traffic on the original motorway where there was little room for widening. This bridge spans the motorway with two spans of 37.55 m and 31.34 m and is continuous across the pier. The bridge is semi-integral and is supported on a reinforced earth wall with a bank-seat (Figure 4.5). The bridge is 11.8 m wide and consists of four constant-depth girders curved in plan to follow the highway. As before, the bridge has been sized for load model 1 (LM1), uniformly distributed load (UDL) and tandem axle load (TA).

4.4.1 Loads and analysis

The loads imposed on the bridge are determined as in the previous examples. The modelling of the bridge is carried out as a grillage to estimate deck and soil loads in a similar manner as in Example 3.1. However, as the bridge is continuous some complications arise at internal supports. Three methods of analysis are available.

- Method 1. Analyse the bridge using uncracked composite section properties and assuming that the full concrete area is even over the pier. The results of the analysis are used to estimate the tensile stresses in the concrete. If the tensile force in the concrete slab exceeds N_{ct} it is assumed that the section has cracked and that the sagging moments from the analysis have increased by 10%, with no reduction in hogging moment.
- Method 2. Calculate the section properties of midspan sections as above, but at the pier and up to approximately 15% of the span to each side use section properties that ignore any concrete in tension (any reinforcement in the slab should be considered, see Appendix B) but any tension stiffening effects are ignored.

Figure 4.5 Details of Example 4.1, Walsall Lane Bridge

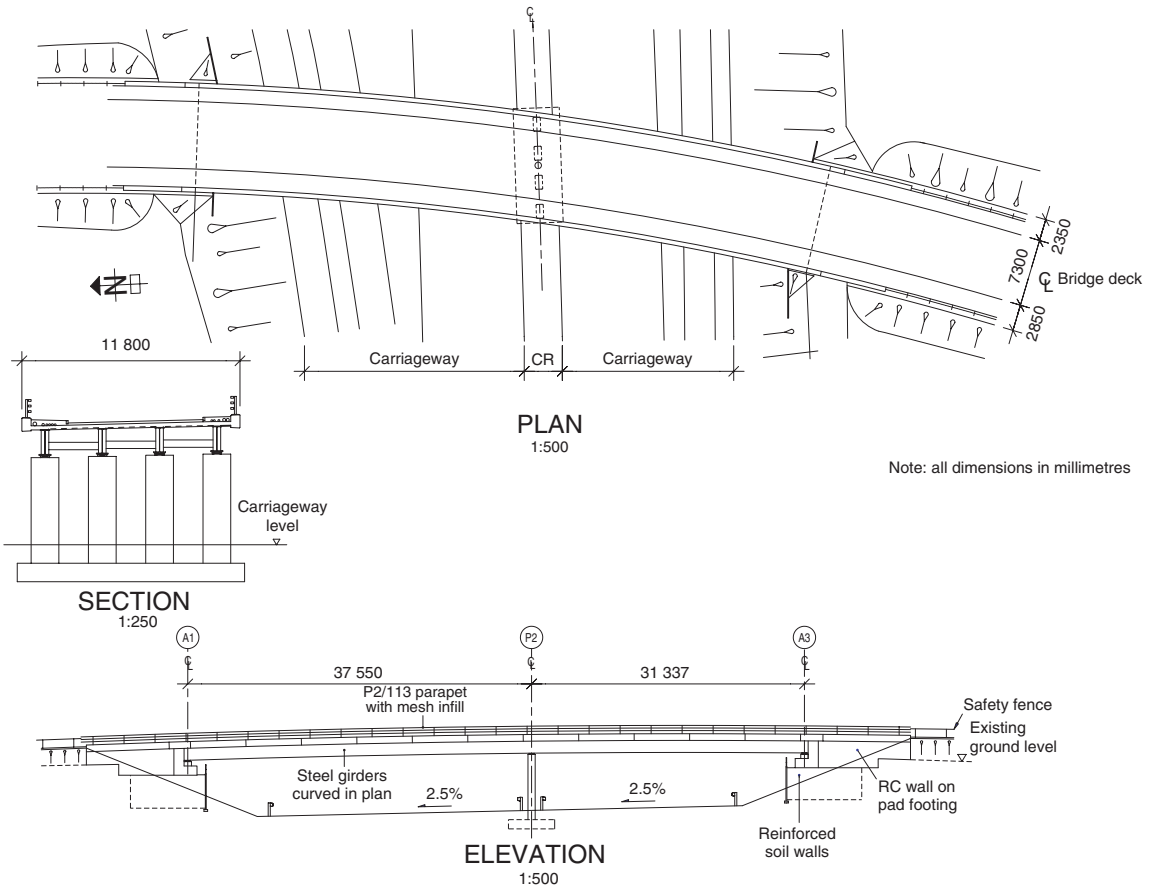

- Method 3. Analyse the bridge using uncracked composite section properties and assuming that the full concrete is area even over the pier. The results of the analysis are used to estimate the tensile stresses in the concrete. Where tensile forces in the slab exceed N_{ct} cracked section properties using tension stiffening are assumed, and where tensile forces in the slab exceed $2N_{ct}$ fully cracked section properties are assumed. The bridge is reanalysed using these revised section properties and a new set of results is obtained for bending and shear design.

Method 2 is most commonly used as with current computing methods it is relatively simple to carry out; generally it will give slightly lower design moments than method 1. Method 2 should generally be used for bridges with approximately equal spans; where spans vary significantly method 3 should be used. It should also be noted that these various methods of analysis are for moment, vertical shear and cracking only. For the design of the connectors and interface shears, method 1 results should be used.

For Example 4.1, method 2 is used. The moment and shear diagrams for analysis are shown in Figure 4.6. The moment envelope has been factored taking into account the relative section moduli

Figure 4.6 Analysis results: (a) bending moments; (b) shear

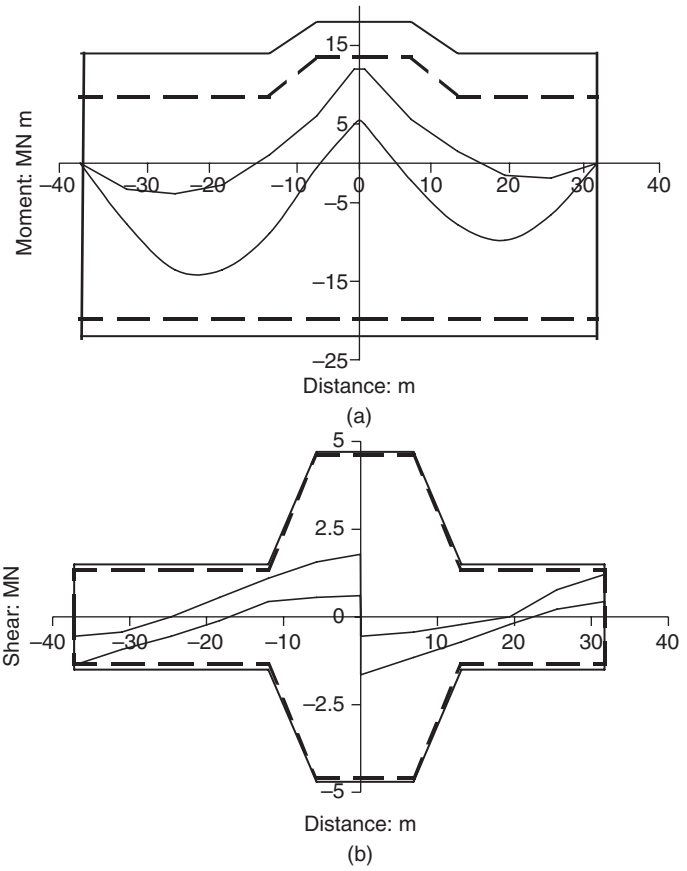

as outlined in Chapter 3 (see Equation 3.6b). It should also be noted that the values for the peak moments at the supports have been rounded.

4.5. Moment rounding

Moment rounding is common for concrete structures (Menn, 1990; Benaim, 2008) where a spread of the load from the bearing plate to the neutral axis can be visualised (Figure 4.7a). For a steel girder where the compression path has to follow stiffeners to prevent the buckling of plates, the spread of load is less clear. If a single leg stiffener is used then rounding will be small, for a multi-leg stiffener there is a greater spread of load (Figure 4.7b). The reduction in moment M' is dependent on the reaction and the width of spread

$$M' = Ra/8 \tag{4.8}$$

where R is the reaction (3.3 MN in this example) and a is the length of the effective support (1200 mm in this case):

$$M' = Ra/8 = 3.2 \times 1.2/8 = 0.5 \text{ MN m}$$

Figure 4.7 Moment rounding for: (a) a concrete structure; (b) a steel structure

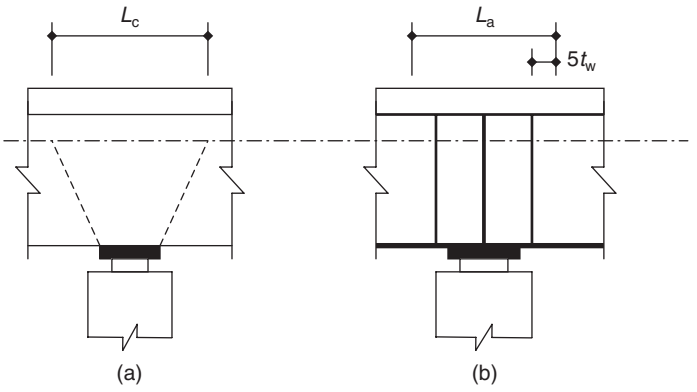

The section properties of the girder have been calculated using the steel section (Figure 4.8) and the two layers of T16 reinforcing bars at 150 mm centres in the slab (see Appendix B). $W_b = 0.058\ m^3$, $W_t = 0.045\ m^3$ and the transverse radius of gyration of the steel section (i) is 372 mm. The section is class 3.

Figure 4.8 Steelwork details for Example 4.1

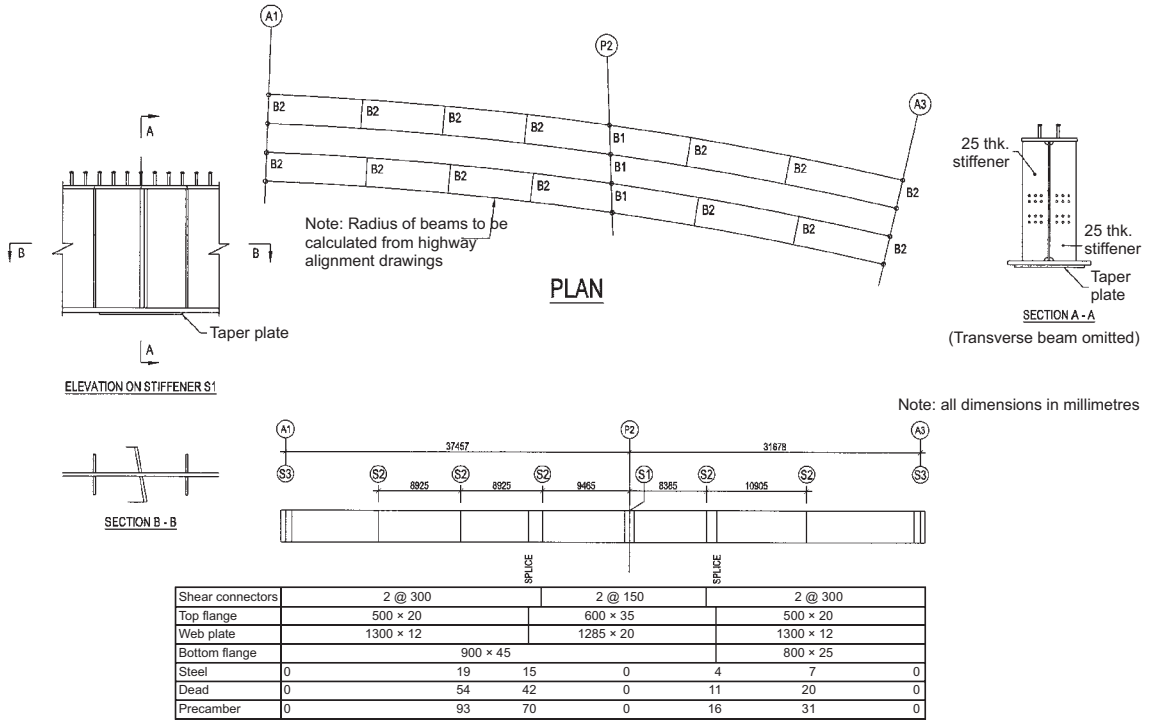

Shear connectors	2 @ 300			2 @ 150		2 @ 300	
Top flange	500 × 20			600 × 35		500 × 20	
Web plate	1300 × 12			1285 × 20		1300 × 12	
Bottom flange	900 × 45					800 × 25	
Steel	0	19	15	0	4	7	0
Dead	0	54	42	0	11	20	0
Precamber	0	93	70	0	16	31	0

The bottom flange is in compression, so the limiting compressive stress is to be estimated. For the completed bridge the slab is in place, and this has a large lateral inertia preventing a lateral torsional buckling failure mode; the mode of failure is a more local mode involving bending of webs and stiffeners. Bracing at the pier and 9.0 m either side of it are provided. Using the basic lateral torsional buckling slenderness parameter (λ) as a conservative estimate of behaviour (see Equation 2.5c)

$$\lambda = k_1 k_2 k_3 L_e / 77 i \tag{4.9a}$$

where $k = k_1 k_2 k_3$, and k_1 depends on the type and class of section and is taken as 0.95–1.0 as the girder is a fabricated section. The moment drops significantly from the support to the bracing, meaning that k_2 is usually less than 1; the compression flange has a transverse inertia less than the deck slab, so k_3 is greater than 1. For moderate spans, at the support the equation simplifies to

$$\lambda = L_e / 70 i \tag{4.9b}$$

For this example, the distance from the support to the effective brace is 9 m. Using Equation 4.9b:

$$\lambda = L_e / 70 i = 9000 / 70 \times 372 = 0.35$$

From Figure 2.7, at this value buckling is not an issue and the full moment can be carried. Using Equation 1.8d, for the bottom flange

$$M_D = f_y W_b = 335 \times 0.058 = 20.5 \text{ MN m}$$

and for the reinforcement (note the lower material factor normally used for the reinforcing steel)

$$M_D = 0.87 f_{ys} Z_t = 0.87 \times 500 \times 0.045 = 19.5 \text{ MN m}$$

The bending capacity of the beam, ignoring the web, is

$$M_{flange} = f_y A_f D \tag{4.10}$$

where D is the distance between flanges. For the bottom flange

$$M_{flange} = f_y A_f D = 0.95 \times 335 \times 0.0405 \times 1.450 = 19.7 \text{ MN m}$$

and for the top flange and reinforcement

$$M_{flange} = f_y A_f D_f + 0.87 f_{ys} A_s D_s = 335 \times 0.021 \times 1.325 + 435 \times 0.00837 \times 1.340 = 13.7 \text{ MN m}$$

The tensile capacity of the composite top flange is the lowest and most critical. M_D and M_{flange} at the support and midspan are plotted on Figure 4.6a. It can be seen that at all locations the applied moment is less than the resistance moment.

For the web $h_w/t = 1285/20 = 64$ and the web panel aspect ratio $a/h_w = 8500/1285 = 6.6$. This means that Equation 1.9b can be used:

$$V_{web} = V_d = 0.58 f_y t_w h_w = 0.58 \times 355 \times 1.285 \times 0.020 = 5.3 \text{ MN}$$

These values together with those for the midspan section are plotted on Figure 4.6b. It can be seen that at all locations the applied shear is less than the shear resistance. From Figure 4.6, it is clear that $M < M_f$ and $V < V_w$, and so no M–V interaction check is required. However, the M–V interaction diagram is drawn in Figure 4.3 using the properties of this example.

4.6. Cracking of concrete

Over a pier support of a continuous beam the deck slab is in tension, as outlined in the previous section on tension stiffening. If the stress in the concrete exceeds its limiting tensile strength then cracking will occur and the force in the concrete will be transferred to the reinforcement. For structures built in stages with the concrete initially carried by the steel section, the stresses in the reinforcement will be lower than the stresses in the steel section (Figure 4.9).

The amount of and size of cracks in the slab will depend on the stress in the reinforcement and the spacing of reinforcement bars (s_b). At the serviceability limit state the limiting crack width (w) can be approximated as

$$w = 2.8 a_s \varepsilon_m \tag{4.11}$$

where a_s is the distance from the reinforcement to the point where the crack width is considered (see Figure 4.9) and ε_m is the strain at that point. For design of uniform sections without re-entrant corners with 40–60 mm cover and bars at 125–175 mm spacing Equation 4.12 may be rearranged to give the limiting stress:

$$f_{sc} = \frac{E_s w}{1.6 s_b} \tag{4.12a}$$

For European standards (BSI, 2005b), the stress is limited in a similar way, and for bars at a spacing (s_b) of 200 mm or less the limiting stress is

$$f_{sc} = 200 - \frac{0.4 f_{ct} b h}{\alpha A_s} \tag{4.12b}$$

Figure 4.9 Build up of stresses in a composite section in hogging regions of a deck. Stresses in the reinforcement are usually lower than those of the steel girder

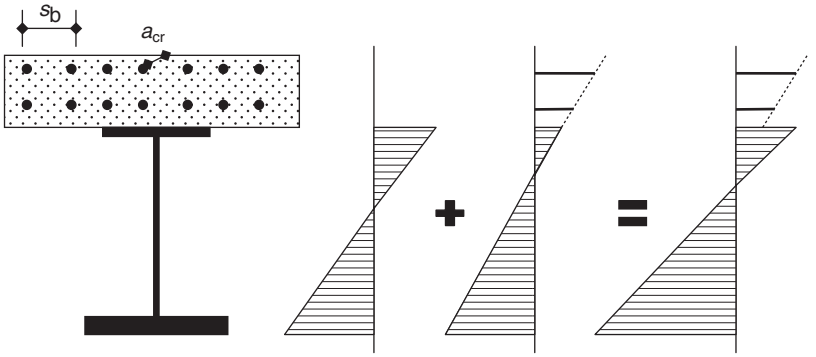

where f_{ct} is the tensile strength of concrete and α is the ratio of the area and second moment of area (AI) of the composite and non-composite section:

$$\alpha = \frac{(AI)_{a-c}}{(AI)_a} \tag{4.13}$$

The standards also recommend a minimum amount of reinforcement:

$$A_s = 0.9k_c \frac{f_{ct}}{f_s} bh \tag{4.14a}$$

f_s is dependent on the bar diameter, and so smaller bars giving higher stresses. For bars of 20 mm diameter or less, the ratio f_{ct}/f_s can be taken as 0.01. For most beam and slab bridges k_c is 1.0 and the equation simplifies to

$$A_s = 0.9A_c/100 \tag{4.14b}$$

For Example 4.2, using Equation 4.15b with $b = 3100$ mm and $h = 225$ mm,

$$A_s = 0.9bh/100 = 0.9 \times 3100 \times 225/100 = 6277 \text{ mm}^2$$

With T16 bars at 150 centres the area provided is 8308 mm^2, and so is more than the minimum requirement. Using Equation 4.13a with a crack width of 0.15 mm:

$$f_{sc} = \frac{E_s w}{1.6 s_b} = \frac{210\,000 \times 0.15}{1.6 \times 150} = 131 \text{ N/mm}^2$$

Using Equation 4.13b with $f_{ct} = 2.5$ N/mm^2 and α from Equation 4.8 using the properties from Appendix C:

$$\alpha = \frac{(AI)_{a-c}}{(AI)_a} = \frac{(0.87 + 0.008) \times 0.034}{0.087 \times 0.029} = 1.29$$

$$f_{sc} = 200 - \frac{0.4 f_{ct} bh}{\alpha A_s} = 200 - \frac{0.4 \times 2.5 \times 3100 \times 225}{1.29 \times 8308} = 135 \text{ N/mm}^2$$

As would be expected, similar limiting stresses are obtained for both methods.

4.7. Bearing stiffeners

At the pier a high reaction is transferred from the girder to the fixed bearing via a stiffener. The stiffener is required to carry this and prevent buckling of the web. If the stiffener thickness (t_s) is greater than $h_w/60$ and the stiffener to each side of the web has an outstand ratio of $10t_w$ or less, then overall and local buckling of the stiffener will not occur and the squash load of the section can be used:

$$N_s = (A_s + A_w)0.85 f_y \tag{4.15}$$

where A_s and A_w are the area of the stiffener and the web, respectively, acting with the stiffener ($30t_w$, see Figure 4.8; and similar to Figure 2.9 for intermediate stiffeners). Assuming a 250 mm by 25 mm

stiffener each side of the 20 mm web,

$A_s = 12\,500\ \text{mm}^2$

$A_w = 12\,000\ \text{mm}^2$

$N = (12\,500 + 12\,000) \times 0.85 \times 345 = 7.2\ \text{MN}$

This is significantly more than the applied reaction of 3.3 MN. The large stiffener is used to give sufficient room to bolt on the cross-beams stabilising the system. To allow future jacking for bearing replacement, additional stiffeners are located each side of the main stiffener; the jacking stiffeners are 20 mm thick. The final multi-stiffener layout gives a very robust arrangement.

4.8. Precamber

Bridges deflect under load. While there are no limits to deflections specified for highway structures, there are limits to the deflection of the steelwork supporting the concrete during construction (BSI, 2004, 2005a):

$$\delta = (L + 40)/2000 \tag{4.16a}$$

For rail bridges, particularly those on high speed lines (HSLs), deflections are more critical, and typical limits are outlined in Table 4.2. These limits lead to stiffer, deeper structures for bridges carrying railways. A significant proportion of the load of a bridge may be the weight of the structure and its finishes, and these deflections are normally precambered out such that at the end of construction the bridge is at its intended level. For a composite bridge, the deflections will occur in stages. Under the bare steel with wet concrete, the short-term composite and the long term as creep and shrinkage affect the section. The deflections at these stages should be calculated and set on the steelwork drawing to allow them to be incorporated when fabricated (see Figures 3.5 and 4.8). Generally, it is sufficient to give the deflection under steel only (such that this can be measured in the fabrication shop if required), the deflection when concrete is placed, and the total precamber.

The designer and builder should accept that there will be some inaccuracy in the prediction of deflection and precamber, as factors that affect the accuracy are numerous. The steelwork will be

Table 4.2 Deflection limits for railway bridges

Type of movement	Limit
Span/deflection limit at mid span	350 for 1 or 2 adjacent spans 450 for 3–5 adjacent spans 1250 for high-speed railway
Twist of track	0.0025 rad on any 3 m length 0.0005 rad for high-speed railway
End rotation at joint	0.005 rad for direct fixing 0.010 rad for ballasted track 0.0035 rad for high-speed railway

Figure 4.10 Slab construction sequence for Example 4.1. (a) Single pour: the pour must be complete before the concrete starts to set in order to avoid movement and weakening of the steel–concrete interface. (b) Span–span–pier casting sequence

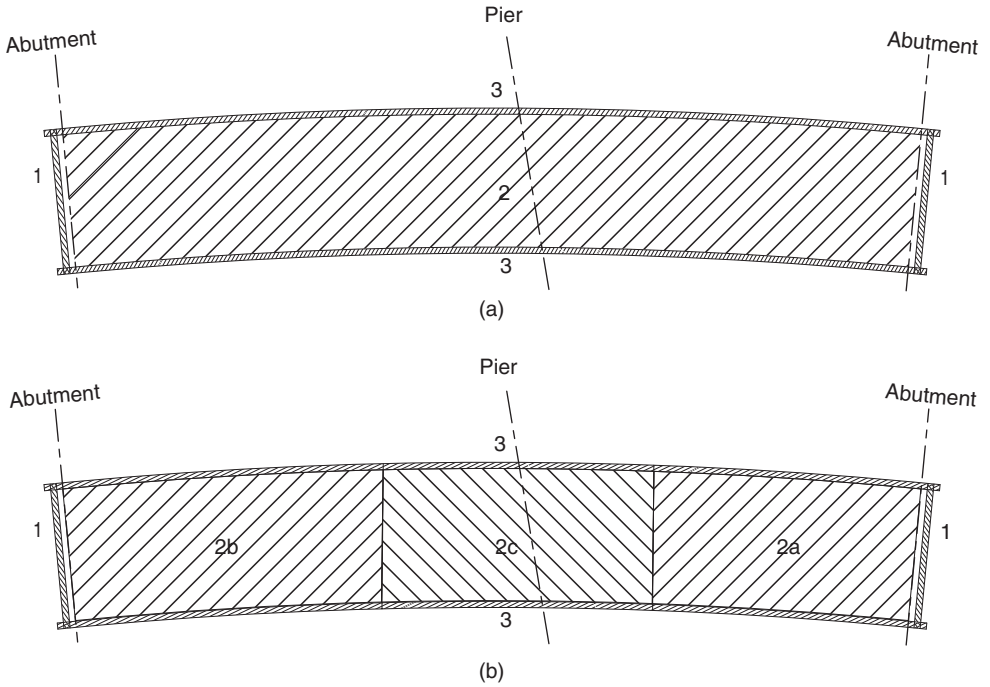

fabricated using welding; some weld shrinkage will occur, and the fabricator will make some allowance for this. Standards (BSI, 2005c, 2006) allow for inaccuracies in fabrication. A typical allowance for such inaccuracies would be the section length divided by 1000; for a section of girder near the transport limit of 27.4 m this is 25–30 mm. The thickness of the concrete slab is specified, but again there may be some variation, which will cause the deflection to vary slightly. The sequence of placing the concrete may also affect deflections. A bridge constructed using a span–span–pier technique (Figure 4.10a) will have a different deflection to one where the slab is cast in one pour (Figure 4.10b). As noted in Table 1.1 there is some variation in concrete modulus. All this will lead to a variation in girder stiffness and a range of possible deflections.

For a continuous bridge the concrete at supports is unlikely to be cracked straight after construction, leading to some difference with the idealised cracked section of design. The thickness of the surfacing will also vary slightly. The designer should consider these factors and allow some additional precamber if necessary; an allowance of span/1000 or one-third of the live-load deflection of a highway bridge has been found to be a reasonable allowance. If the bridge is relatively flat this allowance will also ensure that there is a slight upward precamber, although horizontal flanges can look as though they are sagging due to an optical illusion. The designer should also consider any additional long-term deflections. If the bridge is at its correct level during construction then some sag below this will occur in the longer term, and if precamber for this is added then the bridge will not be at the correct level at the end of construction. This issue tends to become more important on longer composite spans.

For the example of the Walsall Lane Bridge the midspan deflections are tabulated in Figure 4.8. Given that fully cracked section properties were used over the pier, values of the permanent load plus $L/1000$, or the permanent load plus one-third of the live load, are likely to be overestimates; a precamber of 93 mm is used.

The deflection for concrete is 53 mm (see Figure 4.8), and the limit for Equation 4.17 is 39 mm, so consideration needs to be given to the construction sequence, which must be specified on the drawings (as in Figure 4.10). Given these values, the deflection limit can be increased to

$$\delta = L/300 \tag{4.16b}$$

The example is comfortably within this limit.

4.9. Natural frequency

The natural frequency (f_n) of a structure is a function of its mass (m) and stiffness (K):

$$f_n = \frac{1}{2\pi}\frac{K^{1/2}}{m} \tag{4.17a}$$

The stiffness is the ratio of load to deflection; hence the first frequency of a bridge can be estimated by knowing only its deflection under permanent loads:

$$f_n = \frac{1}{2\pi}\left(\frac{9.81}{\delta}\right)^{1/2} \tag{4.17b}$$

The frequencies of various bridge structures are shown in Figure 4.11. Highway structures tend to be a little lower in frequency than rail bridges for a given span. For highway bridges on motorways or major roads vibration is not usually an issue, although movement under traffic loading may be noticed. Vibration of highway structures is normally only an issue where it is of large amplitude, as on

Figure 4.11 (a) The variation in natural frequencies with span length. (b) Results of a dynamic model showing displacement and acceleration at midspan

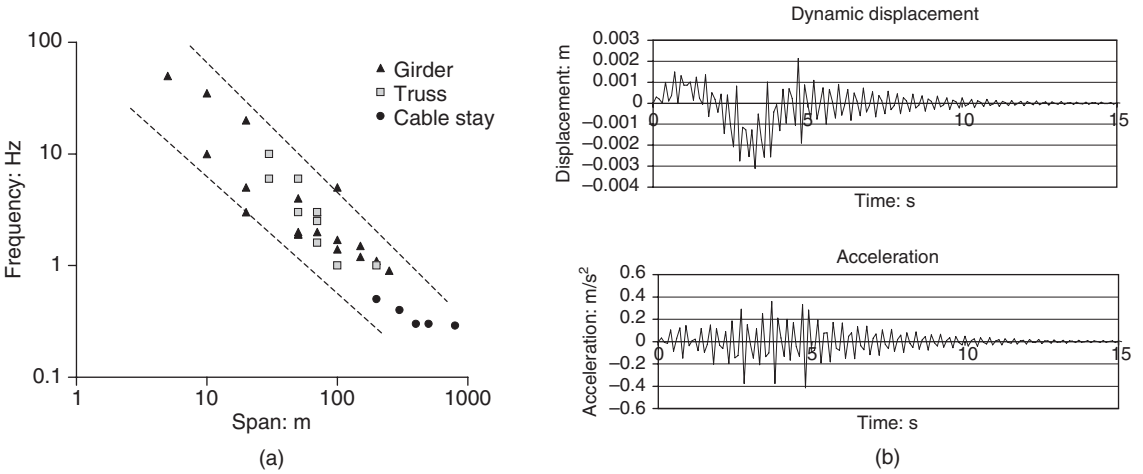

long-span structures (see Chapter 10), or if pedestrians use the structure as well as traffic. It is desirable to avoid vibration that may be near resonant frequencies or vibration that people will notice. The natural frequency of a typical vehicle is in the range 1–3 Hz, and simple dynamic checks should be undertaken if the structure frequency is in this range. A 20 tonne vehicle driving over the structure has been used as a forcing function.

For the Walsall Lane Bridge, the deflection under dead load, from the precamber table in Figure 4.8, is $19 + 53 = 72$ mm. This is calculated using the non-composite section properties; for the calculation of natural frequencies the deflection on the short-term composite is required. The short-term composite second moment of area is approximately 3.8 times greater than the non-composite one, and so the deflections will be 3.8 times smaller, and the deflection from the surfacing and other permanent loads (6 mm) will also be added. $\delta = 6 + 72/3.8 = 25$ mm. Using Equation 4.18:

$$f_n = 0.16 \times (9.81/\delta)^{1/2} = 0.16 \times (9.81/0.025)^{1/2} = 3.6 \text{ Hz}$$

A 20 tonne vehicle travelling at 50 km/h (13.9 m/s) is assumed to be travelling over the structure. The results of the analysis are given in Figure 4.11b, where the maximum amplitude and accelerations are plotted.

The limits of acceleration or deflection are subjective. For the 20 tonne vehicle a limit of the combined acceleration and displacement is

$$\Delta a = 0.003 \text{ (in units of } m^2/s^2) \tag{4.18}$$

where Δ is the dynamic deflection and a is the acceleration. For pedestrian-only bridges the acceleration would be limited to

$$a = 0.5(f_n)^{1/2} \tag{4.19}$$

For Example 4.1 the maximum acceleration is $0.4\ m/s^2$ and the amplitude is 0.003 mm. Using Equations 4.19 and 4.20, the calculated values are well below the limiting values, and so the bridge should not feel 'lively' to pedestrians when vehicles are passing.

For railway bridges vibration and dynamics are a more significant issue, the higher speeds of trains causing a greater dynamic loading of the structure. For railway bridges limits on natural frequencies are specified in Eurocode 1: Part 2, 'Actions on structures. Traffic loads on bridges' (BSI, 2003), these limits depend upon the type of railway. Table 4.3 summarises the requirements. Composite bridges on

Table 4.3 Frequency limits for rail bridges

Span, L: m	Limiting frequencies: Hz		
	$f_{min} > 120$ km/h	$f_{min} > 200$ km/h	f_{max} all speeds
10	8	6.3	17
15	5.3	3.7	12.5
25	3.5	2.3	8.5
40	2.7	1.8	6
80	1.8	1.8	3.6

Figure 4.12 Variation in load and in connector strain in a composite bridge. Based on Kiu *et al.* (2009)

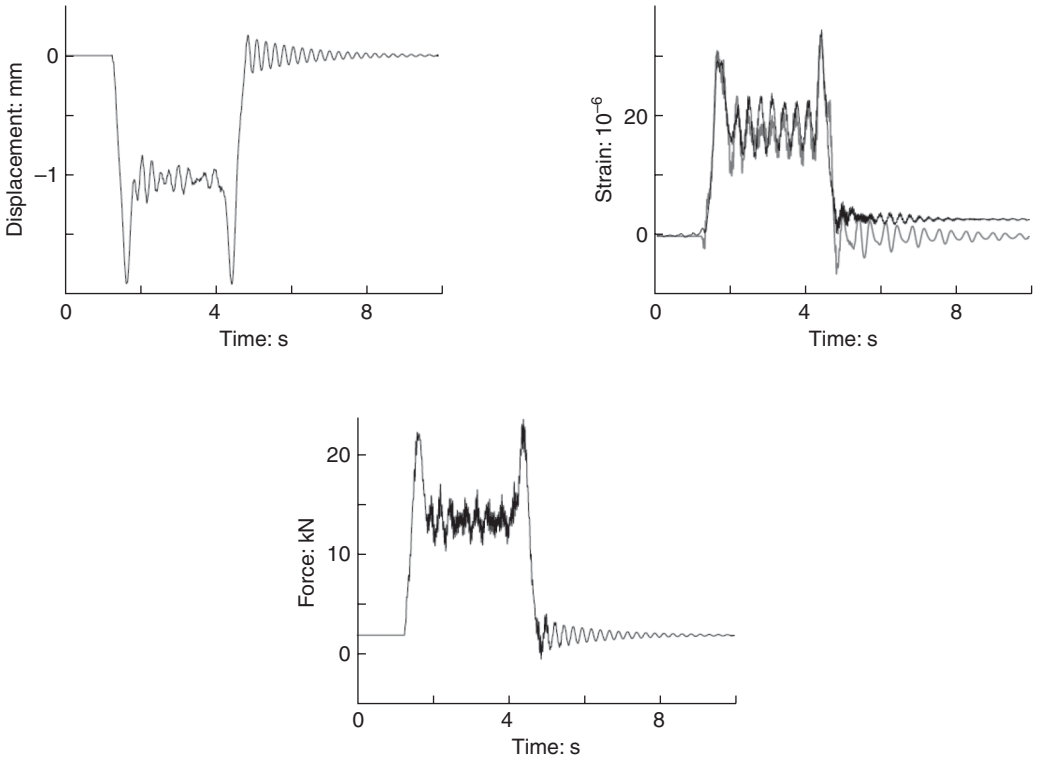

high-speed railways have been instrumented (Kiu *et al.*, 2009), showing that frequencies can be affected to some degree by the stiffness of the track and track slab and by the additional mass of the train. The variation in the connector strain also follows closely the loads applied by the train (Figure 4.12).

4.10. Loads on railway bridges

In Eurocode 1: Part 2, 'Actions on structures. Traffic loads on bridges' (BSI, 2003), the primary railway loading is the load model 71 (Figure 4.13a), this in its characteristic form is identical to RL-type loads commonly used in the UK and other parts of the world where British Standards are used. This characteristic load is multiplied by various factors for design:

$$Q_{\mathrm{E}} = Q_{71} a d \varphi \gamma_{\mathrm{q}} \tag{4.20a}$$

where a is a coefficient, ranging from 0.75 to 1.45, which modifies the characteristic loads. For normal railways in the UK, a is taken as 1.0. Where only lighter rolling stock is used and the trains are primarily for passengers rather than freight, factors below 1.0 may be used. A value of $a = 0.65$ gives a load similar in effect to RL loads (Figure 4.13b). RL is a common loading throughout the world for mass-transit systems (O'Connor and Shaw, 2000). d is a dynamic factor that varies with the span of the structure (or subelement), the frequency f_{n} of the bridge (or subelement) and the speed of the train (Figure 4.14), and φ and γ_{q} are the load coefficients and load factors which may be taken as 1.0 and 1.4, respectively, for the ultimate limit state. The basis of the type 71 loading is

Figure 4.13 Primary railway loads: (a) type 71 or RU loading; (b) type RL; (c) type SW0 loading; (d) SW2 load; (e) HSL; (f) fatigue loading

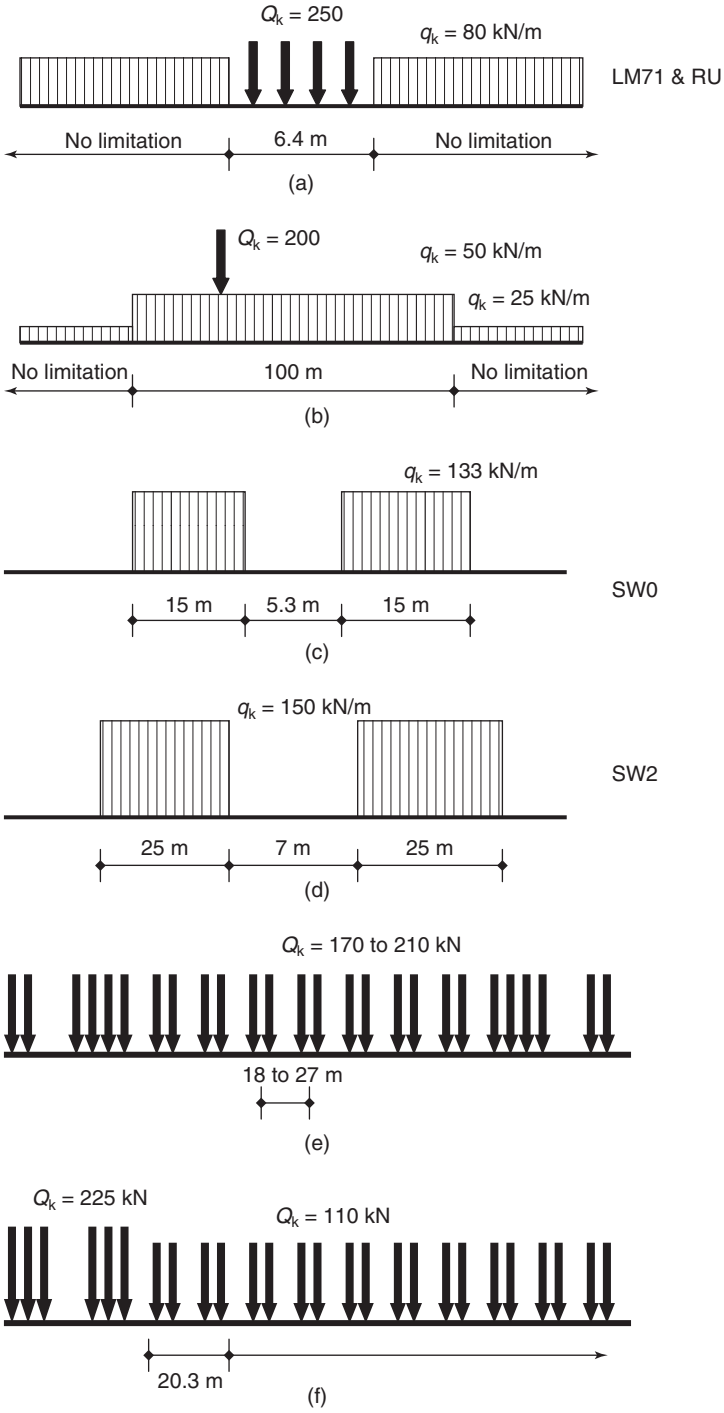

Figure 4.14 Dynamic coefficients for railway bridges

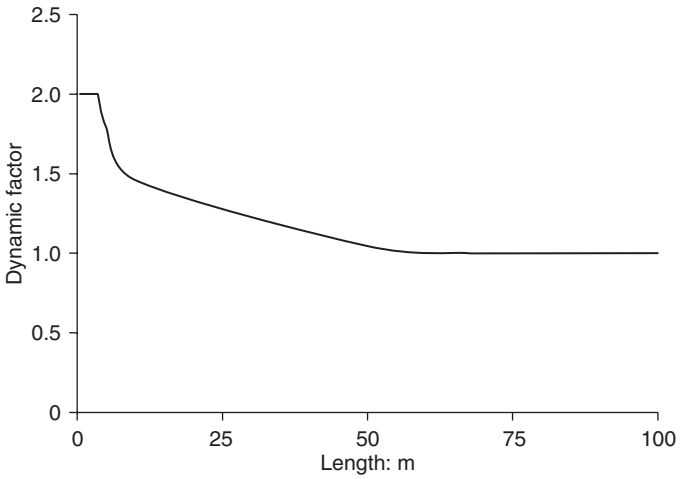

outlined in annex D of Eurocode 1: Part 2 (BSI, 2003), and for more detailed fatigue designs should this be required.

For continuous bridges, the type 71 loading should be supplemented by SW0 loading (Figure 4.13c), this is a shorter, heavier load with a variable gap between the two primary load elements. This load may govern for some load cases over continuous supports. Identical a, d, φ and γ_q factors apply to the SW0 load as to the type 71 load. Eurocode 1: Part 2 (BSI, 2003) also defines a heavy loading (type SW2), this is very similar to the SW0 load but with an a coefficient of 1.11. The type 71 loading using a static analysis with the multiplication of the load using the dynamic factors etc. is applicable to many bridges, particularly typical continuous girder or simple box bridges. Eurocode 1: Part 2, however, notes that a dynamic analysis may be required. Figure 4.15 gives a flowchart outlining when this is needed; typically it is only required for non-standard structures or structures on HSLs.

$$Q_E = Q_{SW} ad\varphi\gamma_q \tag{4.20b}$$

The type 71 loading is applicable to speeds up to 200 km/h (55 m/s); for speeds above this a special HSL load is used (see Figure 4.13d). the HSL consists of a series of axles, for which a dynamic analysis is likely to be required; however, for shorter spans an equivalent static analysis can be carried out using the type 71 loading with $a = 0.75$ and a dynamic factor of 1.4.

$$Q_E = Q_{HSL} ad\varphi\gamma_q \tag{4.20c}$$

4.11. Through-girder bridges

Through-girder, or U-frame, bridges have the deck at lower flange level between the main girders (Figure 4.16a). The main reason for this is to limit the structural depth below the rail or road level. The transverse beams determine the structure depth below the rail. The width of a through-girder bridge would typically be limited to a single-carriageway road (two lanes with footway) or twin-track railway. A U-deck has been developed for smaller spans (Sadler and Wilkins, 2003), and here the girders and deck are a single fabrication (Figure 4.16b). The through-girder bridge layout is not

Figure 4.15 Flowchart for dynamic analysis

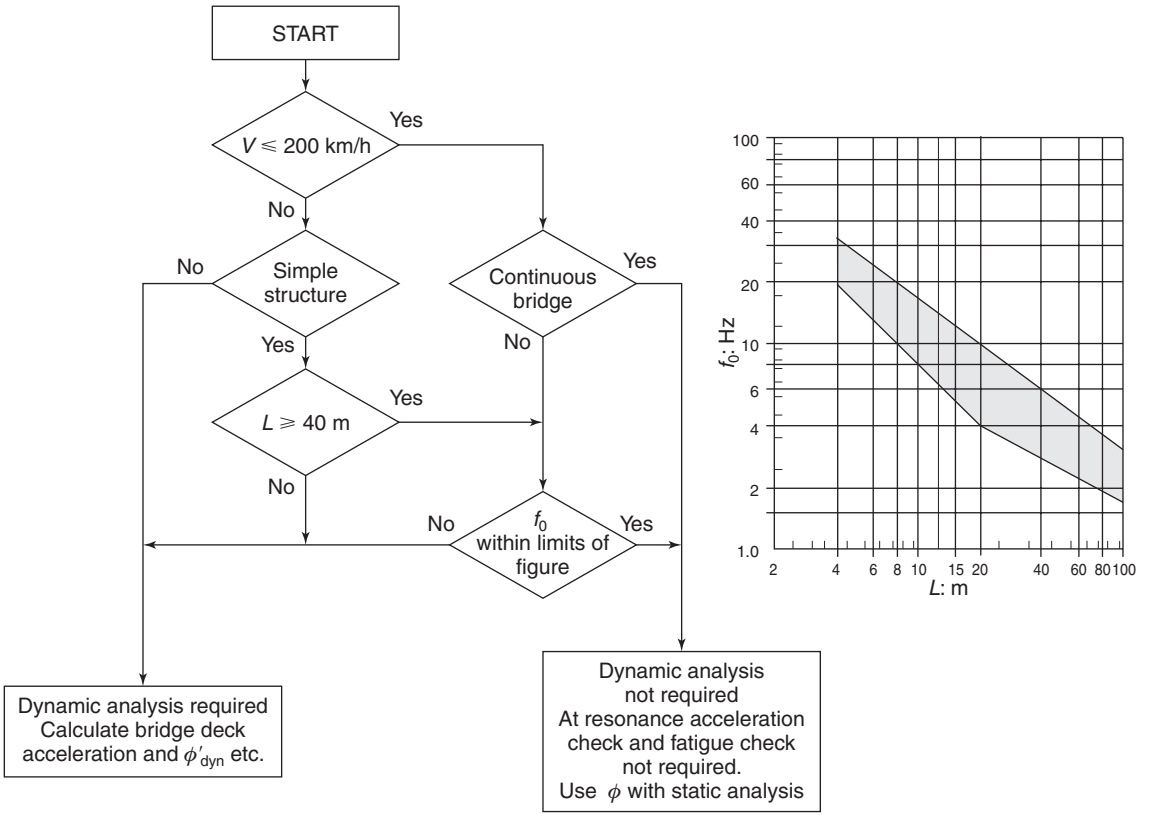

ideal for steel–concrete bridges, as the concrete deck is predominantly in the tension zone and the top compression flange is unrestrained for most of the bridge length.

The transverse deck beams and transverse web stiffeners are used as a U-frame restraint (Figure 4.17) to partially restrain the flanges. The effective length of the flange for buckling depends on the stiffness of the U-frame:

$$L_e = \pi k(EI_u L_u\ \delta)^{0.25} \tag{4.21}$$

If $L_e < L_u$ the U-frame is stiff and flange buckling will occur only between frames. If $L_e > L_u$ the U-frames only partially restrain the flange. k is a factor that depends on the support stiffness and whether the load is applied to the tensile or compression flanges. For a rigid end support $k = 0.8$, while for flexible end supports $k = 1$. If the load is applied to the compression flange the factor k should be increased by 20%. For stability, the design will tend towards the use of stiffer U-frames. However, the stiffer frames will lead to larger live-load moments at the girder to cross-beam connection. Through-girder bridges carrying railways have experienced fatigue problems at this location, and for fatigue the design will tend towards the use of more flexible connections. A key part of the bridge design will be resolving these conflicting requirements of stability and fatigue.

Figure 4.16. (a) Through-girder deck; (b) U-deck

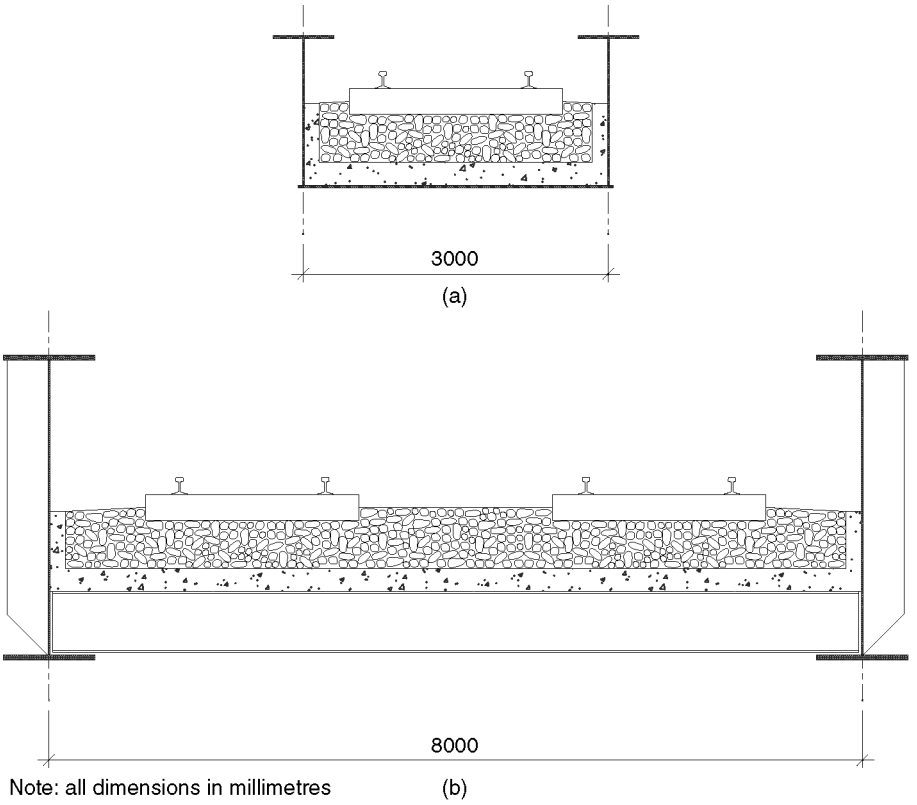

Figure 4.17 U-frame action

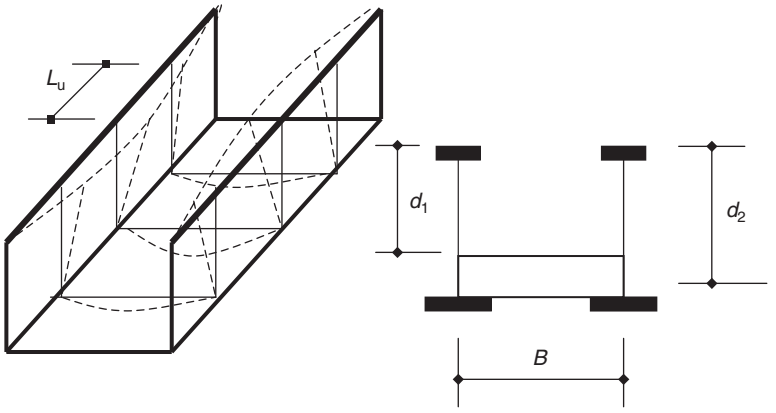

The U-frame deflection δ is calculated as

$$\delta = \frac{d_1^3}{3EI_1} + \frac{Bd_2^2}{2EI_2} + \frac{d_2^2}{S_j} \tag{4.22}$$

The first term estimates the deflection of the web stiffening, the second term the deflection caused by the cross-beam rotation, and the third term the deflection from the joint rotation. d_1, d_2 and B are defined in Figure 4.17. S_j is the joint stiffness, which varies from 100 MN m/rad or more for a relatively rigid welded and stiffened connection to 20 MN m/rad or less for an unstiffened bolted joint.

4.12. Joint stiffness

The design of joints in steel structures is outlined in Eurocode 3: Part 1-8, 'Design of steel structures. Design of joints' (BSI, 2005d). The strength design is outlined in Chapter 8 of this book. Previous UK standards (BSI, 2000) outlined typical joint stiffness as 20 MN m/rad for flexible joints, and 50 and 100 MN m/rad for more rigid welded joints. The Eurocode defines three broad types of joint – unstiffened, part stiffened and rigid – and the code also gives ways of calculating the stiffness of these joints:

$$S_j = M/\phi \tag{4.23a}$$

If the moment is considered as a force couple with force F_j and lever arm z, the equation can be written as

$$S_j = F_j z^2/\mu\Delta_j \tag{4.23b}$$

The various deformations may be calculated using test data, from codified values or using simpler methods (Collings, 2008). Table 4.4 outlines the deformations that should be considered for various joint types. Based on this, the author has calculated various joint stiffnesses, and these are presented in Figure 4.18 together with results of various tests (Collings, 2008). The values from previous UK standards are also plotted. It is clear that there is a relationship between joint stiffness and beam depth, and the old code recommendations seem valid only for shallow girders, while for deeper beams more accurate calculations (or tests) should be carried out.

Table 4.4 Deformations to be considered for various joint types when determining stiffness

Type of movement	Limit
Span/deflection limit at midspan	350 for 1 or 2 adjacent spans 450 for 3–5 adjacent spans 1250 for high-speed railway
Twist of track	0.0025 rad on any 3 m length 0.0005 rad for high-speed railway
End rotation at joint	0.005 rad for direct fixing 0.010 rad for ballasted track 0.0035 rad for high-speed railway

Figure 4.18 Joint stiffness plotted against beam depth, showing calculated values, test data and previously codified stiffness values

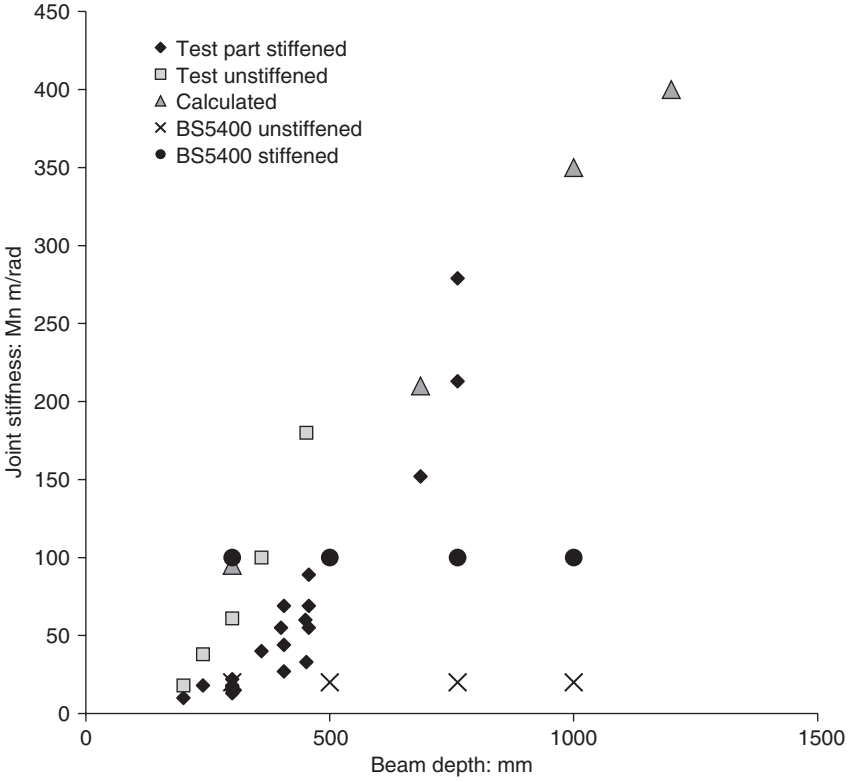

Composite joints tend to be stiffer than all-steel joints, Eurocode 4: Part 1-1, 'Design of composite steel and concrete structures. General rules and rules for buildings' (BSI, 2004) modifies the formula for joint stiffness to

$$S_{jc} = kS_j \tag{4.23c}$$

$$S_j = F_j z^2/\mu\Delta_j + \Delta_v + \Delta_c \tag{4.23d}$$

where Δ_v and Δ_c are the deformations of the connectors at the steel–concrete interface and the deformation of the concrete, respectively.

4.13. Example 4.2: A through-girder bridge

This is the first of the railway bridge examples; a three-span through-girder structure carrying a light rail (metro) system across highly skewed mainline tracks. In order to avoid the substantial construction issues associated with large-skew abutments adjacent to the railway, an extra span is added at each side, resulting in a continuous structure with three spans. The span lengths are 30–31 m, 42–43 m and 32–33 m. A benefit of this arrangement is that, structurally, the girders and cross-beams have no significant skew; the arrangement is also visually more open. The steel girders vary from 2.5 m

to 3.5 m deep. Cross-beams at 3 m centres span the 9–15 m between girders and are 500–700 mm deep. A grade 40 concrete slab, 250 mm thick, spans between cross-beams and supports track plinths (no ballast is used on the bridge).

4.13.1 Loads

The structure is designed using RL loads. As noted above this is equivalent to type 71 loading with $a = 0.65$. The dynamic magnification factor is taken from Figure 4.14 as 1.2 for both longitudinal and transverse analysis.

4.13.2 Analysis

Analysis of the structure can again be carried out using a grillage. However, the deflection of the transverse beams will induce lateral loads in the top flange of the main girders that cannot be obtained directly from the grillage. The moments in the flange can be estimated using simplified equations or a beam on elastic foundation analysis. Alternatively a three-dimensional frame analysis could be used to determine coexistent moments in both the vertical and horizontal directions. The beam on elastic foundation model is a useful analysis method for many structural forms, including box girders (see Chapter 7). For this example, the transverse moments are determined using this method. The results of the various analyses are summarised in Figure 4.19.

4.14. Shear lag

For the multi-beam bridge examples considered so far with spans of 30–40 m and a beam spacing of 3–3.6 m ($b/L = 0.1$), we have assumed that plane sections remain plane and that the full width between beams can be utilised. For twin-girder bridges, where the width is relatively large, these assumptions

Figure 4.19 Results of the Metro flyover structural analysis

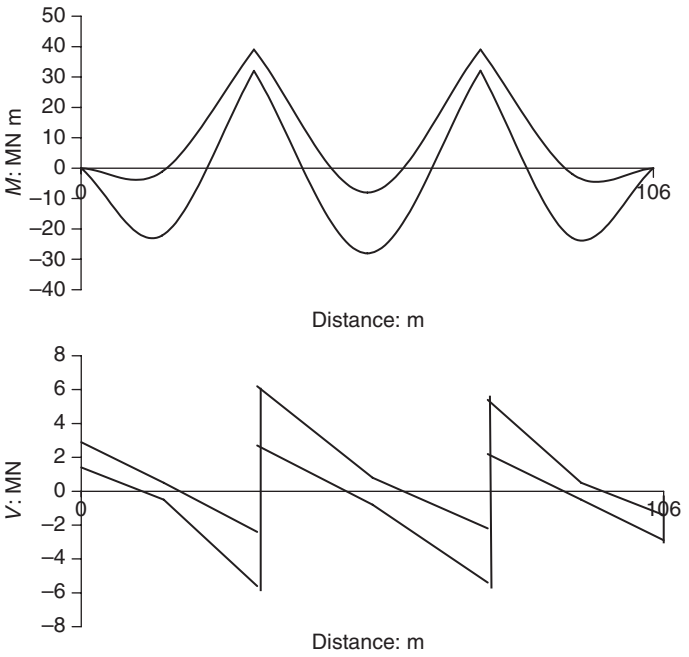

Figure 4.20 Variation in stress across a flange due to shear lag

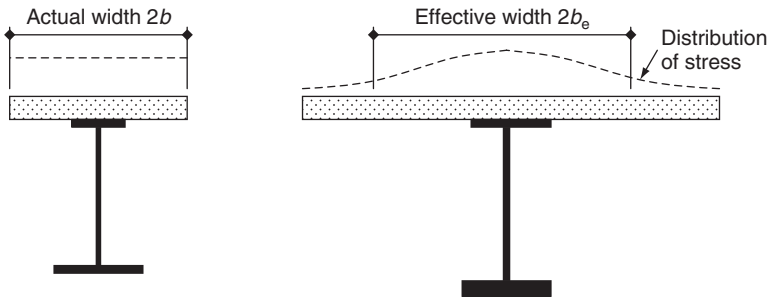

may not be correct. The slab has some in plane flexibility, and when loaded a small displacement occurs; the wider the slab the more flexible it is, and the larger the shear displacement or lag. The shear lag causes a variation in longitudinal stress across the section, with the stress dropping as the distance from the beam web increases (Figure 4.20).

For steel structures the shear lag is commonly allowed for by using an effective width factor. The factor varies with the width/span ratio (b/L), the type of span (simply supported or continuous), and the location on the span and the type of load applied. Point loads cause more shear lag than uniform loads. The effective width factors are tabulated in codes (Collings, 2005).

For concrete structures a simpler approach is often taken, and the effective width is taken as the width of the beam plus one-tenth of the span (BSI, 1992). For steel and concrete composite structures, where the shear lag generally affects the concrete slab, the simpler approach seems logical, and the latest Eurocodes (BSI, 2004, 2005f) use a similar approach:

$$b_{\text{eff}} = b_{\text{o}} + L_{\text{c}}/8 \tag{4.24}$$

where b_{o} is the width across the connectors on the beam and L_{c} is the distance between points of contraflexure.

For calculation of section properties at the serviceability limit state and for fatigue, shear lag should be taken into account. At the ultimate limit state, shear lag can be neglected. However, it is often taken into account, as this saves calculation of more section properties. As slab stresses are rarely critical, the degree of conservatism is small. For the Metro flyover the slab is not continuous beyond the beam and stops at the web, $b_{\text{o}} = 0$. The span between points of contraflexure is 30 m ($0.7L$), and at the pier the distance between points of contraflexure is 11 m. Using Equation 4.25

$b_{\text{eff}} = 0 + 30/8 = 3.75$ m, at midspan

$b_{\text{eff}} = 0 + 11/8 = 1.4$ m, at the pier

It can be seen that the effective width at the support is significantly smaller than at midspan. Both widths are significantly smaller than the half width between girders (6.5 m). Section properties for the midspan and pier girder sections together with the cross-beams are summarised in Appendix C.

Having ascertained the section properties and the effect of shear lag, the investigation of the U-frame behaviour is continued. For Example 4.2, using Equation 4.17 and assuming a flexible beam to girder connection:

$$\delta = \frac{d_1^3}{3EI_1} + \frac{Bd_2^2}{2EI_2} + \frac{d_2^2}{S_j} = \frac{2.6^3}{3 \times 210\,000 \times 0.0032} + \frac{13 \times 3^2}{2 \times 210\,000 \times 0.01} + \frac{3^2}{20}$$

$$\delta = 0.09 + 0.03 + 0.45 = 0.57 \text{ m}$$

which is the flexibility of the stiffener and the joint contributing most significantly to this deflection. To stiffen the U-frame the stiffener could be formed using a T-section, stiffening this element by a factor of almost 3, and reducing the U-frame deflection to 0.51 m. Alternatively, the joint at the girder to cross-beam connection could be stiffened, reducing the deflection to about 0.15 m. Using Equation 4.22 to estimate the effective length with a flexible frame:

$$L_e = \pi k (EI_u L_u \delta)^{0.25} \tag{4.21}$$

$$L_e = \pi k (EI_u L_u \delta)^{0.25} = \pi \times 1 \times (210\,000 \times 0.0019 \times 3 \times 0.51)^{0.25} = 15.6 \text{ m}$$

which is approximately five frames long and significantly shorter than the span.

The slenderness parameter (λ) is determined using Equation 4.10a. As the steel and slab weight are a significant proportion of the load, the properties used may be those of the beam (ignoring the slab):

$$\lambda = k_1 k_2 k_3 L_e / 77i = 1.2 L_e / 77i$$

which for this example is approximately $\lambda = 1.4$.

Once the slab has been cast the structure is significantly more rigid transversely – overall lateral torsional buckling will not occur, the buckling will involve only the top flange. The slenderness parameter for this is lower than 1.4; however, the more conservative figure will be used. From Figure 2.7 the limiting moment is 40% of the full capacity:

$$M_D = \chi W f_c = 0.176 \times 0.4 \times 335 = 23.54 \text{ MN m}$$

This is greater than the applied moment of 20.1 MN m.

For the top flange, the transverse bending is $W = 0.051$ m^3, so

$$M_{DT} = W f_c = 0.051 \times 0.5 \times 335 = 8.5 \text{ MN m}$$

This is again greater than the applied moment of 5 MN m. Both the primary and transverse bending will induce compressions in the flange, and the interaction between primary and transverse bending is checked as

$$\frac{M}{M_D} + \frac{M_T}{M_{TD}} < 1$$

$$\frac{20.1}{23.5} + \frac{0.5}{8.5} = 0.85 + 0.06 = 0.91 < 1 \tag{4.25}$$

and so is satisfactory.

Figure 4.21 Typical stress ranges with cycles to failure

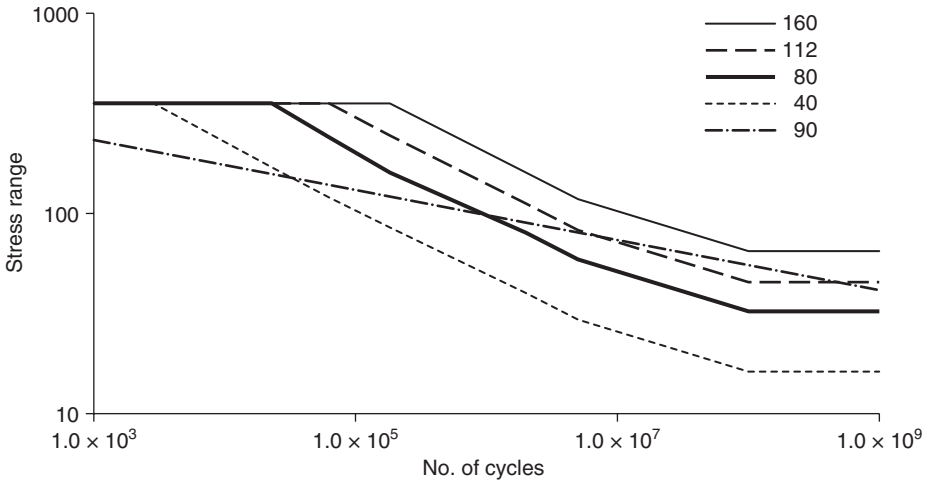

Having designed the structure, the assumptions can be reviewed, and account can be taken of the composite connection with the cross-beam, thus reducing the effective length and perhaps reducing the steelwork content by a few per cent.

4.15. Fatigue

A steel component subject to a series of load cycles may fail if the stress range during the cycles is large. Figure 4.21 shows an indication of the critical stress range for a shear stud connector (detail 90) and a steel flange, with welded attachments (details 80 and 40) and without welded attachments (details 120 and 112), with various loading cycles. Unwelded reinforcement bars have a 162 N/mm^2 stress range similar in shape (but not identical) to the unwelded steel section. From Figure 4.21, it can be seen that there is a wide range in the fatigue strength of the various details, with the unwelded reinforcing bar and steel section being the strongest, and the steel flange with welded attachments, which are potential fatigue-crack propagators, being the weakest. Broadly speaking, this means that fatigue is generally not an issue in a reinforced concrete structure, but is likely to be so in a steel structure if the design requires cleats, stiffeners, transverse girders, one-sided welds, etc. The details are classified by the reference stress ($\Delta\sigma_R$) measured at 2 million cycles (N_R). The stress limit at other cycles can be estimated as

$$\Delta\sigma_R^m N_R = \Delta\sigma_c^m N_c \tag{4.26}$$

where $m = 3$ for steelwork details at less than 5 million cycles, or $m = 8$ for shear connectors. For railways 10^7 cycles are often assumed (Collings, 2010) (although the Eurocodes define the number of cycles according on the tonnage carried per year), for a passenger line 2×10^6 trains is a good first estimate; 3×10^8 small vehicle cycles is appropriate for structures on busy motorways, and 2×10^6 cycles for heavier vehicles. For design, the limiting stress is estimated as

$$\Delta\sigma_d = \Delta\sigma_c/\gamma_{fm} \tag{4.27}$$

where γ_{fm} depends on the maintenance regimen and the importance of the structure. Assuming the bridge will have the usual maintenance and inspections over its required life, γ_{fm} may be taken as 1.35 for areas that are structurally important and as 1.15 for less important details.

Fatigue assessment for both rail and highway loads can be carried out using a simplified procedure that estimates a limiting stress range, or using a more complex damage summation calculation method (Palmgren–Miner rule). For design, the simplified method is preferred, although it may be a little more conservative. However, given the significant changes in the loading for both highway and railway structures over the last 50 years, some conservatism is justified. The tonnage of freight carried by rail has plunged significantly over this period, while that carried by road has risen. The simplified procedure involves first: determining the stress range in the connector, or other component being assessed from the fatigue load model ($\Delta\sigma_L$). For railway bridges, the stress range is calculated using the LM71 train (see Figure 4.13). For road bridges, the stress range is calculated using a 480 kN vehicle (load model FLM3). This stress is then modified by a series of factors to get the effective stress:

$$\Delta\sigma_L = |\Delta\sigma_{max} - \Delta\sigma_{min}| \tag{4.28}$$

$$\Delta\sigma_E = d\varphi\lambda\Delta\sigma_L\gamma_{fL} \tag{4.29}$$

where d is a dynamic factor for railway bridges (see Figure 4.14), φ is a local dynamic factor for parts adjacent to expansion joints, and γ_{fL} is 1.0. The term λ is a factor that accounts for damage effects, traffic volume, design life, etc. Typically, $\lambda_{max} = 2$. The structure is designed such that the stress range of the effects of the loads are less than the design limiting stress:

$$\Delta\sigma_E < \Delta\sigma_d \tag{4.30}$$

For Example 4.2, based on static longitudinal shear requirements, six connectors per linear metre are required near the quarter point. At this location there is both a longitudinal shear and a direct tension effect from the transverse cross-beam, and fatigue of these connectors may be a significant design issue. The shear on the main girder at this location from the RL load is 1002 kN/m. From Appendix C, $V_l/V = 0.156$, so $V_l = 156$ kN/m. The tension in the slab caused by transverse bending is 140 kN, and this force is assumed to be concentrated over a 1 m wide strip near the stiffeners. Using Equation 1.19, the connectors will be subject to the following combined shear and tension load:

$$V_{l\,max} = (V_l^2 + 0.33T^2)^{1/2} = (155^2 + 0.33 \times 140^2)^{1/2} = 174 \text{ kN}$$

The load in one connector is

$$P = V_l/n = 174/6 = 29 \text{ kN}$$

The stress in a connector is calculated as

$$\Delta\tau_L = P \times 425/P_u \tag{4.31}$$

In this case,

$$\Delta\tau_L = 29 \times 425/108 = 114 \text{ N/mm}^2$$

$$\Delta\tau_E = d\varphi\lambda\Delta\tau_L\gamma_{fL} = 1.2 \times 1.0 \times 1.4 \times 114 \times 1 = 191 \text{ N/mm}^2$$

At 2×10^6 cycles, $\Delta\sigma_c$ is 90 N/mm^2. The main girder is structurally important, and so γ_{fm} is 1.35:

$$\Delta\tau_d = \Delta\tau_c/\gamma_{fm} = 90/1.35 = 67 \text{ N/mm}^2$$

The effects of the fatigue load are clearly significantly larger than the limiting stress range, and significantly more connectors are required. A more refined analysis may reduce the difference, but a modification to the static design is required to meet the fatigue requirements. As there is a tension in the slab and connector, additional reinforcement will be placed to carry the tension and to prevent splitting of the slab. Tests indicate that splitting of the slab may occur prior to connector failure where connectors are placed at the end of a slab. Eurocode 4: Part 2 (BSI, 2005e) also gives further advice on this aspect, in his example the use of an upstand or down-stand at the slab–girder interface will give more space to place connectors and avoid these splitting issues.

REFERENCES

Arya C and Vassie P (2004) Whole life cost analysis in concrete bridge tender evaluation. *Proceedings of the ICE – Civil Engineering* **159(1)**: 9–18.

Benaim R (2008) *The Design of Prestressed Concrete Bridges: Concepts and Principles*. Taylor & Francis, London.

BSI (1992) BS 5400-4:1992. Steel, concrete and composite bridges. Code of practice for design of concrete bridges. BSI, London.

BSI (2000) BS 5400-3:2000. Steel, concrete and composite bridges. Code of practice for design of steel bridges. BSI, London.

BSI (2003) BS EN 1991-2:2003. Eurocode 1. Actions on structures. Traffic loads on bridges. BSI, London.

BSI (2004) BS EN 1994-1-1:2004. Eurocode 4. Design of composite steel and concrete structures. General rules and rules for buildings. BSI, London.

BSI (2005a) BS EN 1991-1-6:2005. Eurocode 1. Actions on structures. General actions. Actions during execution. BSI, London.

BSI (2005b) BS EN 1992-2:2005. Eurocode 2. Design of concrete structures. Concrete bridges. Design and detailing rules. BSI, London.

BSI (2005c) BS EN 1993-1-1:2005. Eurocode 3. Design of steel structures. General rules and rules for buildings. BSI, London.

BSI (2005d) BS EN 1993-1-8:2005. Eurocode 3. Design of steel structures. Design of joints. BSI, London.

BSI (2005e) BS EN 1994-1-2:2005. Eurocode 4. Design of composite steel and concrete structures. General rules. Structural fire design. BSI, London.

BSI (2005f) BS EN 1994-2:2005. Eurocode 4. Design of composite steel and concrete structures. General rules and rules for bridges. BSI, London.

BSI (2006) BS EN 1993-2:2006. Eurocode 3. Design of steel structures. Steel bridges. BSI, London.

Collings D (1994) M5 parallel widening. *New Steel Construction* **2**.

Collings D (2005) *Steel–Concrete Composite Bridges*. Thomas Telford, London.

Collings D (2008) Double composite steel concrete composite bridges. *Proceedings of the ICE – Bridge Engineering* **161**: 45–48.

Collings D (2010) *Steel–Concrete Composite Buildings*, *Designing with Eurocodes*. Thomas Telford, London.

Highways Agency (1992) BD 36, Evaluation of maintenance costs in comparing alternative designs for highway structures. In *Design Manual for Roads and Bridges*, Vol. 1. The Stationery Office, London.

Isles D (ed.) (1992) *Replacement Steel Bridges for Motorway Widening*. Steel Construction Institute, Ascot.

Kiu K, Lombarert G, Deroek G, Chellini G, Nordini L, Salatore W and Peters B (2009) The structural behaviour of a composite bridge during the passage of high speed trains. *Structural Engineering International* **19(4)**: 427–431.

Menn C (1990) *Prestressed Concrete Bridges*. Birkhauser-Verlag, Basel.
O'Connor C and Shaw P (2000) *Bridge Loads an International Perspective*. Spon, London.
Rockey K and Evans H (eds) (1981) *The Design of Steel Bridges*. Granada, London.
Sadler N and Wilkins T (2003) Short span railway underbridges: developments. *New Steel Construction* **Nov/Dec**: 18–19.

Steel–concrete Composite Bridges
ISBN 978-0-7277-5810-1

http://dx.doi.org/10.1680/scb.58101.103

ice Institution of Civil Engineers publishing

Chapter 5
Viaducts

. . . the most efficient form of structure . . . is a two-girder system . . .

5.1. Introduction

Viaducts are major linear structures with multiple supports; they utilise the same beam-and-slab layout as outlined in previous chapters. Due to the repetitive spans, it is more usual to look for the optimum span and structural layout. The construction method used can often have an influence on the bridge form, and again some repeatable process is likely to be the most economic. Viaducts have been built in many forms (Figure 5.1). However, experience has shown that simply supported spans or forms with large numbers of joints and bearings can create maintenance issues on highway structures. On railways, simply supported spans are still often used to minimise rail–structure interaction issues. Today, continuous forms minimising bearings and joints are encouraged for highway bridges (Highways Agency, 2001a).

5.2. Concept design

The first stage in a viaduct design is to determine the most economic material, and a steel–concrete composite structure may not necessarily be the best form. Cost differences between well-designed all-concrete structures (or even an all-steel structure for longer spans) and a steel–concrete composite structures are relatively small. Often the founding conditions or the nature of the obstacle to be crossed influences the choice. Where shorter spans can be used and where founding conditions are good, a concrete scheme may be better. For larger spans, or where the lighter deck of a steel–concrete composite structure leads to significant savings in pile numbers, a composite structure is the logical choice. The obstacle to be crossed may also dictate the use of certain construction methods (i.e. launching or cantilevering), and the experience of the contractor building the structure will heavily influence this form. The anticipated maintenance regimen will also affect the choice, and many clients require the additional costs of the future repainting of steel elements to be taken into account when considering options (Highways Agency, 1992).

Assuming a steel–concrete composite structure is chosen, its form must then be ascertained. Up to now the examples used in previous chapters have generally involved multi-beam forms (Figure 5.1a). Sometimes, in order to try to minimise the number of piers and bearings, the piers may be inset (Figure 5.1b), and this feature will lead to complex details at diaphragms and increase the steelwork tonnage, particularly where piers are at a skew. The intersection of main girders and cross-diaphragms will give rise to issues with lamella tearing, and may require a higher quality steel or additional testing. The multi-beam form is relatively simple on straight bridges but can become complex for curved structures. The multi-beam type is also not the most efficient form, particularly for wider structures, as each individual beam has to be designed to carry its share of a heavy abnormal vehicle (the TA of LM1 loading or LM3 loading, see Chapter 2), leading to more steel in the webs and flanges.

Figure 5.1 Deck forms: (a) multi-beam on piers; (b) multi-beam with integral crosshead; (c) ladder beam; (d) ladder beam with cantilevers; (e) twin beam with stringer beam; (f) twin girder

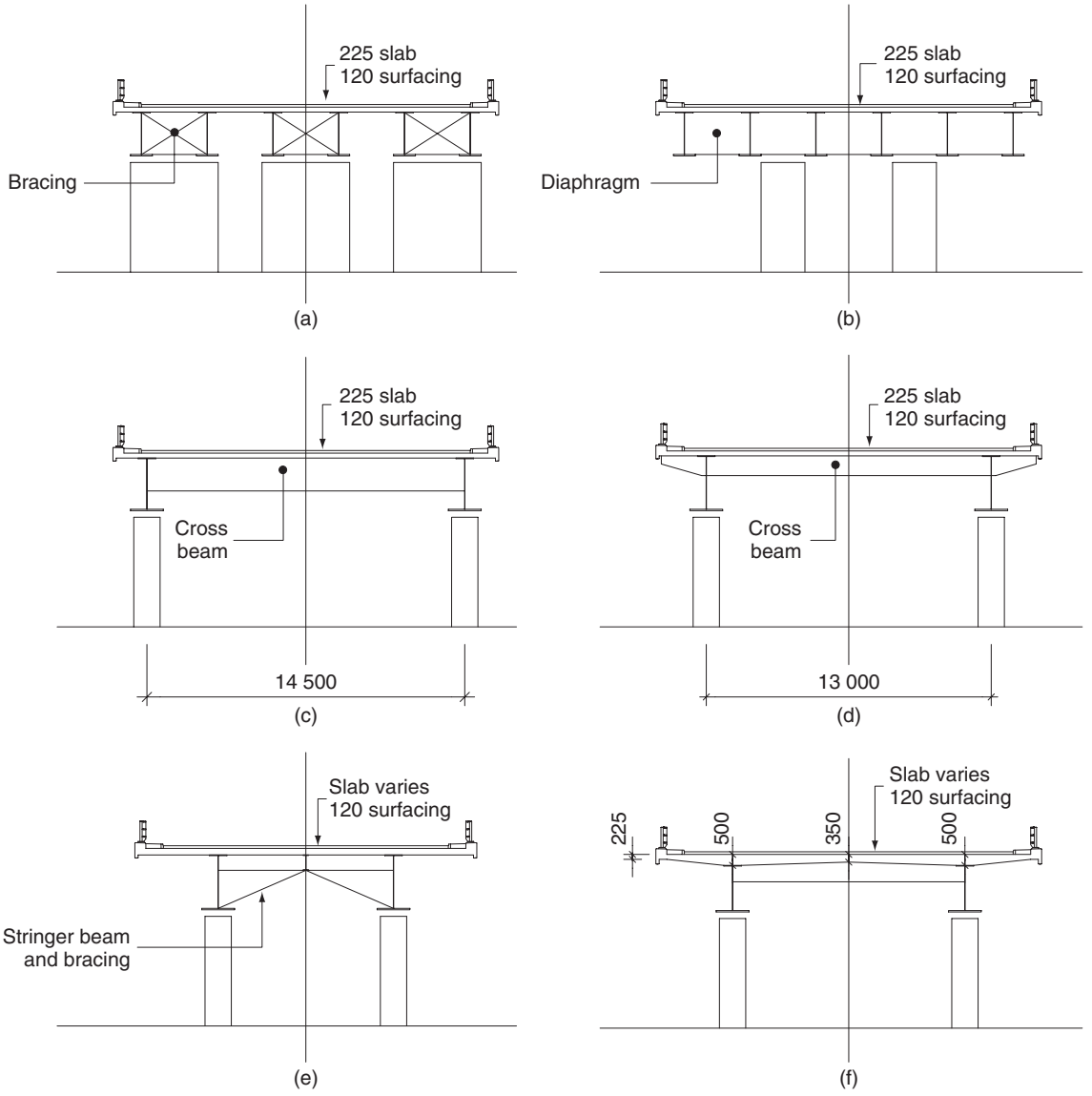

Note: all dimensions in millimetres

The most efficient form of structure for a viaduct is a two-girder system, and a number of variations on this form are viable. The most common twin-girder form is the ladder beam (Figure 5.1c), which has two main longitudinal girders with transverse cross-beams at a longitudinal spacing of 3–4 m. Permanent formwork is often used to form the slab between cross-beams. The forming of the edge cantilevers is often the most difficult feature, and so the cantilever overhang is generally limited to about 1.5 m. However, for long spans with deep girders, the short cantilevers can be visually

distracting. A variation on the ladder form is to extend the cross-beams beyond the girders to form steel cantilevers (Figure 5.1d). This allows the whole deck to be constructed using the permanent formwork system, but will increase steelwork tonnage and can significantly complicate fabrication at the girder to cross-beam connection.

Another variation on the twin-girder form is the stringer beam system (Figure 5.1e). This reduces the slab span but can again increase fabrication complexity because of the truss system supporting the stringer. The final variation considered is the plain girder system (Figure 5.1f), where the primary steelwork is limited to the main girders with the minimum bracing to provide stability. The slab is profiled and designed to carry all the loads spanning transversely. The slab thickness for this form is greater than the others, and may lead to additional steel tonnage (but not fabrication costs). A formwork gantry system would normally be used to form the slab.

5.3. Example 5.1: A viaduct structure

It is not always easy to decide on the best form of structure or the best materials. The preferences of the client, designer and builder can drive a broad spectrum of solutions. It is often simpler to look at a proposed design and assess it against the key criteria, and then modify it or propose an alternative. The first example in this chapter is the Doncaster North bridge viaduct. In the first part of the example the thought process that led to the design is explored.

The need for a road bypassing the centre of Doncaster, UK, had been required for some time, the form of the viaduct had been chosen as a post-tensioned, twin concrete box design on spans of approximately 40 m (Figure 5.2a). This form is economic, and a number of structures of this type have been constructed – the author has designed a similar concrete structure as an alternative to the proposed steel–concrete composite at another location (Collings, 2001). A prestressed concrete box can be challenging to construct for those without previous experience, and two alternatives were considered: a steel–concrete composite twin ladder beam design, and an in situ concrete twin rib design (Figures 5.2b and 5.2c). The original design primarily used spans of 40–45 m, as this was the length required to span the river, canals and railways along the line. A study of the most economic spans indicates a relatively flat curve over the 30–50 m range, and tends to show the concrete and steel–concrete composite options to have very similar costs. The steel design offered offsite pre-fabrication of the deck, which could then be launched or lifted in place; the concrete design, with its minimum materials, reduced the number of structural elements and required simpler foundations, but was more difficult to build over the railways. A fourth scheme was developed that took the minimal elements of the concrete rib and applied it to a steel–concrete composite scheme, reducing the number of main longitudinal girders from four to two, and had the pier on single pile foundations (Figure 5.2d). This design was chosen as the preferred scheme and was worked up in detail.

The viaduct superstructure consists of a steel–concrete composite ladder beam form. The twin main girders consist of 2.4 m deep constant-depth steel girders, and the top and bottom flanges were of a constant width with the thickness varying to suit the bending moments; visually this is far neater than varying the width of the flange plate. Transverse cross-beams at 3.8 m centres span the 16 m between girders. A 225 mm thick grade 37 concrete slab spans across the beams. The viaduct runs for 620 m – starting near the Yorkshire Canal, it runs north across marshy industrial land and railway sidings, and then curves across the east coast main line railway and other lines that converge at Doncaster, finally crossing the River Don and ending at an embankment on the flood plain. Flexible pier foundations were used to provide an articulation with multiple fixed bearings.

Figure 5.2 Alternative forms considered for the Doncaster viaduct: (a) prestressed concrete boxes; (b) four-girder steel–concrete composite; (c) concrete twin rib; (d) steel–concrete composite ladder beam (© Benaim)

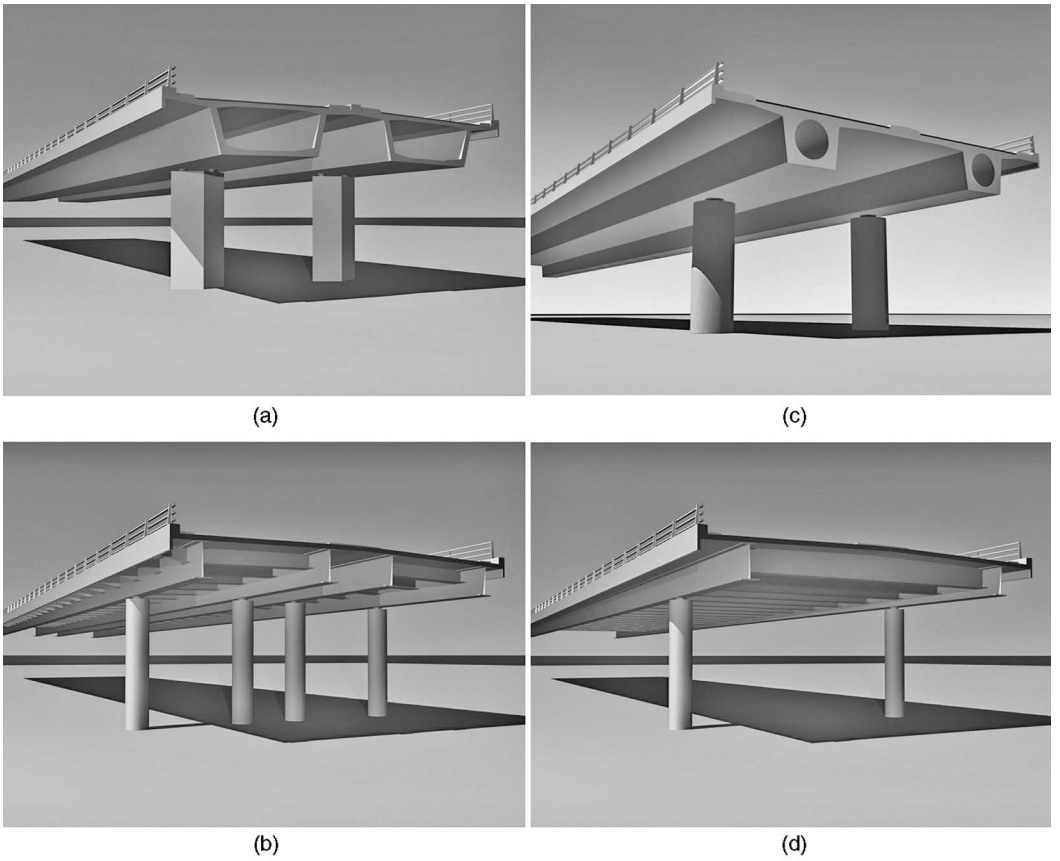

5.4. Articulation

For short spans it is possible to design bridges without bearings or joints. In the UK, for lengths up to approximately 80 m it is possible to use integral bridges without joints (see Chapter 3). For bridges over 80 m long, both joints and bearings are usually used. The bearings allow the structure to move and accommodate the strains imposed by temperature, creep or shrinkage, without inducing significant stresses. Expansion joints are used at the ends of the bridge to accommodate the movement, and to allow vehicles or trains to pass over the gap. It is possible to design long bridges without bearings if the piers can be made flexible enough; for example, the 1600 m long Stonecutters Bridge (see Chapter 10) has 70 m high piers fully built into the deck of the back spans, and no bearings.

Expansion joints and bearings have a shorter design life than the main structural elements of the bridge and will need to be replaced a number of times over the life of the structure. The number of joints and bearings should normally be reduced to a minimum. Proprietary expansion joints and bearings for highway structures can accommodate movements of +1000 mm, meaning that continuous lengths of viaduct of 2 km are possible (Collings, 2001). For railways, joints of a similar size to the highway

Figure 5.3 Articulation arrangements for railway viaducts: (a) continuous structure; (b) multi-structure form

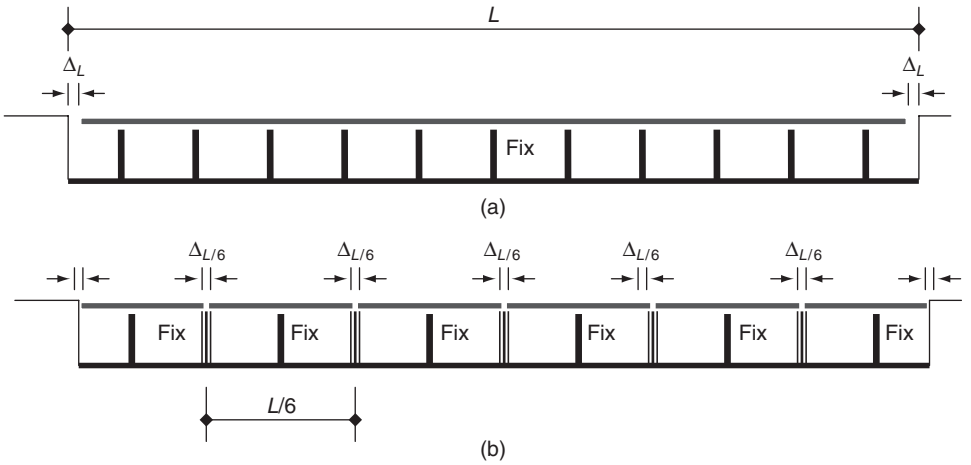

joints have been used, but these tend to be complicated and expensive. A maximum length of 1200 m has been used for recent high speed lines (Johnson, 2003). A shorter length of approximately 80 m is the limit for unjointed continuously welded track. To avoid track joints, railway viaducts are often formed of a series of short structures, each less than 80 m long (Figure 5.3b).

Traditionally, bearings have been laid out with a fixed point near the centre of the structure, with guided or free bearings beyond this, all pointing towards this bearing. This arrangement tends to require a large bearing at the fixed point, and often a larger pier and foundation to resist the applied loads. For curved alignments the movement at the expansion joints using this articulation also involves some transverse movement of the joint, which can lead to joint tearing in some situations. An alternative, 'flexible fixity', articulation is to make the piers flexible, and fix (or make integral) several bents, spreading the load to a number of piers. Beyond the fixed section the bearings are aligned parallel to the bridge girders, and for a curved alignment this means that at the expansion joint movements are only along the structure. However, there are additional transverse forces on the piers.

The layout of the fixed bearings in the Doncaster example is shown marked on the aerial view in Figure 5.4. For this viaduct with 15 spans of approximately 45 m, the permanent reaction (R) at a pier is 10 MN. Assuming a maximum coefficient of friction (μ) of 4% and a minimum of 2% (Collings, 2001), the longitudinal force on any typical pier will be

$$F = \mu R \tag{5.1}$$

$$F_{\max} = 0.04 \times 10 = 0.4 \text{ MN}, \quad F_{\min} = 0.02 \times 10 = 0.2 \text{ MN}$$

With a single fixed bearing line near the centre of the bridge the bearing will be required to carry the out-of-balance friction load:

$$F_{\mathrm{F}} = \sum F_{\max(F-i)} - \sum F_{\min(F+i)} \tag{5.2a}$$

For the example, $\sum F_{\max} = 7 \times 0.4 = 2.8$ MN and $\sum F_{\min} = 7 \times 0.2 = 1.4$ MN.

Figure 5.4 Aerial view of the Doncaster viaduct showing fixed bearings and joint locations. (Image courtesy of Morgan Sindall © unknown)

$F_F = 2.8 - 1.4 = 1.4$ MN, which is significantly larger than the typical force on other bearings, and larger than the live-load braking and traction loads defined in standards (BSI, 2003).

If now we consider the central four pier lines to be flexibly fixed, there are less piers each side of the fixed zone. $\sum F_{max} = 6 \times 0.4 = 2.4$ MN and $\sum F_{min} = 6 \times 0.2 = 1.2$ MN. At the fixed section the load is spread between the increased number (N) of fixed pier lines:

$$F_F = \left(\sum F_{max(F-i)} - \sum F_{min(F+i)}\right)\frac{1}{N} \tag{5.2b}$$

For this articulation on the viaduct, $F_F = (2.4 - 1.2)/4 = 0.3$ MN, which is similar to the forces on the other piers and significantly less than that of the single fixed-pier articulation.

5.5. Construction methods

For the steelwork of a major viaduct like the one in Example 5.1, the design is optimised, as a small saving in the weight of an element used many times can be significant overall. The optimisation will be done using methods outlined in previous chapters, and the number of iterations is selected to develop the best design. A key issue is the method of construction.

The method of construction will affect the girder size, the need for wide stable girders in crane-erected sections, or thicker webs where girders are launched. For elements lifted into place independently, the

Figure 5.5 A big lift of a complete span over the railway at Doncaster. (Image courtesy of Morgan Sindall © unknown)

first elements should be sized to be stable without the subsequent elements. For the Doncaster viaduct example, the viaduct beyond the railway and river was built element by element, with the main girders being placed prior to lifting in the numerous cross-beams. Over part of its length the viaduct is curved, and this curvature means that there is a tendency for the girder to twist sideways. To prevent twisting, temporary counterweights are used until the cross-beams are placed. The flanges are sized to give a stable structure for the girders plus the counterweights, without the stabilising cross-beams. The majority of small to medium span composite bridges are built using cranes, as for bridges with good access and space to manoeuvre a crane this method is simple and very economical. Components must be of a size that is transportable to the site; in the UK this generally means a maximum length of 27.4 m and a width or height of 4.3 m.

Over the railway and rivers at Doncaster the bridge was placed in a single 'big lift' of the steelwork and permanent formwork (Figure 5.5). During lifting the support locations for the steel will be different from those of the final situation, and may require checking. The buckling mode in this case involves two girders and the transverse beams. In this structure, the stability of the girders during concreting will be the more critical condition. The loading at this stage involves the steelwork, permanent formwork, concrete and an allowance for live loading during concreting. This allowance is assumed as 2.5 kN/m^2, and allows for minor plant, men and some mounding of the concrete as it is placed before being spread (BSI, 1996). Eurocode 1: Part 6, 'Actions during execution' (BSI, 2005), also

gives advice on loads to be considered during construction. The total design load at the ultimate limit state during construction of the bridge deck is 10.5 MN. The moment on the deck (resisted by two girders) is estimated as

$$M = 0.072GL = 0.072 \times 10.5 \times 42.5 = 32.1 \text{ MN m}$$

If the stiffness of the transverse beams is such that the beams form a stiff U-frame (such that $L_e < L_u$ using Equation 4.22), then for a single girder the buckling length will be limited to the girder spacing. This is a short length, and the buckling of a single beam is therefore unlikely to be critical; however, the transverse beams must be sufficiently deep and stiff to achieve this. For the pair of girders, instability may occur with the lateral movement and rotation of the frame, the elastic critical moment (M_{cr}) being dependent on the torsional and warping strengths of the system (Timishenko and Gere, 1961; Pandey and Sherbourne, 1989):

$$M_{cr} = (M_{cT}^2 + M_{cW}^2)^{1/2} \tag{5.3a}$$

$$M_{cT} = \frac{\pi}{L}(EIGJ)^{1/2} \tag{5.3b}$$

$$M_{cW} = \frac{\pi^2}{L^2}E(IC_W)^{1/2} \tag{5.3c}$$

where G is the shear modulus, J is the torsional constant (see Appendix E) and C_W is the warping constant. The slenderness parameter of the girder system is estimated using Equation 2.5:

$$\lambda = (M_E/M_{cr})^{1/2} \tag{5.4}$$

For most plate girder bridges the torsional resistance (M_{cT}) is small, and most of the resistance comes from the warping resistance of the girder pair, $M_{cr} = M_{cW}$. The warping resistance (M_{cW}) is primarily dependent on the distance between girders (Timishenko and Gere, 1961):

$$C_W = B^2\frac{D^3 t_w}{24} \tag{5.5}$$

$$C_W = 15^2\frac{2.4^3 \times 0.02}{24} = 17 \text{ m}^2$$

For the beams in the Doncaster example, using Equations 5.3 and 5.4,

$$M_{cW} = \frac{\pi^2}{L^2}E(IC)^{1/2} = \left(\frac{9.9 \times 210\,000}{42.5^2}\right)(0.2 \times 17)^{1/2} = 2200 \text{ MN m}$$

$$\lambda = (M_E/M_{cr})^{1/2} = (32.1/2210)^{1/2} = 0.12$$

From Figure 2.7, this means that the full capacity of the section can be carried. Using Equation 1.8c, for the two girders

$$M_D = 2 \times 345 \times 0.071 = 47 \text{ MN m}$$

which is greater than the applied moment of 32.1 MN m.

Figure 5.6 Moment and shear envelope for a launched viaduct

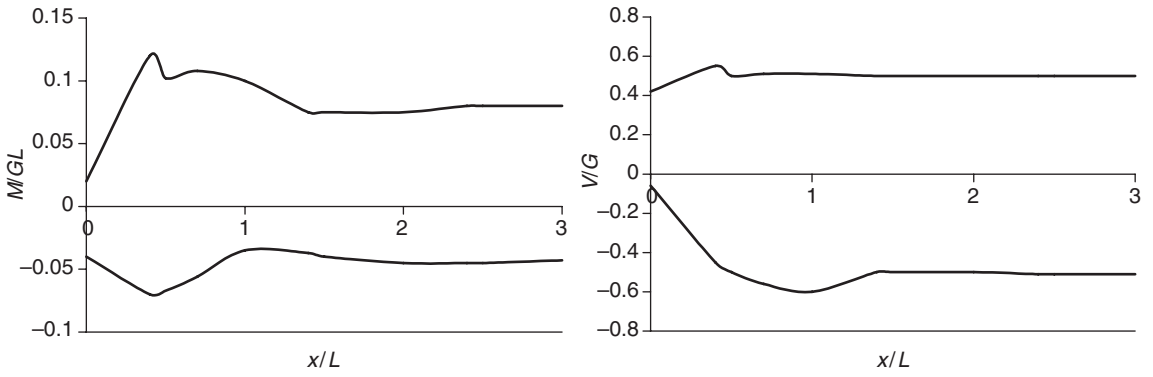

An unpropped crane-erected method of construction, which has been used in all the previous examples, is the most economic method for short and medium spans. Propping of the steelwork can be used instead of bracing to reduce the span and the effective length during construction; this also reduces the moment on the non-composite section, and allows some reduction in both the top and the bottom flanges. Propping the steelwork prior to concreting can aid slender or non-compact sections; the majority of the load is immediately carried by the composite section when the props are removed. If a single prop is used, the moment in the steelwork is approximately 25% of the unpropped value, and the top flange can be reduced. As the steel and concrete dead load accounts for about one-third of the total design load, which is now largely carried by the composite section with a 30% greater modulus, it may be possible to reduce the bottom flange. Overall, propping may save 5–15% of the girder steelwork tonnage. There will be little change in the fabrication and painting costs as the number of stiffeners, weld volume and overall painted area will be little affected. The cost of the temporary prop towers and their foundations will need to be added to the erection costs, and usually exceed the cost of the saved material. Propping is more often used for larger spans in combination with a launched construction method (see Chapter 8).

Launching of the Doncaster viaduct across the east coast main line railway was considered at an early stage, but the large lift was felt to be more appropriate for the site situation. A number of viaducts over railways have been launched into position (Calzon, 2001; Clough and Parsons, 2007). Launching involves the sequential building and launching of a viaduct from one abutment out over the obstacle, with a new section being added to the rear at each stage. A launching nose is normally used to limit the cantilevering stresses in the steelwork. The nose is shaped such that it compensates for the cantilever deflections, gradually bringing the steelwork back to level. A nose length of approximately 70% of the span is normally used for a concrete deck, less if only steelwork is launched.

The moment range in the structure during launch is shown in Figure 5.6. It can be seen that all sections of the structure need to be designed to cope with a significant moment range. The support points of the structure move as launching progresses and will bear on unstiffened portions of the web, so a check on crippling and buckling may be required unless an overthick web is used (see Chapter 8). It is common to launch the steelwork only, as this limits the moments and shears in the structure and limits the jacking forces required. The launching of the steel–concrete composite section can, however, limit the work required over the railway or other obstacle, and has been successfully carried out at, for

Figure 5.7 Sheppey bridge during launched construction

example, the Sheppey bridge (Figure 5.7). In this structure, two halves were launched from each bank and joined in the middle (Clough and Parsons, 2007).

5.6. Deck slab

The final aspect of the Doncaster viaduct to be considered in more detail is the issue of the deck-slab design and construction. The trend in UK construction practice is for maximum off-site prefabrication with minimised on-site work. The steel elements of a steel–concrete composite viaduct fit with this trend, but the in situ deck slab does not. A fully in situ deck slab requires formwork and falsework to support the wet concrete, and this has to be removed from between the girders after the slab has cured. A safer way to form the slab is to use permanent formwork, allowing some off-site prefabrication and avoiding the need to strip the soffit of formwork. If the formwork is designed to participate with the deck slab to carry loads, some economy in deck-slab reinforcement may result. The use of a full-depth precast slab with in situ stitches gives maximum prefabrication. For the full-depth precast slab, the joints between units and over beams need to be detailed carefully to achieve continuity (Figure 5.8).

Slabs for composite bridges have been traditionally designed as bending elements using fully elastic methods of analysis (Pucher, 1964), and it has been known for some time (Csagoly and Lybas, 1989; Hillerborg, 1996; Collings, 2002) that this leads to a conservative design. For most slab panels, except those of cantilever edge panels, some arching action (Collings, 2002) or compressive membrane action (Peel-Cross *et al.*, 2001) will exist (Figure 5.9), and the design issue is how to take this into account. For relatively robust slabs with a span/depth ratio of 15 or less and a span below 3.2 m, full arching action may be assumed (Highways Agency, 2002). A relatively simple internal arch within the slab is assumed to carry the wheel load. The slab capacity is estimated assuming a

Figure 5.8 Details of an in situ stitch on a precast deck slab (Ito *et al.*, 1991)

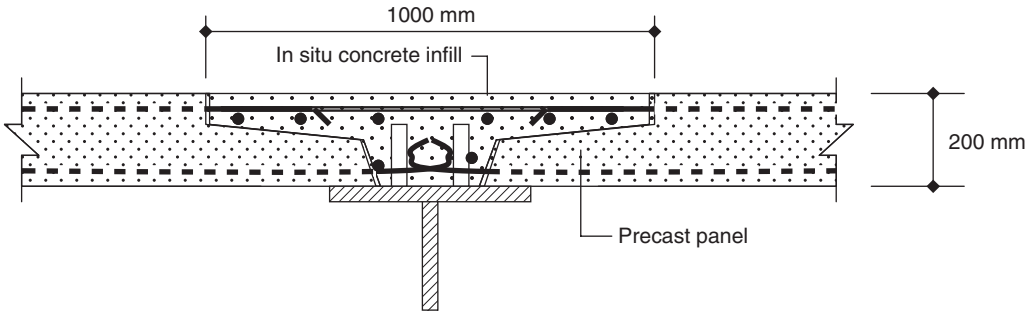

punching shear failure:

$$V_{\text{arch}} = 1.25\ (2r + d)d(f_{\text{ck}})^{1/2}(100\rho)^{1/4} \tag{5.6a}$$

$$\rho_{\text{v}} = \frac{kf_{\text{ck}}b^2}{300d^2} \tag{5.6b}$$

where ρ is an effective reinforcement ratio, r is the radius of the loaded area, d and h are the slab depth and thickness, and k is a coefficient dependent on the span/depth ratio and the strain at which plasticity of the concrete occurs (see Figure 5.9b).

For spans above 3.2 m or those with a span/depth ratio greater than 15, some arching action will occur with bending. Tests in relatively slender building structures indicate that significant arching action can still occur (Peel-Cross *et al.*, 2001). In order to estimate the degree of arching action, the relative stiffness of the in-plane and bending components need to be evaluated. The stiffer the in-plane strength of the slab, the greater the proportion of load that will be carried as an axial thrust (N) rather than bending (M).

Figure 5.9 (a) Arching action in a slab. (b) Coefficient k for arching action in a slab for various span/depth ratios and elastic strains

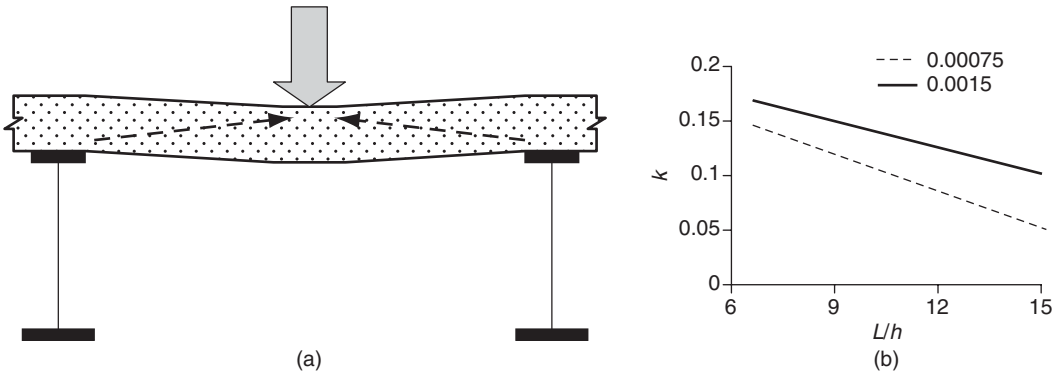

Arching action assumes an internal arch within the slab (Figure 5.9a), with the compression diagonals thrusting against adjacent concrete panels. For internal panels the restraint may be approximated as

$$K = Eh \tag{5.7}$$

Where the panel is nearer the edge of the bridge the restraint will be less (Peel-Cross *et al.*, 2001; Collings, 2002), while for cantilever edges or panels adjacent to joints no restraint should be assumed. The geometry of the arch will have a significant effect on the arch capacity; it will be dependent on the depth of slab in compression. Typically, a compression depth of $0.2h$ to $0.3h$ may be assumed, but this should be confirmed during the analysis, particularly if there are significant deflections under load.

The analysis method involves the modelling of a representative beam strip, with the beam, arch and restraints included. The slab of the Doncaster viaduct is used as an example of the method. The deck slab is of grade 40 concrete, is 225 mm thick and spans approximately 3.8 m between transverse cross-beams; it carries the LM3 abnormal vehicle loading. For this structure, the abnormal vehicle specified is identical to the HB as defined in previous UK standards (BSI, 1978; Highways Agency, 2001b) (45 units at the ultimate limit state, and 25 at the serviceability limit state). The critical design loading is with two axles of the LM3-HB bogie slightly offset from the slab midspan (Figure 5.10).

The use of a conventional strip, influence line or a simplified finite-element analysis indicates an ultimate peak hogging moment of 60 kN m/m and a sagging moment of 90 kN m/m. Using Equation 1.5 with $d = 0.75h$, or 170 mm, the ultimate capacity of the slab based on compression of the concrete is:

$$M_u = 0.2bd^2 f_{ck} = 0.2 \times 1000 \times 170^2 \times 40 \times 10^{-6} = 230 \text{ kN m/m}$$

which is two to three times the applied moment, and so the depth in compression will be significantly less than the half of the slab depth assumed (see Chapter 1). A neutral axis depth of $0.25h$ at the support and midspan will be assumed for the analysis, giving an arch rise of $0.5h$, say 100 mm. The restraint stiffness of the slab at the arch springing is estimated using Equation 5.7, assuming $E_c = 34\,000 \text{ MN/m}^2$ (see Table 1.2) and $h = 225$ mm:

$$K = Eh = 34\,000 \times 0.225 = 7600 \text{ MN m}$$

Analysis of the slab strip with the internal arch indicates an ultimate hogging moment of 55 kN m/m and a sagging moment of 78 kN m/m. The arch thrust is 350 kN/m and the midspan deflection of the slab 12 mm.

Figure 5.10 Slab strip layout showing applied load and arch geometry assumptions

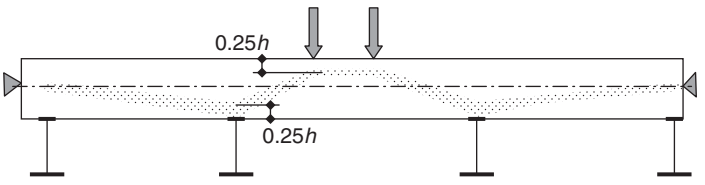

Figure 5.11 *M–N* interaction curve for a 225 mm slab, and the reinforcement requirements

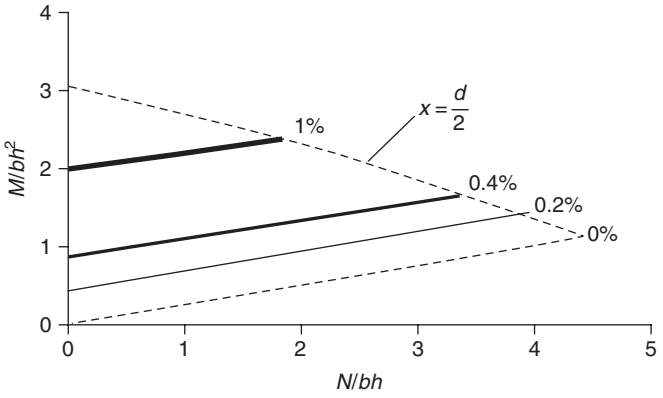

The bending capacity of a reinforced concrete section is increased by the application of a moderate co-existent axial load. An interaction curve for a 225 mm thick slab of grade 40 concrete, with various reinforcement percentages, is shown in Figure 5.11. It can be seen that there is some bending capacity with axial load, even for unreinforced slabs. At high compressive stresses the amount of reinforcement makes little difference to the slab bending capacity.

From the interaction curve for the slab without arching the reinforcement requirement for pure bending is 1300 mm^2/m for the 85 kN m/m moment. For the arched slab, the reinforcement requirement is 750 mm^2/m for the 77 kN m/m moment with 350 kN/m axial load. Figure 5.11 also outlines when the neutral axis reaches the limiting (d/2) value in the slab for various reinforcement amounts; for the arch the neutral axis depth is estimated at approximately 40 mm. Reviewing the arch geometry, a revised estimate of the arch rise is

$$r = h - 2x - \delta \tag{5.8}$$

For this example, this is 133 mm, which is larger than the rise originally assumed, and so the original assumptions are conservative. If the analysis is reiterated using the new arch geometry, a reduced reinforcement requirement is obtained due to an increased axial load and reduced moment.

A check on the punching shear capacity of the slab is also carried out. Punching shear is assumed to occur at 1.5d from the wheel load (Figure 5.12). The ultimate shear force (V) is the vehicle bogie weight of 644 kN and the shear perimeter (L_v) calculated at 10 m.

The limiting shear stress (v_c) of a grade 40 concrete slab is (Ryall *et al.*, 2000):

$$v_c = 0.74 k_1 k_2 \left(\frac{100 A_s}{L_v d} \right)^{0.33} \tag{5.9}$$

where k_1 is a coefficient dependent on the concrete strength, and is 1.0 for grade 40 concrete or more, and k_2 is a coefficient dependent on the concrete depth. For a 225 mm thick slab, k_2 is 1.22. The shear

Figure 5.12 Punching shear on the deck slab.

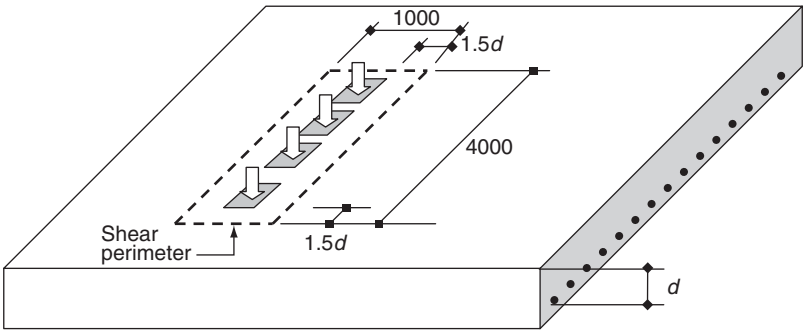

resistance of the concrete section is

$$V_{Dc} = L_v d v_c \tag{5.10}$$

For this example, the shear resistance must be at least 645 kN. Rearranging Equation 5.10,

$$v_c = \frac{V_{Dc}}{L_v d} = \frac{645\,000}{10\,000 \times 170} = 0.38 \text{ N/mm}^2$$

Rearranging Equation 5.9,

$$\frac{100 A_s}{L_v d} = \left(\frac{v_c}{0.174 k_1 k_2}\right)^3 = 0.075$$

The minimum steel in a slab is typically 0.15% of the concrete area (twice the calculated requirement), and so punching shear is not critical in this example.

REFERENCES

BSI (1978) BS 5400-2:1978. Steel, concrete and composite bridges. Specification for loads. BSI, London.

BSI (1996) BS 5975:1996. Code of practice for falsework. BSI, London.

BSI (2003) BS EN 1991-2:2003. Eurocode 1. Actions on structures. Traffic loads on bridges. BSI, London.

BSI (2005) BS EN 1991-1-6:2005. Eurocode 1. Actions on structures. General actions. Actions during execution. BSI, London.

Calzon J (2001) The abacus system for the launching of large span constant depth composite bridges. *Types and possibilities. Composite Bridges – State of the Art in Technology and Analysis, Proceedings of the 3rd International Meeting*, Madrid.

Clough R and Parsons J (2007) Design and construction of the new Sheppey Crossing, UK. *Proceedings of the ICE – Bridge Engineering* **160(3)**: 101–108.

Collings D (2001) The A13 viaduct: construction of a large monolithic concrete bridge deck. *Proceedings of the ICE – Structures and Buildings* **146(1)**: 85–91.

Collings D (2002) Design of bridge decks utilising arching effects. *Proceedings of the ICE – Buildings and Structures* **152(3)**: 277–282.

Csagoly PF and Lybas JM (1989) Advanced design method for concrete bridge deck slab. *Concrete International* **11**.

Highways Agency (1992) BD 36, Evaluation of maintenance costs in comparing alternative designs for highway structures. In *Design Manual for Roads and Bridges*, Vol. 1. The Stationery Office, London.

Highways Agency (2001a) BD 57, Design for durability. In *Design Manual for Roads and Bridges*, Vol. 1. The Stationery Office, London.

Highways Agency (2001b) BD 37, Loads for highway bridges. In *Design Manual for Roads and Bridges*, Vol. 1. The Stationery Office, London.

Highways Agency (2002) BD 81, Use of compressive membrane action in bridge decks. In *Design Manual for Roads and Bridges*, Vol. 3. The Stationery Office, London.

Hillerborg A (1996) *Strip Method Design Handbook*. E&F Spon, London.

Ito M, Fujino Y, Miyata T and Narital N (eds) (1991) *Cable-stayed Bridges. Recent Developments and their Future*. Elsevier, Oxford.

Johnson P (2003) CTRL section 1: Environmental management during construction. *Proceedings of the ICE – Civil Engineering* 156(Special Issue).

Pandey M and Sherbourne A (1989) Unified v. integrated approaches in lateral–torsional buckling of beams. *The Structural Engineer* **67(13)**.

Peel-Cross J, Rankin G, Gilbert S and Long A (2001) Compressive membrane action in composite floor slabs in the Cardington LBTF. *Proceedings of the ICE – Structures and Buildings* **146(2)**: 217–226.

Pucher A (1964) *Influence Surfaces of Elastic Plates*. Springer-Verlag, Berlin.

Ryall MJ, Parke GAR and Harding JE (eds) (2000) *Manual of Bridge Engineering*. Thomas Telford, London.

Timishenko S and Gere J (1961) *Theory of Elastic Stability*, 2nd edn, McGraw Hill, New York.

Steel–concrete Composite Bridges
ISBN 978-0-7277-5810-1

http://dx.doi.org/10.1680/scb.58101.119

ice Institution of Civil Engineers
publishing

Chapter 6
Haunches and double composite action

... a double-composite structure ... providing composite action to both the top and bottom flanges ...

6.1. Introduction

For short- to medium-span bridges the constant-depth girder is an economic solution, as fabrication is relatively simple. For longer spans the cracked concrete section over supports becomes less efficient. In order to improve the effectiveness of a continuous structure at intermediate supports, the section can be improved by haunching (increasing the girder depth locally), or by the use of double composite action (the addition of concrete to the lower flange). Both, haunching and the use of a double composite section will affect the distribution of forces in the girder and the shear flow at the steel–concrete interfaces.

6.2. Haunches

Visually, constant-depth girders can look heavy, particularly if the deck overhang is small. In general, the deck overhang should always be at least the depth of the girder, and preferably more. Haunching of the beams (Figure 6.1) allows beams with larger span/depth ratios to be used over the midsection of the span (see Table 4.1).

The moment diagram for a bridge or viaduct span (Figure 6.2) shows that deepening the girder adjacent to supports, where the moments are larger, could form a more structurally efficient arrangement. The deepening of the girder increases the stiffness and draws further moment to the support. The extent of haunching should be carefully considered, as drawing too much moment or shear to the support can be detrimental; the web slenderness increases, reducing the limiting shear stress, but also the composite section is less efficient with the upper deck in tension and the lower steel flange in compression.

The form of the haunching could be a straight haunch (Figure 6.3a), a gradual curving change in depth (Figure 6.3b) or a corbel type (Figure 6.3c) (Chen and Wang, 2009). The haunching of the steelwork will affect the design process and detailing. For the straight haunch, stiffeners are required to resolve forces where the flange changes direction. For the curved or parabolic haunch, additional in-plane forces are generated in the web, with some local transverse bending of the flange; these forces are usually small enough to avoid the need for stiffening. For both types, the flanges are not parallel, and so the shear–moment (M–V) interaction criteria (outlined in Chapter 4) may not be valid, as this method assumes some post-buckling strength. Testing has generally been confined to parallel flange beams (Rockey and Evans, 1981); where flanges are significantly non-parallel the use of an elastic buckling criteria design method (see Chapter 10) may be more applicable, leading to thicker webs. Eurocode 3: Part 1-5, 'Plated structural elements' (BSI, 2006a), limits the use of parallel-flange design methods to flanges 10° out of parallel, with the slenderness at the deepest point used to determine its class slenderness parameters.

Figure 6.1 Sketch of alternative bridge forms for a motorway, with a constant-depth girder (top) and haunched girders (bottom)

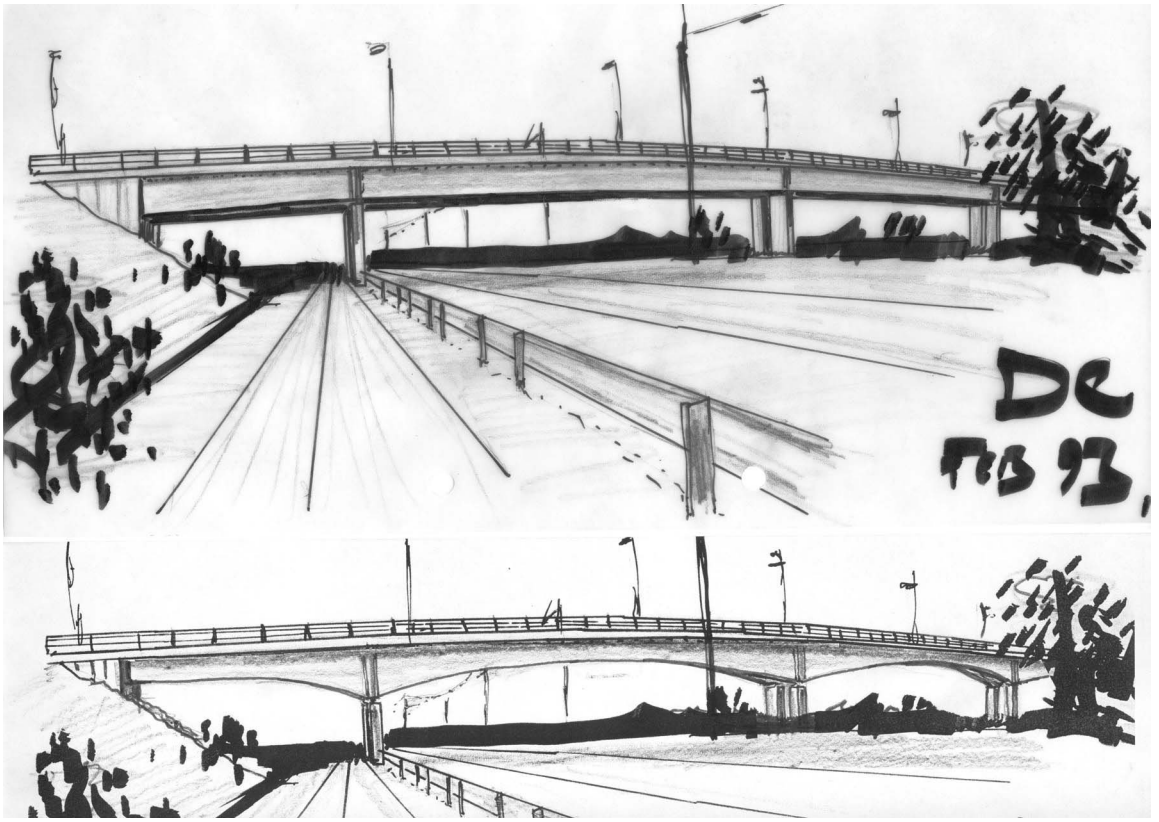

Figure 6.2 Moments on a viaduct span with increasing relative haunch stiffness

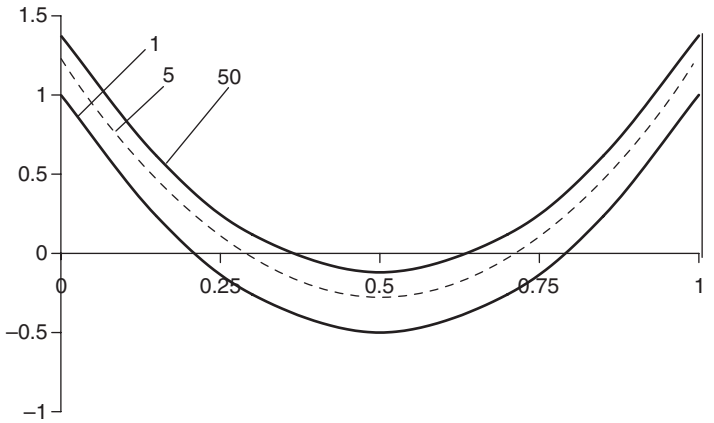

Figure 6.3 Forms of haunching: (a) curved; (b) straight; (c) corbel

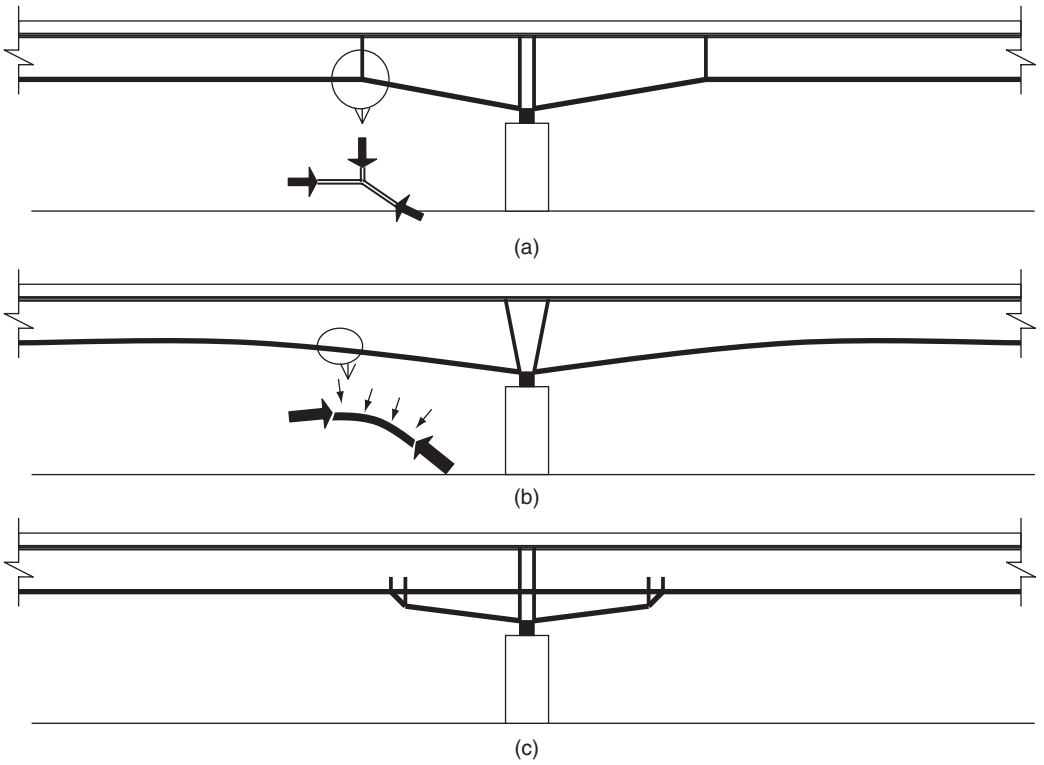

6.3. Longitudinal shear at changes of section

The longitudinal shear is determined from the rate of change of force in the composite flange adjacent to the interface (Equation 1.14). For constant-depth girders, this was simplified for design purposes to Equation 1.16b:

$$V_1 = \frac{VA_c y}{I_{a-c}} \tag{6.1a}$$

For a haunched girder, additional forces are generated due to the change in section. For a constant-depth girder element under a uniform moment there is no change in force, while for a girder with a changing depth there is a change in force due to the depth change ($M = zN$, Equation 2.1). The longitudinal shear due to the change in depth is

$$V_1 = M \frac{\mathrm{d}}{\mathrm{d}x}\left(\frac{A_c y}{I_{a-c}}\right) \tag{6.1b}$$

The total longitudinal shear on the interface for a haunched girder is the sum of Equations 6.1a and 6.1b:

$$V_1 = \frac{VA_c y}{I_{a-c}} + M \frac{\mathrm{d}}{\mathrm{d}x}\left(\frac{A_c y}{I_{a-c}}\right) \tag{6.2a}$$

Where the flanges are large and the web slender:

$$V_1 = \frac{VA_c y}{I} + \frac{D_2}{D_1} \tag{6.2b}$$

where D_1 and D_2 are the distances between flanges at each end of the section over which the longitudinal shear is being calculated.

6.4. Hybrid girders

Eurocode 3: Part 1-5, 'Plated structural elements' (BSI, 2006a), includes a mention of hybrid girders, that is, girders that contain different grades of steel. The Eurocode clarifies that it is assumed that the flanges will use higher grades of steel than the web. The logic behind hybrid girders is that high-grade steel can be fully used in the tension flanges to resist the bending effects, while in the webs, which on large girders usually have stresses limited by slenderness parameters, a lower grade of steel is more effective.

At the ultimate limit state, if the section is class 1 or 2, or if the section is slender and class 4, the moments can be assumed to redistribute from the web (see Section 6.7) to the flange, and a hybrid girder may be appropriate. However, care must be taken at the serviceability limit state to ensure that the degree of yield in the lower grade of steel is not so large that deflections etc. are affected.

6.5. Double-composite action

A way of further improving the effectiveness of a steel–concrete composite structure at intermediate supports is to use a double-composite section. In a double-composite structure, an additional concrete element is added to the lower (compression) flange, providing composite action to both the top and bottom flanges. The lower concrete flange allows the steel elements to be reduced in size, due to both the sharing of load between the steel and concrete sections, and the elimination of lateral buckling modes by the introduction of the slab with a high lateral inertia. The design of sections with double-composite action follows the basic rules outlined for conventional composite structures, but with both interfaces requiring design. Appendix F outlines the calculation method for a double-composite section.

The author has made a study of the effectiveness of double-composite action for a range of bridge forms and spans (Collings, 2008). The forms of bridge considered were: a constant-depth plate girder (30–100 m spans); a haunched plate girder (50–150 m spans); and a continuously profiled box girder (100–250 m spans). The results of the study are shown in Figure 6.4. In all cases, the double-composite section has less steel than the standard composite section. However, there is only a small saving in steel on the unhaunched girders and on smaller spans. The additional construction complications of casting the lower concrete are only worthwhile on larger spans or in box girders (see Chapter 7).

6.6. Example 6.1: A haunched girder

This example considers a steel–concrete composite river bridge (Collings *et al.*, 2003) with a series of 110 m spans. The large 110 m spans are used in the river where ship impact and seismic requirements govern the design. On-shore shorter spans are used. A number of interesting features are used on the bridge. First, the section is haunched. Second, the lower flanges have a concrete slab between them, creating a double-composite structure. Third, the structure uses a twin-girder arrangement with

Figure 6.4 Results from a study on double-composite bridges: (a) the steelwork tonnage for composite and double-composite bridges of various spans; (b) the saving in steelwork with span

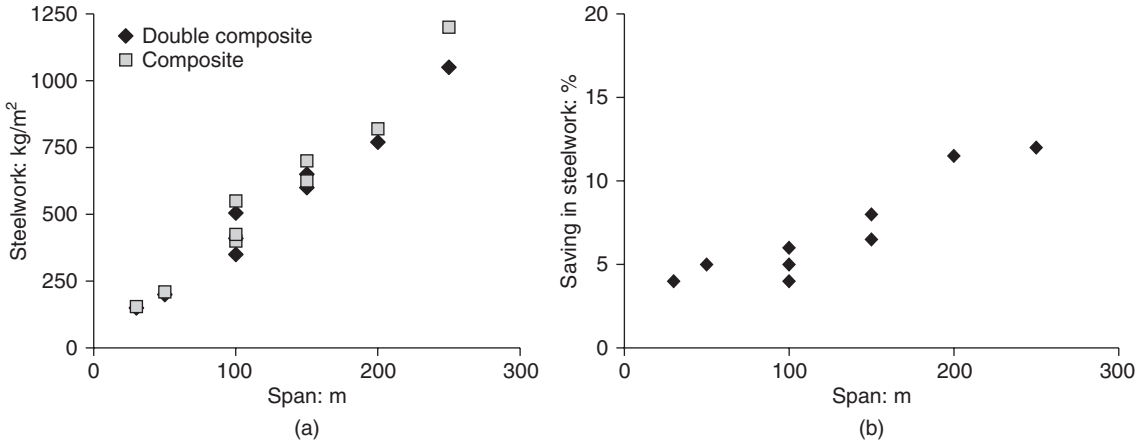

minimum bracing and cross-girders, the profiled slab forming the primary transverse member of the 19 m wide deck. Finally, a twin-pier arrangement is used to increase stiffness further (Figure 6.5).

6.6.1 Loads and analysis

The self-weight of the steelwork and concrete deck are approximately 225 kN/m. Near the pier the lower double-composite slab adds a further 80 kN/m. Surfacing and parapets add 75 kN/m, and the unfactored live load is approximately 65 kN/m. Analysis of the bridge is by a simple line beam model. A twin-pier arrangement is used to increase the stiffness of the system; this arrangement is often used on concrete bridges, but less so on steel–concrete composite structures. For live loads, this arrangement doubles the midspan stiffness, and is particularly useful for long-span railway structures, where deflection limits often govern section sizes.

At the pier the girder is 6.6 m deep. This depth of girder is difficult to fabricate and transport, and so the steelwork is formed of two sections – the lower with a small top flange and the upper with a small bottom flange, the smaller flanges being bolted together to form the larger girder section (see Figure 6.5). The depth of the section also affects the behaviour of the web.

6.7. Slender webs

For deep class 4 girder sections the web slenderness is large and the web is not fully effective, and there is a tendency to shed stress from compression areas. This may be approximated by ignoring the part of the web in compression, known as the 'effective width method', or by using a reduced effective thickness for the web when calculating the stresses.

6.7.1 Reduced area or effective thickness method

In this method (Dubas and Gehri, 1986), if the depth of the web exceeds the limits for the web of a class 3 section (see Table 1.3) then a reduced area of the web in the compression zone is taken. First, the section properties of the full section are determined and the location of the neutral axis found. If the depth of the web in compression exceeds $63t_w$, then only the web within $25t_w$ of the compression flange and $20t_w$ of the neutral axis is considered; the part of the web between these is ignored.

Figure 6.5 Double-composite section with upper and lower steel–concrete composite flanges the pier section of Example 6.1

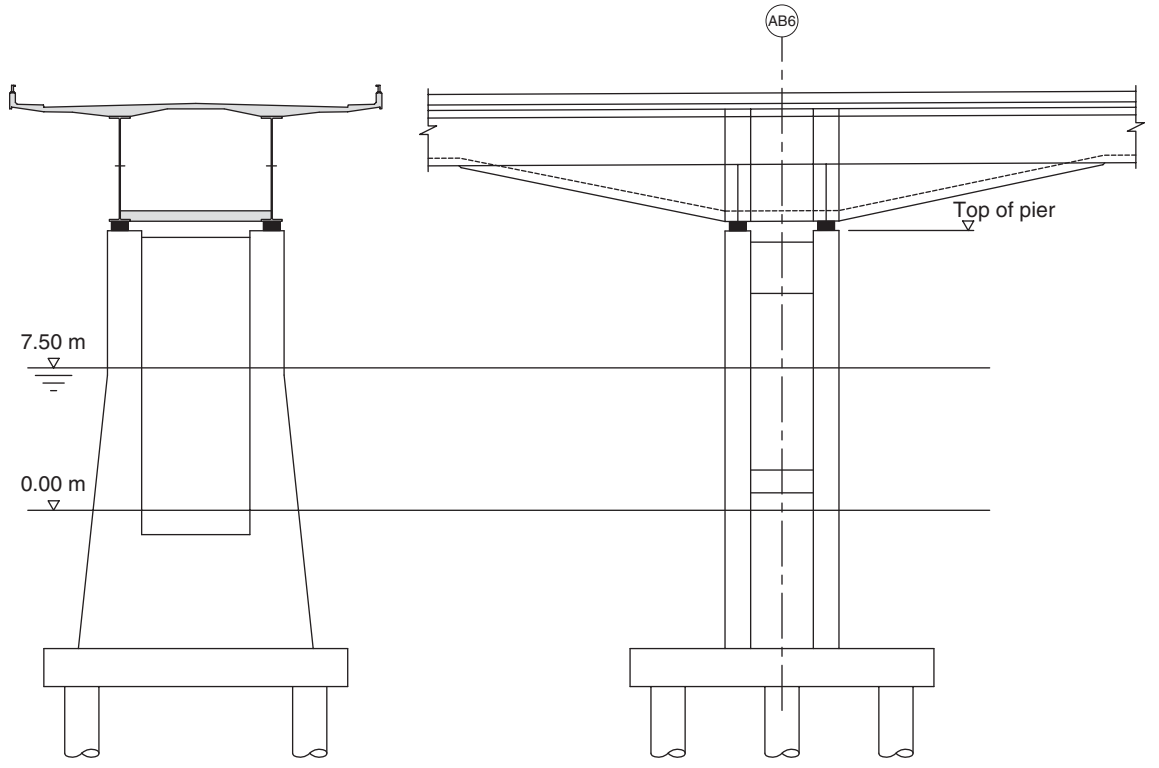

6.7.2 Reduced effective web method

In this method (Rockey and Evans, 1981; BSI, 2000), if the depth of the web exceeds the limits for the web of a class 3 section (see Table 1.3) then a reduced thickness of the web is taken. If the depth of web in compression (y_c) is greater than $67t_w$, it is classed as slender, and a reduced section should be used for calculating the section properties (bending and axial stresses). The reduced effective web is estimated using

$$t_{we} = 1.425t_w - 0.00625y_c \tag{6.3}$$

If the depth in compression exceeds $228t_w$, then the effective web thickness is zero, and all bending is assumed to be resisted by the flanges only.

6.8. Web breathing

Slender panels of web will achieve their ultimate strength with some local buckling or movement of the webs. At the serviceability limit state some movement, known as 'breathing', may occur under the application of live loads. Eurocode 3: Part 2, 'Steel bridges' (BSI, 2006b), limits the slenderness of webs. For highway bridges the limit is

$$h_w/t_w \leq 30 + 4L \leq 300 \tag{6.4a}$$

For railway bridges the limit is

$$h_w/t_w \leq 55 + 3.3L \leq 250 \tag{6.4b}$$

For Example 6.1, which is a highway bridge, the limiting h_w/t_w ratio for web breathing is 300. As the actual slenderness is approximately 260, this aspect is satisfactory. The depth of the web in compression is initially estimated as 3000 mm, so for a 25 mm web the slenderness is

$$\frac{y_c}{t_w} = \frac{3000}{25} = 120$$

When calculating the section properties, a reduced area or a reduced effective web needs to be used. The author prefers the effective web method. Using Equation 6.3:

$$t_{we} = 1.425t_w - 0.00625y_c = (1.425 \times 25) - (0.00625 \times 3000) = 17 \text{ mm}$$

For the steel section this reduces the section moment of area by 9%; if the other method is used a similar reduction is found. For the composite section, the reduction in section moment of area is only 5%.

The bridge is constructed by cantilevering of the steelwork from the stable twin-pier arrangement; the lower concrete flange is placed prior to linking of the cantilevers. The upper deck slab is constructed in two stages using moving formwork gantries, from the pier outwards on the continuous girders. The stresses build up stage by stage on the various sections: the non-composite steel section, the section with a composite lower flange, and the final section with a composite upper and lower flange. Table 6.1 outlines the moment at each stage of construction and the stresses induced.

The total shear on the section at the ultimate limit state is approximately 324 MN (16 MN per girder). The composite section will carry 85% of the shear. For this girder, the V_l/V ratio is approximately 0.12 for both the upper and the lower shear interface, and the slope of the haunch is approximately 10°. Using Equation 6.2b

$$V_1 = \frac{VA_c y}{I} + \frac{D_2}{D_1} = 0.85 \times 16 \times 0.12 \times 1.03 = 1.7 \text{ MN/m}$$

Table 6.1 Moment and stress build up for a double-composite section in Example 6.1

Construction stage	M: MN m	Z_t: m^3	Z_b: m^3	f_{at}	f_{ab}	f_{ct}	f_{cb}
Steel cantilever	20	0.55	0.39	−36	51	0	0
Single-composite section	40	1.02	0.85	−39	47	0	4
Double-composite section	70	1.04	1.37	−67	51	−68	4
Parapets and surfacing added	50	1.04	1.37	−48	37	−49	3
Live loading	60	1.07	2.24	−56	27	−57	5
Total stress: N/mm^2				**246**	**213**	**174**	**16**

Figure 6.6 Connector details for the upper and lower slab in Example 6.1

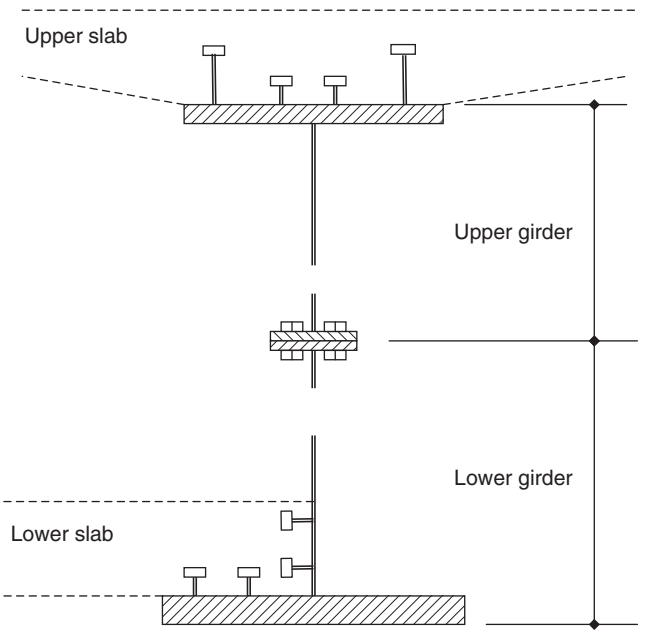

Using Equation 1.20 with 22 mm diameter connectors (see Table 1.5), the number of connectors required is

$$n = V_l/0.71P_u = 1.7/0.71 \times 0.139 = 17$$

The requirements equate to four connectors at 200 mm centres. The layouts of the upper and lower connectors are shown in Figure 6.6. Longer connectors are used at the outside edges of the upper flange (Gimsing, 2000), as there is also some uplift on these connectors from local vehicle loads, particularly adjacent to stiffeners (see Chapter 4 for connector design with additional tensile loads).

6.9. Lightweight concrete

Concrete with a reduced density, from 14 to 24 kN/m^3, may be used in composite structures, particularly long-span bridges, reducing the overall dead weight of the span. Typically, densities of 21–23 kN/m^3 can be achieved with the use of a lightweight aggregate; to get below 20 kN/m^3 the finer aggregate (sand) will also need to be replaced. The strength of concrete is dependent largely on the strength of the aggregate, and generally lightweight concrete can achieve similar strengths to normal concrete. The letters LC adjacent to the grade designates 'lightweight concrete'.

The properties of lightweight concrete are slightly different from normal-density concrete. The coefficient of thermal expansion is lower, typically 9×10^{-6}/°C rather than 12×10^{-6}/°C, which means that additional longitudinal shear may be induced by changes in temperature. Lightweight concrete is usually less permeable than conventional concrete, and creep is usually higher, by 20–60% depending on the aggregate. At the steel–concrete interface the reduction in the elastic

modulus is the most important difference:

$$E_{CL} = \left(\frac{\rho}{22}\right)^2 E_C \tag{6.5}$$

where E_{CL} is the modulus for lightweight concrete of density ρ, compared with a conventional concrete of the same strength. The capacity of the connectors is dependent to some degree on the stiffness of the concrete, and Equation 1.21b is modified for lightweight concrete:

$$P_{UL} = P_U \left(\frac{E_{CL}}{E_C}\right)^{1/2} \tag{6.6}$$

Equations 1.26, governing the ultimate shear strengths of the possible shear planes in the concrete, are also affected:

If lightweight concrete of density 20 kN/m^3 and grade LC 40 is used for the deck in Example 6.1, the longitudinal shear will reduce to approximately 1.5 MN/m. However, as the modulus and connector capacity also reduce, very similar connector requirements are obtained.

REFERENCES

BSI (2000) BS 5400-3:2000. Steel, concrete and composite bridges. Code of practice for design of steel bridges. BSI, London.

BSI (2006a) BS EN 1993-1-5:2006. Eurocode 3. Design of steel structures. Plated structural elements. BSI, London.

BSI (2006b) BS EN 1993-2:2006. Eurocode 3. Design of steel structures. Steel bridges. BSI, London.

Chen BC and Wang TL (2009) Overview of concrete filled steel tube arch bridges in China. *Practice Periodical on Structural Design and Construction* **14(2)**: 70–80.

Collings D (2008) Double composite steel concrete composite bridges. *Proceedings of the ICE – Bridge Engineering* **161**: 45–48.

Collings D, Mizon D and Swift P (2003) Design and construction of the Bangladesh–UK Friendship Bridge. *Proceedings of the ICE – Bridge Engineering* **156(4)**: 181–190.

Dubas P and Gehri E (eds) (1986) *Behaviour and Design of Plated Structures*. ECCS, Switzerland.

Gimsing N (2001) Composite action and high strength steel in the Oresund bridge. *Composite Bridges – State of the Art in Technology and Analysis. Proceedings of the 3rd International Meeting*, Madrid.

Rockey K and Evans H (eds) (1981) *The Design of Steel Bridges*. Granada, London.

Steel–concrete Composite Bridges
ISBN 978-0-7277-5810-1

http://dx.doi.org/10.1680/scb.58101.129

ice Institution of Civil Engineers publishing

Chapter 7
Box girders

. . . a triangular shaped structure . . . is stiffer and less susceptible to distortion than the conventional . . . forms . . .

7.1. Introduction

The first metal box girder bridge was built in 1850 by Stephenson over the Menai (Ryall, 1999). Although a riveted wrought iron structure, it had the basic stiffened plate form used by many bridges in the twentieth century. In the 1970s, a series of collapses in the UK, Europe and the Far East highlighted that the box form had developed beyond the knowledge of known behaviour, a phenomenon that possibly occurs with every generation (Sibley *et al.*, 1977; Collings, 2005). Extensive research followed the collapse enquiries (Merison, 1971). The use of large steel box girder bridges is still relatively uncommon, their major use being on larger cable-suspended spans (see Chapter 10). Concrete boxes are more tolerant of the shear lag, warping and distortional effects that affect thin steel plated sections, and often diaphragms are not required, making them simpler to construct. Concrete boxes are a common form for 40–200 m spans. Composite boxes are an intermediate type; they have an advantage over the all-steel box in that they avoid the use of the fatigue-sensitive steel orthotropic deck (Beales, 1990). However, the design complications of warping, distortion and shear lag still occur, and need consideration. Intermediate steel diaphragms are used to limit distortion. The fabrication costs of boxes are relatively high compared with plate girders, because of access difficulties for welding inside the box. The use of an open-top steel box with the concrete deck forming the top flange is often preferred to avoid this access issue.

Steel–concrete box girders are today most common on moderate spans, often for aesthetic purposes (Dickson, 1987). The box gives a potentially sleeker appearance, uncluttered by flange plates and stiffeners. However, care needs to be taken, as without features the structure may appear dull or monotonous. The details of the box to slab joint, the size of overhangs and the parapet type will affect the aesthetics. If the box structure is sleek but the substructure is not designed to complement this then the aesthetics of the box will be lost (see Chapter 9 for more on aesthetics).

7.2. Behaviour of boxes

When subject to bending, box girders behave in a similar way to plate girders – they are subject to buckling, shear lag and local slenderness effects. As with plate girders, the importance of these issues will depend on the class of the structure. Compact class 1 or 2 boxes have been built (Dickson, 1987), but generally the box will be relatively large and have elements that are class 3 or 4. When subject to a torsional moment, either from eccentric loading or from curvature of the structure, the box forms a much stiffer structure than does a plate girder. The resistance to torsion in a box is from a shear flow around the box (Figure 7.1a). The shear flow around the box is uniform:

$$v_w t_w = v_f t_f \tag{7.1}$$

$$T = BD(v_w t_w + v_f t_f) \text{ or } 2A_o vt \tag{7.2}$$

Figure 7.1 Distortion of the box: (a) shear flow around section; (b) idealised distorted shape; (c) distortion with transverse bending

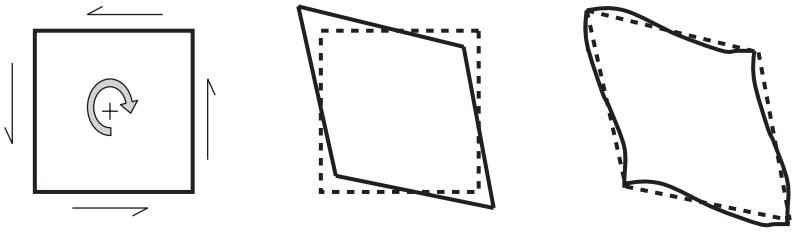

where v_f and v_w are the shear stress in the flange and web, A_o is the area within the box centreline ($B \times D$) and T is the total torsion moment at the section. The torsional shears in the web will add (or subtract) directly to those shears due to vertical loads (v_v), meaning that for a curved bridge one web of the box and one of the shear interfaces with the deck slab will have larger shears than the other:

$$v_1 = v_v + v_w \tag{7.3a}$$

$$v_2 = v_v - v_w \tag{7.3b}$$

The shear stresses around the section cause a distortion of the box, which is idealised as a parallelogram (Figure 7.1b), but in real structures it involves some transverse bending due to the rotational stiffness at the plate intersections (Figure 7.1c).

Conventional plate girders can carry torsional moments if the torsion is resisted by the warping of a girder pair, with one girder moving upwards and the other down. A similar warping occurs in the box section but, because the webs are connected by the flanges, the distribution of stresses are slightly modified.

Intermediate diaphragms within the box span will reduce the effects of warping and will restrain distortion, causing some secondary restraining stresses. The relative magnitude of the stresses depends on the structure geometry. The stresses can be derived from an analysis of the box (using a beam on elastic foundation (Horne, 1977) or a finite-element model) or from simplified equations (BSI, 2000), provided certain geometric limits are satisfied. The simplified method will give an indication of the stresses. Where the stresses are significant, a more complex analysis may be required, or a more efficient structural arrangement sought. At the junction of the web and flange, when subject to an increment of torque (T_i), the longitudinal stress induced by the restraint to torsional warping is

$$f_{TW} = \frac{DT_i}{J} \tag{7.4}$$

where J is the torsional constant (see Appendix E). This stress drops rapidly each side of the applied torque at a distance y from the applied torque:

$$f_{TWx} = f_{TW}\, e^{-(2y/B)} \tag{7.5}$$

This means that, generally, there is little interaction between increments of torque further apart than the box width. The longitudinal distortional warping stress (f_{DW}) can be estimated as

$$f_{DW} = \frac{k_1 {L_D}^2 T_{UD}}{B W_e} \tag{7.6}$$

where L_D is the diaphragm spacing and T_{UD} is the applied uniformly distributed torque.

When βL_D is less than 1.6, k_1 is a constant at 0.22 (where β is an effective length parameter and L_D is the distance between diaphragms). When βL_D is greater than 1.6:

$$k_1 = \frac{1}{1.66(\beta L_D)^2}$$

$$\beta L_D = \left(\frac{k_1 {L_D}^4}{EI}\right)^{1/4} \tag{7.7}$$

$$k_2 = \frac{24 D_{YT} k_3}{B^3}$$

where k_3 is obtained from Figure 7.2a and depends on the relative transverse flexural rigidity of the top and bottom flanges (D_{YT} and D_{YB}) and webs (D_{YW}).

The longitudinal torsional and distortional warping stresses will add directly to (or subtract directly from) the bending stresses in the girder:

$$f = f_b + f_{TW} + f_{DW} \tag{7.8}$$

Figure 7.2 (a) Coefficient k_3 for longitudinal distortional warping. (b) Coefficient k_6 for transverse distortional bending

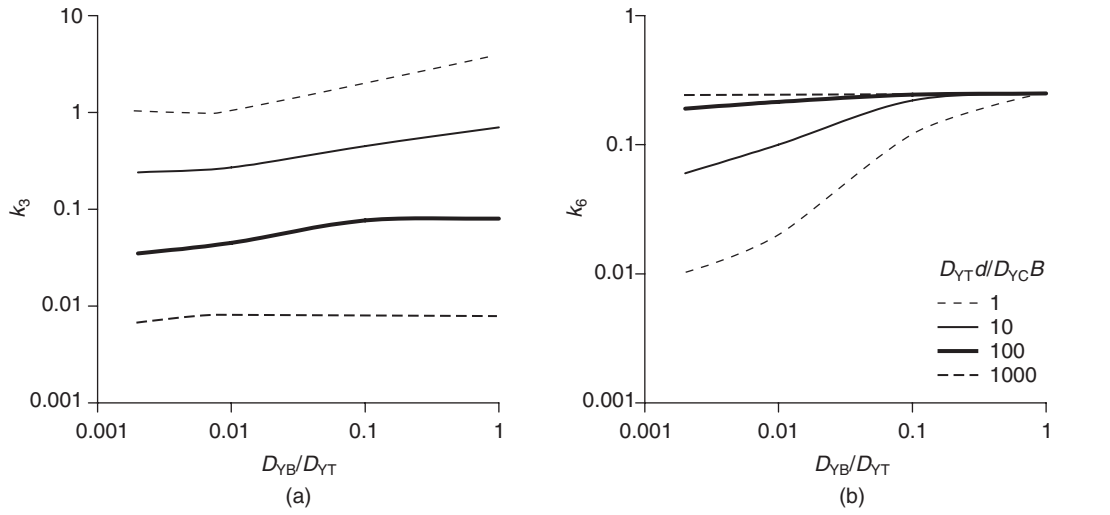

Transverse bending (f_{DB}) effects from the distortion (see Figure 7.1c) can be estimated from

$$f_{DB} = \frac{k_4 k_5 T_{UD}}{B W_f} \tag{7.9}$$

where W_f is the transverse flange modulus. When βL_D is greater than 2.65, $k_4 = 1$; when βL_D is less than 2.65,

$$k_4 = 0.5(\beta L_D)^{3.7}$$

$$k_5 = 0.5 B k_6$$

where k_6 is obtained from Figure 7.2b, and again depends on the relative flexural rigidity of the flanges and webs.

7.3. Diaphragms

The behaviour of the box is influenced by the stiffness and spacing of the diaphragms. Typically, diaphragms will be at 2–4 times the box depth to limit the distortion and warping stresses. The diaphragms should also be stiffer than the box section, and a figure of at least 1500 times that of the box is recommended (BSI, 2000). For Equations 7.6 and 7.9 to be valid, a minimum diaphragm stiffness (K_D), as shown in Figure 7.3a, is required; the stiffness is determined from the application of a series of diagonal loads applied to the corners of the diaphragm (Figure 7.3b).

Three forms of diaphragm are commonly used: the plate diaphragm, the braced diaphragm and the ring diaphragm. The plate diaphragm is relatively simple to fabricate and has a good stiffness. Access requirements through the box will complicate the diaphragm layout, and additional stiffening will be required. The ring diaphragm is even simpler, and allows maximum access through the box, but it is more flexible. The braced diaphragm allows a compromise between access and stiffness to be achieved. In practice, the types of diaphragm are often mixed with stiffened plate diaphragms at supports with ring diaphragms between, perhaps with every third or fourth ring being braced. Figure 1.8 shows a 3D fabrication drawing of a box with ring diaphragms.

Figure 7.3 (a) Minimum diaphragm stiffness requirements. (b) Force system to determine the diaphragm stiffness across the diagonal

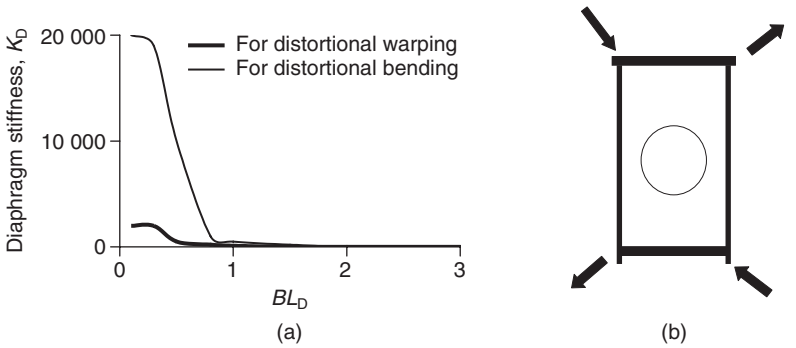

In the UK, steel boxes have been a popular form for railway bridges. The box is more stable than a conventional plate girder, provides a stiffer U-deck and is relatively simple to construct quickly during railway possession. The first example in this chapter is a box of this type.

7.4. Example 7.1: Railway box

The example is a 22 m span twin box bridge carrying a railway over a road in the midlands. The form of the structure is a U-frame (see Chapter 4) with the deck between the boxes. The U-frame action provides only limited restraint, as the torsional stiffness of the girder is relatively large and the joint at the cross-beam connection is flexible (see Section 4.12 in Chapter 4). The layout of the steelwork is shown in Figure 7.4. The box, cross-beams and detailing of the box to beam connection is designed to allow fast assembly during a railway possession, one face of the box being inclined to provide more space and ease assembly of the deck beams.

Figure 7.4 Typical standard box railway bridge details

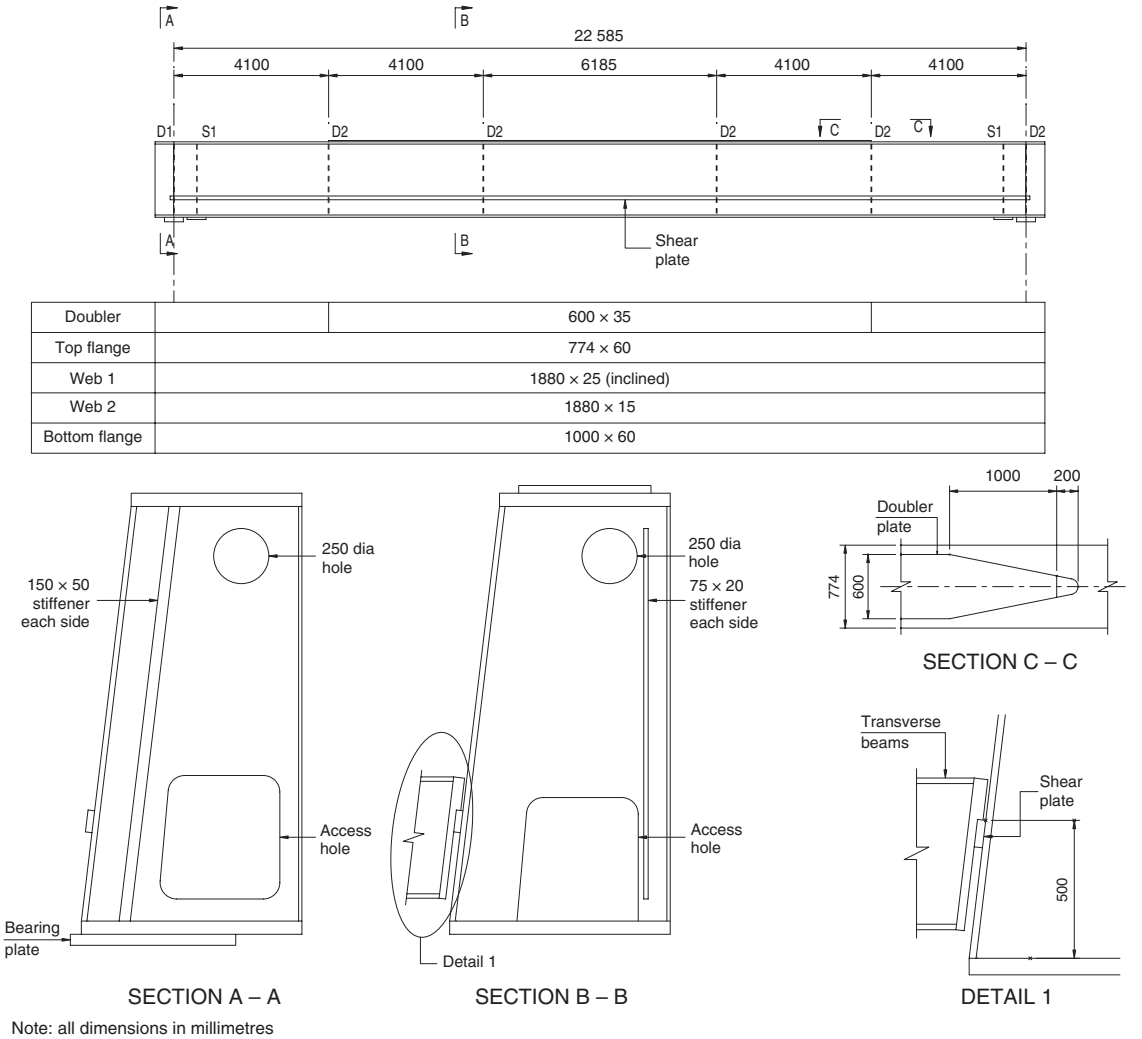

7.4.1 Loads and analysis

The bridge carries its self-weight, a layer of ballast and full RU loading, type SW2 (see railway loading in Chapter 4). At the ultimate limit state, the loading on the girder is approximately 330 kN/m, and this load is applied to the edge of the box via the cross-beam connection, inducing both a moment and torsion in the box. The total load on the 22 m span $(G + Q)$ is 7.3 MN, giving $M = 20$ MN m, $V = 3.9$ MN, $T_{UD} = 0.15$ MN m/m and $T = 1.6$ MN m. The torsional properties of the box are summarised in Appendix E and the bending properties in Appendix C.

The vertical and torsional shears in the box are calculated as

$$v_v = \frac{V}{dt_w} = \frac{3.9}{1.88(0.025 + 0.015)} = 83 \text{ N/mm}^2$$

The torsional shear is estimated from a rearrangement of Equation 7.2:

$$v_T = \frac{T}{2A_o t} = \frac{1.6}{2 \times 1.8 \times 0.025} = 18 \text{ N/mm}^2$$

Using Equation 7.3, the maximum shear stress is estimated as

$$v = v_v + v_w = 83 + 18 = 101 \text{ N/mm}^2$$

From Figure 1.6, with $d/t = 80$ and a panel aspect ratio of 2, the limiting shear stress is $0.86v_y = 167$ N/mm^2. This is greater than the applied shear, and so the web plate is satisfactory.

The bending stress at midspan of the box is calculated as

$$f_b = M/W = 20/0.08 = 250 \text{ N/mm}^2$$

The width of the box is small, so in this example T_i is similar to T_{UD}. The longitudinal stress due to torsional warping is (Equation 7.4)

$$f_{TW} = DT_i/J = 2.0 \times 15/69 = 0.4 \text{ N/mm}^2$$

To determine the longitudinal distortional stress, the various coefficients are determined:

$$\frac{DD_{YT}}{BD_{YW}} = \frac{2 \times 3.8}{0.9 \times 0.14} = 60 \qquad \frac{D_{YB}}{D_{YT}} = \frac{3.8}{3.8} = 1$$

From Figure 7.2a, $k_3 = 0.12$, so

$$k_2 = \frac{24D_{YT}k_3}{B^3} = \frac{24 \times 3.8 \times 0.12}{0.9^3} = 15$$

and

$$B_{LD} = \left(\frac{k_2 L_D^4}{B^3}\right)^{1/4} = \left(\frac{15L_D^4}{210\,000 \times 0.81}\right)$$

Solving this gives $\beta = 0.17$.

Table 7.1 Longitudinal warping and transverse distortional bending stress in Example 7.1 for various diaphragm spacings

Diaphragm spacing: m	2	4	6	9	11	15	22
βL_D	0.34	0.68	1.0	1.6	1.9	2.7	3.8
f_{DW}: N/mm^2	2	8	18	45	45	45	45
f_{DB}: N/mm^2	0	0	1	5	10	34	34

Using Equation 7.6 the longitudinal warping stress can be calculated for various diaphragm spacings. From Table 7.1 it can be seen that the longitudinal distortional warping stress increases with diaphragm spacing, but is constant beyond $\beta L_D = 1.6$. From Figure 7.4 the diaphragm spacing near midspan is 6 m and $f_{DW} = 18$ N/mm^2. The peak longitudinal stress is the sum of the bending, distortion and warping stresses (Equation 7.8):

$$f = f_b + f_{TW} + f_{DW} = 250 + 6 + 18 = 274 \text{ N/mm}^2$$

The limiting stress for a 60 mm thick flange plate is $0.95 f_y = 308$ N/mm^2; again this is satisfactory.

For the transverse distortional bending effects, again the relative rigidity of the web and flanges is used to determine coefficient k_6 from Figure 7.2b as 0.25, and k_5 as 0.113. Using Equation 7.9, the value of the transverse bending stress is tabulated for various diaphragm spacings. From Table 7.1 it can be seen that the transverse distortional bending increases with diaphragm spacing but is constant beyond $\beta L_D = 2.65$. For the 6 m diaphragm spacing used in this example, the transverse stresses are small.

The transverse bending stresses will need to be carried around the welded joint between the flange and the web. These stresses will be in addition to any local bending from the application of the load and any longitudinal shear stresses. For a railway structure of this type, the use of a full penetration butt weld is advisable to avoid fatigue issues (Figure 7.5a). For highway structures the welds may be reduced to partial-penetration welds (Figure 7.5b), but a double-sided weld should be used to avoid bending of

Figure 7.5 Weld details for box connections: (a) standard railway box; (b) composite highway box

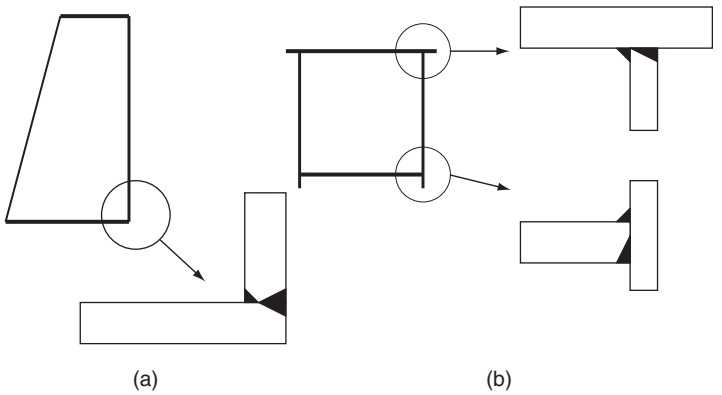

the weld itself. In both details the primary weld is formed from the outside of the box in order to limit work inside the box.

The stresses in the bridge were also checked using a finite-element analysis. Eurocode 3: Part 1-5, 'Plated structural elements' (BSI, 2006), outlines some recommendations for the use of finite-element analysis in steel plated structures where buckling of plates is an issue. The maximum bending stresses are similar to those estimated using the equations. Finite element analysis is a useful tool, but the author would recommend caution in its use. It is a good way to verify a design that has been carried out using simpler methods, or to point out its flaws; but it is less useful as a design tool when starting from scratch! The web shear stresses are higher near the support, but this is not related to the box behaviour. The stresses are significantly different from the average stresses assumed for design, and for larger boxes with limited post-buckling capacity this elastic shear distribution may become critical and additional stiffeners be required to limit buckling at serviceability limit states.

7.5. Efficient box girders

A review of the behaviour of composite box girders indicates that the stresses induced are a result of the relative flexibility of the steel plate elements of the box. The use of a composite top flange will increase the rigidity of this element. Reducing the bottom flange to the bare minimum size then leads to a triangular shaped structure, a form that is stiffer and less susceptible to distortion than the conventional rectangular or trapezoidal forms. Where a conventional box shape is required, the rigidity of the web can be significantly increased by the use of a folded plate (for more on folded plates see Chapter 11). The folded plate gives a shear and torsional stiffness similar to that of a conventional web, but the transverse rigidity is increased by a factor proportional to the square of the fold amplitude (a). The folded plate effectively provides a continuous, but relatively weak, ring diaphragm, and is a valid option with regard to the practical diaphragm stiffness requirements at low βL_D ratios (see Figure 7.3).

The Maupre Bridge, France (Subedi, 2003), is an example of a structure where the triangular box and folded web have been exploited to remove all intermediate diaphragms (Figure 7.6). The behaviour of a folded-plate web will be different from a conventional web; the increased distortional stiffness is accompanied by a reduction in longitudinal stiffness, such that the web can carry almost no longitudinal bending. Further consideration of folded web plates is set out in Chapter 11. A number of innovative composite box girder forms have been developed in France (BSI, 2008), particularly on the various sections of the high-speed railway (Plu, 2001). The development of

Figure 7.6 Details of the Maupre Bridge, combining a triangular form with a folded web

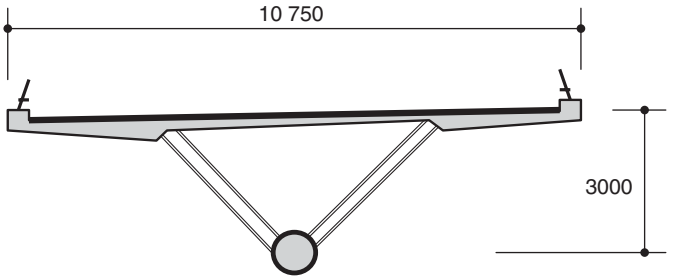

Note: dimensions in millimetres

composite sections for high-speed railways serves as an interesting example of the strengths of this structural form.

7.6. Example 7.2: Types of composite box

The construction of high-speed railways across Europe has required the construction of many bridges and viaducts in various forms. In the UK, the major structures have tended to be concrete box girders (Figure 7.7a) (Johnson, 2003), with only a few steel–concrete plate girders being used (Figure 7.7b). The multiple girder structure has also been used in Europe (Detandt and Couchard, 2003), and it has advantages in that the girders are directly beneath the rails. The use of a twin composite box girder section (Figure 7.7c) increases the stiffness of the section, particularly for skew crossings. The inclined webs give improved aesthetics, although the twin boxes are still relatively expensive to fabricate and erect.

Through the longer lengths of high-speed railway constructed in France and Spain, other forms of composite bridge have been developed. The twin girder (Figure 7.7d) increases the structural efficiency

Figure 7.7 High speed viaduct forms: (a) concrete box; (b) steel girders; (c) twin boxes; (d) twin girder; (e) composite box; (f) double-composite box

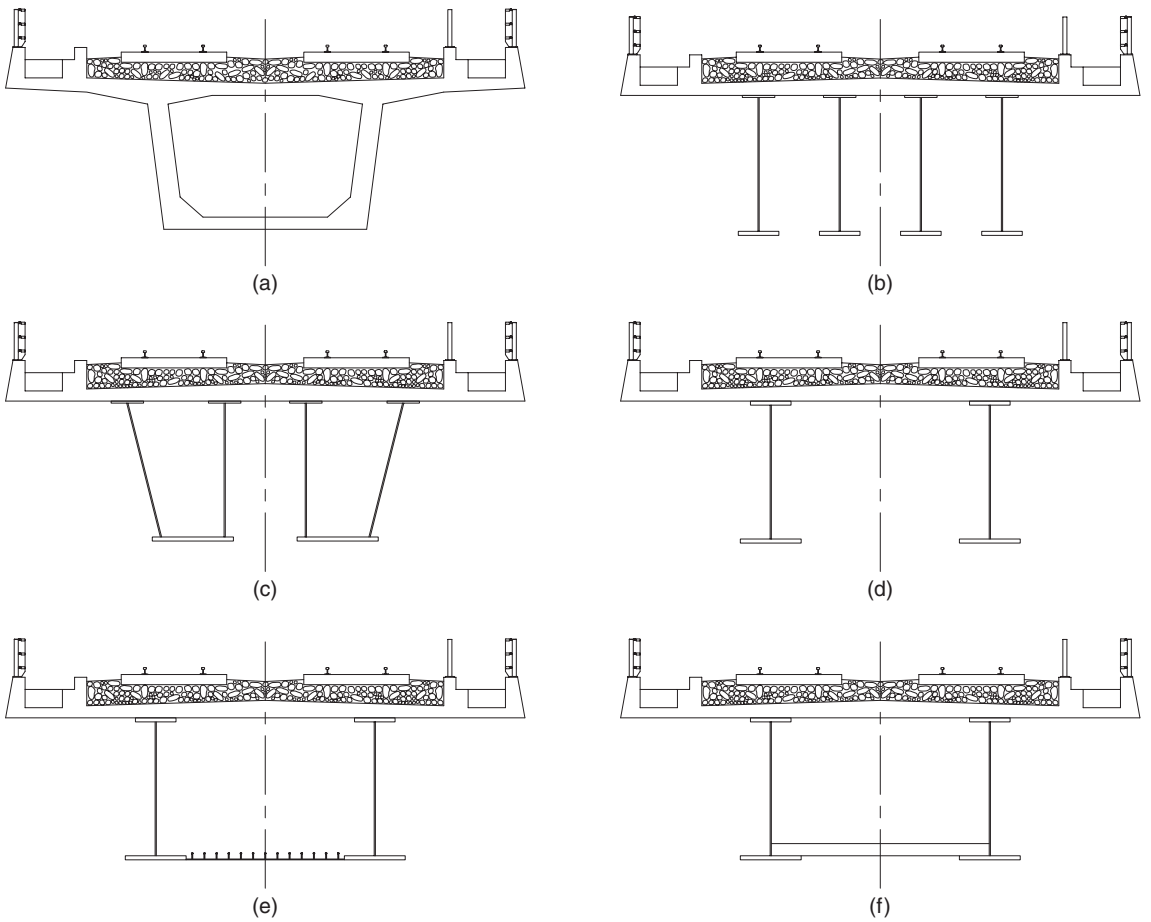

(see Chapter 5) and is simpler to build, particularly if launched. However, for the twin girder, the load transfer is less direct, involving slab bending, and for asymmetric loading this involves some transverse rotation of the passing train. The limits of deflection and rotation for high-speed lines are more onerous than those for conventional railways (see Table 4.2), and often govern the size or layout of a bridge. To improve the rotational stiffness of the twin-girder structure, the addition of a lower steel plate between the girders (Figure 7.7e) has been used to form a box, with its improved torsional inertia. On more recent structures the use of a lower concrete slab between the girders (Figure 7.7f) has been used to form the box structure, and this also improves the acoustic performance of the structure. The slab is not continuous longitudinally at midspan, but the panel lengths are sufficient to allow torsional shears to be transferred. This form gives the relatively simple fabrication and construction form of the twin-girder bridge, with the improved rotational and acoustic properties of the concrete box. For a given span the vertical deflection under load is broadly similar for all forms, as it needs to be within the limits outlined in Table 4.2. The rotational stiffness of the box forms is significantly enhanced, as rotations of box forms are about three times less than those for girder forms for the single loaded track scenario.

7.7. Noise from bridges

The construction of new railways and highways is often constrained by environmental issues such as noise. Noise can be mitigated by the choice of an appropriate bridge design (Cooper and Harrison, 2002). The noise associated with a road or railway tends to come from three sources: the vehicles or rolling stock, the wheel–rail or wheel–road interface, and re-radiated structure-borne noise.

The noise from vehicle or rolling stock, motors, air-conditioning etc. is largely controlled by the performance specification of the vehicles, and the bridge form has no influence on this noise source. Wheel–rail or wheel–road interaction noise is related to the roughness of the road or railway. This noise generally increases with the age of the road or railway, and for most situations this is the primary source of noise. Noise from points, switches or joints at the ends of bridges also contributes to this noise source. The noise from wheel–rail interaction and vehicle or rolling stock can be controlled by the use of noise-absorbing barriers. For railways, the barriers are more effective if placed adjacent to the track. For both rail and road bridges large structural parapets should be used with care, as the increased area may increase the re-radiated noise if the parapets are not designed correctly.

Structure-borne noise is generated by vibrations from the wheel–rail interface being transmitted through the structure and re-radiated. This is largely a dynamic phenomenon, and depends on the mass, stiffness, natural frequency and damping of the structure (Brown, 1997). Massive or highly damped structures emit less noise. The exposed surface area of the structure also affects the amount of noise generated, and so should be minimised where possible. Figure 7.8 outlines the relative noise generated by a high-speed train on the various viaduct forms. The box sections are less noisy than the girder forms. The concrete box and double-composite steel–concrete box are the best at limiting re-radiated noise. For the steel composite forms, the webs are the major sources of noise; the natural frequencies tend to be in the range generated by the train, leading to some resonance. The use of thicker webs and additional stiffening or damping can be used to reduce this noise.

Analysis of the radiated noise is a relatively complex procedure. An initial estimate of the relative noisiness of various structural forms can be made by assessing the vibration frequency of the primary elements. Estimation of the actual noise generated involves significantly more complex analysis. The initial problem is to estimate the input energy; this will require modelling track and wheel defects. Having defined the input criteria, the behaviour of the structure must be modelled, usually by

Figure 7.8 Relative noise emission from various viaduct structure forms

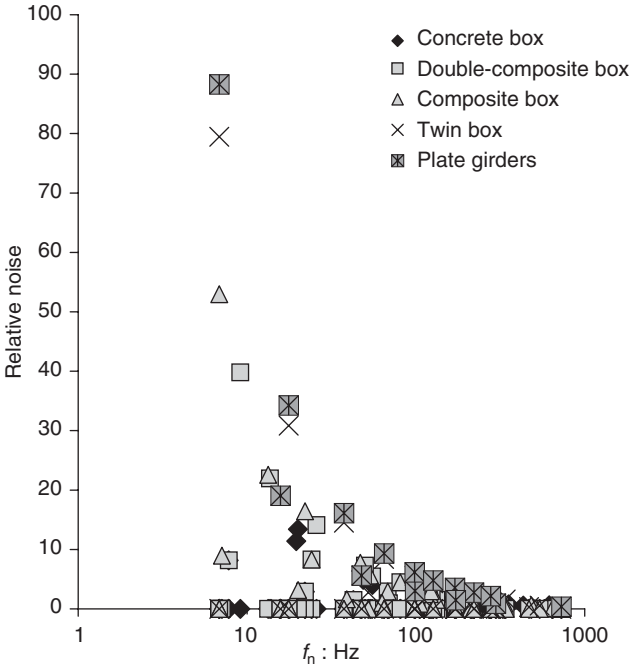

finite-element techniques. The modelling required to achieve frequency outputs to about 300 Hz requires a model that is more refined than is usual for stress analysis (Cooper and Harrison, 2002).

7.8. Shear connectors for composite boxes

For an open topped box (Figure E.1b in Appendix E), the behaviour of the steel–concrete interface is similar to that of a conventional girder, and the shear flow is calculated from Equation 1.16 (but taking into account the additional torsional shears). The shear failure planes will be as in Figure 1.11. For a closed box (Figure E.1a) of a similar size, logic indicates that a similar number of connectors should be satisfactory; this is generally true, but with some complications. The top flange layout is not symmetrical about the web, and so the connectors previously provided outside the web are added inside, increasing the connector density locally near the web. The majority (approximately 90%) of the effective connectors should be within the effective width of the girder; connectors outside the effective width will be required to carry local or transverse effects, or the small longitudinal shear spread beyond the effective width. The nominal connector spacing requirements (see Table 1.3) also apply in this area.

The load in any connector at a distance a from the web of a closed box is given by

$$P = \frac{VI}{n}\left[k\left(1 - \frac{a}{b_w}\right)^2 + 0.15\right] \tag{7.10}$$

where V_1 is the longitudinal shear derived for one web, b_w is the width of the box from the web to the box centre line, and n is the number of connectors within b_w (all are assumed to be of the same type).

Figure 7.9 Distribution coefficient k for shear connectors in a closed box

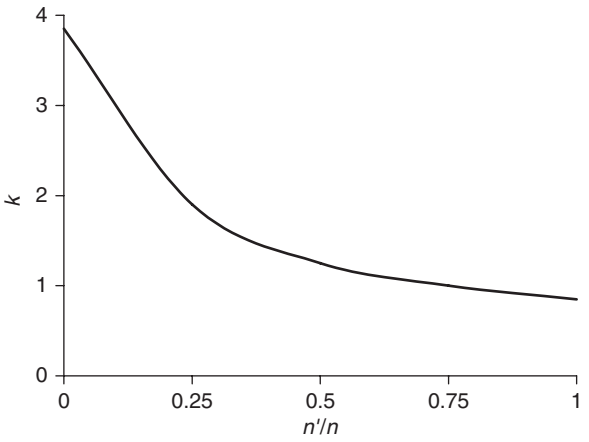

k is a coefficient taken from Figure 7.9 and n' is the number of connectors within a nominal 200 mm strip adjacent to the web. Where connectors are not of the same type, the effective number of connectors may be estimated as follows:

$$n = n_1 + n_2 P_{u2}/P_{u1} \tag{7.11}$$

Where a closed box is used, there are additional local stresses and connector requirements due to local bending, shear and torsion in the composite plate.

7.9. Composite plates

The top flange of a closed box girder will initially provide support for the wet concrete; it will also assist the embedded slab reinforcement in carrying local wheel loads. The flange can be considered as providing a tie restraint for arching action on smaller spans (see Chapter 5), or as providing additional bending reinforcement on larger spans.

During construction of a box girder, the top flange will be subject to a direct in-plane compression (or tension) induced in the flange by the bending of the box section. To prevent buckling of the flange it should satisfy the shape limitations outlined in Table 1.4, unless stiffening is added. The plate will also be subject to direct loading from the wet concrete, and in this situation the deflection of the plate should be limited. For a 200–300 mm deck slab the deflection should be limited to span/300 (see Equation 4.12) or 10 mm, whichever is the lesser. A plate thickness of approximately span/60 will be required for unstiffened plates; where the span is larger, stiffening of the plate will be required.

For the design of the composite plate to resist local wheel loads, two design methods are used. The simplest method is to ignore the capacity of the plate and provide embedded reinforcement to carry the local wheel loads; shear connectors at a nominal spacing only are provided to ensure that the plate and concrete remain together. This method is conservative but useful, particularly on multiple box structures where only part of the slab soffit has a composite plate. The second method considers the steel plate as reinforcement; the required area is derived using Equation 1.5b. The longitudinal shear is estimated using Equation 1.16b, and the spacing of the shear connectors is obtained using

Figure 7.10 Failure mechanisms for composite plates (Subedi, 2003): (a) yielding of the plate in the bending tensile zone; (b) buckling of the plate in the bending compression zone; (c) plate ineffective for local shear failure

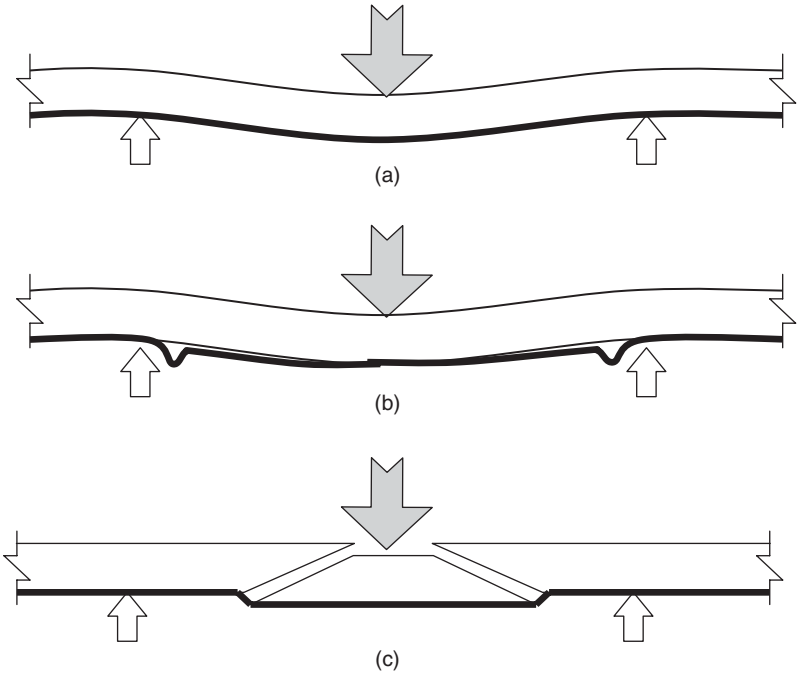

Equation 1.18a as other steel–concrete composite sections. Where the slab is subject to moments that cause compression in the plate, the connector spacing should be such that local buckling of the plate does not occur (Figure 7.10b). In practice, failure of short spans is often by punching shear (Figure 7.10c) and, again, unless the connectors are at an increased spacing, the slab will not act as effective reinforcement for this failure type.

7.10. Example 7.3: Trapezoidal box

A series of viaducts consisting of twin trapezoidal box girders was proposed for new grade separated highway intersections in Kuala Lumpur. The road alignment was highly curved and the pier positions were restricted by existing roads and services. Typically, 55 m spans were used (Figure 7.11). At midspan a closed box, and nearer the supports an open box, were proposed. At the piers the boxes were haunched, and a lower concrete slab placed within the box to form a double-composite section (see Chapter 6).

Due to the curved alignment, closed-box behaviour was required during construction to carry the wet concrete loading, and a plan-bracing layout was used to achieve this. For the torsional analysis, the bracing was assumed to act as a plate, with the effective thickness of the plate being estimated as

$$t_{\text{eff}} = \frac{A}{b} \cos\theta \sin\theta \tag{7.12}$$

where A is the area of the brace, b is the distance between webs and θ is the brace angle.

Figure 7.11 Typical viaduct for the curved interchange structure in Example 7.3

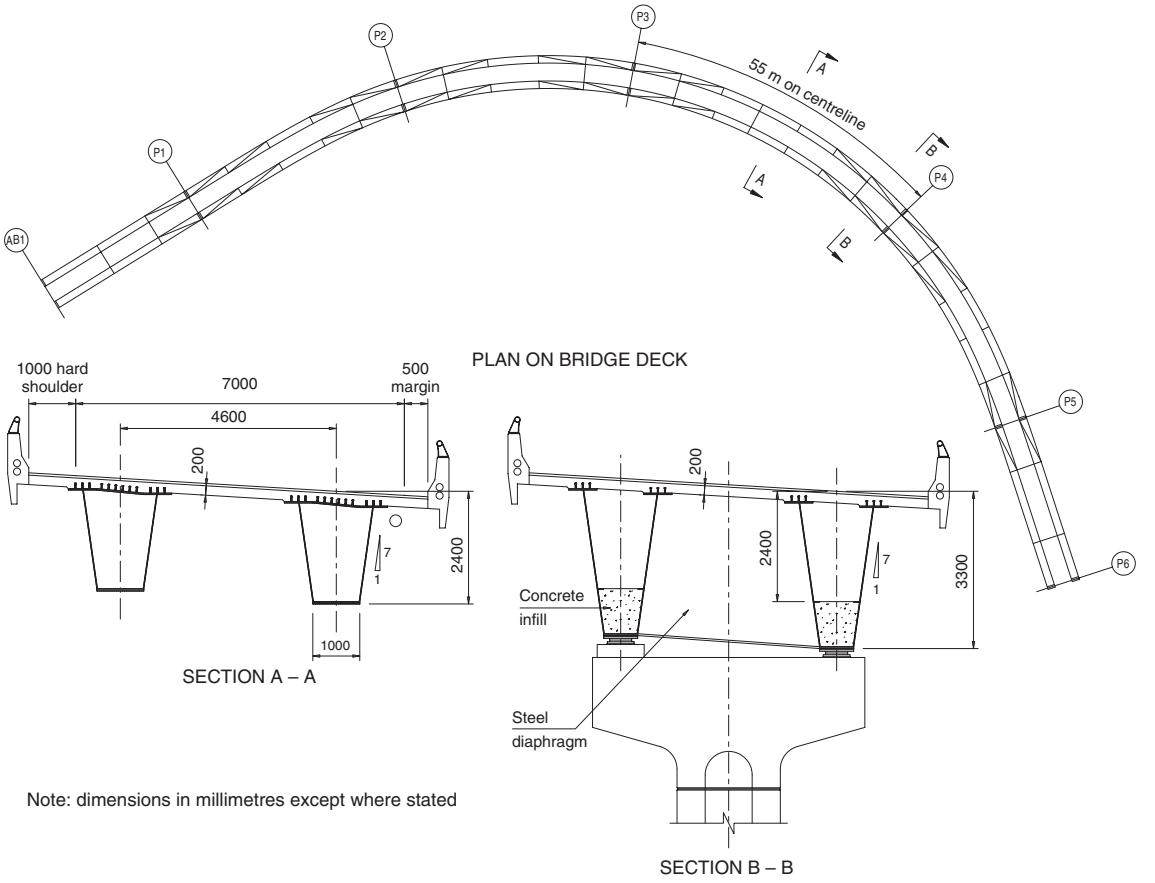

7.10.1 Loads and analysis

For a 55 m span, the permanent load on the non-composite section is 2.6 MN, and the load on the composite section is 4.5 MN. The characteristic live load for a single lane giving maximum torsion is 2.1 MN. Analysis of the structure, using a grillage method, gives estimates of shear and torsion near the quarter span (where the section changes from an open to a closed box). The section properties and torsional properties are calculated as in Appendix B, E and F, and given in Tables C.1 and E.1.

For the box, the effective shear on a web can be estimated by rearranging Equation 7.2:

$$V_T = T/2B \tag{7.13}$$

For this example, with $T = 1.6$ MN m and $B = 1.25$ m,

$$V_T = T/2B = 1.60/(2 \times 1.3) = 0.67 \text{ MN}$$

$$V_l = (0.81 + 0.5 \times 1.02) \times 0.24 = 0.32 \text{ MN/m, or } 320 \text{ kN/m}$$

Figure 7.12 Distribution of force in the connectors for the open and closed box in Example 7.3

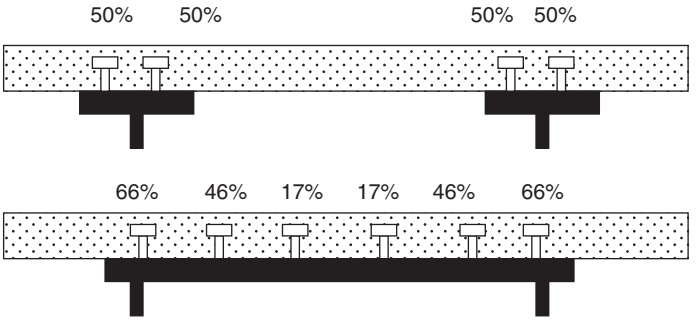

Using Equation 1.18a to estimate the number of connectors,

$$n = V_l/0.71P_u = 320/0.71 \times 108 = 5$$

so pairs of connectors at 300 centres are sufficient.

Using Equation 7.10 the distribution of force in the connectors is as shown in Figure 7.12.

REFERENCES

Beales C (1990) *Assessment of Trough to Crossbeam Connections in Orthotropic Steel Bridge Decks*. Research Report 276. Transport and Road Research Laboratory, Wokingham.

Brown C (1997) *Reducing Noise Emission from Steel Railway Bridges*. Technical Report 173. Steel Construction Institute, Ascot.

BSI (2000) BS 5400-3:2000. Steel, concrete and composite bridges. Code of practice for design of steel bridges. BSI, London.

BSI (2006) BS EN 1993-1-5:2006. Eurocode 3. Design of steel structures. Plated structural elements. BSI, London.

BSI (2008) NA to BS EN 1991-1-4:2008. UK National Annex to Eurocode 1. Actions on structures. General actions. Wind actions. BSI, London.

Collings D (2005) Lessons from historical failures. *Proceedings of the ICE – Civil Engineering* **161(6)**: 20–27.

Cooper JH and Harrison MF (2002) Development of an alternative design for the West Rail viaducts. *Proceedings of the ICE – Transport* **153(2)**: 87–95.

Detandt H and Couchard I (2003) The Hammerbruke viaduct, Belgium. *Structural Engineering International* **13(1)**: 16–18.

Dickson DM (1987) M25 orbital Road, Poyle to M4: alternative steel viaducts. *ICE Proceedings, Part 1* **82(2)**: 309–326.

Horne M (1977) *Structural Action in Steel Box Girders*. CIRIA Guide 3. Construction Industry Research and Information Association (CIRIA), London.

Johnson P (2003) CTRL section 1: Environmental management during construction. *Proceedings of the ICE – Civil Engineering* **156**(Special Issue).

Merison (1971) *Inquiry into the Basis of Design and Method of Erection of Steel Box Girder Bridges*. Interim Report of the Committee on Steel Box Girder Bridges. HMSO, London.

Plu B (2001) TGV Mediterranean railway bridges. *Composite Bridges – State of the Art in Technology and Analysis. Proceedings of the 3rd International Meeting*, Madrid.

Ryall MJ (1999) Britannia Bridge: from concept to construction. *Proceedings of the ICE – Civil Engineering* **132(2)**: 132–143.

Sibly PG, Bouche T, Walker AC, Cooper T, Stephenson R and Moisseiff LS (1977) Structural accidents and their causes, L. *ICE Proceedings*, *Part 1* **62(2)**: 191–208.

Subedi N (2003) Double skin steel–concrete composite beam elements: experimental testing. *The Structural Engineer* **Nov**.

Steel–concrete Composite Bridges
ISBN 978-0-7277-5810-1

http://dx.doi.org/10.1680/scb.58101.145

ice
Institution of Civil Engineers
publishing

Chapter 8
Trusses

> ... the simpler truss types ... with linked bracing between bays or bracing that is directly in line give the best forms ...

8.1. Introduction

The heyday of the truss was in the nineteenth century, when many types were developed empirically (Figure 8.1), all aimed at carrying the relatively heavy rolling load of the train. Today the relatively high fabrication costs of truss members and, in particular, the numerous joints, have meant that they tend to be economic only for larger spans or heavier loads such as railways.

The truss tends to be of two basic forms: the through truss, where the railway passes between a pair of trusses; and the underslung truss, where the railway rides over the truss. Composite action in the truss may occur in a number of ways. Usually the deck slab is formed of a concrete slab composite with steel transverse beams, the beams being supported by the trusses. This may be a filler joist form, or a beam and slab form. For the simply supported through truss the slab is at the bottom chord level and so is in the tensile zone, it does not act efficiently as a composite section. The underslung truss is more efficient in this respect as the slab forms part of the top compression chord, it also avoids the additional transverse bending effects induced from the cross girders in the through truss form. Occasionally, where a double deck structure is used, both forms are combined. Trusses may also be used on continuous structures (Forsberg, 2001) or cable stay structures (Collings, 1996; Gimsing, 2001).

Typical span/depth ratios for trusses are outlined in Table 8.1. Railway structures will tend to have lower span/depth ratios because of the higher live loads and the tight deflection and rotational limits of modern high-speed railways. The angle of the diagonals should generally be kept constant, in order to keep details standardised and to avoid a cluttered visual appearance. For almost any truss structure, when viewed obliquely, there will be an intersection of elements. Diagonals at 45–65° to the horizontal are generally the most efficient structurally; shallower angles tend to have higher relative loads and are less stiff. The Fink and Bollman trusses (Figure 8.1a and 8.1b) have relatively shallow diagonals and tend not to be used today (although they have in the past been used to produce some stunning structures (Leonhardt, 1982; Dupre, 1998)). The bay length of a truss should be a multiple of the transverse beam spacing, with an even number of bays being preferred in order to avoid crossed diagonals if a modified Warren or Pratt truss configuration is used.

8.2. Example 8.1: Truss efficiency

An analysis of the ten truss types shown in Figure 8.1 has been carried out, assuming a 60 m span and a 10 m height. The structures were sized to carry a 1 MN rolling load. Both through and underslung forms were considered. The results of the analysis are shown in Figure 8.2. A number of conclusions can be drawn, the most obvious being that all the braced forms of truss are significantly lighter than the Vierendeel type. It is also clear that the underslung system utilising a composite beam and slab system

Figure 8.1 Truss types: (a) Fink; (b) Bollman; (c) double Pratt; (d) K brace; (e) X brace; (f) Pratt; (g) modified Warren; (h) Warren; (i) Bowstring; (j) Vierendeel

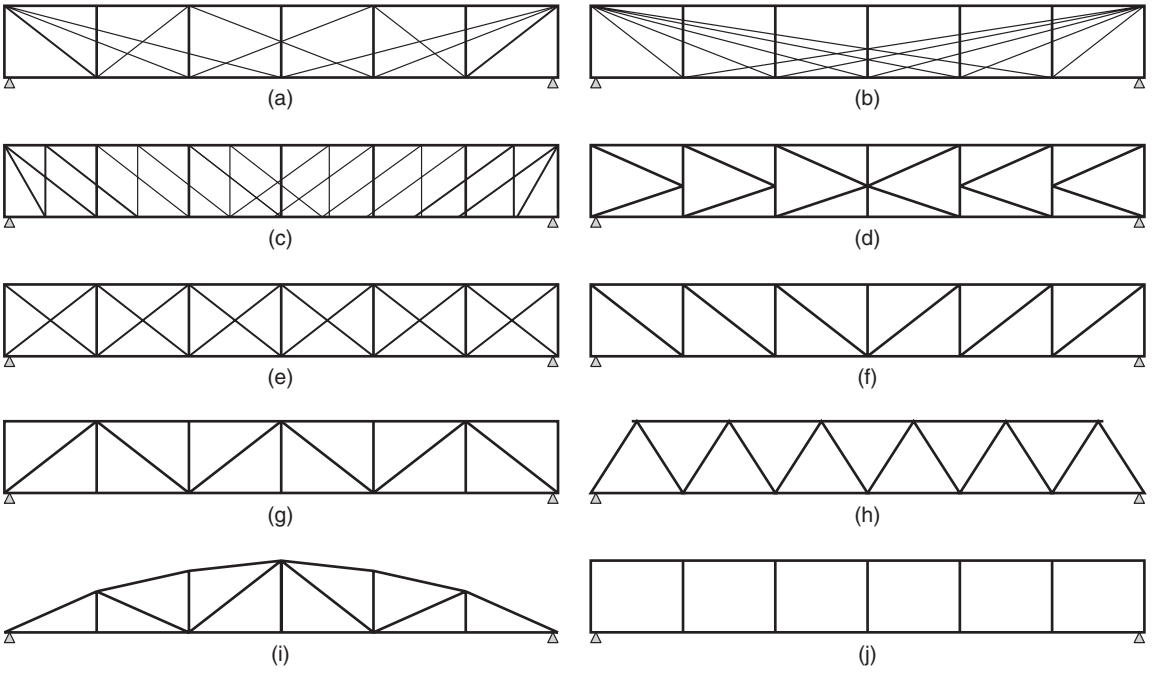

is more efficient than the through truss for all truss types. In general, the stiffer the structure for a given steel tonnage the more efficient the structure (Leonhardt, 1982), the simpler truss types tending to be stiffer. Those trusses with linked bracing between bays (Figure 8.1h) or bracing that is directly in line (Figure 8.1i) give the best forms.

The truss forms were analysed, as is traditional, as pin-jointed frames. This is permitted by codes (BSI, 2000), as the moments at joints induced by deflection are secondary and not required for the equilibrium of external loads. Most well-framed structures have sufficient deformation capacity at joints for this assumption to be valid. Where node eccentricity is present (see Figure 9.12) the moments should be considered. Where truss members are stocky, the moments may also be more significant; and, of course, for untriangulated forms such as the Vierendeel truss (Figure 8.1j) the moments will dominate the design.

Table 8.1 Span/depth ratios for truss bridges

Truss form	Typical span/depth ratio
Simply supported highway truss bridge	10–18
Continuous highway truss bridge	12–20
Simply supported railway truss bridge	7–15
Continuous railway truss bridge	10–18

Figure 8.2 Relative weight and stiffness of the various truss types shown in Figure 8.1

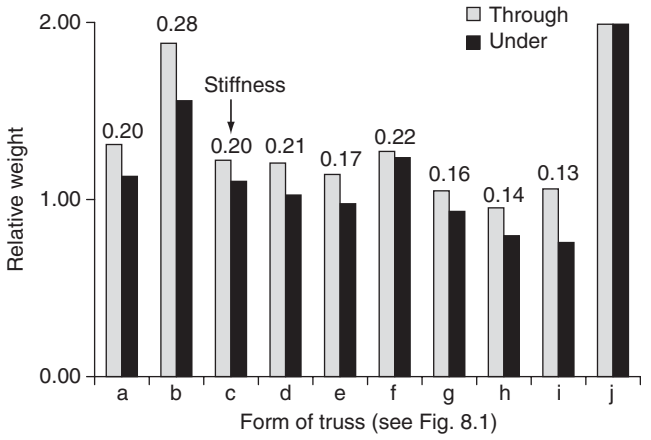

A number of simple criteria for the efficient design of truss bridges have been developed (based on Tianjian (2003)). In order of relative importance these are as follows.

- Each bay of the truss should be braced (not Vierendeel).
- The truss should support the load directly (underslung rather than through).
- The truss layout should exploit the properties of the materials used (composite, with concrete in compression and steel in tension).
- The size of the bracing should reflect the loads carried (using smaller diagonals at midspan where shears are low).
- The bracing between bays should be linked (Warren truss rather than Pratt type).
- The bracing should be linked in a continuous line between bays (a bowstring form).
- The bracing should be at 45–65° to the horizontal (Warren truss rather than Bollman type).
- When additional bracing is added it should follow the above criteria (i.e. the bracing within the bowstring form).

From the above criteria, a steel–concrete composite underslung fish belly or Warren truss emerges as the most efficient form. Both forms have recently been used to support high-speed railways in Europe (Plu, 2001; Detandt and Couchard, 2003). Figure 8.3 outlines these two structures.

8.3. Member types

The type of member used in the truss will depend on the span, the loading and the force it is carrying (tension or compression). For smaller spans and lighter loads, rolled beam, channel or tubular sections may be appropriate. For most bridge trusses, a fabricated section will be used, the form of which will depend on the location of the member. For compression chords, the effective length for buckling out of the plane of the truss is likely to be longer than the in plane length, and so the use of an I-section on its side is more appropriate to maximise the transverse radius of gyration. The vertical I-section is more appropriate for the lower tensile flange (on a simply supported truss), which also carries local bending from the transverse beams. Open I-, U- or C-sections are preferable due to their easier fabrication and because they allow simpler splice–plate connections. Box sections are efficient for larger trusses where internal access can be gained. The use of a concrete-filled section creating a steel–concrete composite section can be used to increase the capacity of the basic steel section.

Figure 8.3 Composite underslung truss: (a) fish belly at L'Arc; (b) Warren truss at Hammerbruke

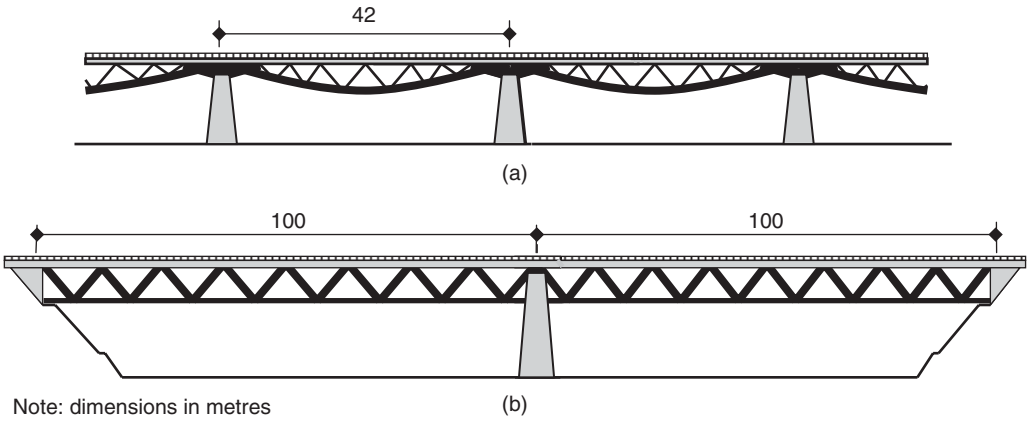

8.4. Steel sections under axial load

In Chapter 1, the basic limitations of steel sections in buckling were outlined, the limiting axial compression load being determined from Equation 1.7 provided that local buckling is prevented by the limits of the plate geometry (see Table 1.3):

$$N_D = \chi A_a f_y \tag{8.1}$$

The limiting compressive stress (χf_y) depends primarily on the member slenderness parameter λ, which for axial loads this is dependent on the effective length (L_e) of the member and its radius of gyration (i), as in the equations used previously for plate girders:

$$\lambda = L_{eff}/77i \tag{8.2}$$

For design there is a variation in capacity for different section types (Figure 8.4), with small, hot-rolled, hollow sections having larger capacities than large fabricated welded sections with thick plates (>40 mm). Rolled beam and column sections or fabricated sections using thinner plates have intermediate relative capacities.

Typical effective lengths for truss members are given in Table 1.4. In general, the out-of-plane buckling of a truss member is more critical than the in-plane buckling, and hence it is preferable to use sections with larger transverse inertia. Typically, where the length of a section exceeds 3.5 times its minimum dimension, buckling will affect the compression capacity to some extent.

8.5. Joints in steelwork – strength

A steel truss bridge is generally made up of a series of chord and diagonal components that are joined together. The joints may form the weakest element in the truss; at nodes the stresses may be complex, with bending and axial loads from various directions being combined and resolved. In general, jointing should be carried out away from the truss nodes, particularly if there is a change in section type (box to I or vertical to transverse I). Two forms of joints in steel structures are common: fully welded joints and bolted joints. The choice of joint type will depend on a number of factors, but particularly the expertise

Figure 8.4 Limiting compressive stress for grade 355 steel for members subject to axial loads: (a) hot-rolled hollow sections; (b) fabricated sections with plates less than 40 mm thick; (c) fabricated sections with plates more than 40 mm thick

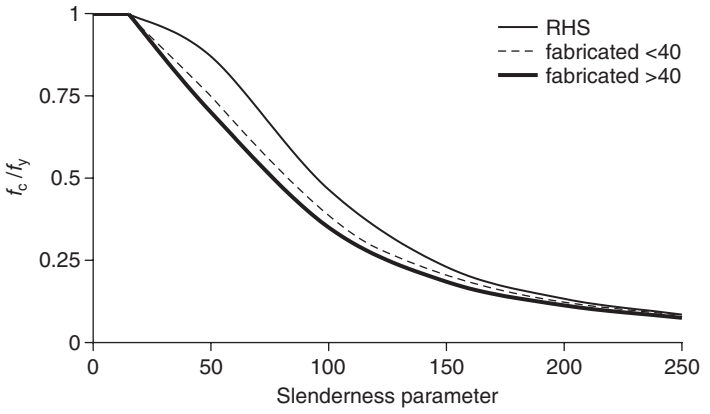

of the contractor and fabricator building the structure, the form of the structure, and the number and size of joints.

8.5.1 Welded joints

Welded joints are suitable for in-line flange or web connections where the full capacity of the section needs to be maintained. Welded joints are also suitable for structures where a protected environment can be created for the fabrication of a number of joints (i.e. viaduct structures) (see Chapter 5) or launched bridges. Full-strength joints will require the use of full-penetration butt welds, and where there is a change in plate thickness on one side of the joint the plate should be tapered at a minimum of 1 : 4 to limit stress concentrations and maintain a reasonable fatigue strength.

8.5.2 Bolted joints

For bridges, all bolted connections between main structural sections should use high-strength friction-grip (HSFG) bolts, which are preloaded and have a low initial slip, giving an almost rigid joint with good fatigue properties (see Chapter 4 for joint stiffness). HSFG bolts are best used in shear using lapped joints or joints with cover plates (Figure 8.5a and 8.5b). The use of end plates where bolts are in direct tension should be avoided, as the connection is more flexible, is subject to additional prying forces, and is generally more difficult to fabricate (Figure 8.5c).

The strength of a joint formed from HSFG bolts will be determined by the lower of: a failure in the elements being connected (usually across the bolt holes as a tension failure (P_T)), a failure in the cover plates (again usually across bolt holes (P_T) or by failure in bearing (P_B)), or a failure of the bolts in shear (P_V). At the ultimate limit state these capacities may be determined using

$$F_T = f_y A_{ae} \tag{8.3}$$

where A_{ae} is the area of the element being connected or of the cover plates, less the area of any bolt holes, and f_y is the yield strength of the element or cover plate.

$$F_v = 0.6 f_{ub} A_s n / \gamma_{m2} \tag{8.4a}$$

Figure 8.5 Bolted joint types: (a) lap joint in single shear; (b) cover plates in double shear; (c) plate joint in tension

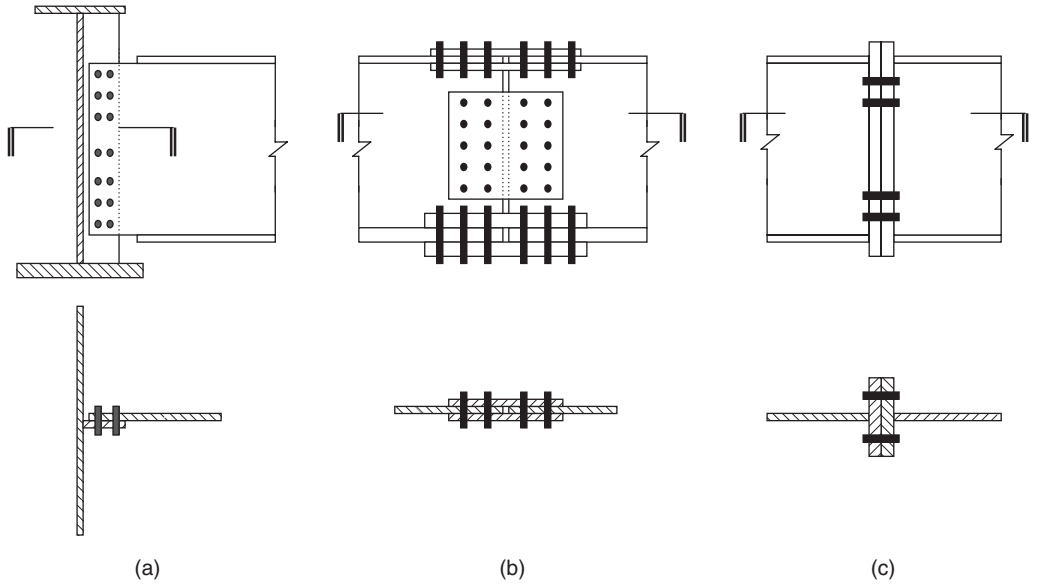

where f_{ub} is the ultimate tensile strength of the bolt (Table 8.2), A_s is the tensile area of the bolt (Table 8.2), and n is the number of shear planes.

$$F_b = k_1 f_u dt/\gamma_{m2} \tag{8.5a}$$

where d is the bolt diameter, t is the thickness of the plate in bearing, and k_1 is a factor based on the joint detail. For an edge bolt:

$$k_1 = 2.8(e_2/d_o) - 1.7, \text{ or } 2.5 \text{ whichever is smaller} \tag{8.6a}$$

$$k_1 = 1.4(p_2/d_o) - 1.7, \text{ or } 2.5 \text{ whichever is smaller} \tag{8.6b}$$

e_2, p_2 etc. are defined in Table 8.3, and d_o is the bolt hole diameter, normally 2 mm larger than the bolt diameter.

Table 8.2 Bolt strengths and areas

Bolt class	**4.6**	**5.8**	**8.8**	**10.9**	
f_{yb}	240	400	640	900	
f_{ub}	400	500	800	1000	
Bolt diameter	**M20**	**M24**	**M27**	**M30**	**M36**
Hole diameter	22	27	30	33	39
A_b	245	353	459	561	817

Table 8.3 Edge distances and spacing

	Minimum	Maximum
Edge distance e_1–e_2 for normal holes	$1.2d_o$	$4t + 40$ mm
Edge distance e_1–e_2 for oversize and slotted holes	$1.5d_o$	
Spacing along the joint p_1	$2.2d_o$	$14t$ or 200 mm
Spacing across the joint p_2	$2.4d_o$	$14t$ or 200 mm

For design purposes, Equations 8.4a and 8.5a can be simplified to

$$F_{vd} = 0.5 f_{ub} A_s n \tag{8.4b}$$

$$F_{bd} = 2 f_u d t \tag{8.5b}$$

The slip resistance of a joint is

$$F_s = k_s n \mu F_p / \gamma m_3 \tag{8.7a}$$

where k_s is a factor depending on the hole type (taken as 1.0 for normal holes, 0.85 for oversized holes and 0.7 for slotted holes). μ is a friction coefficient, determined from a test or taken between 0.4 and 0.5 for unpainted surfaces, but it may be as low as 0.2 for some painted surfaces, and for clean surfaces clear of loose rust and mill scale a value of 0.45 may be used. F_p is the proof load of the bolt:

$$F_p = 0.7 f_{ub} A_s \tag{8.8}$$

For design, at the ultimate limit state if the slip resistance is higher than the shear or bearing force, the lower of the shear or bearing resistance should be used. If the slip resistance is lower than the shear and bearing force, it may be assumed that the joint will slip into bearing or shear, and again the lower of these used. If the slip resistance is significantly less than shear or bearing, a check may need to be made at the serviceability limit state to ensure there is no slip at this state.

So, for design, Equation 8.7a simplifies to

$$F_{sd} = 0.3 f_{ub} A_s n \tag{8.7b}$$

8.6. Example 8.2: Steel truss

The next example in this chapter looks at a steel through-truss bridge constructed to carry a high-speed railway into London. The structure spans 75 m and carries two tracks over the east coast main line to a tunnel portal. The bridge is enclosed with an architectural cladding and has a tubular shape. The track through the bridge is on an isolated track slab to limit noise and vibration.

8.7. Enclosure

Steel requires both water and oxygen to corrode (see Chapter 3), so enclosure of the steel structure with a waterproof enveloping structure is an alternative to painting or the use of weathering steel. Enclosure may also be used as an additional supplementary protection layer to give enhanced durability for important structures (Highways Agency, 1996). To be successful, the enclosure must keep out water

and vermin, but have adequate ventilation to prevent high moisture content in the enclosed air space. The enclosure must also not impede regular inspection of the structural elements, and must itself be simple to maintain and be replaceable relatively easily (the life of an enclosure system is likely to be 30–50 years). Enclosure is a relatively expensive way to protect steelwork from corrosion, but where an enclosure is proposed for other reasons (architectural, fire or noise protection) the additional cost may be offset.

For the structure in Example 8.2, the cladding serves a number of functions. The structure is located at a tunnel portal over the east coast main line, and so a robust structure with enhanced fire protection was deemed necessary. Thick steel sections are used as the primary protection (thick steel sections are less likely to buckle or fail in a fire than are thin sections; see Chapter 12 for fire design), and a fire-resistant cladding is also provided to give added protection. The central London location also imposes environmental issues, including the need to limit railway noise; the internal cladding also assists this. The complete enclosure reduces direct rail and locomotive noise as well as the re-radiated structure noise (see Chapter 7 for noise from bridges). The cladding support structure is isolated from the main truss structure by steel-elastomeric units to limit the transfer of vibration to the cladding, thus limiting the re-radiated or 'rumble' noise. The external panels provide a curved architectural cladding and a waterproof skin. The gap between the main structure and the cladding is also sealed by mesh to prevent rats, pigeons and other vermin from gaining access to the inside of the cladding.

The structural form is a pair of Warren girders with chords and diagonals formed from fabricated girder sections. The top chord and diagonals have the beams oriented transversely to maximise the resistance to lateral buckling (Figure 8.6a). The lower chord is oriented vertically to resist the local bending from train loads and the significant local reactions induced during the launched construction of the bridge (Figure 8.6b). Cross-beams span transversely between the lower chords and support a concrete structural slab. Plan bracing spans transversely between the top chords.

8.7.1 Loading and analysis

The total weight of the bridge (G), cladding and fixings is 25 MN, and the total live loading (Q) is similar. The bridge analysis is carried out using a 3D truss model with continuous joints, such that

Figure 8.6 Chord to diagonal intersection in Example 8.2: (a) upper node; (b) lower node

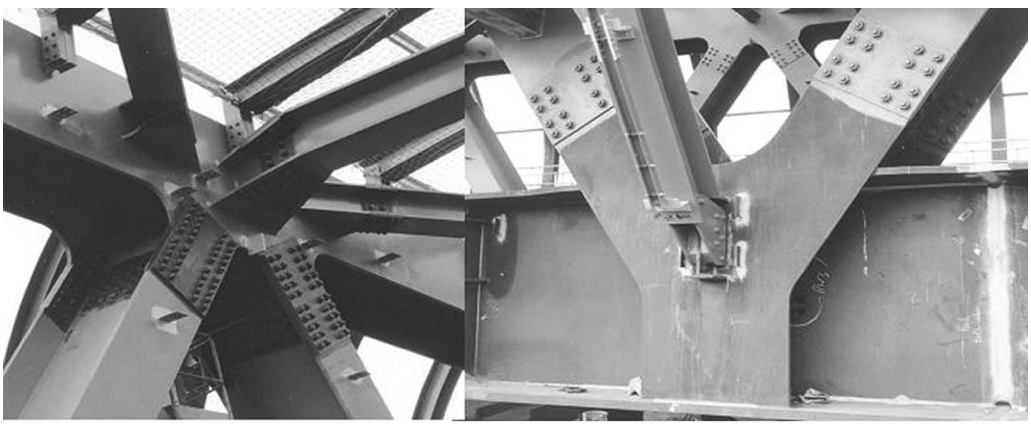

(a) (b)

moments, shears and axial loads are obtained. However, for the primary member design and splice design, the moments are small, and only the primary axial load will be considered.

The load in the chords of a truss may be estimated by assuming the compression and tension in the chords resist the bending moment, and is calculated assuming the truss is a conventional girder:

$$N_C = N_T = M/D \tag{8.9a}$$

Similarly, the forces in the diagonals can be calculated by resolving the calculated shear force through to the inclination of the members:

$$F = V/\sin\theta \tag{8.10}$$

In this example, at the ultimate limit state, $M = 600$ MN m and $V = 32$ MN. The depth between the centre of the chords is 7.58 m, and the angle of the diagonals to the horizontal is 58°. Using Equation 8.6a, the compression in each of the two top chords is

$$N_C = M/D = 600/(7.58 \times 2) = 40 \text{ MN}$$

From the analysis model, the compression is 37.2 MN and there are some associated moments. The width of the section used is 800 mm, and the length/width ratio is 9.5. This is greater than 3.5, and so buckling needs to be considered.

The effective length of the top chord (from Table 1.4) is 0.85 times the length between truss nodes for both in-plane and out-of-plane buckling; $L_e = 0.85 \times 9.4 = 7.7$ m. Section properties for the chord are outlined in Appendix C; the in-plane radius of gyration is the smaller, with i_y being 0.29 m. Using Equation 8.2,

$$\lambda = L_e/77i = 7.7/(77 \times 0.29) = 0.35$$

From Figure 8.4, using the curve for thick fabricated sections, $f_{ac} = 0.87 f_y$. For sections with 65 mm plate, $f_y = 315$ N/mm^2 (see Figure 1.4). Using Equation 1.7b with $A_{ae} = 0.225$ m^2, the capacity of the section is

$$N_D = f_y A_{ae} = 0.87 \times 315 \times 0.225 = 61.6 \text{ MN}$$

which is larger than the applied load of 40 MN.

Using Equation 8.7, the force (compression) in the diagonals adjacent to the support at the ultimate limit state is

$$F = V/\sin\theta = 32/(2 \times \sin 58) = 19 \text{ MN}$$

At the serviceability limit this is reduced to 13.7 MN.

At both the upper and lower node the joint is a fully welded connection with radiused plates to reduce stress concentrations (Figure 8.6a and 8.6b). A bolted connection formed using splice plates with HSFG bolts loaded in shear is placed just away from the node.

The number of bolts in the section may be approximated initially by dividing the force by the bolt capacity:

$$n = N_F/F \tag{8.11}$$

where F is the appropriate bolt capacity in shear, bearing, tension or friction.

Assuming M36 HSFG bolts will be used with $A_b = 817\ \text{mm}^2$ and $f_{ub} = 800\ \text{N/mm}^2$, then from Equation 8.4 for bolts in double shear:

$$F_{vd} = 0.5 f_{ub} A_s n = 0.5 \times 800 \times 817 \times 10^{-3} \times 2 = 653\ \text{kN}$$

The maximum number of bolts required at the ultimate limit state is

$$n = N_F/F_v = 19/0.65 = 30$$

$$F_{sd} = 0.33 f_{ub} A_s n = 0.33 \times 800 \times 817 \times 10^{-3} \times 2 = 431\ \text{kN}$$

$$n = N_F F_{sd} = 19/0.43 = 44$$

The number of bolts is governed by the requirements to limit slip, and this is generally true for most HSFG joints on bridges.

The cover plate sizes are smaller than the main sections, and so a tension check is made through the plates. The area of the plates is 107 000 mm^2, and there are 15 holes of 39 mm diameter across the width, reducing the plate area (A_{ae}) to 77 500 mm^2. Using Equation 8.3,

$$F_T = f_y A_{ae} = 345 \times 0.0775 = 25\ \text{MN}$$

This is greater than the 19 MN applied, and so is satisfactory.

The bridge is constructed adjacent to the railway and launched across it (Figure 8.7). The behaviour of the bridge is significantly altered by this launch; there are tensions in the upper (previously the compression) chord and compressions in the lower (previously the tension) chord (see also Collings and Chiodi, 2011). More significantly, large local patch loading of the lower chord occurs.

8.8. Local loading of webs

The design resistance of a girder subject to a local load on the flange that is transferred to the web and then the rest of the structure, for example, when a bridge is being launched (Figure 8.8), may be estimated as

$$F_R = f_y L_{eff} t_w/\gamma_m \tag{8.12}$$

$$L_{eff} = \chi_F l_y \tag{8.13}$$

where l_y is the effective loaded length of the stiff bearing. Where the flanges are bigger than the web, the effective loaded length may be estimated as the loaded length (s) plus ten times the flange thickness:

$$l_y = s + 10 t_f \tag{8.14}$$

Figure 8.7 Launch sequence for a truss bridge. Construct the bridge adjacent to the railway on the launch track. Place the launch skids and the nose, and construct the temporary tower. Launch the bridge until the nose is on the tower, then remove the central skid. Launch the bridge until it is at the final location. Place the final bearings, and remove the launch skid and nose

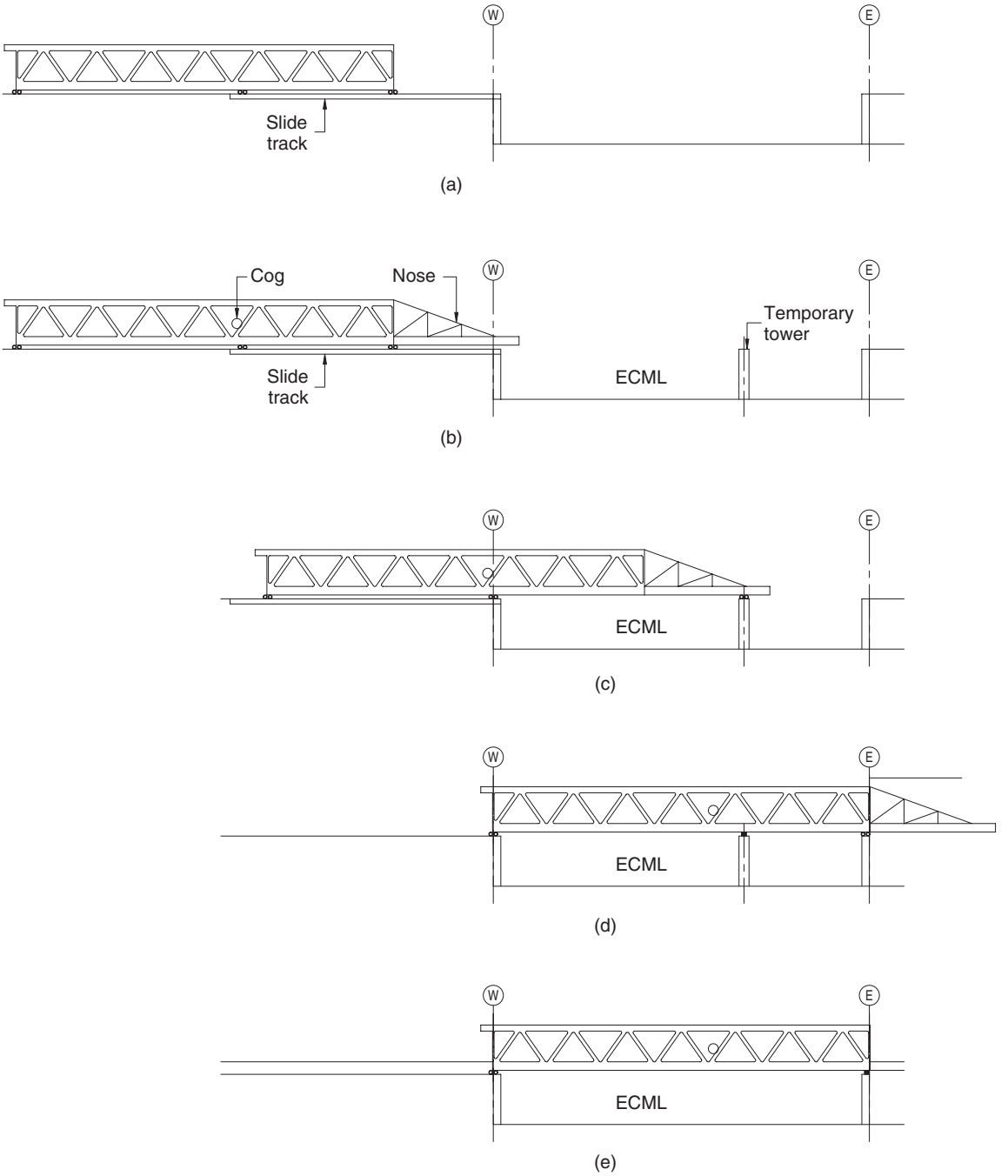

Figure 8.8 Patch loading on the web of Example 8.2, due to launching

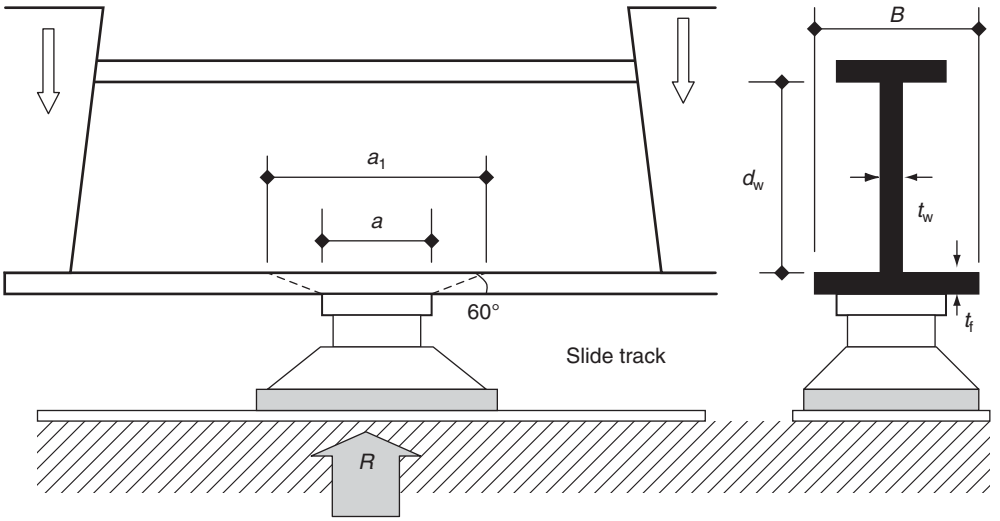

If stiffeners are provided on the web, a less conservative estimate of the effective loaded length may be obtained from Eurocode 3: Part 1-5 (BSI, 2006), but l_y should not be greater than the stiffener spacing.

The reduction factor χ_F for bearing is to take into account local buckling of the web, and is dependent on the web geometry and the critical buckling load F_{cr}:

$$\chi_F = 0.5(F_{cr}/F_y)^{1/2} \tag{8.15}$$

$$F_y = f_y l_y t_w \tag{8.16}$$

When the stiffener spacing is large,

$$F_{cr} = 5Et_w^3/h_w \tag{8.17a}$$

Where the stiffener spacing is closer, such that $h_w/a < 1$,

$$F_{cr} = 7.2Et_w^3/h_w \tag{8.17b}$$

According to Eurocode 3: Part 1-5 (BSI, 2006), the patch loading is verified such that

$$\eta_2 = F_{E/}F_R < 1 \tag{8.18}$$

The author would recommend stiffeners if η_2 is greater than 0.5. With patch loading there is likely also to be some local shear and bending, and a shear bending interaction (see Chapter 4) together with the patch loading may need to be considered. The full *M–V–N* interaction for slender webs is considered in Chapter 10. A simple, but conservative, interaction is

$$F_E/F_R + M_E/M_f + V_E/V_w < 1 \tag{8.19}$$

providing no individual part is greater than 0.5.

In Example 8.2 the launch reaction on one truss chord is approximately 10 MN at the ultimate limit state. The length of the local load (s) is 1000 mm, the web thickness is 60 mm and the flange thickness is 65 mm. For these thick sections $f_y = 325$ N/mm^2. Using Equations 8.15 and 8.17,

$$l_y = s + 10t_f = 1000 + 10 \times 65 = 1650 \text{ mm}$$

$$F_y = f_y l_y t_w = 325 \times 1650 \times 60 = 32.2 \text{ MN}$$

Stiffeners are provided on the web of the chord to support the cross-beams. These are at 1300 mm centres and will be taken into consideration for the web loading using Equations 8.18. Note that the stiffeners themselves should also be verified for the local load (see Chapter 4).

$$F_{cr} = 7.2Et_w^3/h_w = 7.2 \times 210\,000 \times 603/1650 = 198 \text{ MN}$$

$$\chi_F = 0.5(F_{cr}/F_y)^{1/2} = 0.5(198/32)^{1/2} = 1.24$$

χ_F should not be taken as larger than 1.0.

$$F_R = f_y L_{eff} t_w/\gamma_m = 325 \times 1.0 \times 1650 \times 60/1.1 = 29 \text{ MN}$$

The launch load is 10 MN, which is less than the capacity; the local launching stresses are acceptable without additional stiffeners.

8.9. Continuous trusses

The basic trusses considered are simply supported structures. Trusses can be used for continuous structures, often of large span. In the USA, many large variable-depth continuous trusses have been built using steel, the depth varying with the moment such that an approximately constant chord size can be utilised. Rearranging Equation 8.7,

$$D = M/N_a \tag{8.9b}$$

In Europe, a number of continuous trusses have been used, particularly for railway structures (Saul, 1996), and the tendency has been to use composite or double-composite structures (Figure 8.9), giving increased efficiency:

$$D = M/N_{a-c} \tag{8.9c}$$

Underslung continuous trusses tend to be deep structures, allowing the use of double deck structures with two levels of highway, or a highway at one level and a railway at another. For longer spans, the trusses may be cable stayed (Collings, 1996; Gimsing, 2001). The Øresund project in Sweden (Forsberg, 2001) utilised a series of 144 m span double-deck trusses with a 490 m cable-stayed section. The bridge carried a concrete deck supporting the road at a higher level, with a railway on the lower chord. The Øresund Bridge also utilises high-strength steel.

8.10. High-strength steel

Typically, in Europe steel with a nominal yield strength of 355 N/mm^2 is assumed for the design of rolled sections and steel plate. Most of the examples given until now have used this grade, although Eurocodes are based on a 275 N/mm^2 strength steel. Higher strength steel plate is available, and a 460 N/mm^2 grade is now becoming more common. In Japan, steel plate strengths up to 700 N/mm^2 have been used. A number of issues need to be considered when using high-strength steel.

Figure 8.9 Variable-depth continuous truss of the doubly composite Nantenbach Bridge

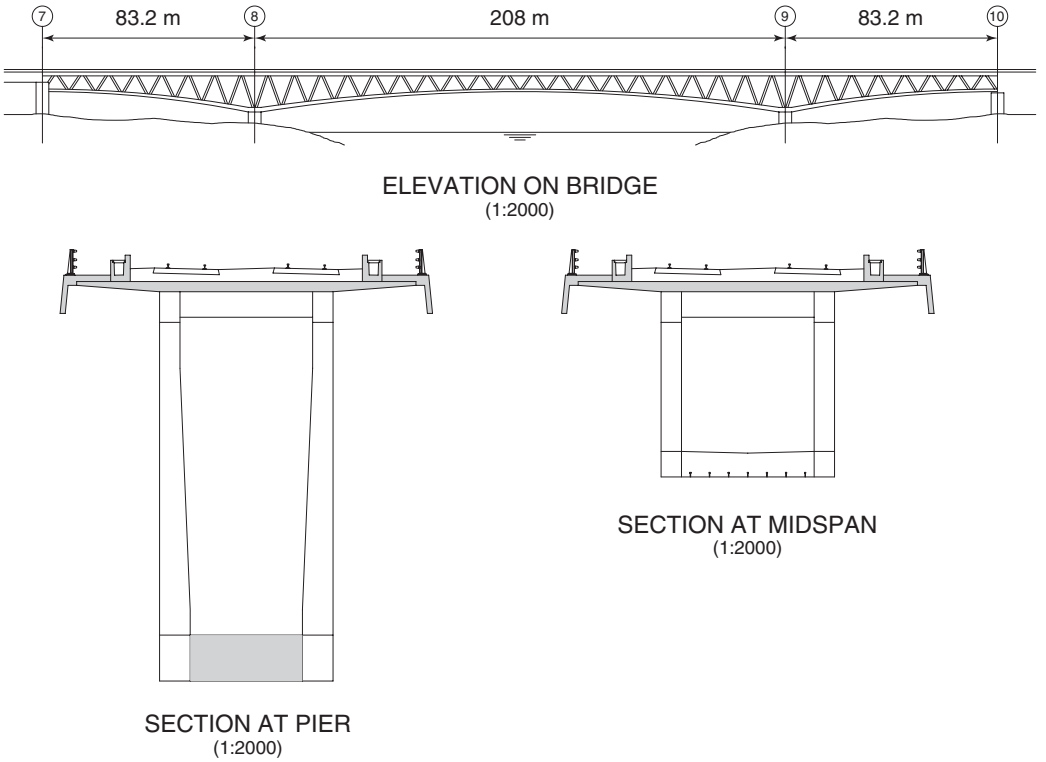

The first issue is weldability and fatigue. High-strength steel requires careful consideration of weld details. The steel is more difficult to weld, the fabrication shop must be set up to accommodate it, and standard production tests must be repeated for the higher grade, and this is unlikely to be economic for small structures. The higher stresses in the section will require additional testing (BSI, 1999). The higher stresses used will also lead to fatigue being more critical, as the limiting fatigue stress (f_A) for various details is not increased with steel grade. The bridge should be designed with this in mind, and details such as doubler plates with a low fatigue classification should be avoided. Second, the reduced steel area obtained for a given load will lead to a reduced stiffness, as the elastic modulus for steel (E_a) is independent of strength. The increased stresses may also cause more cracking at continuous supports. Finally, for steel sections subject to compressive loads, the critical load at which buckling occurs will be affected. The slenderness parameter λ is modified:

$$\lambda = \lambda(f_y/355)^{1/2} \tag{8.20}$$

This means that, for high-strength steel, buckling becomes more critical.

REFERENCES

BSI (1999) BS 5400-6:1999. Steel, concrete and composite bridges. Specification for materials and workmanship, steel. BSI, London.

BSI (2000) BS 5400-3:2000. Steel, concrete and composite bridges. Code of practice for design of steel bridges. BSI, London.

BSI (2006) BS EN 1993-1-5:2006. Eurocode 3. Design of steel structures. Plated structural elements. BSI, London.

Collings D (1996) *Design of Innovative Concrete Bridges for south China. Bridge Management 3*. E&F Spon, London.

Collings D and Chiodi L (2011) Tricky truss: design and construction of bridge GE19, London. *Proceedings of the ICE – Civil Engineering* **CE4**: 177–183.

Detandt H and Couchard I (2003) The Hammerbruke viaduct, Belgium. *Structural Engineering International* **13(1)**: 16–18.

Dupre J (1998) *Bridges*, Konemann, New York.

Forsberg T (2001) The Oresund approach bridges. *Composite Bridges – State of the Art in Technology and Analysis. Proceedings of the 3rd International Meeting*, Madrid.

Gimsing N (2001) Composite action and high strength steel in the Oresund bridge. *Composite Bridges – State of the Art in Technology and Analysis. Proceedings of the 3rd International Meeting*, Madrid.

Highways Agency (1996) BD 67, Enclosure of bridges. In *Design Manual for Roads and Bridges*, Vol. 2. The Stationery Office, London.

Leonhardt F (1982) *Bridges, Aesthetics and Design*. Architectural Press, London.

Plu B (2001) TGV Mediterranean railway bridges. *Composite Bridges – State of the Art in Technology and Analysis. Proceedings of the 3rd International Meeting*, Madrid.

Saul R (1996) Bridges with double composite action. *Structural Engineering International* **6(1)**: 32–36.

Tianjian J (2003) Concepts for designing stiffer structures. *The Structural Engineer* **81(21)**: 36–42.

Steel–concrete Composite Bridges
ISBN 978-0-7277-5810-1

http://dx.doi.org/10.1680/scb.58101.161

ice Institution of Civil Engineers
publishing

Chapter 9
Arches

. . . 'sculpting bridges' . . .

9.1. Introduction

The arch form has been around for millennia, and many masonry arches (and some using concrete) survive from the Roman period 2000 years ago (O'Connor, 1993). The arch carries load using compression, so it is ideal for materials, such as concrete, that have limited tensile strength. Concrete is heavy, and for large spans the higher strength/weight ratio of steel can significantly reduce arch thrusts. The problem with steel arches is that the steel is prone to buckle under compression and requires extensive stiffening and bracing. A composite structure, if carefully considered, can combine the best features of concrete and steel. Figure 9.1 outlines the typical arch forms and the terminology used. The terms 'crown', 'springing', 'rise', etc. are derived from the terms used for masonry structures. Table 9.1 outlines typical geometric ratios used to size this form of structure.

The thrust of an arch (N_A) may be estimated approximately by calculating the equivalent bending moment that would occur on a beam of the same span (providing the arch shape and bending moment shapes are similar), and assuming that the lever arm resisting the moment is simply the arch rise (r). For parabolic arches under uniform loads this method gives good agreement with more complex analytical methods:

$$N_A = M/r \tag{9.1}$$

9.2. Example 9.1: Composite arch

The first example in this chapter is used to explore the behaviour of a composite arch. The example considered is the Runnymede Bridge (Cracknell, 1963) over the River Thames, about 5 km downstream of Brunel's famous shallow red-brick arch, and a similar distance upstream of Hampton Bridge. The aesthetics of the structure were said by Edwin Lutyens in the 1930s to rival the other arches, including those of his bridge at Hampton 'better than any others' (Lutyens, 1991). The structure has the appearance of a white-stone arch with red-brick spandrels. The external appearance is a wonderful example of this form (Highways Agency, 1996). The structure is formed from a thin 225 mm concrete slab spanning 55 m. The slab is stiffened by and acts compositely with steel truss ribs that support the upper deck slab, which carries traffic loads. The structure is now incorporated into the M25, carrying the northbound carriageway, and the A30, with another new structure adjacent to it (Benaim *et al.*, 1980).

9.2.1 Loading and analysis

The key dimensions of the Runnymede Bridge are shown in Figure 9.2. The total dead plus surfacing characteristic load is about 70 kN/m per lane. Assuming a 30 kN/m per lane live load, we have a 100 kN/m per lane total load, say, about 145 kN/m at the ultimate limit state. For a span of 55 m

Figure 9.1 Arch forms and notation

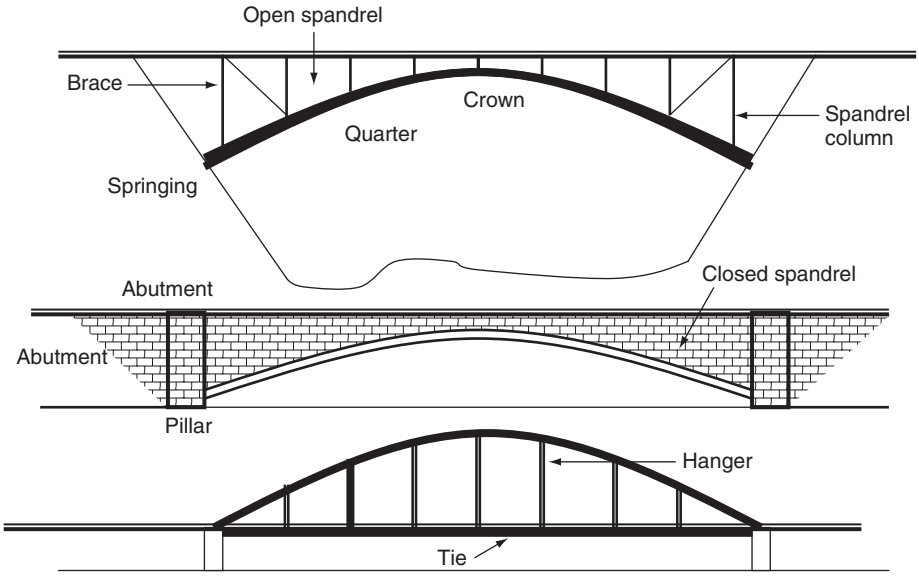

the applied load and resultant forces are

$$G = 55 \times 145 = 8.0 \text{ MN}$$

$$M = 8.0 \times 55/8 = 55 \text{ MN m at the crown}$$

The rise of the arch is 5.5 m, so the midspan thrust (using Equation 9.1) is:

$$N_E = M/r = 55/5.5 = 10.0 \text{ MN}$$

The slab thickness is 225 mm and the cube strength of the concrete is 40 N/mm^2 ($f_{ck} = 32$ N/mm^2, see Chapter 1), so the arch capacity (using Equation 1.4b) is:

$$N_D = 0.57 f_{ck} bh = 0.57 \times 32 \times 3.5 \times 0.225 = 14.3 \text{ MN}$$

Therefore, as $N_D > N_E$, the slab can carry the entire structure. However, traffic loading is seldom uniform in practice, and the bridge will have to carry large abnormal vehicles. The moment diagram

Table 9.1 Typical geometric ratios

Arch type	Span to rise (L/H)
High	1.0
Semi circular	2.0
Typical range	2.5 to 7
Flat	Below 10

Figure 9.2 Runnymede Bridge details

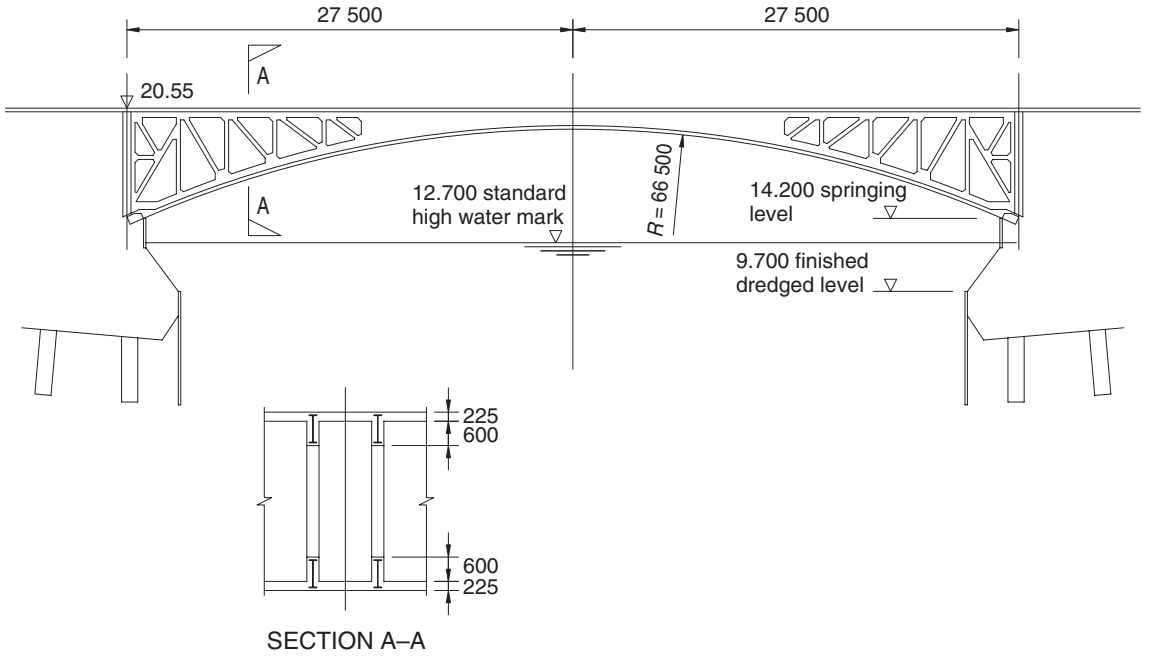

for the abnormal vehicles is not the same shape as the arch (particularly for loads placed near the quarter span), and the resultant thrust occurs outside the arch. Large moments are induced in the slab, together with large deflections, and the slab will buckle unless stiffened (see Figure 9.17).

The slab of the Runnymede Bridge is stiffened by steel ribs at approximately 1.6 m centres. The ribs, which vary from 800 mm deep plate girders at mid-span to 5 m deep trusses near the springing, carry the moments from asymmetric loads. The steel elements themselves are encased in concrete to form a double-composite action (see Chapter 6), which helps to carry secondary, local moments more efficiently. The moment is carried by the ribs and resisted as a couple by the top and bottom elements.

Another major problem with concrete arches is that they require significant falsework support during construction; this centring will fill the entire span and is often a significant structure in its own right. At Runnymede the problem was overcome by using the steel stiffening ribs as the support during construction. The steel rib trusses were built in cantilever from each side of the river. Once the steelwork was closed, formwork for the arch was hung from the steel and the slab concreted in bays, leapfrogging from each springing to crown. This method of construction (Figure 9.3) complicates the stress analysis of the structure, as some of the dead load is now carried by the steelwork rather than all the load being carried by the concrete slab, as previously assumed.

9.3. Composite filled tubes in China

The steel–concrete composite arch form using the steel to carry initial construction loads has been developed dramatically in China in recent years. The development of composite structures in China has taken a different path from that in Europe. In Europe, composite columns have been used in buildings since the 1960s, and have developed into the 3 m by 3 m mega-columns of

Figure 9.3 Runnymede construction sequence

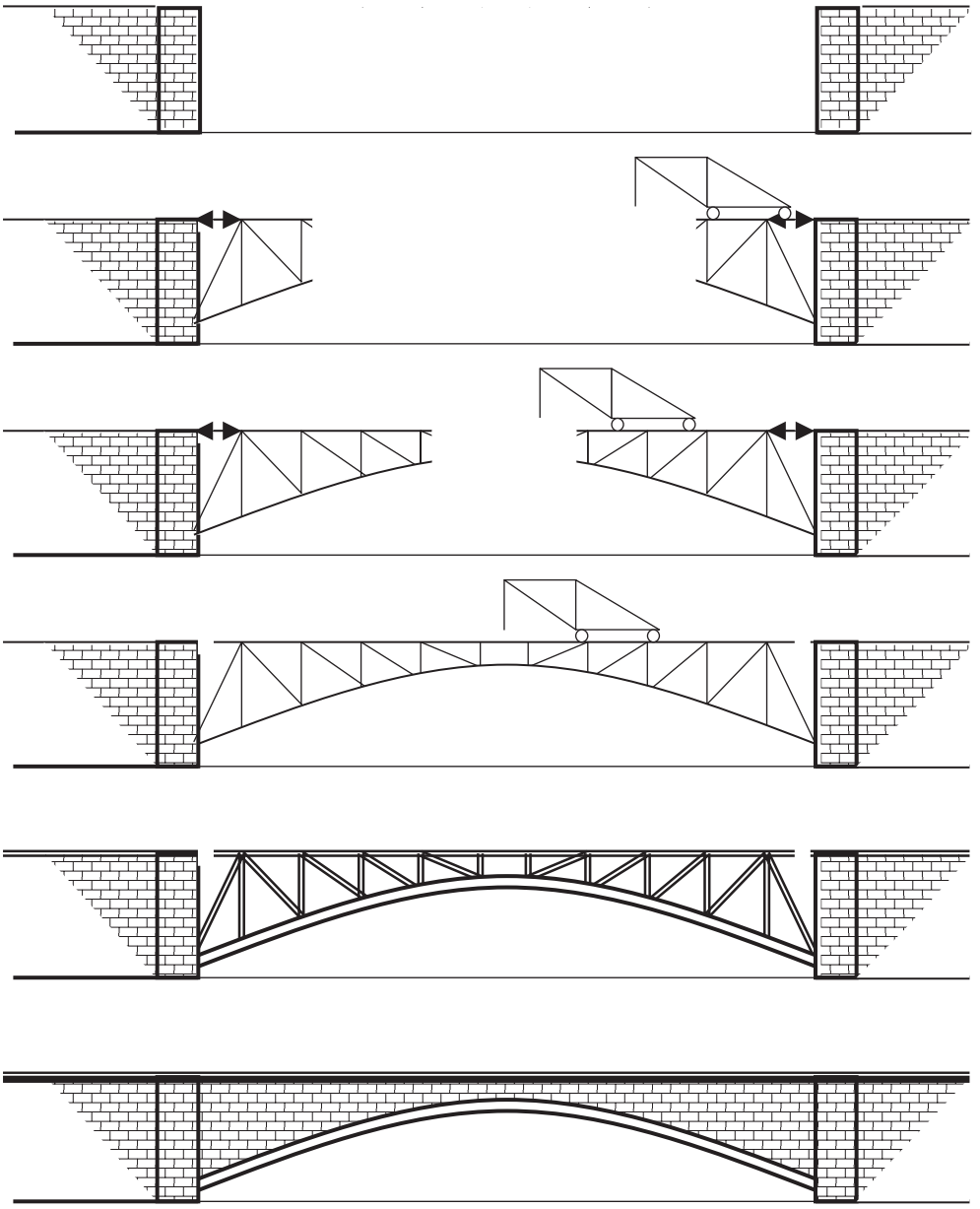

Tower 101 (Collings, 2010). The use of concrete-filled steel tubes (CFSTs) in bridges began in the early 1990s. An early example is the Wanxin Bridge (Yan and Yang, 1997), for which ten 406 mm diameter, 16 mm thick steel tubes fabricated into a braced truss framework were constructed in cantilever using stays, such that a light but stiff steel framework in an arch form spanned 420 m over the Yangzi River. The tubes were then filled with concrete to further stiffen and strengthen them. A travelling formwork

Figure 9.4 Tubular composite arch bridge, the Wanxian Bridge in China (Yan and Yang, 1997)

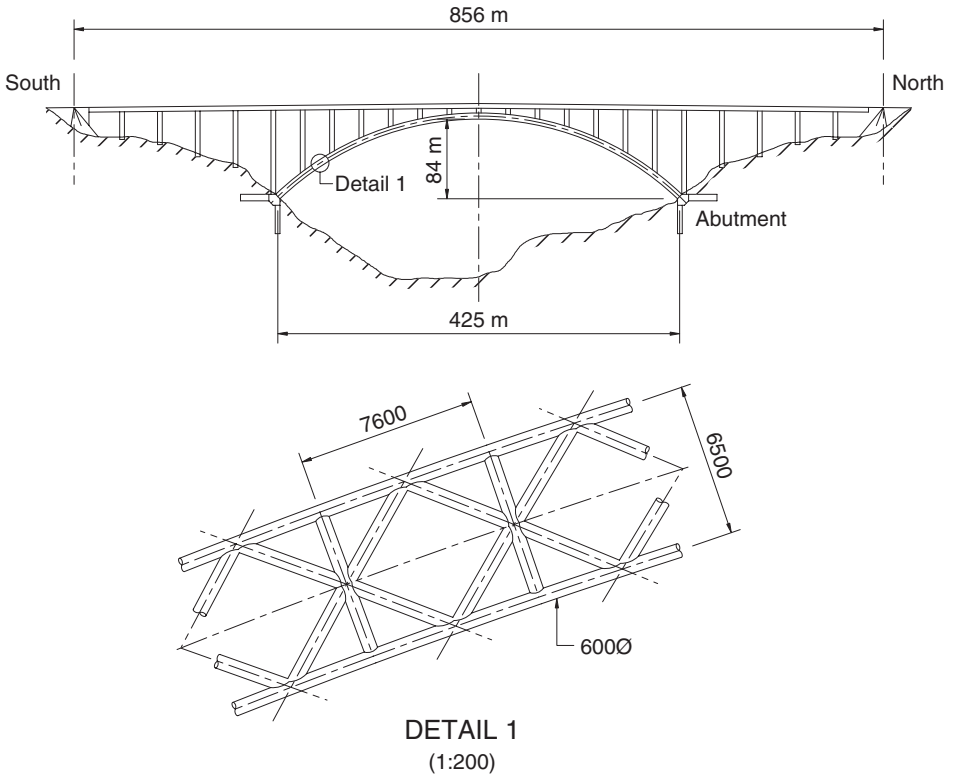

system was then used to construct a concrete box section around the steel frame. The final arch structure is primarily a concrete section with the steel framework embedded within it (Figure 9.4).

Today in China it is more common to use the CFSTs as the final structural form, and not just as a temporary platform (Zang *et al.*, 2004). The CFST bridge started with a single tube of 800 mm diameter on an 80 m span in Zhengjiang province. It developed to a dumbbell form with spans of 270 m on a bridge in Yongjian province, and has developed further to multiple dumbbell types with 750 mm diameter, 20 mm thick tubes filled with grade 60 concrete on a 360 m span at Guanggou (Figure 9.5) (Zuou and Zhu, 1997; Dajun, 2001).

The design methods have developed gradually, and the current methods are comparable with Eurocode methods in terms of both the strength and the stiffness of both the steel tube and the concrete infill. The construction of the bridges has developed with confidence, based on extensive research into the behaviour of CFSTs, including the effects of temperature (not too significant), creep (more significant) (Chen and Chen, 2011) and shrinkage.

Some of the bridges have been constructed on falsework, and in a few cases two halves have been rotated into position, but most have been constructed with the help of cable stays (Ke-Bo *et al.*, 2008) (Figure 9.6). The light steel framework is cantilevered in stages, and then the arch is closed. When the arch has been closed the primary tubes are filled with concrete such that they have their

Figure 9.5 CFST forms: (a) single tube, 800 × 18 mm, spanning 80 m; (b) dumbbell, 800 × 12 mm, spanning 75 m; (c) triple tube, 600 × 12 mm, spanning 100 m; (d) double dumbbell, 1000 × 28 mm, spanning 356 m; (e) multiple dumbbell, 750 × 20 mm, spanning 360 m

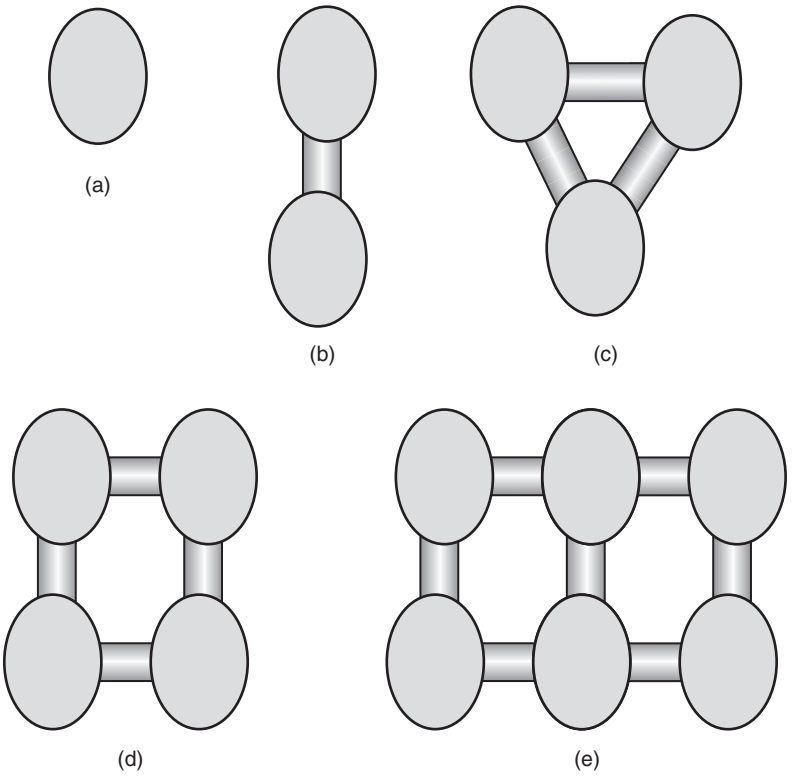

final strength and stiffness. The deck slab is then placed on the arch or hung from it, depending on the type of arch form. In China, four arch-form types are common (Figure 9.7): true arch, half-through, through and fly bird. In a survey of CFST forms (Yan and Yang, 1997), the half-through arch was found to be the most common.

The advantage of CFSTs is that the character of the steel tube changes for the better. It is less prone to local buckling (higher d/t ratios can be used, see Table 1.3), the axial and bending capacity of the steel-only section is improved (see the interaction curve in Figure 9.9), and the stiffness of the section increases.

9.4. Composite compression members

So far in this and previous chapters we have considered composite structures primarily in bending. However, the arch form carries load primarily as direct compression. The maximum axial, or squash, load carried by the steel–concrete composite section can be considered as the sum of its concrete, reinforcement and steel components, provided the steel element or connectors comply with the minimum thickness given in Table 1.4:

$$N_{\mathrm{p}} = kN_{\mathrm{c}} + N_{\mathrm{s}} + N_{\mathrm{a}} \tag{9.2a}$$

Figure 9.6 Construction method using stays for a half-through CFST arch

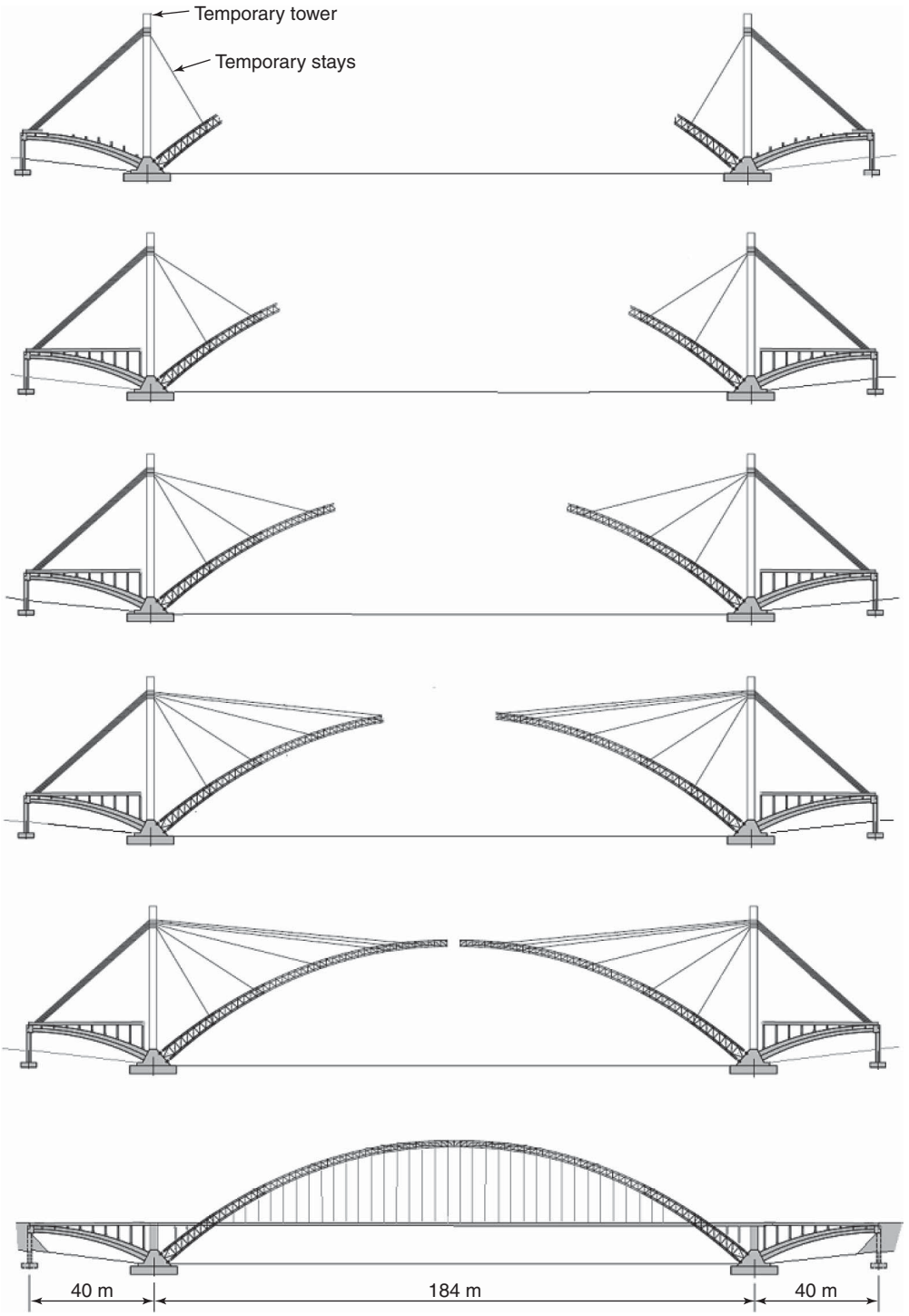

Figure 9.7 Chinese CFST forms: (a) true arch; (b) half through; (c) through; (d) fly bird

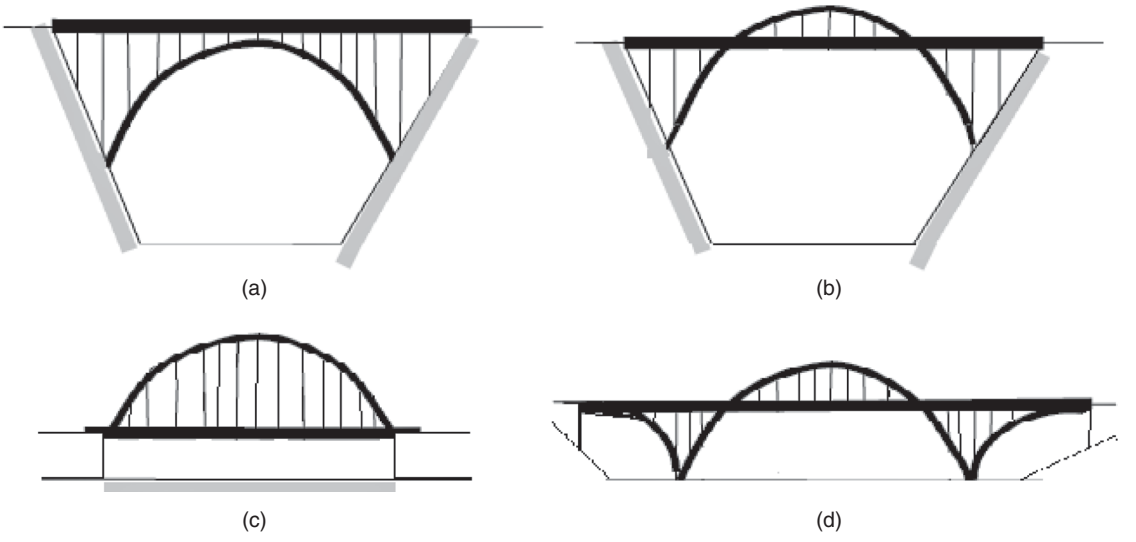

For filled tubes, where reinforcement inside the tube is seldom used, this simplifies to

$$N_p = 0.6 f_{ck} A_c + f_y A_a \tag{9.2b}$$

For encased sections, which usually have some reinforcement around the steel section, this simplifies to

$$N_p = 0.5 f_{ck} A_c + f_y A_a + 0.9 f_{ys} A_s \tag{9.2c}$$

The relative contribution of the steel and concrete elements is measured by the contribution factor α. This is an important parameter for determining the likely behaviour of the composite section. When based on the steel contribution, if α_c is less than 0.2 the section has minimal composite action, and the section may be designed as a concrete section. As the ratio rises, the steel component of the structure becomes more important, and beyond 0.9 the steel will dominate the section.

$$\alpha_a = N_a / N_p \tag{9.3}$$

When L_e/D_o is less than 12, the section can be considered as a short column, and the ultimate capacity of the section taken as in Equations 9.2. Where the section is more slender, the capacity is

$$N_{pd} = \chi N_p \tag{9.4}$$

where χ is determined from buckling curves (such as those shown in Figure 8.4) with the slenderness parameter λ:

$$\lambda = (N/N_{cr})^{1/2} \tag{9.5}$$

$$N_{cr} = (EI)_{eff} \pi^2 / L_e^2 \tag{9.6}$$

where $(EI)_{eff}$ is the stiffness of the composite section.

$$(EI)_{eff} = k_e k_c E_c I_c + E_s I_s + E_a I_a \tag{9.7a}$$

Figure 9.8 Stresses in a composite steel–concrete filled tube: (a) pure tension; (b) moment only; (c) combined axial and bending; (d) pure compression

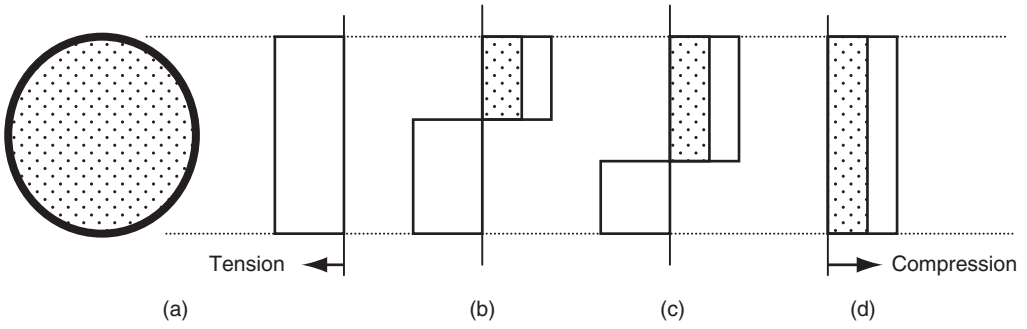

where k_e and k_c are coefficients for creep and shrinkage effects on the concrete. Typically, the stiffness of the reinforcement is small, and the equation simplifies to

$$(EI)_{\text{eff}} = 0.4E_cI_c + E_aI_a \tag{9.7b}$$

Considering a simple steel tube filled with concrete (Figure 9.8), the maximum axial compression load is calculated when there is no moment on the section (from Equation 9.2) and there is a uniform stress distribution across the section. Similarly, the tensile capacity of the section is calculated assuming a uniform stress distribution and ignoring any contribution from the concrete. With no axial load, the bending resistance is calculated assuming a plastic stress distribution, with the compression and tensile forces being equal. If a small axial load is applied a small increase in moment capacity occurs; as more axial load is applied the moment will reduce, until the axial limit is reached with no moment. The values calculated are plotted in Figure 9.9b to show the generalised form of the axial–bending interaction curve. The capacity of the steel-only section is shown in Figure 9.9a, and from the curves it can be seen that the composite section has a greater axial and moment capacity compared to the steel only section.

Figure 9.9 *M–N* interaction curves: (a) generalised comparing steel and composite sections; (b) curve for the 900 mm tube in Example 9.2

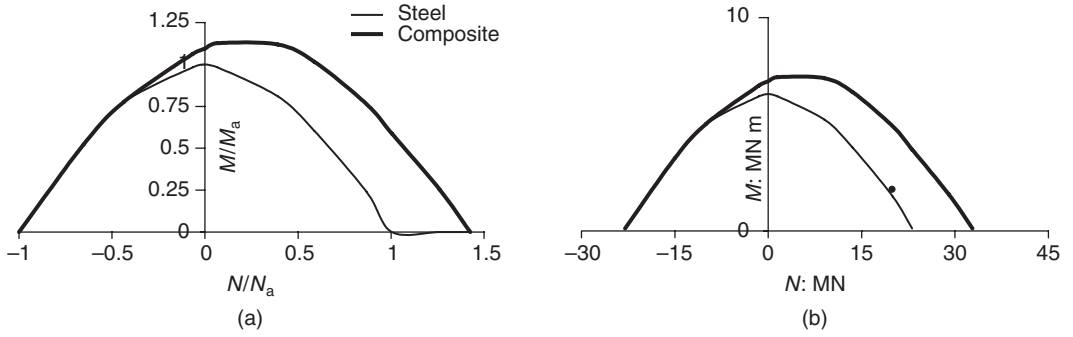

9.5. Example 9.2: Composite tube arch

The second example in this chapter is of an arch frame formed from a concrete-filled steel tube spanning the river adjacent to the structure in Example 9.1. It is shown in Figure 9.10. The structure was conceived to continue the aesthetic qualities of the other crossings. It has a similar arch profile, but with an open structure to allow light to percolate through the total 100 m width of bridge at this location. The structure consists of a monocoque steel–concrete composite deck cantilevering from a central tubular arch frame. The frame consists of three 900 mm diameter main tubes, with 600 mm diameter bracing, the two lower tubes being concrete filled.

9.5.1 Loading and analysis

The total dead load of the new bridge is approximately 18 MN, with a maximum characteristic live load of 13 MN. Analysis of the structure uses a 3D frame model of the combined deck and arch frame. The results of the analysis indicate that, near the quarter span, the lower composite tubes should be designed for a compression of 20 MN and a co-existent moment of 1.8 MN m. This moment includes the additional moment induced due to the curvature of the section between nodes (King and Brown, 2001). For the 900 mm tube filled with grade 45 concrete, using Equation 9.2b, and assuming that no additional reinforcement will be used,

$$N_p = 0.6 f_{ck} A_c + f_y A_a = 0.6 \times 45 \times 0.555 + 355 \times 0.078 = 14.9 + 27.7 = 42.6 \text{ MN}$$

The steel contribution factor (Equation 9.3) is

$$\alpha_a = N_a / N_p = 27.7/42.6 = 0.65$$

indicating that the steel contributes about two-thirds of the strength of the section.

Figure 9.10 Composite tubular arch at Runnymede

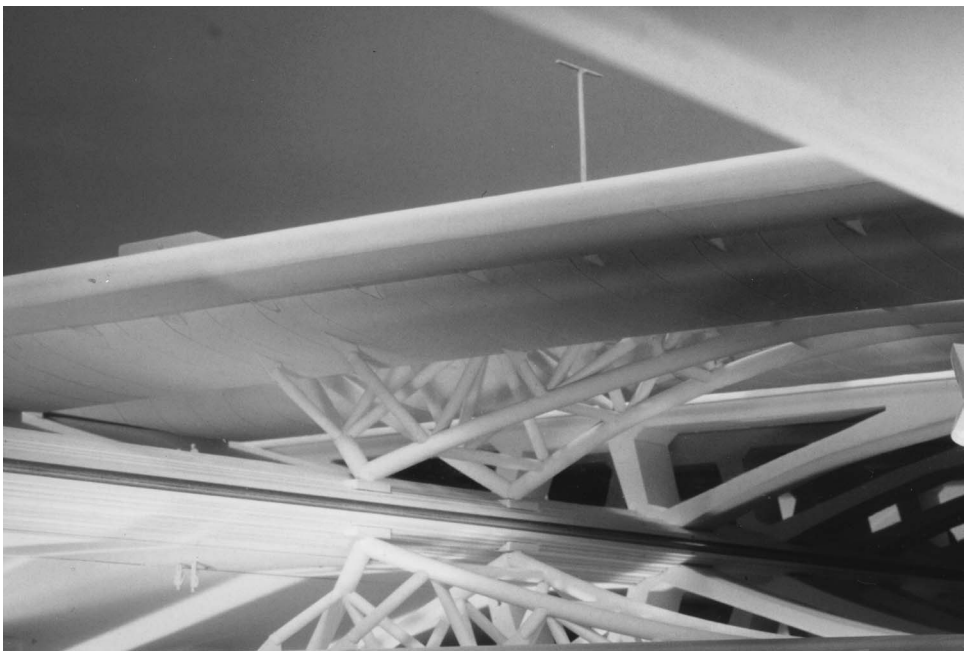

The arch tubes are similar to the chords of a truss, and the effective length will be approximately 85% of the distance between the bracing tubes. In this example, the distance between nodes is 5.5 m. $L_e = 4.7$ and $L_e/D_o = 4.7/0.9 = 4.3$, and therefore the section is not slender and the effects of buckling do not need to be considered.

The tensile capacity is 25.0 MN and the calculated moment capacity is $M_D = 8.3$ MN m. The M–N interaction diagram is constructed (see Figure 9.9b), with the applied forces superimposed. The applied loads are within the curve, so the section is adequate for these loads.

9.6. Fabrication of curved sections

Curved steel elements can be of two types: a true curve, or a faceted curve formed from a series of straight elements. The use of a faceted curve has structural advantages, as it is relatively simple to fabricate and avoids the additional curvature moments between nodes. The truly curved section is, however, often preferred for aesthetic reasons. The bending of steel sections can be carried out by rolling or by induction bending (King and Brown, 2001).

Rolling of a steel section into a curved shape is a cold bending process, and is usually carried out as a continuous three-point bending by rollers. A number of passes through the rollers may be required to achieve the required curvature. The rolling causes a plastic deformation of the steel section and will leave residual stresses locked into the section. These stresses are about 20% of the steel yield stress, but usually have little effect on the ultimate section capacity. Roller bending requires a considerable force, and for larger tubular elements induction bending is preferable.

Induction bending is a hot bending process. The steel section is heated locally by an electric induction coil to 700–1000°C, and at the same time a force is applied from a fixed-radius arm, deforming the heated section. The heat applied in the induction bending process means that the residual stresses will relax and be less than those induced by cold bending.

9.7. Nodes in tubular structures

The nodes for tubular structures can be complex, particularly where more than one plane of bracing is used. The intersections are of two primary types: gap joints (Figure 9.11a) and overlap joints (Figure 9.11b). The strength of the node is greater for the overlap type. Other factors such as the brace angle, the relative size of the chord to the bracing and the thickness of the tubes also influence the node strength (Bergmann *et al.*, 1995).

Rules for the design of nodes between tubular sections have been developed (Wardenier *et al.*, 1991). For the K- and X-joints three failure modes could occur: yielding of the brace member (N_y), plasticisation of the chord (N_p) or punching failure of the joint (N_v). The joint capacity may be estimated using the following equations:

$$N_y = 0.95 f_y A_{a1} \tag{9.8a}$$

$$N_{px} = k_2 f_y t_0^2 \left(\frac{5.2}{1 - 0.81\beta} \right) \tag{9.8b}$$

$$N_{pk} = \frac{f_y t_0^2}{\sin\theta} (1.8 + 10.2\beta) k_2 k_3 \tag{9.8c}$$

$$N_v = \pi v_y t_0 D_1 \left(\frac{1 + \sin\theta}{2 \sin^2\theta} \right) \tag{9.8d}$$

Figure 9.11 Tubular node: (a) X-joint; (b) K-joint

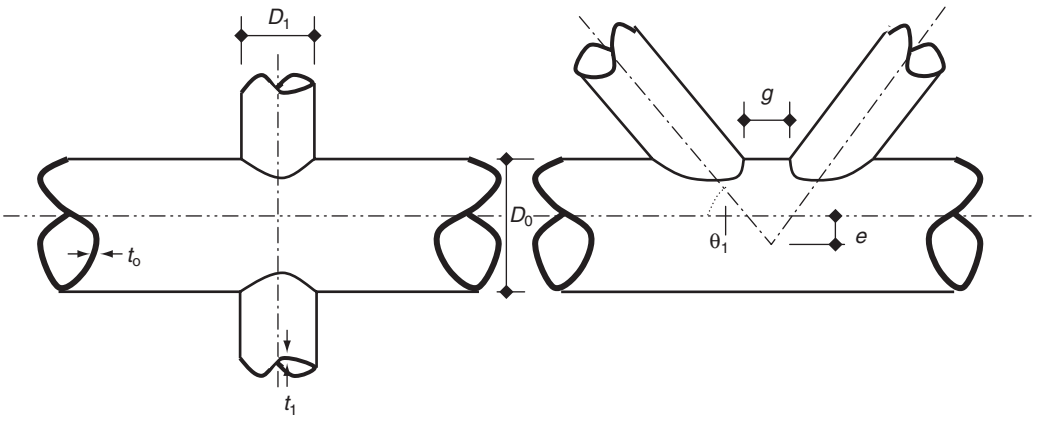

where A_{a1} is the brace area, k_2 is a coefficient dependent on the load ratio of the main chord (Figure 9.12a), k_3 is a coefficient dependent on the overlap or gap in the K-joint (Figure 9.12b), β is the ratio of brace to chord diameters (D_1/D_0), v_y is the limiting shear stress in the steel (Equation 1.10), and D_0, t_0, etc. are shown in Figure 9.11. Where multi-planar joints occur the joint capacity should be reduced to 90% of the calculated X-joint, unless more detailed interaction is considered (Wardenier *et al.*, 1991).

For the large tubes found in bridges, profiling of the tube ends at joints will be required to achieve welding fit-up. Joints can be strengthened by the addition of external plates or internal ring stiffening. For composite structures, the joint will be strengthened by the concrete, and the punching capacity will be increased. The joint may be designed neglecting the contribution of the concrete and assuming that the force from the brace is initially transferred to the steel section. Where the force transfer is large, the local interface shear may be significant and connectors may be required between the steel and concrete. Typically, connectors are required if the shear stress at the tube–concrete interface exceeds 0.4 N/mm^2.

Figure 9.12 Tubular joint capacity coefficients: (a) k_2; (b) k_3

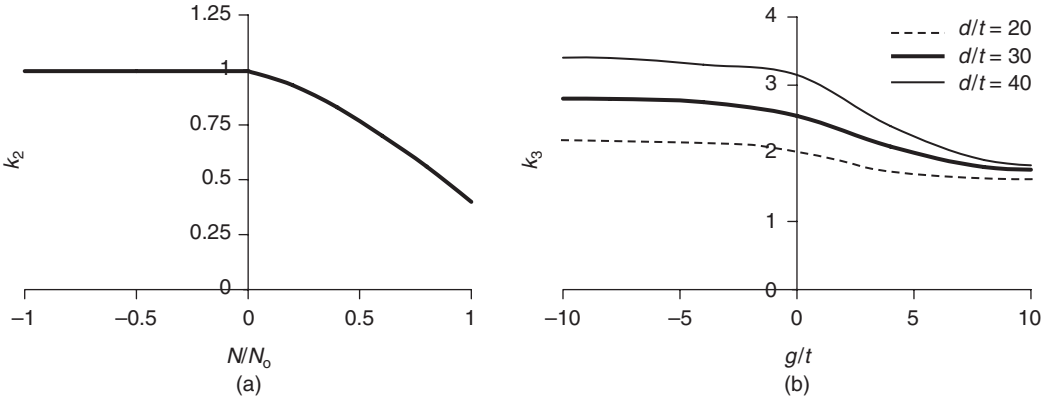

Figure 9.13 Node capacity in Example 9.2

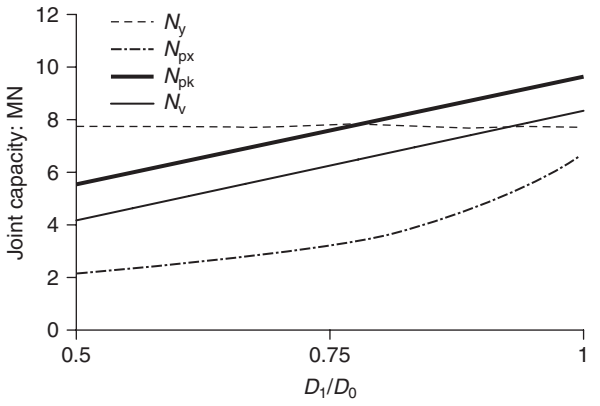

For the tubes in Example 9.2, the capacity of a node is calculated using Equations 9.8a to 9.8d, for various brace diameters. The results are shown in Figure 9.13. For this example, the brace yield and punching failures are not critical, and the capacity is governed by chord plasticisation of the X-joint for a wide range of relative tube diameters and thicknesses. In this example the node capacity can be significantly enhanced by the use of ring stiffening within the tube.

9.8. Aesthetics

The way bridges look, their character, is intimately bound up with the technical decisions taken. The earliest rules of architecture (Vetruvius, 1988) list the requirements of stability, quality, amenity and economy, which are more a guide to the engineering qualities than a checklist for aesthetics. Even in the late nineteenth century the architectural maxim of 'form follows function' was stated (Sullivan, 1958). For early practitioners, the rules of structure, aesthetics and practical construction were interchangeable. The rules of proportion were used to ensure that the structural elements were of the correct thickness for stability as much as for visual quality. Through the twentieth century, with greater specialisation, this holistic approach was partly lost.

Many factors may affect the aesthetic decisions – cultural, political, environmental, historical, technical and, even, current fashion. The political influence is often paramount, as bridges form part of the larger road or rail infrastructure. The need to develop the infrastructure for the benefit of the economy of a country or area will be a political decision. The directives issued will dictate the priorities of the project, and for many schemes speed of delivery or cost will be key requirements. Occasionally, political patronage will demand a statement or landmark structure, where looks, or making an impression, are key requirements. The environment in which a bridge is located is another key factor. Structures located in a beautiful landscape will have a head start in aesthetic merit over those sited in a decaying industrial environment or spanning a motorway. This does not mean that a structure crossing a great river will be beautiful (see the quotation at the start of this chapter), or that an attempt at some aesthetic merit cannot be made for motorway structures (Figure 9.14).

The history of a site may influence aesthetics, particularly if there has been a bridge at the site before. The technical considerations are many, and the length of span will affect the form and character (see Figure 1.1). The load carried will limit the aesthetic choice. Railway bridges, with their heavy loads and

Figure 9.14 Perspective sketch of a fashionable leaning arch structure across a motorway

tight deflection limits, will develop along different lines from, say, footbridges, with their far lower loads. Fashion, or the prevailing taste swirling through society, has its effects and will influence the bridge designer. The ornamentation, or lack of it, will be dictated by the prevailing styles. The ebb and flow of fashion in bridges is not as dramatic as the changes in hemlines on the Paris catwalk, but its influence exists. In the last decade of the twentieth century and into the twenty-first century, the fashion has been to lean arches or towers for visual reasons (see Figures 9.15 and 10.11), to distort the structure from the traditional. Some of these structures will define an era or style, others will date relatively quickly.

The aesthetics of a bridge are governed by visual rules, and these criteria are difficult to quantify in the same way as rules for producing a safe or serviceable structure. They are, perhaps, related as much to art as science, 'sculpting bridges' (Collings, 1994). The rules are open to individual interpretation, and the importance of any of the various parameters will depend on the individual designer and the prevailing influences.

9.8.1 Unity

A bridge should have a visual unity, a feeling of wholeness, 'some configurations are dominated by wholeness, others tend to separate' (Morris, 1992). This property is often found in relatively simple arrangements, in structures with structural continuity, where the elements are clearly seen to be connected, and where the superstructure and the supporting substructure seem related. Without unity the bridge will look like an assemblage of parts. The form of the bridge, the distribution of the visual masses and the degree of symmetry are important parameters to achieving this wholeness.

9.8.2 Scale

The bridge will be perceived by its size, and if the size is appropriate the bridge will seem in scale. This does not mean that the structure has to appear small, as the 'bigness' of a bridge may be appropriate, the dominant scale giving a sense of safety and that it has the strength to span. The bridge should be appropriate at different scales, such that when viewed close up its scale does not appear oppressive.

9.8.3 Proportion

This is the relationship of the parts to each other and to the whole. Geometric ratios, the span/depth ratio, the ratio of the parapet to the beam, the relative size of a span on a continuous (Leonhardt, 1982) bridge, or the solidity ratio of the bays in a truss may all be used to give some proportion.

9.8.4 Rhythm

This is the pattern of repetition of elements, the order in which elements are placed, or the rate of change in proportion. For bridges the rhythm is usually horizontal; from many views the bridge will have a linear arrangement.

9.8.5 Detail

Detail is how the elements are shaped, and brought together with any ornamentation. Poor detailing, or an absence of detail, will affect the wholeness, scale, proportion and rhythm of the bridge. It will affect the play of light and shade, the perceived colour and how the bridge weathers.

To assess the many visual properties of a design, the bridge should be considered from a number of viewpoints: distant, the middle distance and close up. All the criteria need to be assessed from all viewpoints. However, as in most design, some combinations of properties and viewpoints are more critical. Scale and wholeness are more critical for distant views, detail is crucial for close views, and rhythm and proportion are perceived more clearly at the middle distance.

At Runnymede, the influence of aesthetics on the design has been significant for both structures. In the 1930s, when the Staines bypass was proposed, the River Thames at this location was more rural than it is today. When built in the 1960s, there was a political push to develop the nation's infrastructure. By the 1980s, with the extensive development of the area, the M25 motorway (incorporating the original bridge) was heavily congested, and again there was a political push, this time to widen congested motorways (see Chapter 4). Runnymede has now largely lost its rural feel, yet there is still a sense of calm at river level, with light playing on the white soffit, despite the roar of the motorway traffic above.

The brick-faced single span across the river borrows from the nearby 'great leap' double arch of Brunel (Vaughn, 1991). The modern tubular form is influenced by the early tubular bridges of Eads and Baker (Scott and Miller, 1979; Paxton, 1990), which span other great rivers. Its layout is derived from a human hand, as a series of fingers, the 'waiter's fingers' in architectural terms (Bennett, 1997). There could have been other influences – a flying bird, a bulls head and a butterfly have all influenced the styling of other bridges (Sharp, 1996). Both bridges had architectural input, another cyclic fashion that ebbs and flows with the bridge engineer's interest, skill and training in aesthetics.

As we have seen, the earliest forms of architectural advice by Vetruvius (1988) are as much structural rules as visual. Personally, my preference has always been for the practical over the decorative. I am inclined towards what Billington (1983) described as 'structural art'. Sadly, today there are few true practitioners, Benaim (2002) being the nearest I have come to this. I enjoy his methods of: calculating, designing, reviewing, questioning, changing, refining, calculating again, designing . . . . These methods also optimise – optimum structures will have a low carbon and embodied-energy content (see Chapter 2). Rather than have the form follow function, another way to design is to conceive a form and fit the function around it. This approach is very common today. However, this method of thinking of, say, a waveform and designing a bridge to it is usually far from optimum. (On site during the construction of the 'waveform' bridge (Figure 9.15) it was said, rather, that the inspiration was clearly a woman reclining with legs astride, and that the bridge could be seen as a subtle poke at the patriarchal

Figure 9.15 An arch-type bridge in the Middle East: (a) during construction; (b) in its final form (© J. O'Sullivan)

(a)

(b)

society of that part of the world.) In a study for a bridge in the Middle East (Collings, 2006), it was clear that such bridges were not environmentally the best we could achieve. How much should we pay for aesthetics?

9.9. Tied arches

Where the abutments cannot carry arch thrusts, a tied arch form may be appropriate, with the arch thrusts tied through the deck. The large tensions induced in the ties means that they are usually made of steel, although prestressed concrete ties have been used (Chen and Wang, 2009). The tied arch comes in three basic forms: with a dominant arch (Wurth and Koop, 2003), with dominant beams (Hesselink and Meersma, 2003), and with similarly sized arch and beam (Friot and Bellier, 2001). Visually, each form has its own character, with different visual proportions. Structurally, the bridges also have their own character, each behaving differently. With the beam dominant, the arch acts only as the compression chord and carries permanent or uniform loads. Its bending stiffness is significantly less than the deck beam stiffness, so almost all moments are attracted to and carried by the deck beam. Where the arch is dominant, it carries all moments and compressive forces leaving the deck, and carries only the tie force and any local moments from the span between the vertical hangars. In this form the arch is often a large steel truss. Where the arch and deck are of similar stiffness, both share the bending effects of asymmetric loads.

For all tied arches, the connection of the arch to the deck is a critical area. The compression of the arch and the tension of the tie must be resolved, and the vertical components must also be transferred to the substructure and foundations. The hinged arch clarifies this resolution visually to some degree. The connection used will also significantly affect the character of the structure, and must be detailed carefully. Often, the arch and deck may not be in the same plane, and the transfer needs careful consideration of the forces.

9.10. Example 9.3: Composite bowstring arch

The final example considered in this chapter is a design for a composite bowstring arch bridge spanning a river. The form is a continuous twin-girder ladder beam, 330 m long, with a central 187 m arch span. The structure uses composite action on the deck with a conventional ladder beam and slab layout. The arch compression chord is also a composite section formed from a fabricated steel U and box section filled with concrete. The deck of the bridge is continuous through the arch and approach viaducts, thus avoiding a joint and heavy abutment at this location. The continuity improves the durability of the structure, ties the arch and approaches visually, and also has significant structural benefits.

The continuity of the deck beams gives a stiffer structure and results in less moment in the arch. The continuity also helps spread the concentrated arch thrust, and the placing of the arch tie inboard of the deck edge also assists with this spread. Figure 9.16 shows the shear stress contours in the concrete slab of a girder-stiffened bridge deck, with a concentrated in-plane force applied from the arch thrust (Johnson, 2003). At midspan all stresses in the deck are relatively uniform, with 20–25% carried by the deck and 75–80% by the steel girder. Where the arch and tie beam are at the edge of the slab, the shear stress concentration is largest (Figure 9.16a). Where the arch and tie beam are inset, the stress magnitude is similar but occurs over a reduced area (Figure 9.16b). For the bridge with continuity and an inset arch, the magnitude of the stress concentrations are significantly reduced (Figure 9.16c).

9.11. Arch buckling

Where the arch is part of a rigid frame, the effective lengths of the arch members will be similar to those of a truss (see Table 1.4). Where the arch is not restrained in its plane and is free to deflect, the effective

Figure 9.16 Shear stress concentrations from the in-plane tie force from the arch: (a) non-continuous deck with an edge beam; (b) non-continuous deck with an inset beam; (c) continuous deck with an inset beam

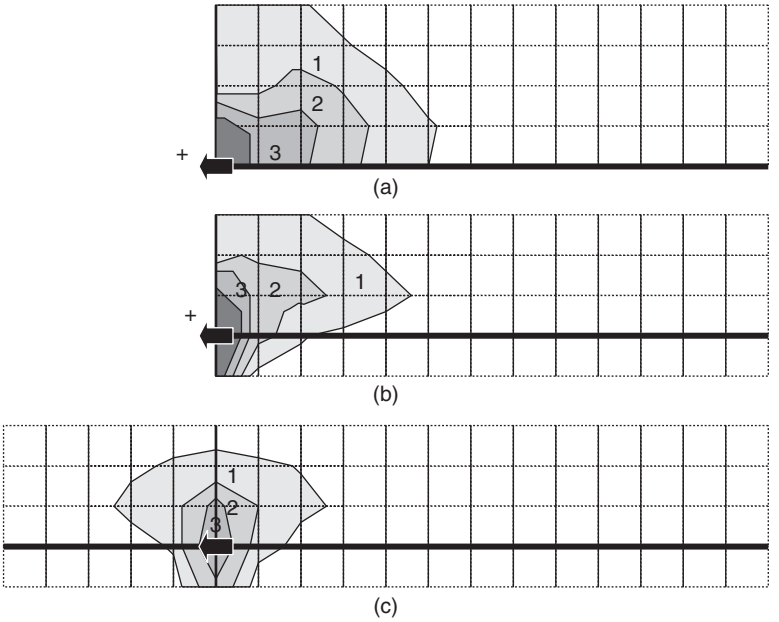

length will be determined by the degree of restraint at the springing point and, to some degree, by the tie and hangar stiffness. Figure 9.17 outlines some approximate effective lengths for in-plane buckling where the arch is the dominant form. In the transverse direction, where the arch is unrestrained by a bracing frame, the U-frame restraint may be calculated (as in Chapter 4). Eurocode 3: Part 2, 'Steel bridges' (BSI, 2006), gives more buckling lengths for arches. Where hangars with no bending stiffness are used, an effective restraint may be estimated from the horizontal force component (F)

Figure 9.17 (a) First in-plane buckling mode. (b) Effective length for in-plane arch buckling for a pinned and fixed arch

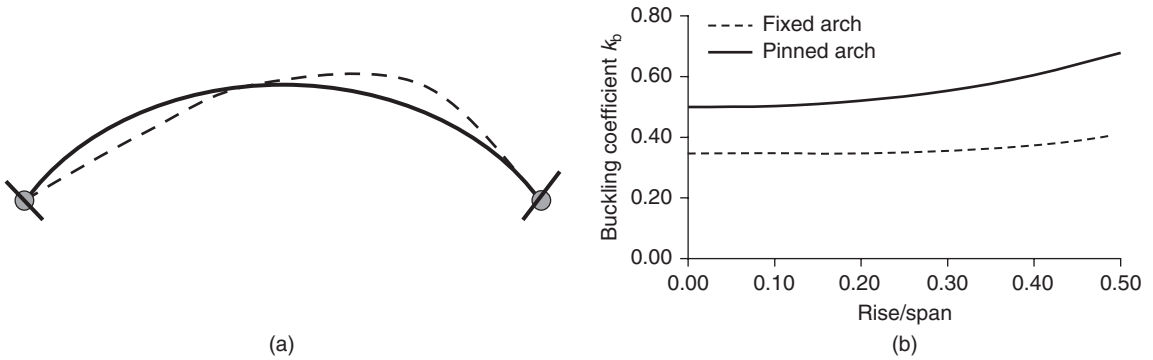

of the hangar load (N_H) as the arch deflects (δ):

$$K_H = F/\delta = N_H/L_H \tag{9.9}$$

9.11.1 Loading and analysis

The weight of the main span structure is 100 MN with surfacing. Maximum characteristic live loads are 40 MN; for the arch and deck design other load cases with more concentrated asymmetric loads will be more critical (as is the case in all the arch examples discussed). For a structure of this kind, a number of frame models and submodels of various elements or connections are required, particularly as the arches lean slightly and moment will occur on both primary arch axes. The results of the analysis of an arch frame are shown in Figure 9.18 for the serviceability limit state, indicating the distribution of moment, axial force and shear in the bridge. Table 9.2 gives the design values at the ultimate and serviceability limit states.

As with all composite structures, the distribution of stresses is, to a large degree, dependent on the construction sequence. For a bridge of this size the sequence is relatively complex, involving launching of the deck steel and propped construction of both the tie beam and the arch. A simplified sequence is shown in Figure 9.19. Due to the propping, the whole self-weight and live load are assumed to be carried on the composite structure.

For the arch the axial load capacity and contributing factors are calculated using Equations 9.2 and 9.3, as before. For this example,

$$N_p = 0.6 f_{ck} A_c + f_y A_a = 122 \text{ MN}$$

$$\alpha_a = N_a/N_p = 0.4$$

Figure 9.18 Analysis results for the serviceability limit state of the tied arch

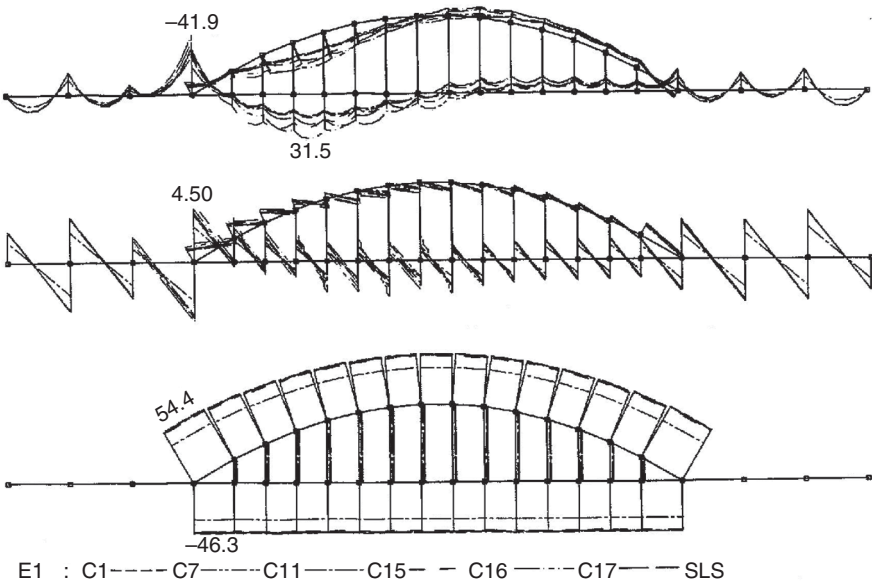

Table 9.2 Analysis results for the tied arch, for design of the arch, tie and arch–tie intersection

Member	Serviceability limit state			Ultimate limit state		
	M: MN m	*V*: MN	*N*: MN	*M*: MN m	*V*: MN	*N*: MN
Arch at springing	6.0	1.0	54			
Tie at springing	4.1	4.5	46			
Arch at quarter				−24	1.0	61
Tie at quarter				−28	3.1	42

indicating that a significant proportion of the capacity is derived from the concrete. In the transverse direction, bracing struts are provided at 40 m centres, giving an effective length of 34 m. In-plane the effective length is estimated from Figure 9.17, conservatively neglecting the restraint from the hangars and tie. For an h/L ratio of 0.2, the effective length factor is 0.35, and

$$L_e = 187 \times 0.35 = 65 \text{ m}$$

Using Equation 9.6,

$$N_{cr} = \frac{(EI)_{a-c}\pi^2}{L_e^2} = \frac{210\,000 \times \pi^2}{65^2} = 490 \text{ MN}$$

$$\lambda = (N/N_{cr})^{1/2} = 0.36$$

From Figure 9.8, $\chi = 0.9$, so

$$N_{pd} = 0.9N_p = 0.9 \times 122 = 109 \text{ MN}$$

The axial capacity of the arch is well above the actual forces in the arch. An interaction diagram (similar to the one in Figure 9.9) can be drawn to show that the axial–bending interaction is satisfactory.

For the tie at the quarter point, the composite girder and slab section will carry a tension and moment. The section properties are given in Appendix C, and the ultimate and serviceability stresses can be calculated. At the ultimate limit state, the tension plus sagging moment is critical for the lower flange. At the serviceability limit state, the stress in the slab is critical, with tension plus a hogging moment. At 125 N/mm^2 the stress in the steel is low enough to prevent extensive cracking of the concrete, provided the reinforcement bars are at 150 mm centres or less (see Chapter 4).

At the arch–tie intersection, the forces from the arch, tie, continuity beam and pier are resolved. The neutral axis of the tie beam with its slab is relatively high, and a large steel top flange is used to draw this up further, such that the primary force is resolved near the top flange without significant transfer to the web and lower flange. This avoids the need for diagonal stiffeners, side plates or split webs. Only the vertical force transferred to the pier (or future jacking point) requires stiffening. The arch–tie joint is shown in Figure 9.20, with the primary forces.

Figure 9.19 Construction sequence for the tied arch bridge in Example 9.3. (a) Construct substructure and temporary foundations in the river; launch the steel deck. (b) Construct the concrete deck in stages, as shown, leaving strips adjacent to the springing. (c) Construct the steel arch on temporary towers; construct the concrete arch. (d) Install the tension hangars; remove the temporary support from the river; construct the concrete slab strips; place finishes

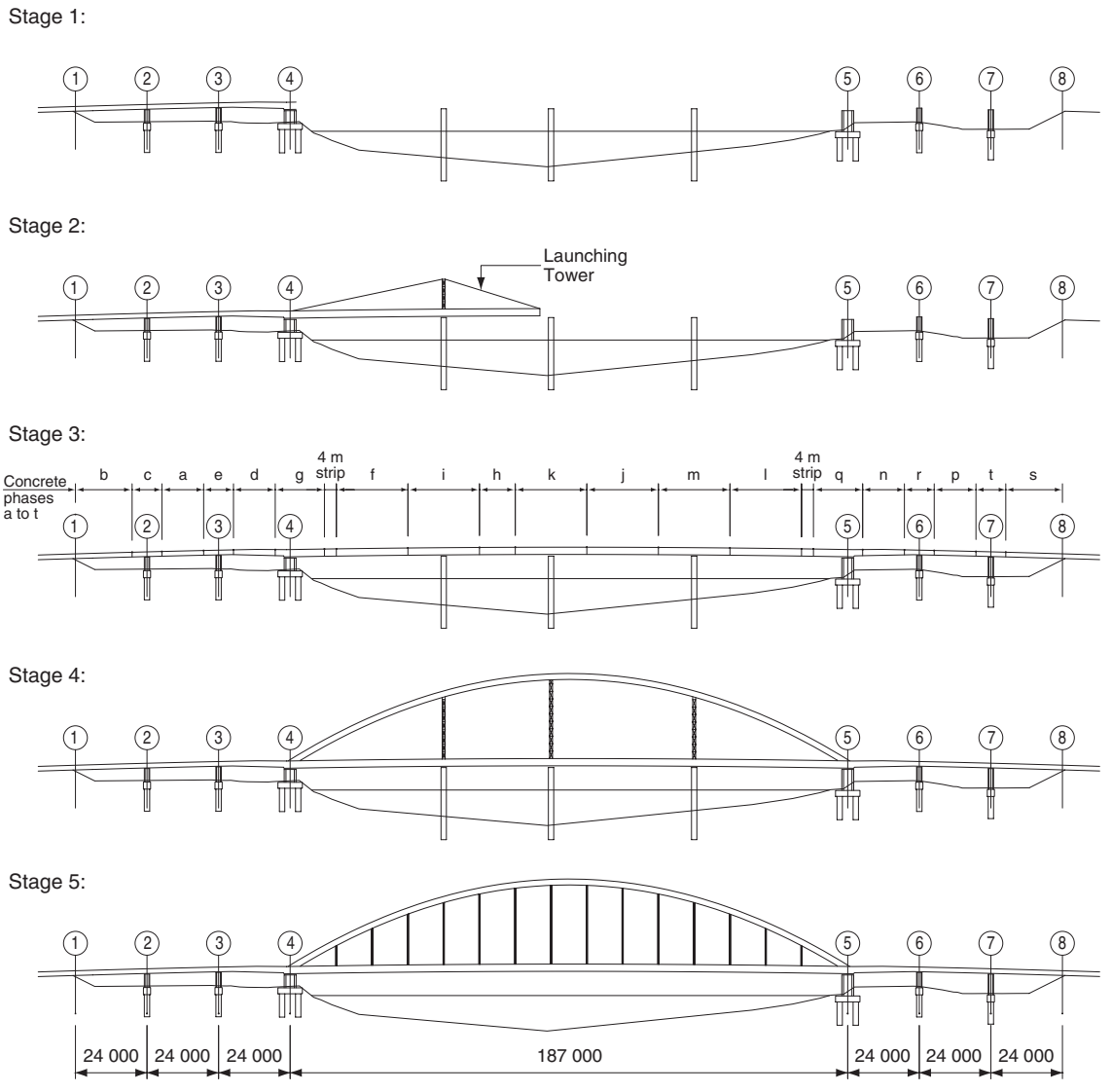

At the arch–tie intersection the force from the concrete arch section has to be transferred to the steel tie. The transfer, via connectors, could occur in the arch such that, at the arch–tie intersection, all the force is in the steel. From the contribution factor, 60% of the force is in the concrete, and the steel arch section must be thickened considerably to carry this additional load. Alternatively, the transfer could occur at the tie–beam connection, with connectors placed on the tie–beam connection to

Figure 9.20 The tie intersection in Example 9.3, showing the serviceability limit state forces

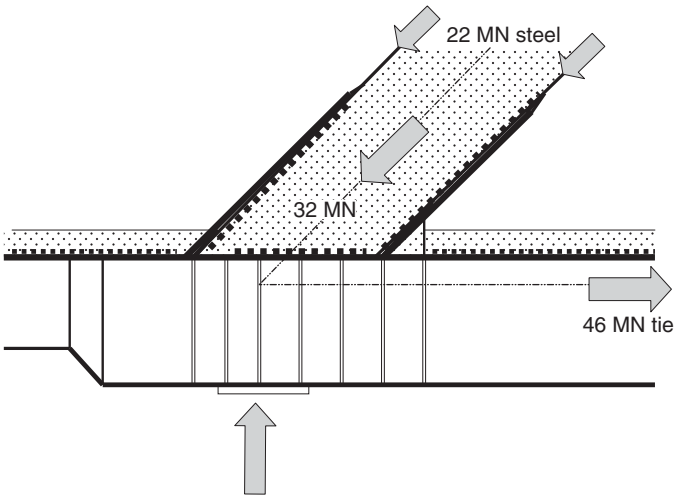

carry the shear at this interface. A large number of connectors will be required. A third option is to use a combination of the two transfer methods, and in this example this method will be used.

At the ultimate limit state the force in the arch is 75 MN (and the tie force is 65 MN). The typical contribution ratio is 0.4 (giving a force of 30 MN in the steel); at the base of the arch the steel thickness is increased and the contribution of the steel is increased to 0.6 (giving a force of 45 MN). To carry the additional load, the top and bottom flanges of the box are doubled in size (the webs are not increased, as additional loads here are more difficult to resolve without using a box section tie beam local to the intersection). Assuming a 4 m length of transfer (based on a 1 : 2 load spread as in Chapter 3), the force to be transferred is

$$V_l = (45 - 30)/(2 \times 4) = 1.9 \text{ MN/m}$$

Using Equation 1.18a with 22 mm diameter connectors, with $P_u = 139$ kN (see Table 1.5)

$$n = V_l/0.7P_u = 1.9/(0.7 \times 0.139) = 20$$

At the steel–concrete intersection on the tie beam the remaining 30 MN in the concrete will require connectors to carry the horizontal component of the force. The force is assumed to be carried on a 2.5 m length of beam. Resolving forces:

$$V_l = (30 \times 65)/(2.5 \times 75) = 10.4 \text{ MN/m}$$

This is a relatively large force, and bar connectors will be used, $P_u = 963$ kN (see Table 1.5):

$$n = V_l/0.7P_u = 10.4/(0.7 \times 0.963) = 15$$

Ten rows of four 50 × 40 × 200 mm bars with hoops will carry this load on the top of the tie within the arch. For both shear planes, reinforcement will be required within the arch across the internal shear plane.

Eurocode 4: Part 1-1, 'Design of composite structures – General rules and rules for buildings' (BSI, 2004), considers only stud connectors; the other connectors noted in Table 1.5 are strictly outside the scope of this standard. Such connectors have been used successfully in the past, and the shortcomings of this standard should not 'embarrass and shackle the progress of improvements' (Vaughn, 1991) and stop their use when appropriate – obviously, some common sense must prevail. The use of mixed systems should be undertaken with care, considering the structural systems involved, and considering stiffness as well as strength. In this case, the serviceability limit state may need to be considered.

At the serviceability limit state the connectors transfer 12 MN from the concrete to the steel:

$$P = V_l/n = 12/168 = 0.071 \text{ MN, or } 71 \text{ kN}$$

This is half of the 139 kN capacity. At the serviceability limit state, if the load in the stud connector is less than 55% of the ultimate capacity, the connector is likely to be behaving in an elastic manner with little slip (see Figure 1.13) and be satisfactory. At the steel–concrete intersection on the tie beam, at the serviceability limit state 17.5 MN is transferred by the bar connectors:

$$F = V_l/n = 17.5/40 = 0.437 \text{ MN, or } 437 \text{ kN}$$

The concrete stress in each connector is

$$f_c = F/A = 437\,000/200 \times 50 = 43 \text{ N/mm}^2$$

which is similar to the value of f_{ck}.

From Equation 1.23 the ultimate capacity is reached at $2.5f_{ck}$, and at the serviceability limit state a stress of f_{ck} will give reasonable behaviour.

REFERENCES

Benaim R (2002) Engineering architecture. *Ingenia* **11**: 6–12.

Benaim R, Smyth W and Philpot D (1980) The new Runnymede Bridge. *The Structural Engineer* **58**.

Bennett D (1997) *The Architecture of Bridge Design*. Thomas Telford, London.

Bergmann R, Matsui C, Meinsma C and Dutta D (1995) *Design Guide for Concrete filled Hollow Section Columns under Static and Seismic Loading*. Verlag TUV Rheinland.

Billington DP (1983) The Tower and the Bridge: The New Art of Structural Engineering. Princeton University Press, Princeton, NJ.

BSI (2004) BS EN 1994-1-1:2004. Eurocode 4. Design of composite steel and concrete structures. General rules and rules for buildings. BSI, London.

BSI (2006) BS EN 1993-2:2006. Eurocode 3. Design of steel structures. Steel bridges. BSI, London.

Chen BC and Chen YF (2011) State of the art creep of concrete filled steel tubular arches. *ASCE Journal of Civil Engineering* **15**: 145–151.

Chen BC and Wang TL (2009) Overview of concrete filled steel tube arch bridges in China. *Practice Periodical on Structural Design and Construction* **14(2)**: 70–80.

Collings D (1994) Personal sketchbook. Discussion at ABK architects.

Collings D (2006) An environmental comparison of bridge forms. *Proceedings of the ICE – Bridge Engineering* **159**: 163–168.

Collings D (2010) *Steel–Concrete Composite Buildings*, *Designing with Eurocodes*. Thomas Telford, London.
Cracknell D (1963) The Runnymede bridge. *ICE Proceedings* **25(3)**: 325–344.
Dajun D (2001) Development of concrete-filled tubular arch bridges, China. *Structural Engineering International* **11(4)**: 265–267.
Friot D and Bellier G (2001) Bonpas tied arch TGV Mediterranee high speed rail bridge over the A7 motorway toll plaza. *Composite Bridges – State of the Art in Technology and Analysis. Proceedings of the 3rd International Meeting*, Madrid.
Hesselink B and Meersma H (2003) Railway bridge across Dintel Harbour, Port of Rotterdam, The Netherlands. *Structural Engineering International* **13(1)**: 27–29 (in Dutch).
Highways Agency (1996) *The Appearance of Bridges and other Highway Structures*. HMSO, London.
Johnson R (2003) Analyses of a composite bowstring truss with tension stiffening. *Proceedings of the ICE – Bridge Engineering* **156(2)**: 63–70.
Ke-Bo Z, Jian-Ren Z and Dong-Huang Y (2008) Model tests of half through CFST tied arch bridge in the process of arch rib erection. *Structural Engineering International* **18(4)**: 396–402.
King C and Brown D (2001) *Design of Curved Steel*. Publication P281. Steel Construction Institute, Ascot.
Leonhardt F (1982) *Bridges*, *Aesthetics and Design*. Architectural Press, London.
Lutyens M (1991) *Edwin Lutyens by His Daughter*. Black Swan Books, London.
Morris R (1992) *Notes on Sculpture. Art in Theory 1900–1990*. Blackwell, London.
O'Connor C (1993) *Roman Bridges*. Cambridge University Press, Cambridge.
Paxton R (ed.) (1990) *100 Years of the Forth Bridge*. Thomas Telford, London.
Scott Q and Miller HS (1979) *The Eads Bridge*. University of Missouri Press, Missouri, MI.
Sharp D (ed.) (1996) *Santiago Calatrava*. Book Art, London.
Sullivan LH (1958) *The Autobiography of an Idea*. Dover Publications, New York.
Vaughn A (1991) *Isambard Kingdom Brunel*, *Engineering Knight-Errant*. John Murray, London.
Vetruvius (1988) *De Architectura*. Harvard University Press, Cambridge, MA.
Wardenier J, Kurobanne Y, Packer JA, Dutta D and Yeomans N (1991) *Design Guide for Circular Hollow Sections under Predominantly Static Loading*. CIDECT.
Wurth GJJ and Koop MJM (2003) Enneus Heerma Bridge, Ijburg, The Netherlands: recent structures in Belgium and The Netherlands. *Structural Engineering International* **13(1)**: 7–10 (in Dutch).
Yan G and Yang Z (1997) Wanxian Yangtze Bridge, China. *Structural Engineering International* **7(3)**: 164–166.
Zang Z, Pan S and Huang C (2004) Design and construction of Tongwamen Bridge, China. *Proceedings of the ICE – Bridge Engineering* **157(1)**: 1–7.
Zuou P and Zhu Z (1997) Concrete filled tubular arch bridges in China. *Structural Engineering International* **7(3)**: 161–163.

Steel–concrete Composite Bridges
ISBN 978-0-7277-5810-1

http://dx.doi.org/10.1680/scb.58101.185

ice Institution of Civil Engineers publishing

Chapter 10
Cable-stayed bridges

... have a system of forces that are resolved within the deck–stay–tower system ...

10.1. Introduction

The development of cable-stayed bridges is contemporary with that of composite structures, both arising primarily in the later part of the twentieth century. All long-span cable-stayed bridges combine steel and concrete elements, and many have some composite components (Virlogeux *et al.*, 1994; Withycome *et al.*, 2002; Collings and Brown, 2003). A cable-stayed bridge consists of a deck stayed by high-tensile wire or strand from towers. The most common form is a single main span with smaller back spans and two towers (see Figures 8.2 and 10.2). Asymmetric layouts hung from a single tower are popular for smaller spans (De Miranda, 1988; Collings and Brown, 2003) and architectural statements (Sharp, 1996). Multi-span cable-stayed structures are now also being developed (Ito *et al.*, 1991; Virlogeux, 2001), with more rigid frame towers. The stay cables are arranged in a harp or semi-fan arrangement (Walther *et al.*, 1988); the true fan arrangement, with all stays converging at one point, is difficult to detail and is rarely used.

Cable-stayed bridges tend to be self-anchored; that is, they have a system of forces that are resolved within the deck–stay–tower system. Earth-anchored systems utilising massive anchorages (similar to suspension bridges) to increase the system stiffness have been proposed as a way of increasing spans (De Miranda, 1988).

The basic stay system is essentially a series of superimposed triangular trusses. A good approximation of the behaviour can be obtained relatively simply. However, the bending, shear and axial load interaction together with non-linear behaviour of the stays, which makes detailed analysis relatively complex. Consider the isolated deck–stay–tower system shown in Figure 10.1. Element 1 of the main span has a weight W_1 and is located at a distance L_1 from the tower. It is attached to a tower of height h_1. A tension T_1 in the stay and compression C_1 in the deck are required for stability.

$$C_1 = W_1 L_1 / h \tag{10.1a}$$

$$C_2 = W_2 L_2 / h \tag{10.1b}$$

$$T_1 = (W_1^2 + C_1^2)^{1/2} \tag{10.2a}$$

$$T_2 = (W_2^2 + C_2^2)^{1/2} \tag{10.2b}$$

To avoid out-of-balance forces at the tower top and in the deck, $C_1 = C_2$, and

$$W_2 = W_1 L_1 / L_2 \tag{10.3}$$

Figure 10.1 Forces in a stay system

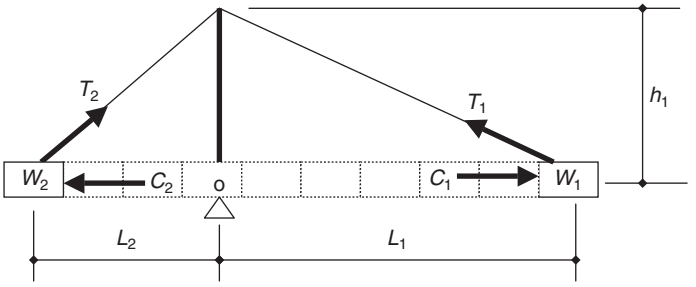

which also gives equilibrium about point O. Hence, if a large span is being planned, then either the back span has to be approximately half the length of the main span, or it needs to be significantly heavier. This leads to the two primary layouts: bridges with stiffening girders and relatively long back spans, or bridges with short, heavy back spans supported on multiple piers. For a 1000 m ($L_1 = 500$ m) span and a 250 m long back span (L_2) the deck in this section would be at least twice as heavy as the main span. If a lighter steel main span is used, then heavier concrete back spans seem logical (Figure 10.2). If a live load is placed on element W_1, then element W_2 needs to be tied down or given sufficient bending stiffness to span the load to the supports.

10.2. Stay design

The overall load on the bridge will not govern the design of an individual stay. However, the load on a shorter length of bridge will govern it, with the axle (T_A) part of LM1 being placed near the stay anchorage. Consideration will also be given to a stay or two being missing due to replacement during maintenance or due to failure of a stay. Eurocode 3: Part 1-11 (BSI, 2008b) contains some rules for these tension elements. It is vital that there is robustness and redundancy in the design of the bridge such that failure of one or two stays does not cause progressive collapse (i.e. the failure of these stays overloads the adjacent stays such that they fail, and an unzipping type failure occurs). Fatigue loads also often govern the stay design.

As a first approximation the author has found that two simple rules will give a good idea of the stay sizes required for strength, robustness and fatigue of high-tensile strand cables. At working loads (serviceability effects) the area required will be the larger of

$$A_{s1} = T_{max}/0.4f_{us} \tag{10.4a}$$

$$A_{s2} = T_L/250 \tag{10.4b}$$

Figure 10.2 Stonecutters Bridge, light steel span (1018 m) with heavy concrete back spans (258 m)

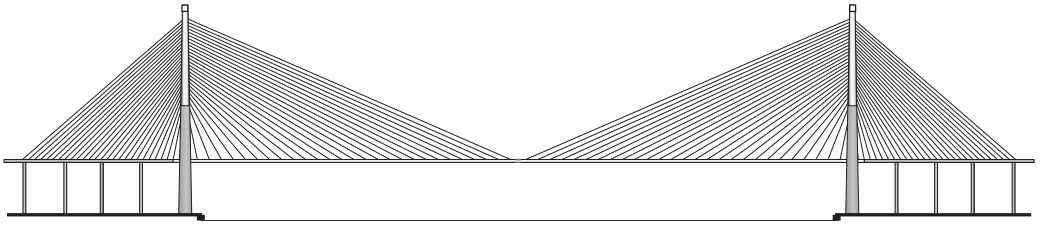

Figure 10.3 Stay-deck connections: (a) Tagus Bridge; (b) Boyne Bridge; (c) Second Severn Bridge

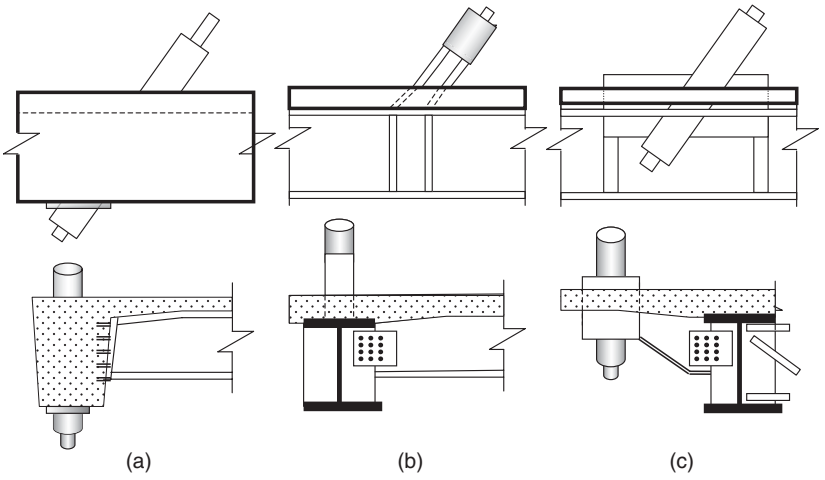

where T_{max} is the maximum total force on the stay, T_L is the force in the stay due to live loads only, and f_{us} is the ultimate strength of the stay steel.

10.3. Deck–stay connection

Composite cable-stayed bridges utilise the best characteristics of the two materials. The vertical component of the stay is resisted by the steel girder and the horizontal component mainly by the concrete deck slab, and ideally the cable connection should permit this.

The connection between the stay and the deck can take a number of forms (Figure 10.3). The stays may be anchored into a large concrete edge beam replacing the longitudinal steel girder, and leaving only the composite cross-beams. The longitudinal and vertical forces are carried entirely by the concrete section only. If the stay is attached directly to the steel girder, all loads are initially carried by the steelwork, and the horizontal component is then largely transferred to the concrete deck (which forms the majority of the section's area) via shear connectors. On the Second Severn Bridge, the connection is via a transfer structure that resolves horizontal loads directly to the deck slab and the vertical components to the main girders (Various authors, 1997).

10.4. Example 10.1: Composite cable-stayed bridge

The first example of a composite cable-stayed bridge is the Second Severn Bridge. This is a 456 m span, 34 m wide structure spanning the shoots channel of the River Severn, 5 km downstream of the first crossing connecting England and Wales. The bridge has a twin stay plane, each with 120 cables in a semi-fan arrangement. The length of the back span is just under half that of the main span, giving a 900 m long cable suspended bridge. A stiffening girder is used to resist live load moments, and the back spans are further stiffened with intermediate piers. The deck stiffening consists of two longitudinal steel plate girders, 2.15 m deep, with transverse composite trusses at 3.6 m centres supporting the deck slab. The slab thickness varies, being 350 mm at the girders, 470 mm at the cable anchorage and 200 mm for the majority of the width between girders. The deck concrete has a cube strength of 70 N/mm^2 ($f_{ck} = 55$).

10.5. High-strength concrete

Typical concrete strengths are within the range 25–50 N/mm^2. With careful consideration of the aggregate type, a reduction in the water/cement ratio, and some cement replacement and additive, concrete strengths of up to 110 N/mm^2 or more are possible. Eurocode 2: Part 1-1, 'Design of concrete structures – General rules and rules for buildings' (BSI, 2004), assumes strengths in the range 20–90 N/mm^2. For steel–concrete composite structures the use of high-strength concrete will allow lower volumes of concrete and lighter structures. The higher strength concrete will also have a higher elastic modulus and lower shrinkage and creep values, leading to an increase in stiffness (Concrete Society, 1998).

For sections with high-strength concrete in compression, the design of the section will be similar to conventional-strength sections (see Equation 1.4). The limiting strain used in design will reduce with strength. At high strengths this may lead to a loss of ductility (see Figure 1.2):

$$\varepsilon_u = 0.0035 - (1.2 f_{ck} - 60)/50\,000 \tag{10.5}$$

The tensile strength of the concrete will also increase. Equation 1.1 is modified as

$$f_{ct} = 0.58(f_{ck})^{1/2} \tag{10.6}$$

The increased tensile strength will increase the load at which first cracking occurs in continuous beam and slab construction at supports. The reinforcement in the tensile zone must be sufficient to limit crack widths, and the increased tensile capacity leads to an increase in the minimum reinforcement. For concrete strengths over 75 N/mm^2 the minimum reinforcement should be

$$100A_s = 0.13(f_{ck}/33)^{0.67} \tag{10.7}$$

The lower water/cement ratio of high-strength concrete (typically below 0.3) means that shrinkage and creep are usually reduced by 20–50%. The stiffness of high-strength concrete elements is also increased, and the elastic modulus will increase (see Table 1.2).

10.5.1 Loads for Example 10.1

For the suspended span, the dead loads – particularly that of the slab – should be minimised in order to reduce the volume of the relatively expensive stay cables. A 200 mm slab is used where possible, as is thickening at the edges, where high local shear stresses occur near the stay anchorages.

10.5.2 Highway loads

The total live load on a bridge varies with span; for longer span lengths the load intensity is generally reduced (Figure 10.4). The loading on a length of highway is dependent on the vehicle weight, vehicle length, axle configuration and the number of vehicles bunched together. For bridges of short span, the impact and overloading factors are also important. For longer loaded lengths, the likelihood of a series of fully loaded heavy vehicles travelling across the structure is reduced, and it is also likely that some of the vehicles will not be fully loaded. The proportion of heavy vehicles depends on the prevailing economic conditions of the country or area in which the bridge is located. It will vary over time, and may be influenced by the bridge itself.

The loading used in the UK has increased over the years. Figure 10.4 shows the HA loading used for the design of the original Severn Bridge from 1966 (BSI, 1958; Chatterjee, 1992) the HA loading used

Figure 10.4 Live load variation with length: (a) HA loads *circa* 1966; (b) HA loads for 2004

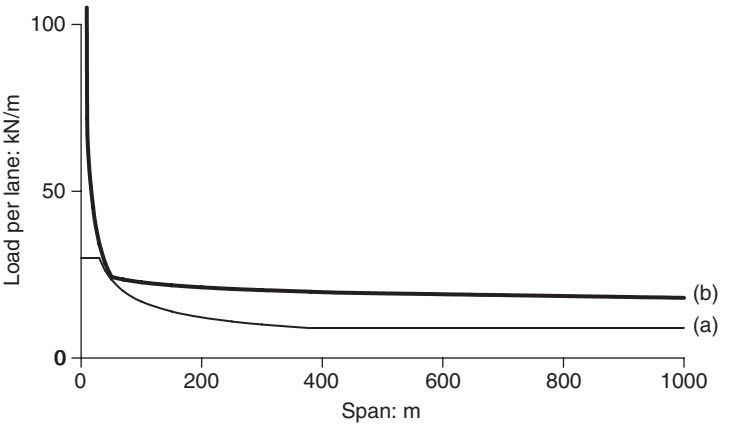

for the Second Severn Bridge and Eurocode loadings. The number of loaded lanes has also increased from a full lane with one-third full adjacent lanes, to a full lane with two-thirds full adjacent lanes, leading to an effective doubling of total load on the highway between the first and second of these bridges.

10.5.3 Wind loads

For long-span suspended structures, wind loading will govern aspects of the design and needs to be considered carefully. The basic wind speed at the site is determined using data given in standards (BSI, 1978, 2005, 2008a; AASHTO, 1996; NRA, 2000), but can be derived from measured values at the site if necessary. Wind velocities have been measured for many years, and there are a lot of data on wind speeds, gusts and direction. For the Eurocode the data has been drawn together and analysed, and a fundamental 10-minute mean velocity at 10 m height in open country with a return period of 50 years (v_{mo}) is used as the basis of calculation.

This wind velocity may be modified for different heights, return periods, seasons and directions, to give a mean velocity (v_m):

$$v_m = c_{dir}c_{sea}c_{prob}c_{alt}c_o c_r v_m \tag{10.8}$$

where c_{dir} is a direction factor, c_{sea} a seasonal factor and c_{prob} a probability factor, c_{alt} is an altitude correction, c_o is an orographic factor, and c_r is a terrain factor, which depends on the distance from the shoreline and the height at which the wind is considered. The mean wind velocity is then used to define a basic wind pressure:

$$q_b = 0.5\rho v_b^2 \tag{10.9a}$$

where ρ is the density of air, taken as 1.25 kg/m^3 (but it may be taken as 1.226 kg/m^3 in the UK). The basic flow pressure is modified to a peak pressure by means of a dynamic component that represents the turbulence and dynamic component of the wind; c_e and c_{et} are dynamic coefficients and may be taken from Figure 7.4b and 7.4c.

$$q_p = c_e c_{et} q_b \tag{10.9b}$$

Figure 10.5 Variation in drag, lift, twist with wind angle: (a) girder bridge; (b) box shape

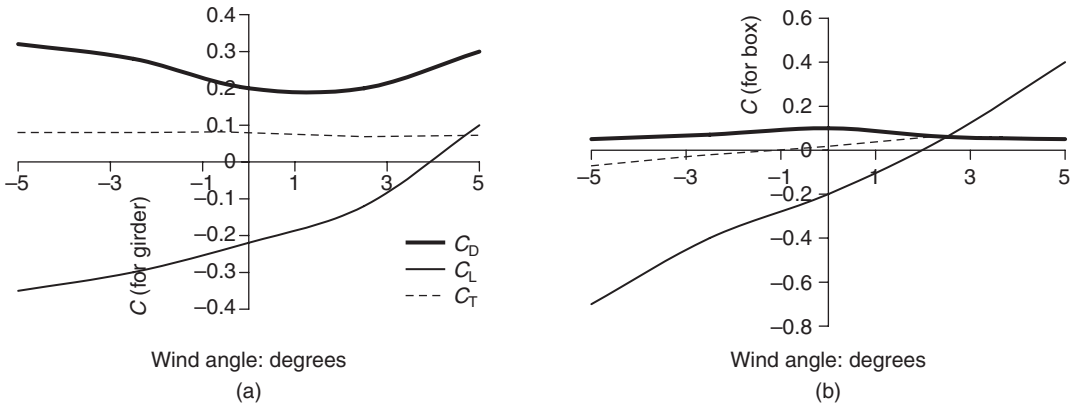

The force on the bridge is derived directly from the peak pressure using a series of factors:

$$F = c_s c_d c_{fd} \Psi_r \Psi_d q_p A_{ref} \tag{10.10a}$$

where c_s is a structural coefficient and c_d is a force coefficient, and c_{fd} is a drag factor, which may be derived from wind-tunnel tests or tabulated data. Figure 10.5 shows the typical variation in drag coefficients with the angle of incidence of the wind for a relatively bluff girder bridge and a more aerodynamic box section. The magnitudes of the coefficients are also affected by the shape and width of the deck. Ψ_r is a factor depending on the radius of the corners, Ψ_d is a solidity factor, and A_{ref} is the projected area of the structure. To a first approximation, in the UK the force due to wind may be taken as:

$$F = 2.5 A_{ref} c_{fo} v_{mo}^2 \tag{10.10b}$$

where c_{fo} is a drag coefficient. The wind imposes load on the structure, causing drag (c_{fd}), lift (c_{fl}) and twisting (c_{ft}) of the suspended deck.

This static loading is only part of the wind effect. Wind velocities vary over time, and gusting causes dynamic effects such as buffeting, flutter and the shedding of vortices. The susceptibility of a bridge to dynamic wind effects can be determined by a factor P (Highways Agency, 2001):

$$P = (\rho b^2/m)\ (44 v_{mo}^2/bLf_b^2) \tag{10.11}$$

where ρ is the density of air, b is the bridge width, L is the span, m is the mass per unit length of the bridge, and f_b is the first bending frequency of the structure. For $P < 0.04$, the structure is unlikely to be susceptible to aerodynamic excitation. For $P < 1$, the structure should be checked against some simplified criteria to check for any aerodynamic instability. If $P > 1$, the structure is likely to be susceptible to aerodynamic excitation, and some changes to the mass, stiffness or structure layout may be required. In addition, in the latter case wind-tunnel testing will be required to verify the structure's behaviour.

Figure 10.6 (a) Vortex shedding from a bridge causing movement of the structure. (b) Flutter of a bridge involving combined vertical and torsional movement

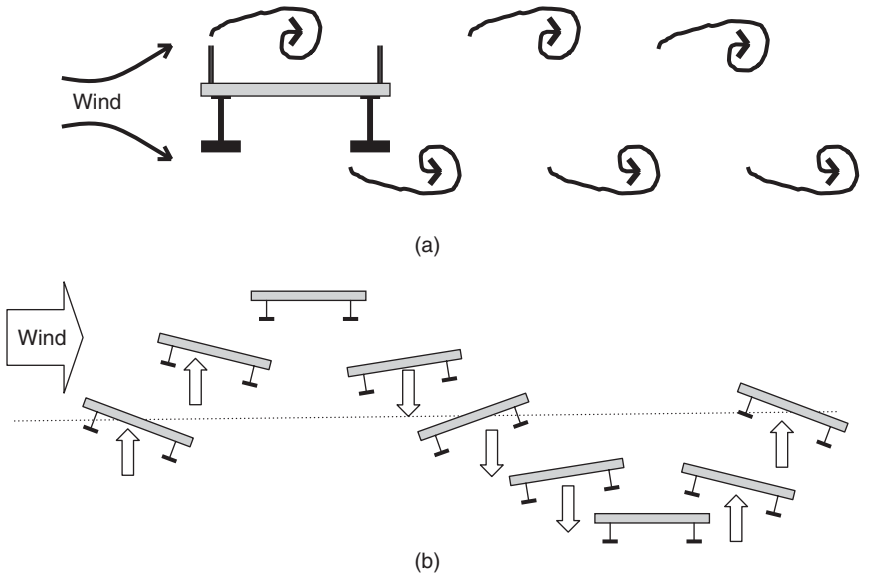

For the Second Severn Bridge, $b = 35$ m, $L = 456$ m, $m = 40\,000$ kg/m and $V_{co} = 22.5$ m/s. The bending frequencies of cable-stayed bridges tend to be lower than those of other beam-, arch- or truss-type structures (see Figure 4.11). In this example, $f_b = 0.33$ Hz (Collings, 2005). Using Equation 10.11,

$$P = \left(\frac{\rho b^2}{m}\right)\left(\frac{44 v_{co}^2}{b L f_b^2}\right) = \left(\frac{1.25 \times 35^2}{40\,000}\right) \times \left(\frac{44 \times 22.5^2}{35 \times 456 \times 0.332}\right) = 0.036 \times 4.3 = 0.15$$

$0.04 < P < 1.0$, so some simplified checks on the two principal causes of wind excitation (vortex shedding and flutter) should be carried out.

Vortex excitation is caused by the shedding of vortices in phase with the natural frequency of the structure (Figure 10.6a). The critical wind speed at which this occurs can be established using

$$v_{cv} = f_b d / S \tag{10.12}$$

where d is the depth of the structure and S is the Strouhal number, which varies from approximately 0.12 for a bluff girder system to 0.3 for a smooth cylinder shape.

In this example, the depth of the structure is approximately 3.1 m. However, wind shielding, 3 m high, is provided at the edge of the bridge to lower the wind loading on traffic. Wind-tunnel testing on the barriers (Irwin *et al.*, 1994; Various authors, 1997) indicated that they have some effect on the aerodynamic behaviour of the deck. Using Equation 10.12, with $d = 3.1$ m and $S = 0.12$,

$$v_{cr} = 0.33 \times 3.1 / 0.12 = 8.5 \text{ m/s}$$

If a larger depth is used to allow for wind shielding,

$$v_{cr} = 0.33 \times 6.1/0.12 = 16.5 \text{ m/s}$$

For high bridges the wind may not always be horizontal, and this may increase the effective depth. In the example the deck is 40 m above the water, and a 3° angle of attack (θ) seems a reasonable assumption:

$$d = d + L \sin \theta = 6.1 + 1.8 = 7.9 \text{ m}$$

Recalculating the critical wind speed,

$$v_{cr} = 0.33 \times 7.9/0.12 = 21.8 \text{ m/s}$$

A large range of critical velocities is calculated, reflecting the various assumptions. All the velocities are lower than the basic site wind speed and may occur relatively frequently; the highest value is a significant proportion of the site wind speed, and may have a significant force input, as the wind force is proportional to the square of the velocity.

Flutter is an aerodynamic phenomenon involving a combined vertical and torsional movement of the bridge deck (Figure 10.6b). The critical wind speed at which this flutter occurs on a thin plate can be estimated as

$$v_{cf} = k_f v_{fd}[1 - (f_b/f_t)^2]^{1/2} \tag{10.13}$$

For bridge deck sections k_f varies from 0.4 for bluff sections to 0.9 for more aerodynamic shapes. f_t is the first torsional frequency and v_{fd} is the divergent wind speed:

$$v_{fd} = (f_b/r_m)(\pi J_m/\rho)^{1/2} \tag{10.14}$$

where J_m is the mass moment of inertia (I_p m/A), r_m is the mass radius of inertia $(J_m/m)^{1/2}$ and I_p is the polar moment of inertia $(I_x + I_y)$.

In this example, $I_p = 88 \text{ m}^4$, $J_m = 4.8 \times 10^6 \text{ kg/m}^2/\text{m}$ and $r_m = 10.9$ m. The torsional frequency of the bridge is 0.47 Hz and, using Equation 10.12,

$$v_{fd} = (f_b/r_m)(\pi J_m/\rho)^{1/2} = (0.47/10.9) \times (3.14 \times 4.8 \times 10^6/1.25)^{1/2} = 149 \text{ m/s}$$

And, using Equation 10.13, with $k_f = 0.45$,

$$v_{cf} = k_f v_{fd}[1 - (f_b/f_t)^2]^{1/2} = 0.45 \times 149[1 - (0.33/0.47)^2]^{1/2} = 48 \text{ m/s}$$

This velocity is higher than the basic wind speed, but given that the accuracy of the calculations above is limited, wind-tunnel testing of the bridge cross-section is required to confirm the critical flutter velocities and to ensure that any vortex excitation is of limited amplitude.

A series of wind-tunnel tests was carried out on the structure in Example 10.1 (Irwin *et al.*, 1994; Maury *et al.*, 1994; Macdonald *et al.*, 2002). The first tests on a 1 : 50 scale sectional model looked at the effect

of removing the enclosure shown on the original design. Removal of the enclosure affects the drag (similar to as in Figure 10.5), but also changes the flutter and vortex response, increasing v_{cf} and showing some vortex shedding. A second series of sectional models was then formulated for the section, with the primary steel stiffening girders in various locations. It was found that layouts with girders near the edge (which are structurally more efficient) caused more vortex shedding than did those with girders nearer the centre of the section. The final deck girder layout had the girders inset from the edges, which was a compromise between conflicting structural and aerodynamic requirements. The testing of this section showed some limited vortex-induced response under smooth flow, but no response where turbulent flow was used. A final set of tests was carried out on a 1 : 125 scale model of the bridge (stays, deck and towers). These tests showed vortex shedding in smooth flow at a wind inclination of 2.5°, while at horizontal inclinations or with turbulent flow no vortex shedding response was recorded.

The bridge has now been constructed (see Figure 10.9), and in the first winter of operation the bridge exhibited some vertical oscillation. The structure was instrumented and the response to the wind measured. After analysing the wind and the structure's response to it, a further series of wind tunnel tests was carried out to replicate the measured response. Based on these studies it was concluded that both the structural damping and the wind turbulence were lower than assumed for design. These conclusions are relevant to many other bridges of this type (Macdonald *et al.*, 2002). It is also clear that changing the cross-section has a significant effect on the design. A further set of wind-tunnel tests was then made on a modified structure – two longitudinal baffle plates were placed between the girders for approximately one-third of the span. The tests indicated that this modification would suppress vortex oscillations. The baffles were then fitted to the real structure, and measurements indicate that vortex-induced oscillations have ceased.

10.5.4 Analysis

A first estimate of cable loads can be obtained from the structure geometry. To estimate deflections, moments and shears in the girders and towers, a more complex model with a high degree of redundancy is required. To understand the behaviour, a series of simple models is generally preferable to a single large complex model. A two-dimensional linear elastic representation of the towers, piers, deck and cables with spring supports representing the foundations will usually be adequate. Depending on the stresses in the cables, some modification of the material modulus may be required to allow for the cable sag (Walther *et al.*, 1988), particularly for long-span structures.

During the life of the structure it is likely that the stays will need to be replaced, and this will be carried out with traffic on the structure. It is also possible that one or more cables could fail, shedding load to adjacent cables, so it is important that the structure is robust and that a progressive 'unzipping' failure does not occur. For the cable-out scenarios a 3D model of the bridge or a section of deck will usually be required. This model is also used to confirm the torsional frequencies of the bridge under wind loads.

Local models may also be required to represent the transfer of load from the stay to the deck, and the use of a strut and tie model (Menn, 1990) will also give a good estimate of likely load paths. Figure 10.7 shows the global moment and shear of the deck for live loads based on the 2D model with stays and decks joined at a node on the longitudinal girder. The stays are located at the edge of the slab and the girder is inboard of this; the connection is via an anchorage beam and two cantilever beams, and this spreads the load and thus reduces the peak moments and shears on the girder.

Figure 10.7 Analysis results for Example 10.1: (a) moment; (b) shear; (c) axial load for live load

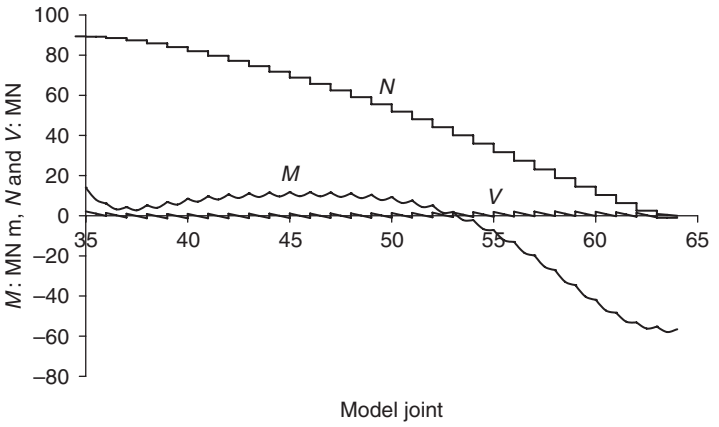

10.6. Buckling interaction

For a slender steel–concrete composite section subject to shear, bending and axial loads, the buckling of the relatively slender components may occur. In Chapter 4, it was noted that there is an interaction between bending and shear, and in Chapters 8 and 9 the interaction of moments and axial load was explored. For a composite cable-stayed bridge deck, the girder system is resisting bending and shear with a large axial load, and there will be an interaction of all three (Rockey and Evans, 1981; BSI, 2000). The web of a girder in a cable-stayed bridge is particularly prone to this buckling. For a web panel, the buckling interaction equation is

$$m_c + m_b + 3m_v < 1 \tag{10.15}$$

where

$$m_c = 0.95 f_c / k_c f_y$$

$$m_b = (0.95 f_b / k_b f_y)^2$$

$$m_v = (0.95 v / k_v f_y)^2$$

k_c, k_b and k_v are coefficients that vary with the web slenderness and degree of edge restraint (Figure 10.8).

For the bridge in Example 10.1, the design forces for the girder near the quarter point are obtained from Figure 10.7. At this location the girder is formed from a 20 mm web and a 750×90 mm bottom flange. The section properties are obtained from Appendix C. The stress at the ultimate limit state are

$$f_{top} = \frac{N}{A} + \frac{M}{Z_t} = \frac{102}{0.535} + \frac{16}{1.47} = 190 + 11 = 201 \text{ N/mm}^2$$

$$f_{bot} = \frac{N}{A} - \frac{M}{Z_b} = \frac{102}{0.535} - \frac{16}{0.21} = 190 - 76 = 114 \text{ N/mm}^2$$

Figure 10.8 Buckling interaction coefficients for restrained and unrestrained panels

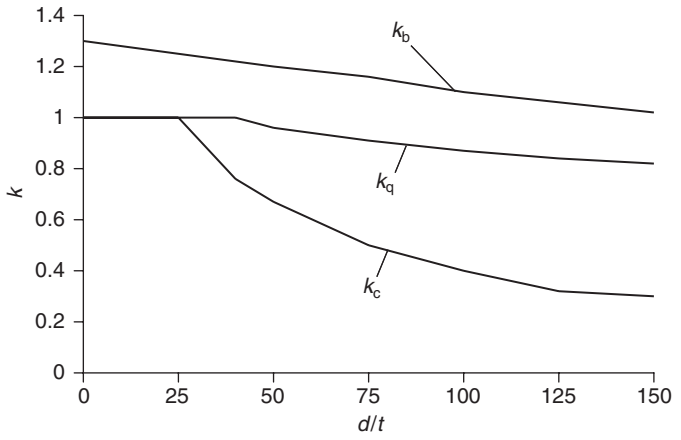

$$f_c = (f_{top} + f_{bot})/2 = 158 \text{ N/mm}^2$$

$$f_b = f_{top} - f_c = 52 \text{ N/mm}^2$$

$$v = V/dt = 2.7/2.1 \times 0.020 = 64 \text{ N/mm}^2$$

If the web is unstiffened, $d/t = 2100/20 = 105$. From Figure 10.9, $k_b = 1.2$, $k_v = 0.94$ and $k_c = 0.4$.

$$m_b = (0.95 \times 52/1.2 \times 355)^2 = 0.01$$

$$m_v = (0.95 \times 64/0.94 \times 355)^2 = 0.03$$

$$m_c = (0.95 \times 158/0.4 \times 355) = 1.05$$

$$m_c + m_b + 3m_v = 1.08$$

which is greater than 1, and so buckling may occur. It can be seen that, in this example, the axial buckling dominates the design. To increase the capacity of the section, stiffening is required. For the built structure, two longitudinal angle stiffeners were used, dividing the web into three sections. For the stiffened web, $d/t = 35$, $k_b = 1.22$, $k_v = 1$, $k_c = 0.8$ and $m_c = 0.63$:

$$m_c + m_b + 3m_v = 0.66$$

which is now satisfactory. It is also possible to avoid buckling of the web by using a corrugated web (see Chapter 11).

10.7. Shear connection

In Chapter 1, it was noted that the force transferred across the steel–concrete interface is related to the rate of change of force in the slab (Equation 1.16a). For many bridges, this can be simplified to the rate of change in bending, in proportion to the vertical shear (Equation 1.16b). For cable-stayed bridges, where there is a significant axial load, the rate of change in axial loads needs to be taken into account.

Figure 10.9 Cantilever construction of the Second Severn Bridge (© T Hambley)

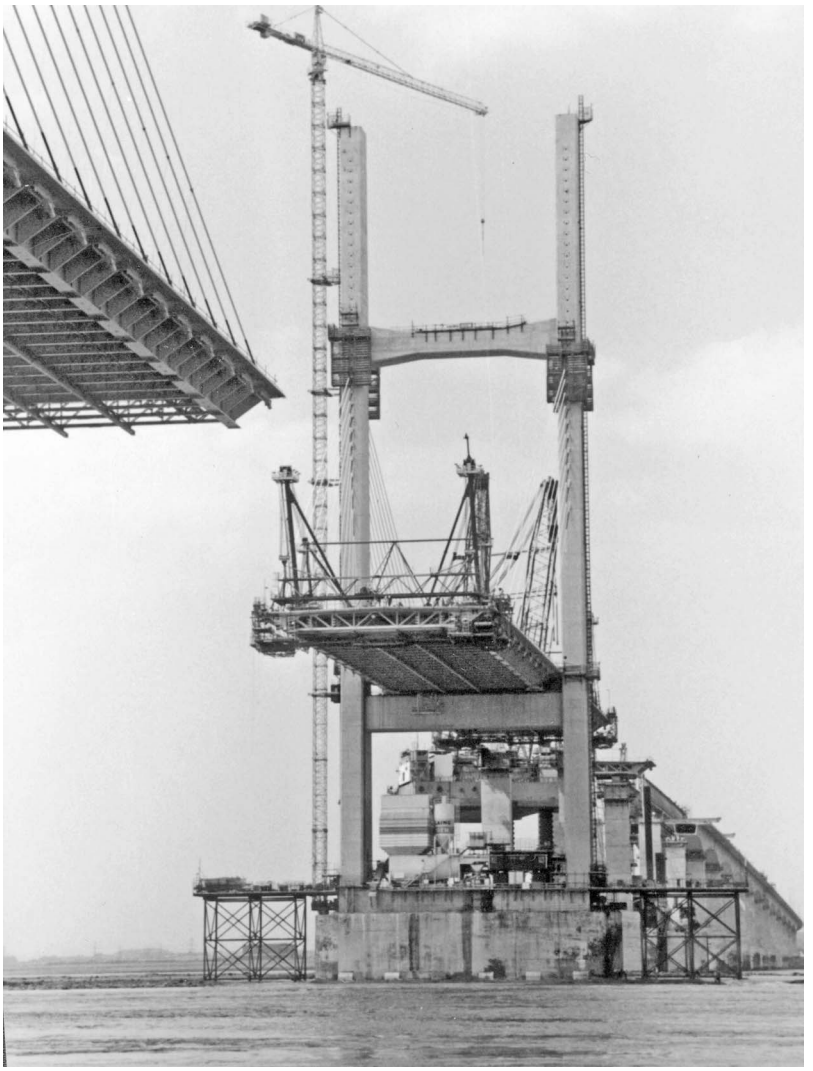

The rate of change in axial force can be visualised by considering the construction method used for the bridge (Figure 10.9). The bridge in this example was constructed using a cantilever technique, with a 7.4 m segment of deck and stay added at each face. Each deck section is supported by a stay and puts a small increment of axial force into the deck. The force in this example is applied directly to the deck concrete (see Figure 10.3c). Part of this force will be carried by the deck steelwork, and shear connectors will be required to transfer the load across the interface.

$$\delta N = N A_{\mathrm{a}} / (A_{\mathrm{a}} + A_{\mathrm{c-n}}) \tag{10.16}$$

$$V_{\mathrm{l}} = \delta N / L_{\mathrm{s}} \tag{10.17}$$

where L_s is the length over which the force is transferred. With stays at 7.4 m centres it is likely that using $L_s = 7.4$ m will give a reasonable distribution of connectors. The length over which the force is transferred depends on the stiffness of the connectors, and can be estimated using Equation 3.13.

For the Second Severn Bridge, near the quarter point $V = 2.0$ MN at the serviceability limit state, and the increment in axial force between stays is 4.7 MN. From Appendix C, $V_l/V = 0.44$, $A_a = 0.13$ m^2, $A_c = 4.8$ m^2 and the modular ratio is 12.

$$\delta N = 4.8 \times 0.13/(0.13 + 4.8/12) = 1.18 \text{ MN}$$

$$V_{lN} = \delta N/L_s = 1.18/7.4 = 0.16 \text{ MN/m}$$

$$V_{lm} = 0.44 \times 2 = 0.88 \text{ MN/m}$$

The total longitudinal shear $V_l = 0.16 + 0.88 = 1.04$ MN/m. Using Equation 1.18a, with 25 mm connectors $P_u = 183$ kN (see Table 1.5), limiting the force in the stud connector to only 55% of its ultimate capacity:

$$n = 1040/0.55 \times 183 = 11$$

Two 25 mm diameter connectors at 150 mm centres are satisfactory at this location.

10.8. Towers

The towers of a cable-stayed bridge provide much of its character. For a given span the taller tower of the asymmetric span will be more prominent than the smaller towers of the symmetric layout. Many of the monumental cable-stayed structures have exploited this asymmetric layout (Highways Agency, 1996; Sharp, 1996; Troyano, 2004). Towers are of three basic forms: the H-shape is a simple and economic layout for medium-span bridges with two planes of cables (see Figure 10.9 for the towers for the Second Severn Bridge); the single-leg tower and the inverted Y-form (Collings and Brown, 2003; Kumarasena *et al.*, 2003), both have the stays anchored in a line, either by the use of a single plane of cables, or by inclining cables on a twin plane of stays. The use of this latter form gives some triangulation and increases the torsional stiffness of the deck–stay–tower system, and is used for larger spans.

The three basic forms may be modified in many ways to achieve some architectural statement or visual interest. Single towers are often inclined in an attempt to dramatise the structure, and backward-leaning towers can achieve a certain sculptural dynamic from some views (Figure 10.10). However, from other views the tower can appear to lean forwards, leading to a more unstable perspective, particularly from the drivers' viewpoint. The viewpoint for structures with a high degree of aesthetic input is often chosen to flatter and compliment the design. When judging such structures other viewpoints should normally be requested in order to avoid the possibility of a mediocre structure being selected on the basis of one viewpoint or image.

The leaning of towers and other elements of the structure usually make the structure less efficient, more costly and of a larger carbon footprint. Consider a simple single-leg tower structure similar to the one shown in Figure 10.10. If the towers are leant backwards or forwards, the relative volume of material in the tower and stays changes. Figure 10.11 shows the change in volume of materials for various inclinations – the steeper the lean, the less efficient the structure becomes.

Figure 10.10 Leaning towers, front and rear views

10.9. Tower top

For the common semi-fan form of cable layout the tower can be divided into two sections: the upper section in which the stays are anchored, and the lower section. The lower section carries the axial force to the foundations and provides the bending resistance to overturning (hence the usually tapered form, widening to the base). The forces in the upper tower section are more complex. Although this section has to resist smaller overall bending, shear and axial effects, it also has to resist the high local loads from the stay anchorage. For the majority of cable-stayed structures the stays have been anchored to the sidewalls of the tower, leading to a significant tension effect across the tower. For smaller structures (Collings and Brown, 2003), anchoring to the far side of the tower can reduce this complexity. For concrete towers, the splitting can be resisted by transverse prestress (Menn, 1990; Benaim, 2008). The layout and anchoring of this prestress can be complex, and many recent bridges (Virlogeux *et al.*, 1994; Kumarasena *et al.*, 2003) have used a steel–concrete composite box arrangement to transfer this tensile load.

Figure 10.11 Variation in structure material volume with tower inclination

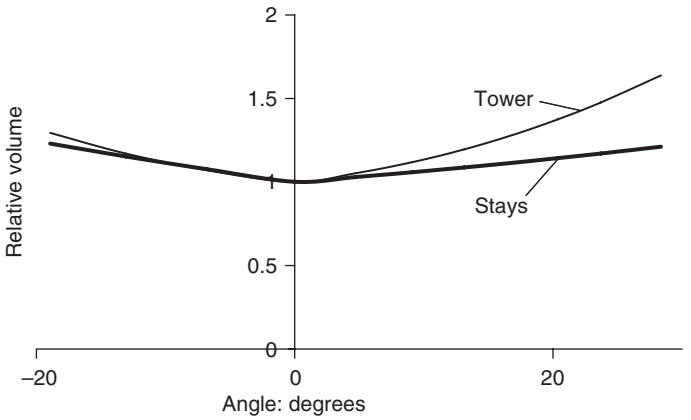

For the tower composite box structure, the inclined tension force of the stays is resolved horizontally and vertically. The horizontal component of the stay tension is resolved across the box, so the transverse area of the box must be large enough to resist this tension. The vertical component of the stay causes compression on the box, and locally this is carried by the steel section only. In a composite steel–concrete tower, this force is then transferred via connectors to the concrete. If the vertical components on each side of the box are not the same, some bending will be induced in the section, and additional reinforcement in the concrete, or an external steel skin may be used to resist this moment.

More recently, the author has used a saddle arrangement on two 300 m span bridges. The saddle gives a continuous stay from deck to deck, without anchorage in the tower. For this form of structure, it is important to avoid large differences in stay forces on each side of the tower, which could induce slip in the saddle (Annan and Gnagi, 2010). Saddles are more appropriate for concrete, rather than steel, towers.

10.10. Example 10.2: Composite tower

The transfer of forces in the top of a tower are complex due to the various angles of the stay anchorage. This complexity is explored in the second example of this chapter, the Stonecutters Bridge (see Figure 10.2). Stonecutters Bridge is a large 1018 m span cable-stayed bridge across the Rambler Channel in Hong Kong. The bridge is located between the Kwai Chung container port (formerly Stonecutters Island) and Tsing Yi Island. The bridge deck consists of twin box concrete girders in the side spans, and twin box steel girders around the towers and in the main span. The deck boxes are separated by an air gap but are interconnected by transverse members at 18 m intervals, an arrangement that significantly improves the flutter response of the structure (Richardson, 1991). It is a cable-stayed bridge with two tapered, cylindrical, single-leg towers, each 298 m tall (Figure 10.12). The cables are arranged in a semi-fan configuration.

The lower sections of the towers from the top of pilecap to 175 m are formed of reinforced concrete. The upper sections to 293 m are of composite construction, with an internal high-strength-steel box structure composite with a concrete surround and a stainless steel outer skin. The top 5 m of the towers are glazed and house lighting features. The upper tower tapers from 10.9 m diameter to 7 m diameter, with a wall thickness varying from 1400 mm to 820 mm. The steel skin is a 20 mm thick stainless steel plate and forms the outside face of the concrete tower. Composite action of the skin and the concrete wall is achieved by connecting the skin to the wall by means of shear studs. The design of the towers has developed from the original design (Withycome *et al.*, 2002), which proposed an all-steel top section. The steel–concrete composite section was used in order to increase stiffness and reduce costs.

10.11. Stainless steel

The twin properties of corrosion resistance and good aesthetics are the primary reasons for using stainless steel. Like weathering steel (see Chapter 3), stainless steel forms a passive oxide film of corrosion products on its surface, which further limits corrosion and means that painting is not required. The oxide film can be damaged by abrasion, atmospheric pollution or a marine environment. There are a number of types of stainless steel (European Stainless Steel Development Association, 2002). For structural use in bridges, austenitic and duplex stainless steels are the most common. Of these types the duplex is most tolerant of pollution and coastal environments.

The structural properties of stainless steel are similar to those of normal steel, although the elastic modulus is slightly lower at 200 kN/mm^2, and the coefficient of thermal expansion is higher at $16 \times 10^{-6}/°C$. The stress–strain profile of stainless steel has a less pronounced yield point than

Figure 10.12 A tower of the Stonecutters Bridge with a composite upper section (© Arup)

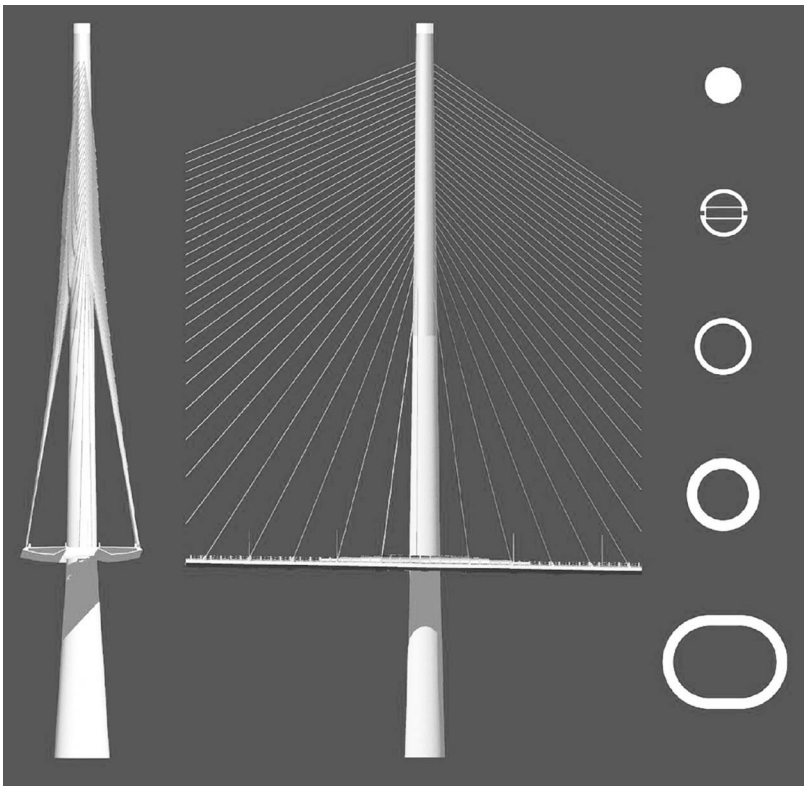

normal steel plate (see Figure 1.5), and the strength is usually based on the 0.2% proof strength. For austenitic stainless steel, the strength is typically 200–250 N/mm^2, while for duplex stainless steel it is 400–480 N/mm^2. Eurocode 3: Part 1-4, 'Supplementary rules for stainless steels' (BSI, 2006), contains supplementary rules for the design of stainless steel structures (Figure 10.13).

10.11.1 Loads for Example 10.2

The Stonecutters Bridge spans a major shipping channel and is located in a moderately seismically active area. The bridge is also located in an area subject to typhoon storm loads, and so wind loads are also significant, adding transverse bending effects to the tower. These criteria are important for the lower tower and its foundations, but less so for the upper tower. For the upper section, the dead and live loads transferred from the deck via the stays are the major influence.

10.11.2 Analysis

The design of the bridge involved a series of analyses at the various stages of design development, from concept through to the detailed design phase. The final analysis consists of a 3D frame analysis of the bridge (deck, stays, piers and towers), with stay non-linearity being taken into account. The tower consists of a tall structure with significant axial loads, and second-order (P-delta and critical buckling) effects were also taken into account. The forces for the upper tower were then processed in a series of spreadsheets to extract maximum and minimum values of axial force and bending, together with their co-existing effects.

Figure 10.13 The Stonecutters Bridge during construction (© VSL)

Considering a stay in the middle of the composite tower section, the reaction at the ultimate limit state from the stays above is 280 MN. At this section the stay forces are 16 MN from the main span and 22 MN from the back span. Resolving the stay forces gives an applied local axial load of 7.0 MN and a horizontal component of 13 MN. The effective depth of the tie across the box is assumed to be 1.2 m with a thickness of 20 mm. Using Equation 1.7,

$$N_{\mathrm{Dtie}} = f_{\mathrm{y}} A_{\mathrm{ae}} = 2 \times 420 \times 1.2 \times 0.02 = 20 \text{ MN}$$

which is more than the applied loads. A local 3D finite-element analysis of the steel skin, concrete tower and anchor box were also undertaken to confirm the local effects on the tower. The local and global effects are added together to determine the final stresses in the system.

The vertical component of the force will be transferred via connectors. The distance between stays is approximately 3 m, and 70% of the local vertical component is reacted on the back-span side of the box:

$$V_{\mathrm{l}} = 25 \times 0.7/3 = 5.8 \text{ MN/m}$$

Using Equation 1.18a and assuming 22 mm diameter connectors ($P_{\mathrm{u}} = 139$ kN from Table 1.5),

$$n = V_{\mathrm{l}}/0.7P_{\mathrm{u}} = 5.8/0.098 = 60$$

These connectors are spread across the box face in a staggered layout, keeping the centres below 600 mm (see Table 1.3).

The box and steel skin are formed of relatively thin (generally 20 mm thick) steel plates, with the concrete section and its reinforcement forming a larger area. The tower section was therefore designed using methods similar to those used for reinforced concrete sections (Menn, 1990), where stresses are derived from strains. The steel skin contributes to both the vertical and the hoop reinforcement. The stainless steel skin is formed in a series of 2–4 m tall sections with bolted splices. The splices are considered as compression-only elements, the tension capacity being conservatively neglected.

10.12. Strain-limited composite section (class 4)

Steel–concrete composite compression members with a steel contribution factor (α_a) less than 0.2, or where the steel element thickness is outside the limits of Table 1.4, will be governed primarily by the behaviour of the concrete. The steel element will rely on connectors to prevent it buckling locally. The behaviour will be similar to that of the steel sandwich panels sometimes used in buildings (Liang *et al*., 2003; Collings, 2010). The axial and bending capacities of the section will be limited by the strain distribution across the section; not all of the section will be at yield (Figure 10.14).

Figure 10.14 Typical stress and strain distribution across a tower at the ultimate and serviceability limit states

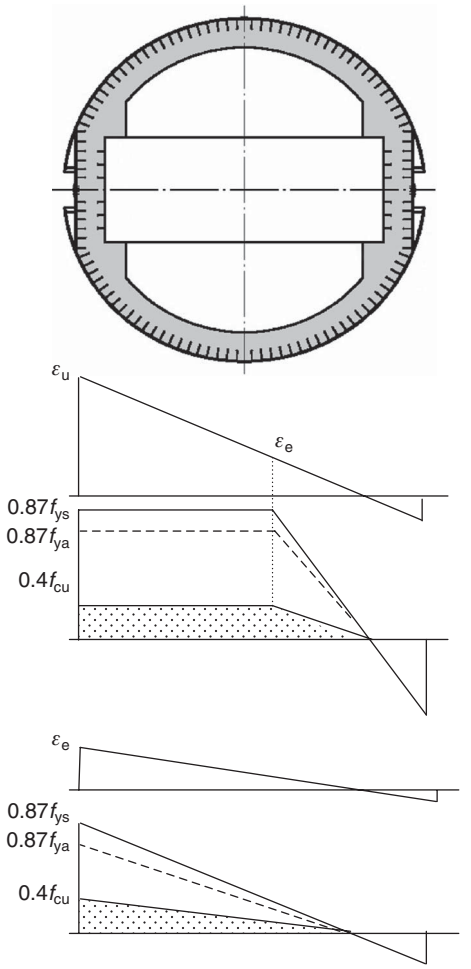

The extreme tension and compression capacities of the section will be similar to a more compact or steel-governed section; the bending capacities of the section will be reduced.

For the Stonecutters tower the axial capacities of the composite section (N_{UL}) and the stainless steel skin (N_{ua}) are 760 MN and 225 MN, respectively, giving a steel contribution factor (α_a) of 0.3. An M–N interaction curve for the tower can be constructed (Figure 10.14); the applied moment and axial load are well within the section capacity. The shear at the interface of the stainless steel skin can be calculated. However, like the internal box plates, the connector spacing is likely to be governed by the nominal spacing requirements to ensure local buckling of the thin plates cannot occur. For this structure the connectors are at $15t_f$ (300 mm) spacing. 300 mm long connectors are used to ensure a firm connection to the concrete.

REFERENCES

AASHTO (American Association of State Highway and Transportation Officials) (1996) *Standard Specifications for Highway Bridges*, 16th edn. AASHTO, Washington, DC.

Annan R and Gnagi A (2010) Development and tests of a high performance saddle system. *Proceedings of the 3rd FIP International Congress*, Lisbon.

Benaim R (2008) *The Design of Prestressed Concrete Bridges: Concepts and Principles*. Taylor & Francis, London.

BSI (1958) BS 153:1958. Steel girder bridges. BSI, London.

BSI (1978) BS 5400-2:1978. Steel, concrete and composite bridges. Specification for loads. BSI, London.

BSI (2000) BS 5400-3:2000. Steel, concrete and composite bridges. Code of practice for design of steel bridges. BSI, London.

BSI (2004) BS EN 1992-1-1:2004. Eurocode 2. Design of concrete structures. General rules and rules for buildings. BSI, London.

BSI (2005) BS EN 1991-1-4:2005. Eurocode 1. Actions on structures. General actions. Wind actions. BSI, London.

BSI (2006) BS EN 1993-1-4:2006. Eurocode 3. Design of steel structures. General rules. Supplementary rules for stainless steels. BSI, London.

BSI (2008a) NA to BS EN 1991-1-4:2008. UK National Annex to Eurocode 1. Actions on structures. General actions. Wind actions. BSI, London.

BSI (2008b) NA to BS EN 1993-1-11:2008. UK National Annex to Eurocode 3. Design of steel structures. Design of structures with tension components. BSI, London.

Chatterjee S (1992) Strengthening and refurbishment of Severn Crossing. *Proceedings of the ICE – Structures and Buildings* **94(1)**: 1–5.

Collings D (2005) Lessons from historical failures. *Proceedings of the ICE – Civil Engineering* **161(6)**: 20–27.

Collings D (2010) *Steel–Concrete Composite Buildings, Designing with Eurocodes*. Thomas Telford, London.

Collings D and Brown P (2003) The construction of Taney Bridge, Ireland. *Proceedings of the ICE – Bridge Engineering* **156(3)**: 117–124.

Concrete Society (1998) *Design Guidance for High Strength Concrete*. Technical Report 49. Concrete Society, Camberley.

De Miranda F (1988) Design – long span bridges. *ECCS/BCSA International Symposium on Steel Bridges*.

European Stainless Steel Development Association (2002) *Design Manual for Structural Stainless Steel*, 2nd edn. Steel Construction Institute, Ascot.

Highways Agency (1996) *The Appearance of Bridges and other Highway Structures*. HMSO, London.

Highways Agency (2001) BD 49, Design rules for aerodynamic effects on bridges. In *Design Manual for Roads and Bridges*, Vol. 1. The Stationery Office, London.

Irwin P, Mizon D, Maury Y and Schmitt J (1994) History of the aerodynamic investigations for the Second Severn crossing. *Proceedings of International Conference*, Deauville.

Ito M, Fujino Y, Miyata T and Narital N (eds) (1991) *Cable-stayed Bridges. Recent Developments and their Future*. Elsevier, Oxford.

Kumarasena S, McCabe R, Zoli T and Pate D (2003) Zakim. Bunker Hill Bridge, Boston, Massachusetts. *Structural Engineering International* **13(2)**: 90–94.

Liang Q, Uy B, Wright HD and Bradford MA (2003) Local and post-local buckling of double skin composite panels. *Proceedings of the ICE – Structures and Buildings* **156(2)**: 111–119.

Macdonald J, Irwin P and Fletcher M (2002) Vortex-induced vibrations of the Second Severn Crossing cable-stayed bridge – full-scale and wind tunnel measurements. *Proceedings of the ICE – Structures and Buildings* **152(2)**: 123–134.

Maury Y, MacFarlane J, Mizon D and Yeoward A (1994) Some aspects of the design of Second Severn Crossing cable stayed bridge. *Proceedings of International Conference*, Deauville.

Menn C (1990) *Prestressed Concrete Bridges*. Birkhauser-Verlag, Basel.

NRA (National Roads Authority) (2000) *Design Manual for Roads and Bridges*, Folio A: Vols 1 and 2. NRA, Dublin.

Richardson J (1991) The Development of the Concept of the Twin Suspension Bridge. National Maritime Institute, Chittagong.

Rockey K and Evans H (eds) (1981) *The Design of Steel Bridges*. Granada, London.

Sharp D (ed.) (1996) *Santiago Calatrava*. Book Art, London.

Troyano L (2004) *Bridge Engineering a Global Perspective*. Thomas Telford, London.

Various authors (1997) Second Severn crossing. *Proceedings of the ICE – Civil Engineering* **120** (Special Issue 2).

Virlogeux M (2001) Bridges with multiple cable stayed spans. *Structural Engineering International* **11(1)**: 61–82.

Virlogeux M, Foucriat J and Lawniki J (1994) Design of the Normandie bridge, Cable stayed and suspension bridges. *Proceedings International Conference AIPC-FIP*, Deauville.

Walther R, Houriet B, Isler W and Moia P (1988) *Cable Stayed Bridges*. Thomas Telford, London.

Withycome S, Firth I and Barker C (2002) The design of the Stonecutters Bridge, Hong Kong. *Current and Future Trends in Bridge Design, Construction and Maintenance. Proceedings of the International Conference*, Hong Kong. Thomas Telford, London.

Steel–concrete Composite Bridges
ISBN 978-0-7277-5810-1

http://dx.doi.org/10.1680/scb.58101.205

ice
Institution of Civil Engineers
publishing

Chapter 11
Prestressed steel–concrete composites

... prestressing using high-tensile-steel strand ... allows a significant reduction in steel volume compared with conventional bar reinforcement ...

11.1. Introduction

The prestressing of a structure involves the application of a state of stress to improve its behaviour. The prestressing may be done by applying displacements to the supports, preflexing the beam, or by applying load from pre-strained or tensioned steel strand. Prestressing using high-tensile-steel strand or bars is common for concrete structures; the use of strand with an ultimate strength of 1880 N/mm^2 (Table 1.2) allows a significant reduction in steel volume compared with conventional bar reinforcement with its 460 N/mm^2 yield strength. This four-fold reduction allows sections to be smaller and lighter with less congested detailing. The prestressing of steel–concrete composite structures is less common (Troitsky, 1990), but it can be seen that there is scope for reducing the size of the conventional 355 N/mm^2 steel plate. The main disadvantage of prestressed steel–concrete composites is that tendon anchorages or deviators attached to the steel elements tend to significantly increase fabrication complexity, and thus increase cost.

11.2. Displacement of supports

The raising or lowering of supports may be used to change the stress in a continuous structure. For a two-span continuous girder of constant section, movement of the central support vertically (δ) will induce a moment of

$$M = 3E_{\mathrm{a}}I_{\mathrm{a-c}}\delta/L^2 \tag{11.1}$$

For a multi-span structure, the use of support movement to change moments is more complex. To induce a uniform moment along the beam, each support must be moved by a different amount. Initially, the beam would be constructed on jacks such that a constant radius of curvature (r_{j}) was formed, and the section would then be lowered to the final curvature (r_{f}):

$$M = E_{\mathrm{a}}I_{\mathrm{a-c}}/(r_{\mathrm{f}} - r_{\mathrm{j}}) \tag{11.2}$$

For both Equations 11.1 and 11.2, the girder stiffness ($E_{\mathrm{a}}I_{\mathrm{a-c}}$) is a critical parameter. For a steel–concrete composite structure the girder stiffness will depend on the age and state of stress of the concrete element. The moment initially jacked into the section will reduce as creep changes the effective stiffness of the section (see Equation 1.3). For use in prestressed sections the effective elastic modulus is estimated using a modified form of Equation 1.3:

$$E_{\mathrm{c}}' = E_{\mathrm{c}}/(1 + k\Phi) \tag{11.3}$$

where Φ is the creep factor (see Chapter 1) and k is a modification coefficient that depends on the variation in stress over time and the properties of the section. For prestress by jacking $k = 1.5$, while for prestressing using tendons $k = 1.1$. These factors are noted in Eurocode 4: Part 1-1, 'General rules and rules for buildings' (BSI, 2004).

11.3. Preflex beams

Preflex beams (Staquet *et al*., 2010) use an applied curvature in a similar way to the displacement of supports. However, the curvature is applied in a different way, usually at the fabrication shop of the beams. Figure 11.1 outlines the method (based on Staquet *et al.* (2010). The beam is fabricated with a given curvature (Figure 11.1a), and then loads are applied to the beam to straighten out the curvature (Figure 11.1b). Concrete is cast around the bottom of the beam (Figure 11.1c) and the loads are released, locking compressive stresses into the beam bottom flange and the concrete

Figure 11.1 Stages in stressing a preflex beam

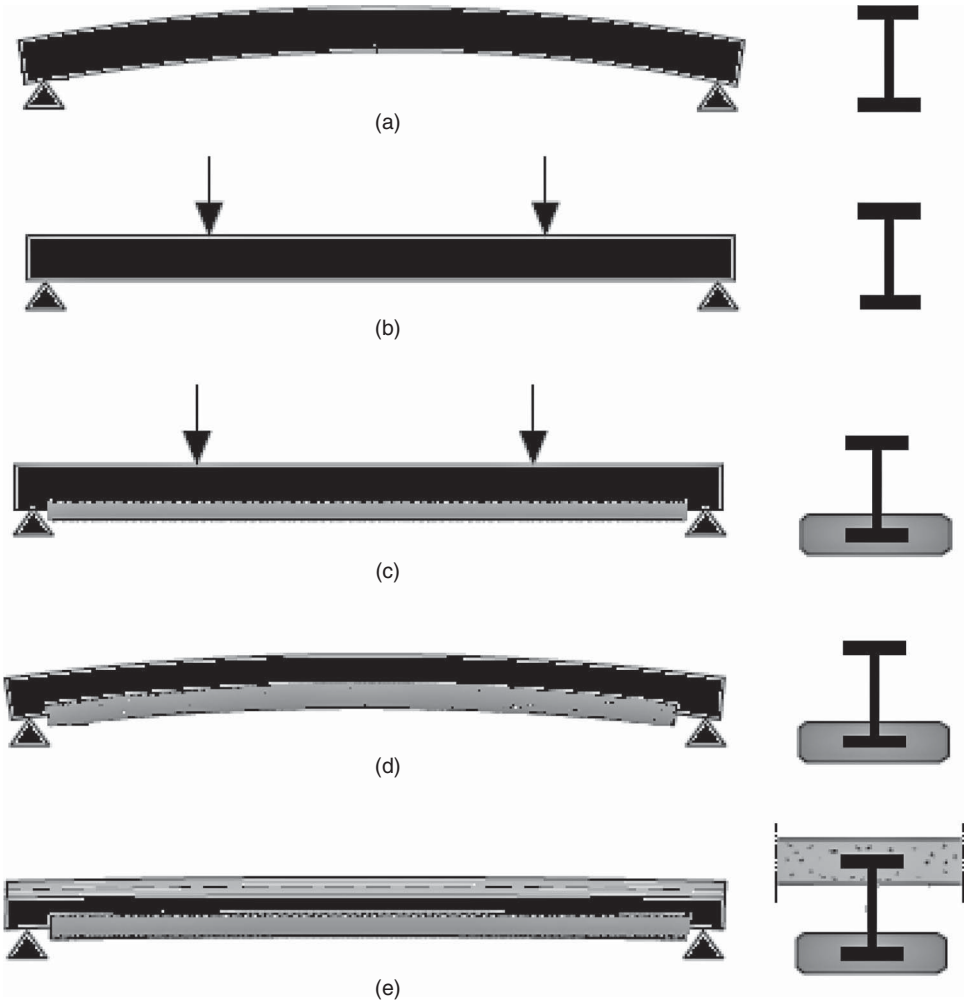

(Figure 11.1d). Finally, the beam is placed in the bridge and the concrete deck slab is cast (Figure 11.1e). The preflexing increases the stress range of the beam, allowing it to carry more load. The stresses locked into the beam will depend on the amount of creep that takes place in the concrete; it has been noted (Staquet *et al*., 2010) that the use of high-strength concrete can reduce the effects of creep significantly.

11.4. Prestress using tendons

Prestressing of a structure using tendons will usually be of one of two types: bonded or unbonded. For bonded prestress, the tendon is enclosed within and bonded to the structure. For unbonded prestress, the tendon is unbonded from the structural components, only touching the structure at anchorages and intermediate deviators (this unbonded, sometimes called 'external', prestress may be inside a box girder to improve durability).

Bonded prestress is usually used in the concrete element of a structure, as it is difficult to get an adequate bond between prestressing tendons and a steel structure. For bonded prestress, the concrete is cast with ducts (empty flexible tubes) inside it to the required profile, with an anchorage casting at each end. The strands are threaded through the ducts when the concrete has cured. The strand is stressed from one of the anchorages (the live end), while the other end is held at the other anchorage (the dead end) and, once the required force has been stressed into the strand, the anchorage is locked off. The duct is then grouted to provide protection to the strand. For durability, the grouting should be carried out carefully and the material used should have a low bleed (separation of water from the grout mix) (Concrete Society, 2002). This method has been used (mainly in Europe) to provide prestress over supports, to induce compression in the slab and to avoid cracking.

Unbonded prestress again utilises tendons, but the loads are applied only to the structure at anchorage and deviator locations. The anchorages may be embedded in the concrete (similar to anchorages for bonded prestress) or attached to the steel element by a series of plates and stiffeners. Deviators are located at intermediate locations along the structure. The tendons change direction at the deviators, and this change in direction must be in a gentle curve, the radius of curvature depending on the tendon size. The deviators are again fabricated plates and stiffeners on the steel elements, or reinforced concrete blocks on concrete elements. Again, the tendons are threaded through the tubes and stressed from the anchorage. For durability, the tendons are grouted, and the grouting medium may be a cement based (at the internal tendons) or a petroleum-wax based (as is common with cable stays). With the wax-based medium the tendons could be destressed and replaced, provided sufficient strand is left in the anchorage cap.

The primary difference between bonded and unbonded prestress is that bonded prestress is physically bonded to the structure by grout, such that at the ultimate limit state, if the concrete is strained sufficiently, the tendon stress will increase up to the ultimate strength. For unbonded prestress, there is no bond and very little additional strain, so that at the ultimate limit state the force in the tendon will not increase far beyond that already in the tendon. An advantage of external prestress is that the tendons are accessible and can be inspected or replaced.

11.5. Design of prestressed composite structures

For a non-prestressed composite structure the stresses on the section are summed at the various stages of construction as the load is applied (Figure 11.2a). For a prestressed composite structure additional stresses are induced, tending to increase the range of the live load that can be added (Figure 11.2b). The additional prestressing stresses comprise an axial and a bending component. The axial stress is simply

Figure 11.2 Comparison of stresses in a conventional composite section and a prestressed composite section

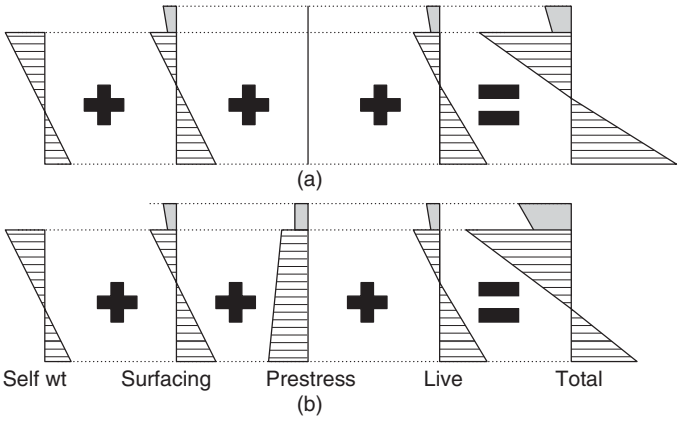

the prestress force divided by the area of the composite section:

$$f_{PA} = P_o/A_{ac} \tag{11.4}$$

The bending stress is derived from the moment applied by the prestress, the moment being the prestress force multiplied by the eccentricity of the force from the section neutral axis (although it is more complex for continuous structures (Menn, 1990; Benaim, 2008)):

$$f_{PZ} = P_o e/Z_{ac} \tag{11.5}$$

Like other steel concrete composites, consideration needs to be made of each stage of construction. For prestressed composites the stage where prestress is transferred to the structure may be critical. Both the ultimate and the serviceability limit state again need to be considered; Table 11.1 outlines

Table 11.1 Limiting stresses for prestressed steel–concrete composite structures

Stage	Ultimate limit state	Serviceability limit state
During concreting	$f_a < 0.95f_{ac}$	
	$f_a < 0.95f_y$	$f_a < f_y$
At transfer	$f_a < 0.95f_{ac}$	
	$f_a < 0.95f_y$	$f_a < f_y$
	$f_c < 0.5f_{cu}$	$f_c < 0.4f_{cu}$
	$f_c > 0.5f_{ct}$	$f_c > -1$ N/mm^2
	$f_p < 0.95f_{pu}$	$f_p < 0.8f_{pu}$
With full loads	$f_a < 0.95f_{ac}$	
	$f_a < 0.95f_y$	$f_a < f_y$
	$f_c < 0.4f_{cu}$	$f_c < 0.3f_{cu}$
	$f_p < 0.95f_{pu}$	$f_c > -3.5$ N/mm^2
		$f_p < 0.7f_{pu}$

the limits of stresses in a prestressed girder. The shear interface will also require checking at the serviceability limit state with the additional longitudinal shear induced by the prestress. It may be assumed that this is transferred over a length L_s in a similar way to that outlined for a cable-stayed anchorage (see Chapter 10), and can be determined using Equation 3.13.

11.6. Prestress losses

An initial force (P_i) is stressed into the tendons during construction and transferred to the bridge. Some loss of prestress will occur straight away, and more will occur over time to leave a lower force (P_o). The primary causes of loss are slip, relaxation, elastic shortening, wobble, cable curvature, shrinkage and creep. The loss of prestress (α) is expressed as a percentage of the initial force:

$$\alpha = \frac{100}{P_i}(P_i - P_o) \tag{11.6}$$

The anchorage of tendons is typically via a system of conical wedges that grip the individual strands. When initially installed these wedges may slip by a small amount (Δ), usually 4–6 mm. The loss is related to the strand area (A_s), the elastic modulus (E_s) and the length (L_{st}) and slip:

$$\alpha_{sl} = \frac{100E_sA_s}{P_iL_{st}}\Delta \tag{11.7}$$

Relaxation of the strand will occur, the amount being dependent on the type of strand and the amount of load applied. The losses are approximately 10% for a standard strand and 3% for a low relaxation strand when stressed to 75% of the strand ultimate tensile strength.

As the tendon is stressed, the composite girder will shorten slightly, causing a loss of prestress related to the relative area of the tendon and the short-term composite section (A_{acs}):

$$\alpha_A = 100A_s/A_{acs} \tag{11.8}$$

For bonded tendons there may be some misalignment or movement of the duct during concreting, and this misalignment or wobble will cause some loss due to friction (μ). For unbonded tendons, wobble may be ignored, unless the deviator length is a significant proportion of the cable length.

$$\alpha_w = \sum 100\mu x_s \tag{11.9}$$

As the tendon changes angle (θ) at deviators or within the duct, a further loss will occur due to friction with the duct at any distance x_s from the jacking end:

$$\alpha_\theta = \sum 100(1 - e^{-\mu\theta})$$

Shrinkage of the concrete will cause a shortening of the composite section (see Chapter 4). Using a shrinkage strain of 200×10^{-6} the loss of prestress is

$$\alpha_{sh} = A_sE_sA_{ac}/50P_iA_c \tag{11.10}$$

Over time creep of the concrete will occur, shortening the section and shedding load from the concrete to the steel, and causing a loss of prestress related to the relative area of the tendon and the long-term

composite section (A_{acl}):

$$\alpha_{cr} = \frac{100A_s}{A_{acl}} - \alpha_E \tag{11.11}$$

11.7. Example 11.1: Prestressed composite girder

Ah Kai Sha Bridge (Benaim *et al.*, 1996; Collings, 1996) is a 704 m long, cable-stayed, double-deck truss bridge with a 360 m main span. The upper deck is 42 m wide and carries a dual four-lane superhighway, and the lower deck carries six lanes of local roads. Transversely the deck consists of a prestressed steel–concrete composite frame structure spanning from the outer stay locations and supporting the longitudinal trusses (Figure 11.3). The primary prestressed steel–concrete frames are at 7 m centres and are in line with the verticals of the longitudinal truss. A series of steel–concrete composite stringer beams span between the frames.

11.7.1 Loading and analysis

The bridge was designed to Chinese standards with verification to UK standards. The dead load of the structure is approximately 6.5 MN per frame and the characteristic live load is 2.0 MN. Analysis of the structure was by a series of longitudinal and transverse frames with local finite-element analysis. The detailed analysis confirmed that the main prestressed beam behaved almost as a simply supported beam. The prestressed section is considered at both the ultimate and the serviceability limit state (Figure 11.4). Three primary load cases are considered: two during construction, before prestressing and when the prestress is added but the full dead load of the upper deck has not been placed; and the condition with full dead and live loads.

Figure 11.3 Deck cross-section for Example 11.1 (© RBA)

Figure 11.4 Simplified loading at various stages: (a) non-composite, no prestress, during concreting; (b) short-term, composite at prestress transfer; (c) long-term, composite with prestress after losses

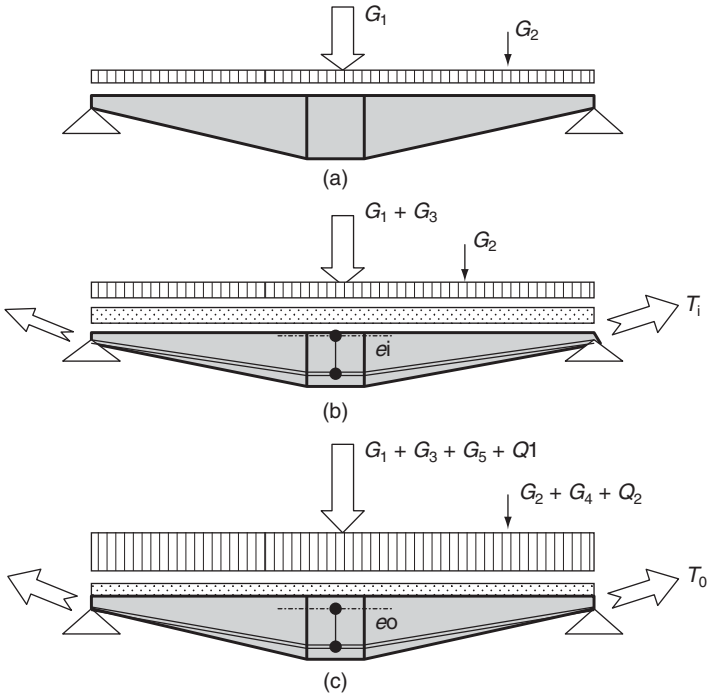

Prestressing of the section consists of two tendons each comprising 19 strands; each strand has an ultimate tensile strength of 265 kN. The tendons are anchored at each stay location and run through the inclined struts and along the lower beam; they are deviated at the beam–strut intersection and at midspan. The tendons are initially stressed to 75% of the ultimate strength, giving an initial prestressing force of 7.6 MN. Loss of prestress will occur, and the losses for Example 11.1 are summarised in Table 11.2, the total losses being 21%. The girder is composed of a fish-belly girder with the deepest section at midspan. The stresses at the girder midspan for the three primary stages are summarised in Figure 11.5.

Table 11.2 Prestress losses for Example 11.1

Type	Amount: %	Remarks
Slip	–	Slip occurs only at ends, not beyond initial deviator
Relaxation	3	Low relaxation strand
Wobble	–	None for unbonded tendons
Curvature	15	Friction coefficient 0.05–0.2
Shrinkage	1	
Creep	2	
Total	21	$T_o = 0.79T_i$

Figure 11.5 Stresses at various stages for Example 11.1

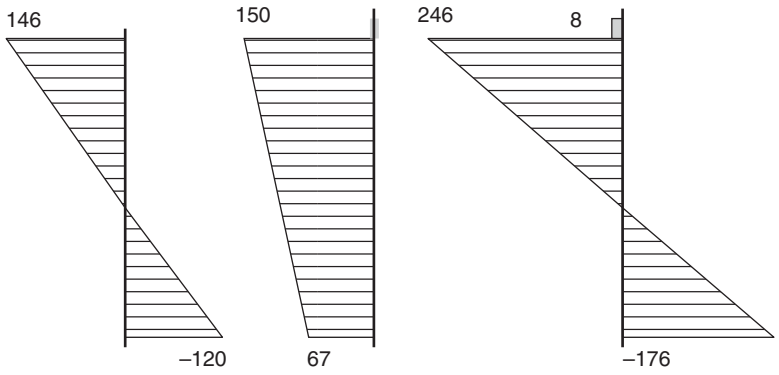

11.8. Durability

For all structures, durability is an issue, and for prestressed structures with steel at permanently high stresses particular care should be taken to ensure durability of the strand and its anchorage system. For prestressed structures a multi-layer philosophy is used (Concrete Society, 2002), with more layers of protection added for structures at higher risk and in more severe environments.

The elements of a multi-layer protection are numerous. The nature of the bridge, the use of continuity and avoidance of joints will improve durability, keeping the tendons away from direct contact with chloride-contaminated water. The use of a low-permeability concrete with small crack widths will be of benefit, as will the use of a high-quality sprayed waterproofing material. Placing the tendons within a box section will lower the exposure category; however, care must be taken at the end anchorage, as these areas are likely to be in a more severe environment. At an anchorage near a joint the anchor head should be kept as far away from the joint as possible and an additional paint (on steel) or waterproofing layer (to concrete) provided to the anchorage area. Over the length of the tendon the strand must be enclosed in a sealed non-corroding duct. Within the duct and any void behind the anchorage cap a grout or wax protection should be used.

11.9. Prestressed composite box girders

The use of prestressed concrete box girders is common. They are often very similar in terms of cost of construction as conventional steel–concrete composite girder and slab construction. Prestressed composite box girder bridges combine both forms of construction. Initial designs for prestressed composite girders used concrete flanges with steel plate webs, the prestress being external but within the box. For this form of structure, the steel web is proportionally stiffer than the concrete and attracts a significant proportion of the prestress from the flanges, lowering the structural efficiency. A more recent development is the use of folded plate webs, which have a low axial stiffness and attract almost no prestress. The folded plate web also has a good transverse stiffness to resist distortion of the box (see Chapter 7).

For the composite prestressed box with a folded plate web, the top and bottom flanges resist the bending effects, the webs carry all the shear, and there is little interaction between the two. A shear connection will be required between the web and the flanges. Using Equation 1.16b, and assuming

that the second moment of area ($I_{a–c}$) is

$$I_{a–c} = 2A_c y^2/n \tag{11.12}$$

then

$$V_l = VA_c y/I_{a–c} n = V/2y = V/d \tag{11.13}$$

where n is the modular ratio. As perhaps expected, this indicates a similar shear flow longitudinally and vertically.

11.10. Corrugated webs

The corrugated steel webs carry the entire shear in a composite steel–concrete box, and almost no other load (Johnson and Cafolla, 1997). The shear capacity of the web will be the lower of the yield or the buckling strength (V_{ai}) of the web. The shear capacity at yield is similar to other steel-plate structures (Equation 1.10):

$$V_y = 0.55tdf_y \tag{11.14}$$

The buckling strength of the web is determined from the interaction of the local (V_{ab}) and overall (V_{ag}) buckling of the panel:

$$1/V_{ai} = 1/V_{ab} + 1/V_{ag} \tag{11.15}$$

Local buckling of one of the folded panels may occur. It is assumed that the geometry of the folds is such that the critical length is that of the panel parallel to the girder axis:

$$V_{al} = \frac{1.1t^2\left(E_a f_y\right)^{1/2}}{b} \tag{11.16}$$

Overall buckling of the web will again depend on the geometry of the folded plate, primarily the distance across the folds:

$$V_{ag} = \frac{55}{d}\left(K_x K_z\right)^{1/4} \tag{11.17}$$

$$K_x = \frac{E_a t^3}{12}\left(\frac{L_l}{L_o}\right) \tag{11.18}$$

$$K_z = \frac{E_a bts^2}{4L_l} \tag{11.19}$$

The overall buckling limit above is for a composite box structure with relatively stiff flanges; if a steel plate flange is used the web capacity should be halved. The geometry and notation for the corrugated web are outlined in Figure 11.6.

11.11. Example 11.2: A structure with corrugated webs

The A13 viaduct in east London is a prestressed box girder structure (Collings, 2001). In this example, a comparison is made with the constructed concrete box and an alternative prestressed steel–concrete

Figure 11.6 Geometry of a corrugated web plate

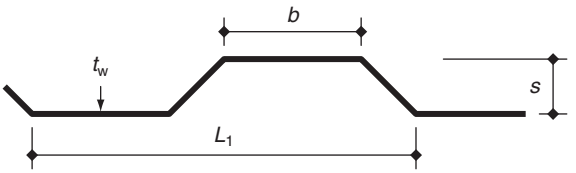

composite box using corrugated webs. The structure is continuous for 1754 m, and consists of a series of spans typically 64 m in length. Each box is 14 m wide, and two boxes are placed side by side to form the typically 28 m wide structure.

For the concrete section, the area of the box is 7.1 m^2 and the dead load on a span is approximately 11.5 MN. For the composite section with corrugated webs, the area reduces to 4.3 m^2 and the dead load decreases by 17% to 9.5 MN. The reduction in the dead load and the area of the structural section will lead to a reduction in prestress requirements.

In this example, a 5 MN ultimate shear occurs on the web near the quarter-span location. A 15 mm web (t_w) with a fold thickness (s) of 350 mm and flat length (b) of 600 mm is used. From this, L_1 is calculated as 1900 mm and L_o as 2187 mm. The depth of the web between flanges is 1830 mm. Using Equation 11.14 the limiting shear capacity is estimated as

$$V_y = 0.55tdf_y = 0.55 \times 0.015 \times 1.83 \times 355 = 5.3 \text{ MN}$$

The local buckling capacity is determined from Equation 11.16:

$$V_{al} = \frac{1.1t^2d\left(E_a f_y\right)^{1/2}}{b} = \frac{1.1 \times 15^2 \times 1830(210\,000 \times 355)^{1/2}}{600} \times 10^{-6} = 6.5 \text{ MN}$$

The global buckling capacity is derived from Equations 11.17 to 11.19:

$$K_x = \frac{E_a t^3}{13}\left(\frac{L_1}{L_o}\right) = \frac{210\,000 \times 15^3 \times 1900}{12 \times 2187} = 51.3 \times 10^{-6} \text{ N mm}$$

$$K_z = \frac{E_a bts^2}{4L_1} = \frac{210\,000 \times 600 \times 15 \times 350^2}{4 \times 1900} = 30.5 \times 10^{-9} \text{ N mm}$$

$$V_{ag} = \frac{55}{d}\left(K_x {K_z}^3\right)^{1/4} = \frac{55}{1.83}\left(51.3 \times 10^{-3} \times 30.5^3\right)^{1/4} = 185 \text{ MN}$$

By inspection, the buckling interaction will be small and the yield capacity of the web is the governing criterion. The 15 mm web is adequate at the quarter point, but a thicker section will be required nearer the support.

11.12. Extradosed bridges

The idea of an extradosed bridge was conceived initially as a girder with low external prestress cables, a hybrid between externally prestressed bridges and cable stayed bridges. Research carried

Figure 11.7 Japanese extradosed bridges: (a) Himi Bridge with 180 m main span; (b) Rittoh Bridge with 160 m spans

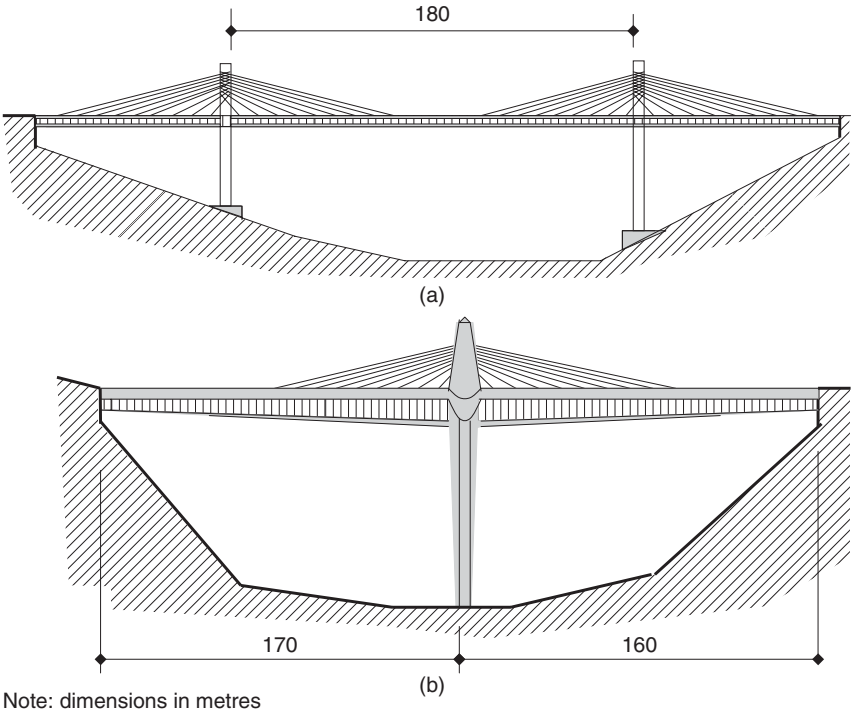

out by the author (Collings and Santiago, in press) has shown that most of the bridges of this form are a special class of cable-stayed bridge where most of the live load is carried by the relatively stiff deck and very little by the stays. This means that there is less fatigue load and the stay can work at nearer 60% of its ultimate strength rather than the 40–45% normally used for typical cable stay bridges (see Chapter 10). Most extradosed bridges have been constructed using concrete box girder decks; some, however, have been constructed using steel–concrete composite girders. Due to the relatively big axial loads in the girder from the stays, steel corrugated webs are often used in order to avoid web buckling issues (see Chapter 10). Steel–concrete composite extradosed bridges have been constructed in Japan, and two, the Himmi and Rittoh bridges, are outlined in Figure 11.7 (Russel, 2004).

The author (Collings and Santiago, in press) has noted that, visually, the extradosed bridge is characterised by a relatively prominent deck, a low tower with shallow stay angles, and stays that are often grouped near the quarter point of the span (with no stays near the tower or at midspan). Figure 11.8b shows that, for most extradosed bridges, the towers are lower than those on cable-stayed bridges. However, the tower height alone cannot define the extradosed bridge, as some of the bridges with low towers are actually shallow cable-stayed structures, not extradosed structures. The depth of the deck, or the deck stiffness, also has a significant influence on the extradosed bridge behaviour (Figure 11.8a), but again there are cable-stayed bridges with stiff decks, and so the deck stiffness alone also does not define the extradosed bridge form.

Figure 11.8 Typical geometric details of extradosed bridges (Collings and Santiago, in press): (a) typical girder depths used for extradosed bridges, compared with girder and cable-stayed bridges; (b) typical tower heights for extradosed and cable-stayed bridges

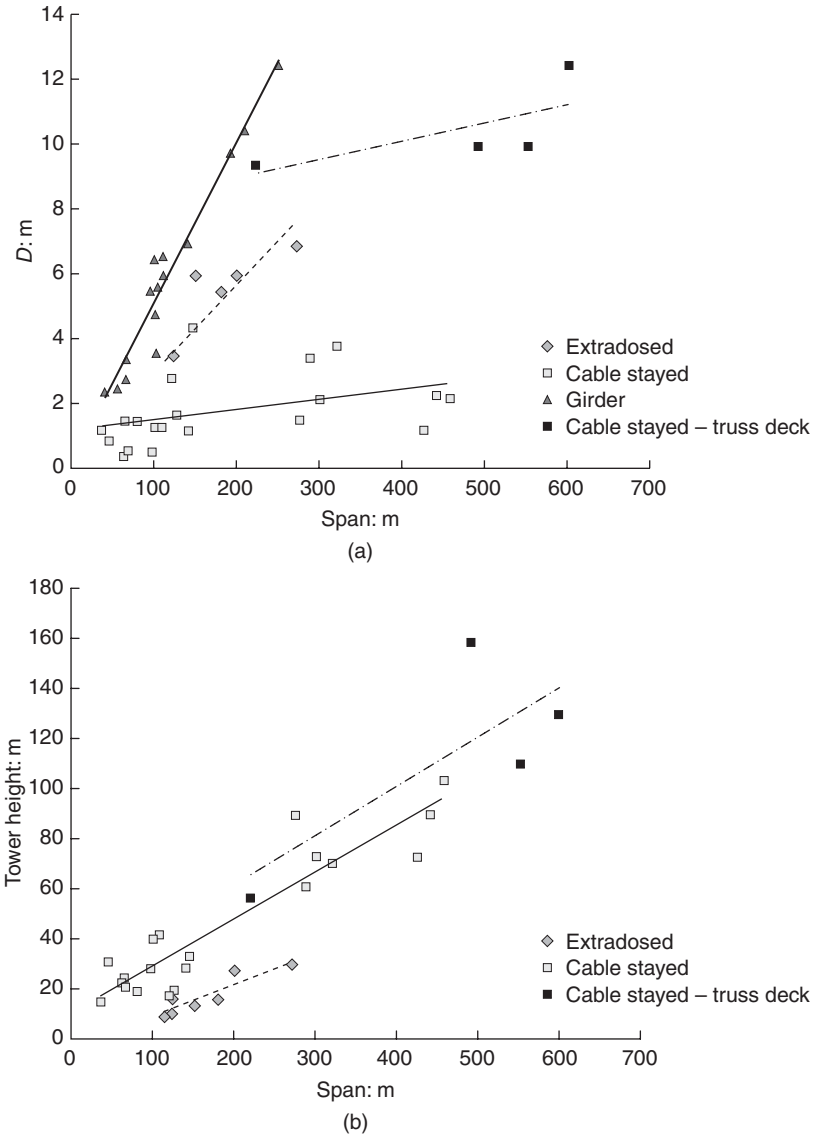

The load distribution factor is a key parameter, and it has been noted (Collings and Santiago, in press) that bridges with a low distribution ratio β had low stay stress variations under live load. The load distribution ratio is defined as

$$\beta = 100F_s/Q \tag{11.20}$$

where Q is the total vertical load and F_s is the vertical component of the stay force.

REFERENCES

Benaim R (2008) *The Design of Prestressed Concrete Bridges: Concepts and Principles*. Taylor & Francis, London.

Benaim R, Brennan MG, Collings D and Leung L (1996) The design of the Pearl River Bridges on the Guangzhou ring road. *FIP Symposium on Post Tensioned Concrete Structures*, London.

BSI (2004) BS EN 1994-1-1:2004. Eurocode 4. Design of composite steel and concrete structures. General rules and rules for buildings. BSI, London.

Collings D (1996) *Design of Innovative Concrete Bridges for south China. Bridge Management 3*. E&F Spon, London.

Collings D (2001) The A13 viaduct: construction of a large monolithic concrete bridge deck. *Proceedings of the ICE – Structures and Buildings* **146(1)**: 85–91.

Collings D and Santiago A (in press) *Proceedings of the ICE – Bridge Engineering*.

Concrete Society (2002) *Durable Post Tensioned Concrete Bridges*, 2nd edn. Technical Report 47. Concrete Society, Camberley.

Johnson R and Cafolla J (1997) Corrugated webs in plate girder bridges. *Proceedings of the ICE – Structures and Buildings* **122(2)**: 157–164.

Menn C (1990) *Prestressed Concrete Bridges*. Birkhauser-Verlag, Basel.

Russel H (ed.) (2004) *Bridge Design and Engineering*. Hemming Group, London.

Staquet S, Espion B and Toutlemonde F (2010) Innovation for railway bridge decks: a prebent steel–VHPC beam. *Structural Engineering International* **20(2)**: 134–137.

Troitsky M (1990) *Prestressed Steel Bridges. Design and Theory*. Van Nostrand Reinhold, New York.

Steel–concrete Composite Bridges
ISBN 978-0-7277-5810-1

http://dx.doi.org/10.1680/scb.58101.219

ice
Institution of Civil Engineers
publishing

Chapter 12
Assessment of composite bridges

. . . sometimes we underestimate the full range of ways a structure can behave . . .

12.1. Introduction

The approach to assessment is different to that of design (Highways Agency, 1996, 2001a). In design, the engineer has freedom to choose a form and provides steel, concrete and connecting elements to suit the forces developed from an analysis of the applied loads. Where parts of the structure are found to be critical, the design can be enhanced. In assessment, the assessing engineer has no choice about the size of elements, or the distribution of materials through the structure, another designer took these decisions long ago. The assessing engineer has to respect the decisions taken and look for the load paths used. Often, in older structures the structural types are different from those that are economic today, many being simple assemblages of beams and concrete not readily analysed by today's design tools. Sometimes we underestimate the full range of ways a structure can behave, and the assessor should take care not to condemn a structure simply because of a lack of understanding of its real behaviour – we tend to think we know things with a greater certainty than we really do. An example is the behaviour of deck slabs under wheel loads. The analysis using plate bending theory often shows existing slabs are under-reinforced, and even yield line analysis may be conservative. However, research has shown that in-plane arching action may dominate shorter spans, and that even larger slab panels will have some degree of arching (Peel-Cross *et al.*, 2001). The use of arching usually shows that a much higher load can be carried by the given reinforcement (Collings, 2002).

12.2. History

Iron has been used in the building of bridges since 1779 with the iron arch over the River Severn at Coalbrookdale (Maguire and Matthews, 1958), and was used in the first long-span box girder over the Menai in 1850 (Ryall, 1999). The first use of steel on a major bridge was Eads' triple arch over the Mississippi at St. Louis in 1874 (Scott and Miller, 1979). The first major use of steel in the UK was the cantilever across the Forth estuary in 1890 (Paxton, 1990). None of these bridges used concrete in the original superstructure, the decking was typically timber balks.

Concrete has been used in bridges for about 2000 years, and many Roman arches used concrete and masonry to form arch structures (O'Connor, 1993). The modern development of concrete started in the 1800s, initially utilising the compressive strength of concrete in arch structures for relatively modest spans. In the 1850s, with the patenting of reinforced concrete by Wilkinson, there was an era of experimentation, with the addition of various bar arrangements or utilising embedded iron or steel sections. The development of reinforced concrete in the UK in a recognisably modern form was by Hennebique and Mouchel in the early 1900s, and many of these bridges used an arch form (of open spandrel construction).

The use of iron joist sections embedded in concrete using a filler joist or jack arch form was used in fireproof slabs in buildings from the 1850s. The first recorded bridge with a combination of iron

Figure 12.1 (a) Embedded joists; (b) brick jack arch; (c) steel hog plates; (d) buckle plate deck

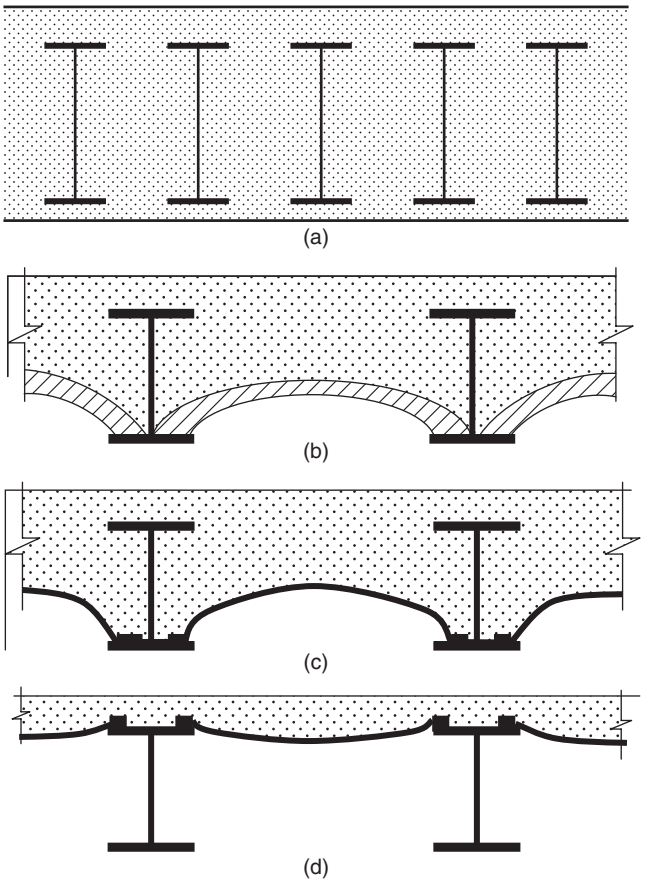

and concrete in the UK was the River Waveney Bridge (Chrimes *et al.*, 1997), dated to 1870, a 15 m span structure comprising a wrought iron arch with a braced spandrel, infilled with mass concrete. However, during the reconstruction work at Paddington, UK, in 2003, an iron-rib and concrete arch by Brunel dating to 1838 was rediscovered (Russel, 2004). The unusual shaping of this structure leads to speculation that it was conceived to utilise some interaction between the iron and the concrete (see Example 12.1). Many of these innovative bridges utilise an arch form. It may be postulated that this was to reduce risk. The way an arch works can be estimated using simple geometry, and the form is well tried and tested. So the only real unknown is the use of the new materials.

The use of embedded joist sections (Figure 12.1a) in concrete is probably the first recognisably modern use of composite steel–concrete construction. The development of steel and concrete remained largely separate for the first half of the twentieth century, with steel bridges generally being preferred for railway bridges and longer span road structures, and concrete being used on shorter spans, primarily carrying roads. When steel was first combined with a concrete deck a composite section was not utilised. Usually the steel element was designed to carry all loads, with the concrete element acting as a deck slab only and carrying local wheel loads. The use of longitudinal stringers supporting the

deck above the main steel ensured a limited interaction. Where the steel and concrete were in contact the provision of composite action was often only accidental, for instance from the joints and connections in buckle plates (Figure 12.1b to 12.1d). Where composite action between steel and concrete was assumed, the steel element was usually fully encased (see Figure 9.2).

12.3. Structure types

The structural forms, from simple beams and boxes, through to arches and suspended spans, outlined in Chapter 1 have all been used before, and may need to be evaluated in an assessment. The details of these structures may be different from those contemplated today. Many girders will not be formed from rolled sections or welded plate, but fabricated from plates and angles using rivets, often using multiple thin plates to achieve the required thickness. Trusses and arches are not simple frameworks of large steel sections or filled tubes, but lattices of battened members with a myriad of intermediate braces in all directions, often forming a very complex structure.

Slabs may be formed from brick arches filled with concrete, or may use steel plates (Figure 12.1b and 12.1c), clearly showing the assumption of arching rather than bending in the original design. Other slabs may use buckle plates or filler beams. On many larger structures the concrete slab may not be fully effective due to inadequate shear connection (by today's standards). The slab may be on a series of stringers separated from the primary structure, and only partially effective as a composite element.

12.4. Inspection

Viewing a structure will give an indication of its overall integrity and condition. A detailed inspection of the individual components and measurement of dimensions will enable accurate estimates of loading and any loss of section. If possible, the bridge should be viewed when fully loaded such that deflections, vibration or the rattling of loose elements can be observed. Inspection just after a period of heavy rain can also be useful for observing leaking joints and cracks.

The concrete elements should be inspected and any cracking, rust staining, spalling or crazing noted. Where penetration by chloride-contaminated water is evident, consideration of testing, such as a survey of the cover to reinforcement, concrete sampling to determine the extent of carbonation and chloride content, and the use of a half cell and resistivity measurements (Ryall *et al.*, 2000; Highways Agency, 2001a) to determine any active corrosion pockets, may also be useful. At the interface of the steel–concrete composite elements signs of corrosion, separation, cracking or longitudinal slip should be noted.

The steel elements should be inspected for defects, including corrosion, cracking, loose or missing bolts, and signs of buckling or out-of-flatness in slender plate panels. For rail bridges in particular, details that are known to be fatigue susceptible should be examined more carefully for cracking.

12.5. Loads

The loading used to assess a structure is likely to initially be the full standard highway or railway load (see Chapters 2, 4 and 10). If the structure is not capable of carrying this load, then the load that it can carry should be determined. The determination of the load limit is carried out on a structure-by-structure basis, as the loading will be influenced by a number of bridge-specific factors.

12.5.1 Highway loading

The UK type HA type loading approximates a 40 tonne vehicle loading. Eurocode loads are also meant to represent real vehicles, and they are derived using worst credible values of vehicle overloading

Figure 12.2 Variation in assessment loading with span and highway classification

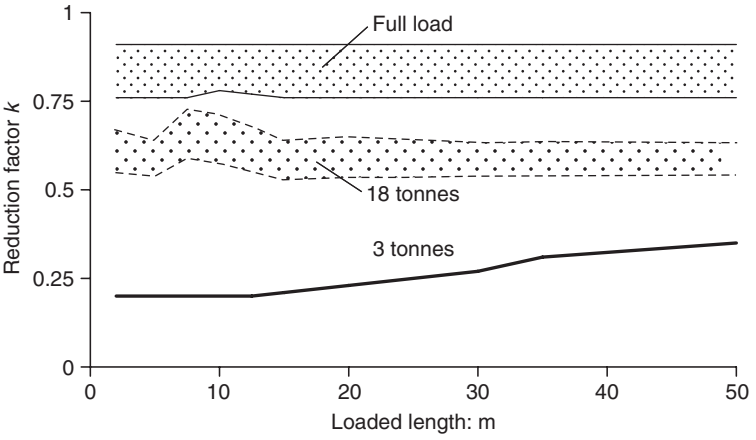

and bunching; for situations where this is not likely, some reduction in loading intensity may be used. Current regulations (Highways Agency, 2001a) define three categories of structure based on traffic flow (high, medium and low), each of these is further subdivided depending on the condition of the surfacing (good or poor). Figure 12.2 shows the variation in the reduction factor (k) from standard loading. The reduction ranges from 0.91 for high traffic flows with poor surfacing, to 0.76 for low flows and good surfacing. The reduction factors were derived using HA loadings as a basis. The traffic on UK roads is the same, even though Eurocodes are now used, but it seems likely that similar reductions can be applied to Eurocode LM1 loads.

If the bridge is still unable to carry this modified full loading, then a reduced loading is considered, usually to 26, 18, 7.5 or 3 tonne loading. Figure 12.2 also shows the reduction factors for these loads, the 3 tonne limit giving a reduction factor of up to 0.2. As an alternative to weight restrictions it may be possible to reduce carriageway widths to limit the number of lanes of full loading on the structure.

12.5.2 Railway loading

For railway bridges in the UK, the assessment is normally carried out for 20 units of RA1 loading (Figure 12.3a) (Network Rail, 2001). For bridges where trains pass at more than 8 km/h, the load should be increased by a dynamic factor (k_D):

$$k_D = 1 + \varphi \tag{12.1}$$

where φ is a dynamic increment depending on the train speed, train–structure interaction, structure length and the natural frequency of the bridge. Figure 12.3b outlines the range of the dynamic increment for various spans and train speeds. The number of units of RA1 loading that can be carried by the structure is determined as

$$N_{RA1} = \text{Effects of 20 RA1 } k_D k_C \tag{12.2}$$

Typically, at least two capacities should be used: first, assuming the load reduction factor (k_C) is 1.0, the limiting value of k_D for 20 units can then be determined; and, second, the dynamic factor for the

Figure 12.3 (a) Type RA1 loading (20 units). (b) Range of dynamic increment for railway assessment loading with span and line speed

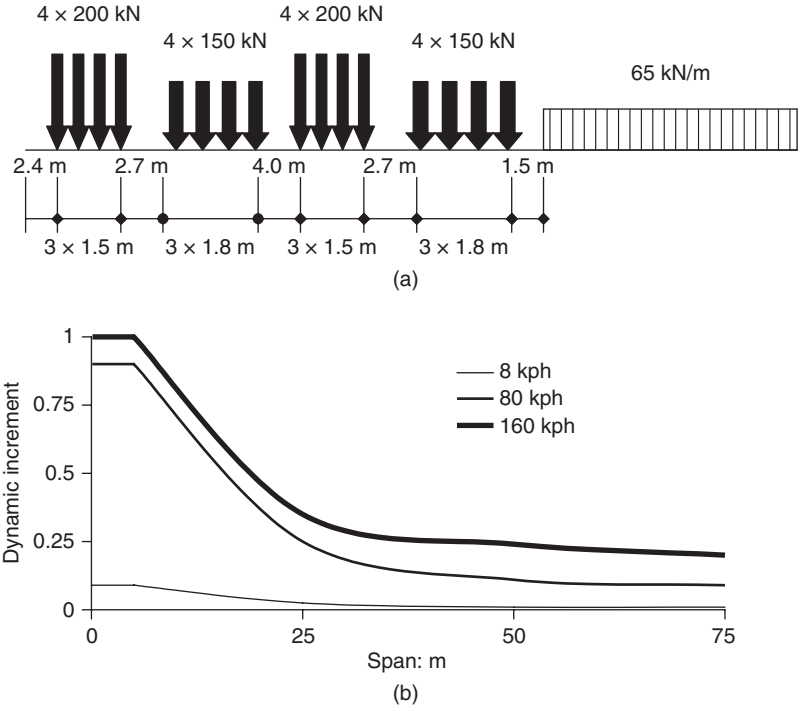

defined line speed is used, allowing a value of k_C to be determined. These calculations will result in an estimate of the speed restrictions to be placed on heavier freight trains (say 90 km/h for 20 units) or an estimate of the weight of lighter passenger vehicles that can travel at the full line speed (say 15 units at 160 km/h).

12.6. Example 12.1: A concrete-encased iron beam

The author was the independent checking engineer for a new steel–concrete composite bridge near Paddington station, UK. The bridge spanned the railway and a canal. The existing bridge over the canal was to be demolished. However, it was found that it was a lost design by Isambard Kingdom K Brunel (Vaughn, 1991).The bridge consists of three small spans, one a masonry arch and the other two slightly arched iron girders, the largest having a span of about 10.7 m (Figure 12.4). The bridge was taken down and its details recorded (Russel, 2004). The shape of the beams is unusual. It was postulated (Tucker, 2003) that Brunel did not fully understand cast iron or that the arching was purely a visual device to make the structure more conventional looking for the period. Having studied and visited many of Brunel's bridges, the author was convinced that Brunel would have shaped the girders for good reason. Some simple calculations show this is true.

The span of the cast iron girders is 10.7 m and the girders are at 1.22 m centres. They consist of a circular top flange (reminiscent, on a small scale, of his later major tubular structures), a web, and a 250 mm wide lower flange curved with a 1 : 20 rise/span ratio. The girder has an area (A) of 0.063 m^2 and a section modulus (W_e) of 0.0091 m^3. The total permanent load (G) on a girder is

Figure 12.4 A concrete-encased iron arch by Brunel (now demolished)

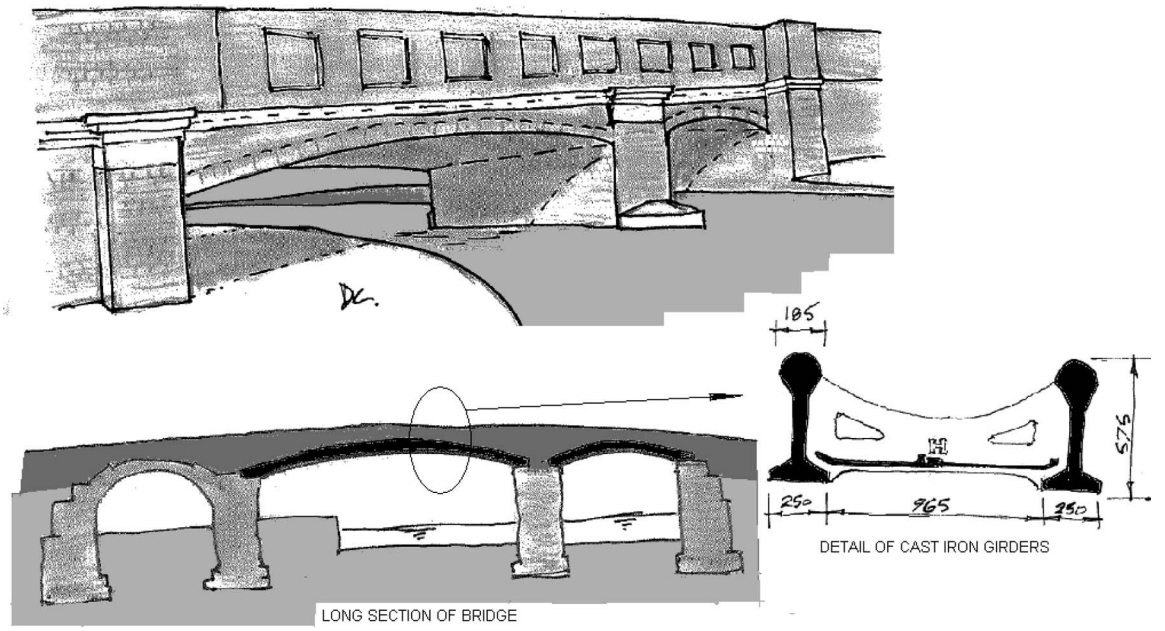

approximately 287 kN. Assuming the bridge behaves as a simple beam,

$$M = GL/8 = 287 \times 10.7/8 = 384 \text{ kN m}$$

$$f_i = M/W_e = -384/0.0091 \times 1000 = -42 \text{ N/mm}^2$$

For cast iron the recommended limit in tension is 46 N/mm^2 (Highways Agency, 2001a), so if we assume the girder behaves only in bending, it has almost no spare capacity for highway loads. The detailing of the lower part of the girder seems to be designed to take some thrust from the brick abutments. These abutments could generate about 100 kN at the end of each beam, and using the arched geometry this would increase the capacity:

$$f_i = 100/0.063 \times 1000 - 42 + 100 \times 0.86/0.0091 \times 1000 = -31 \text{ N/mm}^2$$

This improvement leaves more capacity for live load. The iron girders are encased in a lime-based concrete; the composite iron–concrete structure has a transformed area of 0.074 m^2 and a section modulus of 0.0101 m^3. Recalculating, the stresses in the girder are now –27 N/mm^2, meaning that the bridge probably had a 30 tonne vehicle capacity (although, due to a lack of knowledge about the structure prior to dismantling, it had an 8 tonne weight restriction).

12.7. Materials

The behaviour of the composite structure is heavily influenced by the properties of the component materials. For older structures the properties of the iron, steel and concrete may be different to

those assumed today. Strengths are usually less, the variability in strength is often an issue, and quality-control procedures on some older structures were poor.

12.7.1 Concrete

For pre-1939 bridges, a concrete strength of 12 N/mm^2 may be assumed, while for younger structures 21 N/mm^2 strength is appropriate, unless testing is carried out to determine the strength more accurately. The lower strength of the concrete will affect the elastic modulus, and a long-term value (E_c') of 14 kN/mm^2 is recommended (Highways Agency, 2001a). The shear strength (v_c) obtained using Equation 5.9 is reduced by a factor of

$$(f_{ck}/32)^{1/3} \tag{12.3}$$

The capacity of any shear connection will be reduced; using Equations 1.21d and 1.23 it can be seen that this will be in direct proportion to the lower strength.

12.7.2 Steel

For older structures there may be a considerable variation in strength, for Eads Bridge of 1870 the ultimate strength varied from 400 to 900 N/mm^2 (Scott and Miller, 1979), and typically a 230 N/mm^2 yield strength may be assumed. For more modern structures yield strengths above 250 N/mm^2 will be dependent on the grade of steel used and, unless clearly shown on record drawings or determined from tests, a conservative value is initially assumed.

12.8. Testing of the structure

The strength of the standard connectors outlined in Table 1.5 and Equations 1.21a to 1.21d have been calibrated using tests as outlined in Chapter 1, and the newer forms of perforated plate connectors are also tested as part of the development process (Schlaich *et al.*, 2001). Testing can be used for unusual details found on older bridges; however, the cost of this may be prohibitive, and it is normally only economic when a number of bridges use the same detail. Testing of piled foundations is common for most bridges. In the past, it was often common to test a bridge by driving a convoy of loaded trucks across it. The Eurocode 'Basis of structural design' (BSI, 2002) outlines requirements for testing of structures in annex D. Care has to be taken in determining the load for testing and to understand the implications; the load test should not damage the structure if it is to remain in service. Where testing has been carried out during the life of the structure this can give valuable information for the assessment.

12.9. Analysis

The analysis of an existing structure being assessed will use similar methods to those of design (Hambley, 1991). For most structures, an elastic analysis method is acceptable. However, where the composite section is not slender and is capable of some plastic deformation prior to failure, then some redistribution of moments may be assumed to occur. For the assessment of steel elements it is usually acceptable to use the section modulus calculated at the centre of the flange rather than the extreme edge.

12.10. Incidental and partial composite action

Many older bridges may not have full connection complying with current design requirements. Connectors, where provided, may not be of the modern types, and the connectors may be spaced uniformly along the girder rather than increasing in number towards the supports. The connectors may also be grouped adjacent to stiffeners or cross-beams, with little connection between. Often, part of the shear connection may be only incidental.

Figure 12.5 (a) Partial shear connection, typical variation in span load (F) with the number of connectors (n). (b) Cased beam showing the shear plane used to assess the capacity

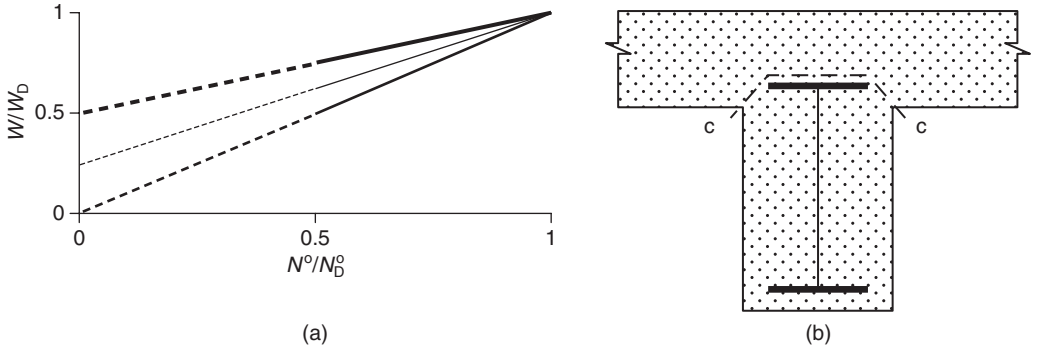

Incidental shear connectors are ends of plate, bolt or rivet heads, stiffeners or trough connections, none of which were specifically designed as connectors but nevertheless provide some connection. Incidental shear connection should not usually account for more than 25% of the longitudinal shear capacity. Incidental shear connection usually has low resistance to uplift. An estimate of the connector capacity can be made by using Equations 1.21 to 1.24 as appropriate, whichever form is nearest.

For girders of less than 20 m span, if insufficient connection is provided to give complete connection then a reduced strength may be derived assuming partial connection. Partial interaction is usually expressed in terms of the maximum design load that the fully composite span could carry:

$$F_d = G_d + Q_d \tag{12.4}$$

For ductile or flexible connectors such as studs or channels, where slip can occur to redistribute load along the connection the capacity is determined by assuming a linear increase in capacity from that of the steel element alone (F_a) to the full design capacity (Figure 12.5). The reduced design load (F) is determined by interpolation from the proportion of the full connector requirements. For stiff connectors, where less slip occurs, the capacity of the section can again be assumed to increase linearly, although from a lower base – either the design dead load (G_D) for unpropped construction, or from zero load for propped construction (see Figure 12.5).

12.11. Cased beams

Fully encasing the steel section with concrete was a popular method of forming early composite structures. Generally, shear connectors were not used and the composite action relies on the bond between the steel and the concrete. The concrete will restrain local buckling of the flange and webs to some degree. Eurocode 4: Part 2, 'Design of composite steel and concrete structures – General rules and rules for bridges' (BSI, 2005), allows the use of class 2 sections if the steel is class 3 but fully encased. When assessing such structures the capacity of the section will often be limited by this bond stress, particularly those sections that are compact and might otherwise develop the full plastic capacity of the section. For cased beams a check of the longitudinal shear across the top of the steel section is carried out (see Figure 12.5b). For design, the bond stress at this interface would normally

be limited to 0.4 N/mm^2 at the serviceability limit state. For assessment a less conservative limit is used, the lesser of Equations 12.5a and 12.5b:

$$V_l = 0.14(f_{ck})^{1/2} L_s \tag{12.5a}$$

$$V_l = 0.7 L_s \tag{12.5b}$$

If the cover around the steel section is less than 50 mm the limiting strength of the interface should be reduced, by 30% for covers of 20 mm.

At the ultimate limit state, where no reinforcement crosses the shear plane the capacity of the shear plane is limited to

$$V_l = 0.5 L_s \tag{12.6a}$$

Where reinforcement passes through the shear plane the capacity may be assessed using modified forms of Equations 1.26b and 1.26c:

$$V_l = 0.9 L_s + 0.7 A_s f_y \tag{12.6b}$$

The minimum amount of reinforcement passing through the shear plane should be

$$A_s = 0.8 L_s / f_y \tag{12.7}$$

12.12. Strengthening

The primary cause of deterioration in bridges is the ingress of chloride-contaminated water at joints, the replacement or removal of joints being the best long-term repair option. Where corrosion has affected the structure's capacity and it can no longer carry the required loading, then strengthening and upgrading will be required. The strengthening of concrete elements can be achieved through the bonding of additional steel or carbon-fibre reinforcement to them with epoxy (Ryall *et al.*, 2000), and in some circumstances the addition of an over-slab bonded to the original slab may be applicable. For steel elements strengthening is often relatively simply achieved by the addition of extra plates and stiffeners using welding or bolting techniques as applicable. For both steel and concrete elements, prestressing by jacking of supports or the use of external unbonded tendons has been carried out successfully (Murry, 1996). Where the interface connection is weak and requires strengthening, repair options are more limited. In some situations it may be possible to break out limited areas of concrete and attach connectors to the steel element in groups. Where there is also concern over the integrity of the deck slab due to chloride ingress or carbonation of the concrete, then the complete removal of the deck may be the only solution, short of complete demolition.

12.13. Life-cycle considerations

The life cycle of a bridge starts at its initial construction, through its useful life (considering inspections, testing, repair or strengthening), up to its final demolition. Decisions made during the initial design will influence significantly the behaviour throughout the life cycle. A whole-life cost (Highways Agency, 2001b) of the bridge through its life cycle may be obtained by placing values on the various operations throughout the structure's life, and these discounted cost methods may be used (see Chapter 4, Equation 4.1). More recently, the environmental life cycle has been considered

(Horne, 1977), looking at the embodied energy and carbon dioxide (CO_2) emissions throughout the life cycle of the structure. Both types of life-cycle study indicate that costs caused by disruption to the use of the structure outweigh the initial construction cost by a significant margin, and this is particularly true for motorway and mainline railway bridges, but is also applicable to smaller structures where the length of any diversion around the structure is significant. Consequently, when planning inspection, testing, maintenance, repair or the rebuilding of a bridge, the minimum disruption to its use should be made.

12.14. Risk assessment

For the engineer looking after a number of bridges, understanding the likely risks to these structures is an important part of the assessment of their adequacy. In order to try to understand possible accidental scenarios and their consequences, a risk assessment should be carried out. Risk assessments may be carried out quantitatively where sufficient information exists to estimate probabilities and allow mathematical modelling of the risk. However, normally such data do not exist or are unreliable, and a more subjective, or qualitative, risk assessment must be carried out. Eurocode 1: Part 1-7, 'Actions on structures – General actions' (BSI, 2006), gives some requirements. All hazards and corresponding accidental load scenarios should be identified. Identification of hazards and accidental load scenarios is a crucial part of risk analysis, and requires an examination and understanding of the structure, its environment and use. A variety of techniques have been developed to assist the engineer in performing this analysis (e.g. HAZOP, fault tree, causal networks, RIM). For many structures a simple risk interaction matrix method of hazard identification is sufficient. This requires an estimation of the likelihood of a hazard occurring and its severity, and then an assessment of acceptability can be made.

The likelihood or probability of occurrence of the hazard should be made, and if no hard data are available the hazard may be classed as 'frequent', 'occasional', 'remote' or 'improbable'. The severity of the hazard can then be defined as 'low', 'medium', 'high' or 'severe'. The two factors (likelihood and severity) may be combined as a risk interaction matrix (RIM) for each hazard, as outlined in Table 12.1.

12.15. Example 12.2: RIM analysis

The bridge designed in Example 2.1 has been standing for 25 years, and a new maintenance company is to be made responsible for the road on which the bridge is located. The new company will need to assess the likely risks on this and other assets they are maintaining. A possible RIM for the structure is carried out as shown in Table 12.2.

Table 12.1 A risk interaction matrix

Severity category	Likelihood			
	Frequent	Occasional	Remote	Improbable
Severe	U	U	U	U
High	U	U	U	T
Medium	U	T	T	T
Low	T	T	A	A

A = Acceptable. T = Tolerable with precautions. U = Unacceptable/undesirable

Table 12.2 Risk interaction matrix for Example 12.2

Hazard	Likelihood	Severity	Initial risk	Mitigation	Residual risk
Overload	Remote	High	U	Bridge was designed to British Standards, carry out assessment to Eurocodes. From past data and bridge location, review the possibility of abnormal vehicles	T
Disproportionate and progressive collapse	Remote	High	U	Assess the effects of failure of parts, such as bearings or bolts. Confirm that structure has sufficient redundancy and that requirements of Eurocode 1 are met	T
Vehicle impact	Occasional	Medium	T	Bridge was designed with standard UK aluminium parapet. Carry out assessment to Eurocodes and using local UK risk assessment methods for parapets	T
Corrosion	Occasional	Medium	T	Review previous inspections. Carry out further inspections at time intervals specified in local UK requirements. If there is corrosion, determine likely loss of section for use in assessment	A
Flooding to beam level	Remote	High	U	Bridge originally designed for flood flows. Review historical river flow data. Assess structure for debris loads and water pressures if required	T
Scouring of foundations	Remote	High	U	Review previous inspections. Carry out further inspections at low flows	T
Settlement of foundations	Occasional	Severe	U	Bridge originally designed for significant movements from ground settlement from mineral extraction. Review extent of current extraction and future extraction; assess effects on structure (bearings and joints in particular)	T
Seismic effects	Remote	Medium	T	Bridge not designed for seismic loads, review local UK requirements. Review robustness of structure and beam-seating requirements in particular	A
Fire	Remote	Medium	T	Review likelihood of storage of hay or other flammable material under structure	A

A = Acceptable. T = Tolerable with precautions. U = Unacceptable/undesirable

REFERENCES

BSI (2002) BS EN 1990:2002. Eurocode. Basis of structural design. BSI, London.

BSI (2005) BS EN 1994-2:2005. Eurocode 4. Design of composite steel and concrete structures. General rules and rules for bridges. BSI, London.

BSI (2006) BS EN 1991-1-7:2006. Eurocode 1. Actions on structures. General actions. Accidental actions. BSI, London.

Chrimes M, Shipway JS, Cox RC, Considere H and Maillart R (1997) The development of concrete bridges in the British Isles prior to 1940. *Proceedings of the ICE – Structures and Buildings* **122(4)**: 499–500.

Collings D (2002) Design of bridge decks utilising arching effects. *Proceedings of the ICE – Buildings and Structures* **152(3)**: 277–282.

Hambley E (1991) *Bridge Deck Behaviour*, 2nd edn. E&F Spon, London.

Highways Agency (1996) BD 61, The assessment of composite highway bridges and structures. In *Design Manual for Roads and Bridges*, Vol. 3. The Stationery Office, London.

Highways Agency (2001a) BD 21, The assessment of highway bridges. In *Design Manual for Roads and Bridges*, Vol. 3. The Stationery Office, London.

Highways Agency (2001b) BD 37, Loads for highway bridges. In *Design Manual for Roads and Bridges*, Vol. 1. The Stationery Office, London.

Horne M (1977) *Structural Action in Steel Box Girders*. CIRIA Guide 3. Construction Industry Research and Information Association (CIRIA), London.

Maguire R and Matthews P (1958) The Iron Bridge at Coalbrookdale. *Assessment Architectural Association Journal* **74**.

Murry M (1996) *Friaton Bridge Strengthening*, *Bridge Management 3*. E&FN Spon, London.

Network Rail (2001) *Railtrack Line Code of Practice. The Structural Assessment of Underbridges*. RT/CE/C/025. Railtrack, London.

O'Connor C (1993) *Roman Bridges*. Cambridge University Press, Cambridge.

Paxton R (ed.) (1990) *100 Years of the Forth Bridge*. Thomas Telford, London.

Peel-Cross J, Rankin G, Gilbert S and Long A (2001) Compressive membrane action in composite floor slabs in the Cardington LBTF. *Proceedings of the ICE – Structures and Buildings* **146(2)**: 217–226.

Russel H (ed.) (2004) *Bridge Design and Engineering*. Hemming Group, London.

Ryall MJ (1999) Britannia Bridge: from concept to construction. *Proceedings of the ICE – Civil Engineering* **132(2)**: 132–143.

Ryall MJ, Parke GAR and Harding JE (eds) (2000) *Manual of Bridge Engineering*. Thomas Telford, London.

Schlaich J, Schlaich M and Schmid V (2001) Composite bridges: recent experience. The development of teeth connectors. *Composite Bridges. Proceedings of the 3rd International Meeting*, Madrid, pp. 760–790.

Scott Q and Miller HS (1979) *The Eads Bridge*. University of Missouri Press, Missouri, MI.

Tucker M (2003) *Canal Bridge – Bishops Bridge Road*. Preliminary archaeological report. Report B/019/2003. English Heritage, London.

Vaughn A (1991) *Isambard Kingdom Brunel*, *Engineering Knight-Errant*. John Murray, London.

Notation

A	area, accidental action
B	width
D	depth of girder; rigidity (EI); diameter
E	modulus of elasticity, effects
F	force or action
G	permanent action, shear modulus
H	height
I	second moment of area
J	torsional constant; mass moment of inertia
K	stiffness of member; soil pressure coefficient
L	length of beam or slab
M	moment
N	axial load
P	connector capacity; wind susceptibility factor
Q	variable action
R	reaction; resistance
S	Strouhal number
T	period
V	shear force
W	section modulus
a	web panel length; weld throat thickness; distance from face of concrete to bar centre
b	width of section
c	outstand length; punching shear perimeter
d	depth to reinforcement centre; bolt or connector diameter
e	eccentricity; edge distance to bolt
f	stress; frequency
g	gap
h	height of section
i	integer
j	integer
k	coefficient; constant
l	length
m	mass per length unit
n	modular ratio; number of connectors or bolts
q	wind pressure
r	radius of gyration; radius
t	thickness
v	shear stress, wind velocity
w	crack width; wind pressure
x	distance along member; distance to neutral axis from compression face
y	distance
z	lever arm
α	factor
β	factor
γ	partial factor
δ	deflection; settlement; connector slip; contribution ratio
ε	strain
η	degree of shear connection

θ	angle; temperature
λ	slenderness parameter
ϕ	creep function, rotation
φ	dynamic increment
ρ	steel ratio
σ	stress
τ	shear stress
χ	buckling reduction coefficient
ψ	load factor

Subscripts

A	arch
E	design effects
R	resistance, strength
T	torsion
a	steel
a–c	steel–concrete composite
b	bottom, bolt
c	concrete
cr	critical buckling
c–s	steel–concrete composite with cracked section
d	design
des	destabilising
eff	effective
f	flange
i	integer
j, *j*	joint; integer
k	characteristic strength
l	length; longitudinal
m	moment
max	maximum
min	minimum
n	axial
o	hole
s	reinforcing steel
st	stiffener
t	top; tension
u	ultimate
v	shear; connector
w	web
x	*x*-axis
y, *y*	yield, *y*-axis
z	*z*-axis
0, 1, 2	general number

Steel–concrete Composite Bridges
ISBN 978-0-7277-5810-1

http://dx.doi.org/10.1680/scb.58101.231

ice Institution of Civil Engineers publishing

Appendix A
Approximate methods

For a girder with approximately equal flange areas (A_f), overall depth D and web thickness t_w, the primary second moment of area of the section may be approximated as

$$I_a = 2A_f(0.5D)^2 + \frac{D^3 t_w}{12} \tag{A.1a}$$

or, rearranging Equation A.1a (Brown, 1988),

$$I_a = 2\left(A_f + \frac{Dt_w}{6}\right)(0.5D)^2 \tag{A.1b}$$

$$W = I_a/0.5D \tag{A.2}$$

Substituting Equation A.2 into A1.b:

$$W = (A_f + 0.167Dt_w)D \tag{A.3}$$

$$M = Wf_a \tag{A.4}$$

$$M = (A_f + 0.167Dt_w)Df_a \tag{A.5}$$

So the moment that the beam will carry may be estimated from the flange area plus one-sixth of the web, multiplied by the permissible stress and the beam depth. This approximation can also be used for girders of unequal flange area.

The transverse second moment of area of the section may be approximated as:

$$I_y = 2B^2A_f/12 \tag{A.6}$$

If the web is of a similar area to the flange,

$$A = 3A_f \tag{A.7}$$

$$i_y = (I_y/A)^{1/2} \tag{A.8}$$

$$i_y = 0.23B \tag{A.9}$$

This approximation can be used for unequal flanges if the average width B' is used.

REFERENCE

Brown C (1988) Plate girders and rolled sections. *ECCS/BCSA International Symposium on Steel Bridges*, London.

INDEX

Page references in *italic* refer figures or tables.

Index Terms	Links		
B			
backfill	*49*	51	52
	53	54	
baffles	193		
bank-seat-type structure	51	*52*	78
bars	*16*	18	*26*
	27	28	46
	61	81	83
	84	99	180
	182	205	219
beams	3	11	*12*
	14	20	*21*
	28	29	33–49
	51–70	75	77
	83	84	85
	91	92	94
	95	96	97
	98	99	109
	110	114	133
	134	147	148
	177	*178*	193
	225	*226*	231
beam layouts for integral bridges	*65*		
calculation of elastic section properties	233–234	241–242	
calculation of plastic section properties	237–238		
concrete-encased iron beam	223–224		
concrete encased steel	226–227		
ladder beam	*104*	105	*106*
multi-beam form, problems with	103	*104*	
preflex beams	205	206–207	
stringer beam	*104*	105	210

E

U